CHARLES UNIVERSITY

FACULTY OF SCIENCE

STUDY PROGRAMME: BOTANY

MGR. MARTIN MACEK

PATTERNS AND PROCESSES IN SPATIAL DISTRIBUTION OF PLANT SPECIES ACROSS SCALES

VZORCE A PROCESY PROSTOROVÉ DISTRIBUCE ROSTLINNÝCH DRUHŮ NAPŘÍČ ŠKÁLAMI

Doctoral thesis / Disertační práce

Supervisor / Školitel: doc. Ing. Jan Wild PhD.

Praha, 2020

PROHLÁŠENÍ

Prohlašuji, že jsem závěrečnou práci zpracoval samostatně a že jsem řádně uvedl všechny použité informační zdroje a literaturu. Tato práce ani její podstatná část nebyla využita jako závěrečná práce k získání jiného nebo obdobného druhu vysokoškolské kvalifikace.

V Praze, dne

Podpis

Table of Contents

PREFACE

„Botanists usually direct their research towards objects that encompass only a very small part of their science. They are concerned almost exclusively with the discovery of new species of plants, the study of their external structure, their distinguishing characteristics, and the analogies that group them together into classes and families. This knowledge of the forms which make up organized beings is no doubt the principal basis for descriptive natural history. It must be regarded as indispensable for the advancement of the sciences that concern the medical properties of plants, their cultivation, or their applications in the arts; even if this knowledge is worthy of occupying a great number of botanists, even if it can be considered from a philosophical point of view, it is no less important to understand the Geography of Plants, a science that up to now exists in name only, and yet is an essential part of general physics. This is the science that concerns itself with plants in their local association in the various climates. This science, as vast as its object, paints with a broad brush the immense space occupied by plants, from the regions of perpetual snows to the bottom of the ocean, and into the very interior of the earth, where there subsist in obscure caves some cryptogams that are as little known as the insects feeding upon them.“

Alexander von Humboldt: Essay on the geography of plants, 1807,
translated by Sylvie Romanowski, 2008.

Caspar David Friedrich: Böhmische Landschaft mit dem Milleschauer, 1808

DEDICATION

This thesis sum up years I've spent by explorations of ecological processes, though it can only bring a tiny fragment of the complex mosaic. Such explorations took diverse forms, including adventurous expeditions to the most remote places on the roof of the world, suffering from mountain sickness and overloaded backpack with scientific equipment and gathered samples, but equally exciting were the late night explorations of the numerical worlds of field data. It is worth mentioning that I was never alone in my struggle – there was always some classmate or colleague around, who shared his/her enthusiasm with me, helped me with the fieldwork, provided critical comments on my results, showed me some tricks in R, shared his own data with me, or 'just' contributed to the inspiring and friendly atmosphere at the department. It's impossible to acknowledge all the people who supported me somehow on my PhD journey without leaving out someone, so I say: "Thank you all!"

Specifically, I'm talkin' about you, Adame, Evo, Honzo, Ingo, Jano, Jardo, Jindro, Jirko, Jitko, Kačko, Leoši, Lucko, Markéto, Martine, Matěji, Míro, Ondro, Pavlo, Pepo, Petře, Pierre, Přemku, Radime, Terezo, Tomáši, Vašku, Věro, Vítku, Vojto, Zdenko, Zdeňku, Zito, Zuzko. However, special thanks belongs to Martin Kopecký and Jan Wild, who guided me since my first steps in the field of science. Finally, very special thanks are dedicated to my wife, Alžběta, and daughters Johana, Marie and Eliška, who suffered most from my occupation and who always welcomed me back home.

ABSTRACT

In this thesis, I aimed to identify factors shaping plant distribution at different spatial scales, correlate them with environmental heterogeneity, identify causal processes and test general hypothesis on the nature of response curve shapes and species richness patterns. General review of the topic is introduced in the first chapter, followed by five chapters presenting three already published studies and two manuscripts.

The first study deals with processes responsible for creation of fine-scaled spatial pattern of spruce seedlings and saplings, emerging after bark-beetle disturbance in mountain spruce forest. Aggregated pattern, replicating previous generation of spruce trees, emerges in consequence to microsite-dependent mortality, as was surveyed through repeated monitoring of the fate of individual seedlings.

The second study explores spatial variability in forest understory temperatures at the landscape scale and its relevance for understory plant distribution. As the main source of variability in understory communities we identified seasonal maximum temperatures. Using GIS modelling approach, we created spatially continuous prediction, which outperformed state-of-art climatic grids used currently by ecologists.

The third study on the shape of species responses along elevational gradients used data from Himalaya collected by L. Klimeš, covering 3500 m wide elevational gradient. Here we show prevalence of asymmetric responses, gradually diminishing towards low elevations and steeply declining towards high elevations. This has practical consequences for ecological model commonly assuming symmetric responses, but it also indicates interesting relations with environment.

In the fourth study we explored patterns in species range size along elevational gradient. Empirical pattern was heavily affected by geographic range truncation. After accounting for this artefact and with a support of our own climate measurements, we had to refuse elevational Rapoport rule, as well as the climate variability hypothesis as the potential explanations of the observed patterns.

The last study focuses on the plant species diversity along elevational gradient, as the synergy of individual species distributions. We used mid-point attractor models to identify central tendency of diversity, accounting for geographic limits of the study.

SHRNUTÍ

V této práci se zabývám procesy a faktory určujícími rozšíření rostlinných druhů na různých prostorových škálách. Studium prostorové distribuce má tři základní kroky: popis pozorovaného vzorce, nalezení prostorových vztahů s dalšími prostorovými jevy a nakonec určení kauzálních vztahů. Tato práce přináší pět případových studií, operujících na různých prostorových škálách, které přináší různou úroveň poznání prostorových vztahů a jejich příčin:

V první studii se zabýváme na jemné škále identifikací procesů, které vedou ke vzniku shlukovitého rozmístění semenáčků smrku v porostech horských smrčin zasažených gradací kůrovce, které je navíc konzervativní v čase – kopíruje totiž předchozí generaci lesa. S pomocí dlouhodobého sledování jednotlivých semenáčků jsme identifikovali rozdíly v mortalitě na mikrostanovištích zodpovědné za prostorové shlukování semenáčků.

Druhá studie zkoumá prostorovou variabilitu teploty v lesních porostech na krajinném měřítku a její vztah k rozšíření druhů bylinného patra. Jako hlavní složku teplotní variability zodpovědnou za rozšíření rostlin jsme identifikovali maximální teploty ve vegetační sezóně. S využitím metod GIS jsme informaci z bodových měření vztáhli k topografii terénu a vytvořili prostorově spojitou predikci mikroklimatu s velmi jemným rozlišením, která obstála při validaci na nezávislém souboru vegetačních snímků před stávajícími klimatickými modely, běžně používanými v ekologii.

Třetí studie se zabývá symetrií tvaru druhové odpovědi na gradientu nadmořské výšky. Tvar druhové odpovědi je nejen důležitým předpokladem nejrůznějších ekologických modelů, ale zahrnuje informaci o vztahu k prostředí jako takovou. Tato studie na velkém měřítku je postavená na datech L. Klimeše získaných v Himalájích, v Ladákhu, které postihují 3500 m dlouhý gradient nadmořských výšek. Výsledkem studie je, že asymetrické křivky s pozvolným vyzníváním druhů do nižších poloh výrazně převládají.

Čtvrtá studie zkoumá zákonitosti rozšíření druhů podél nadmořské výšky ve vztahu k celkové šířce rozšíření jednotlivých druhů. Jako příčinu pozorovaného vzorce odhalujeme artefakty dané částečnou realizací celkové tolerance druhů v mezích zkoumaného území. S podporou vlastních klimatických měření potom odmítáme nejen elevační Rapoportovo pravidlo, ale i hypotézu o rostoucí klimatické variabilitě.

V poslední, páté, studii zkoumáme průběh druhové bohatosti, jakožto synergii rozšíření jednotlivých druhů. S použitím modelu přitahovače středobodů[1] hledáme centrální tendenci druhové diverzity při zohlednění geografických limitů studovaného území.

[1] V originále „Mid-point attractor model“ (Colwell *et al.*, 2016).

Chapter One:
Introduction

Understanding actual physical distribution of organisms in space and time is one of the key goals in ecology, which is as old, as ecology itself, but is still sound (Sutherland *et al.*, 2013). Many fields of ecology are dependent on the knowledge about patterns and processes responsible for spatial distribution of studied species, which propagate to higher organization levels, from community level (Watt, 1947) to global patterns of diversity (Hubbell, 2001; Kier *et al.*, 2005). The occurrence of any individual in certain time on exact location is a result of a myriad processes acting on different time scales, stochastic or deterministic, driven by both physical environment and biotic interactions.

Plant distribution in space: from individuals to species ranges

The spatial arrangement of individuals in space can be generally classified as uniform, random, or aggregated (Wiegand & A. Moloney, 2004). However, it is important to define the scale at which is the pattern analyzed: for example trees exhibit aggregated pattern at the landscape scale because they are restricted to forest patches, but they tend to uniform pattern within the forest stand due to competitive exclusion of neighboring trees. From the processes potentially responsible for creation of aggregated patterns I have to mention namely environmental filtering (because most environmental variables are inherently autocorrelated in space), dispersal of diaspores (because diaspores are more likely to travel shorter distances), or disturbances. Less studied - but potentially important – process forcing spatial aggregation of individuals is the facilitation (Callaway, 1995). Contrary, uniform pattern may stem from intraspecific competition, or positive density dependence in seed predation or parasitism (Janzen, 1970). Random pattern may then arise when none of the above mentioned factors acts, or, more likely, when the antagonistic forces are in equilibrium. Study of spatial patterns is data-demanding, as it preferably require continuously mapped individual positions and also computationally-demanding, when pair-distance matrix is used for inference, and therefore most of the studies of point patterns are of limited spatial extent. Even more difficult is identification of causal relationship, for which either temporally replicated studies tracing dispersal and mortality or manipulative experiments, or advanced statistical modelling tools build upon rigorous ecological knowledge are needed (Lepš, 1990; McIntire & Fajardo, 2009). The Janzen-Connell hypothesis links supposed density-dependent seedling mortality, acting against spatial aggregation of conspecific seedling density, to high species richness in tropics. Later research, as reviewed by Comita et al. (2014), confirmed that negative density dependent or distance dependent mortality is prevailing not only in tropics, but also in temperate zone. On

the other hand, Condit et al. (2000) analyzed patterns from six fully mapped large research plots in tropics, and concluded that aggregated pattern is by far the most common case for tropical trees. Such result indicates that dispersal and environmental filtering are still the dominant drivers responsible for spatial patterning of trees, even at small scales. Considerably clustered spatial pattern was found by Wild et al., (2014) for spruce seedlings in disturbed mountain spruce forest, where spruce seedlings were clustered right around tree trunks. The proposed explanation was built upon observation that the spruce seeds disperse mainly during late winter and supposed that they may be redistributed on the snow into melted holes around tree trunks (called 'tree-wells'), which act as a seed trap. In the chapter two of this thesis, we took a closer look on this phenomenon using a temporally replicated sampling design, which allowed us to describe temporal dynamics of forest regeneration and sapling density differentiation on different microhabitats. Here, we identified that seedling mortality is reduced in microhabitats related to deadwood, or in proximity to tree trunks, suggesting that facilitative effects of (already dead) maternal spruce trees are the driving force of aggregated pattern, rather than the seed dispersal. This facilitative mechanism maintains long-term stability of patterns in spruce forests, which can literally survive its own death.

At intermediate scales, patterns in plant population density are typically studied using presence/absence data or cover/biomass estimates per unit area, which are then related to gradients in environmental or biotic conditions. Because it is usually not feasible to obtain spatially continuous estimates of species density, the entire area is sampled by limited set of plots covering only a fraction of the area, typically using transects, stratified- or random sampling design. Such research typically aims to identify conditions preferred by the species (species optima) and relative importance of various environmental correlates structuring the plant communities. As an example of study at intermediate (landscape) scale, I present the published study focusing on temperature control of plant communities in České Středohoří in chapter three.

At the largest scales, the occurrence of a taxon is usually generalized as the total area of species distribution, i.e. by a spatial polygon bounding the whole population (or contiguous area bounding the majority of population) in geographic space, or by the limits of occurrence in ecological space. Because data on species distribution at large scales are usually compiled from multiple sources, lacking standardized sampling density (see Beck *et al.*, 2014), inference of more detailed information about inner spatial structure is rare at large-scaled studies. Knowledge about the range limits of multiple taxa serve as a basis in search of limiting conditions of species distribution with implications for diversity. Geographical range size reflects ecological tolerance of the species, but its realization may be constrained by many confounding effects, including domain boundaries or dispersal limitations. Range size was reported to increase with increasing latitude, aka 'Rapoport's rule', (Rapoport, 1982; Stevens, 1989).

Climate variability hypothesis provide reasonable explanation for this phenomenon – organisms living in higher latitudes have evolved adaptations to deal with seasonal changes in temperatures, which allows them to tolerate broader range of temperatures also along geographical gradient. In analogy to latitudinal ranges, range size was reported to increase also with elevation (Stevens, 1992). In chapters four, five and six, I present large scale studies from Himalaya, Ladakh. At this large scale, we studied distribution of plants along prominent elevational gradient. Thanks to availability of extensive dataset with unified sampling methodology, I was able to quantify not only limits of distribution along elevational gradient, but also the shape of the species response curve. Here, I question validity of elevational Rapoport's rule – broadening of range size with elevation is a mere artefact of domain truncation and it has nothing in common with fundamental niche of the species.

Linking species distribution and environment heterogeneity

Early formalized attempts to link spatial distribution of organisms and its drivers were developed under niche theory framework, originating in work of J. Grinnell and later refined by G. E. Hutchinson (Grinnell, 1917; Hutchinson, 1957; Vandermeer, 1972). Niche theory accentuated importance of abiotic drivers, with fundamental niche defined by range of condition and resources levels under which the species can survive and reproduce and it's realization in physical space to be realized niche. Hutchinson (1957) discussed two causes of discrepancy between fundamental and realized niche: (1) the physical space could be incomplete subset of possible combinations of factor levels creating fundamental niche, and (2) the competition for resources by two species whose niche overlap resulting in competitive exclusion (aka Lotka-Volterra model).

Grounded in the niche theory, the modern numerical ecology developed multiple tools to describe patterns and identify environmental correlates and demographic processes behind actual distribution of organisms, from simple linear regressions to more sophisticated types of regression analysis including generalized linear models (GLM), generalized additive models (GAM), logistic regression models (Huisman *et al.*, 1993) or direct ordination techniques like redundancy analysis (RDA; van den Wollenberg 1977), canonical correspondence analysis (CCA) and related techniques. Knowledge of environmental drivers and ecological processes is than applied in the species distribution modelling (SDM) (Guisan & Zimmermann, 2000; Austin, 2002), which model either current species distribution based on incomplete set of observation, or potential species distribution under various scenarios of environmental change.

The basic assumption of the most models is the shape of the response curve to the underlying environmental factors. It is clear that 'universal' shape of species response doesn't exist, but for practical reasons e.g. model fitting, generalization of the results and their interpretability, the need of defining universal and simple response curve arise (Jansen & Oksanen, 2013). Many well-established modelling techniques used in ecology

implicitly build on assumption of certain type of response shape, most commonly linear dependence (linear regression, RDA) or Gaussian response (CCA). However, linear response is generally recognized as too simplistic, but can be used with caution in case that fitted gradient is short. Unimodal Gaussian response curve was generally accepted by ecologists in the past as the most appropriate, but later it was questioned (Oksanen & Minchin, 2002), because skewed responses were identified to be relatively common (Lawesson & Oksanen, 2002; Normand *et al.*, 2009; Boucher-Lalonde *et al.*, 2012). In chapter four of this thesis, I present study from Himalaya, showing the prevalence of skewed response shapes along elevational gradient. Skewed responses may arise when different processes act of left and right end of the gradient, e.g. increasing asymmetric competition at warm & productive end of distribution (at low elevations) and physiological barrier caused by low-temperatures at high elevations (Normand *et al.*, 2009; Wisz *et al.*, 2013). However, skewed responses were found also in low-productivity ecosystems with limited competitive interactions among species, like in our study from Himalaya, where low elevations are characterized by increasing aridity, with exception of spatially restricted area along glacial streams and artificially irrigated fields (Fig. 1). More complicated shapes, including splines, bimodal shapes or threshold functions are increasingly used in ecological modelling, but fitting of these models require more intensive sampling design and advanced statistical tools (Oksanen & Minchin, 2002; Jansen & Oksanen, 2015; Michaelis & Diekmann, 2017). It is well-known that "all models are wrong, but some are useful" (Box, 1979), in other words, it is impossible to get perfectly realistic model, but we can learn even from more simple models, when we know their limits.

Figure 1 *Asymmetric species response curve realized along elevational gradient may arise in consequence of interaction of the two different stressors: the low temperature stress uniformly affecting high elevations and the increasing aridity, which is acting in lower elevations (with some local exceptions, responsible for the long-tail of the response curve).*

Besides selection of an appropriate statistical model, the selection of relevant environmental variables entering the model is crucial for successful explanation or prediction of species distribution. Ecologists in countless publications identified important environmental drivers based on extensive field experience, manipulative experiments or regression of occurrence data against multiple environmental factors (comprehensive overview of ecological factors shaping Central European vegetation provides Ellenberg (1988)). However, finding the parsimonious drivers of spatial or temporal dynamics is a challenging task, because the number of possible environmental or biotic drivers and their interactions is virtually unlimited, but the most relevant variables are not always readily available for the modelling (Mod *et al.*, 2016; Körner & Hiltbrunner, 2018), and the correlation is not necessarily a sign of causality (Fig. 2).

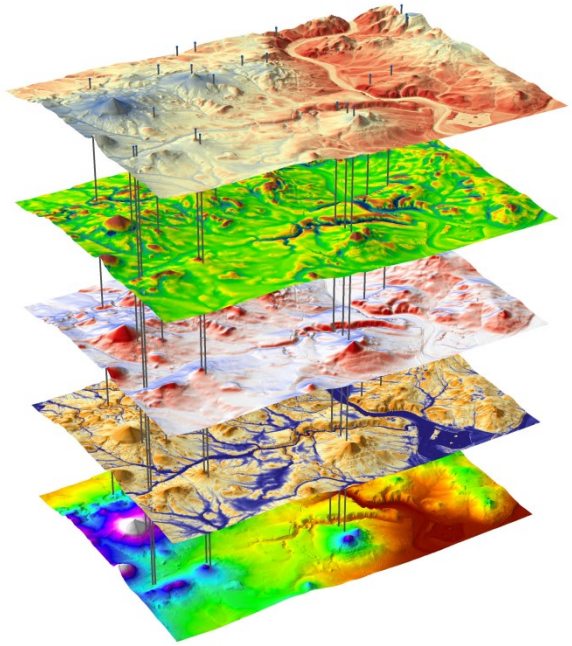

Figure 2 *Environmental heterogeneity of the landscape can be expressed by many ways. Many of them correlate with plant distribution but few of them are the real causal drivers. On the illustrative figure are displayed (from the top): 95th percentile of seasonal maximum temperature, relative topographic position in 250m radius, diurnal anizotropic heating, SAGA wetness index, and elevation for part of study area in České Středohoří (Chapter III).*

Classical regression techniques tend to be sensitive to overfitting and issues caused by collinearity predictors (Guisan *et al.*, 2002). Informed selection of relevant environmental factors entering the model is thus necessary – as Araújo and Guisan (2006) stated: "The use of automated solutions to predictor selection and contribution should not be seen as a substitution for pre-selecting sound ecophysiological predictors based on deep knowledge of the biogeographical and ecological theory". Modern advanced statistical tools using machine-learning like boosted regression trees (BRT, Elith et al. 2008), or maximum entropy modelling (MaxEnt; Phillips et al. 2006) are believed to be less sensitive to limitations of data entering the model (Thibaud *et al.*, 2014) and less attention is also paid to informed pre-selection of environmental variables entering the model (Merow *et al.*, 2013). For instance, the MaxEnt circumvents missing absence data

by producing "pseudo-absences"; the dark side of this approach is that the output provide only relative suitability values, which cannot be scaled to absolute occurrence probability (Guillera-Arroita *et al.*, 2014). Further, even MaxEnt is not immune to overfitting issues, as was documented on species distribution modelling using MaxEnt and set of "pseudo-predictors" (paintings) and a whole set of bioclimatic variables available in Worldclim (Fourcade *et al.*, 2018). This extreme example by Fourcade et al. clearly showed, that fit of the model to the empirical data does not qualify the model for extrapolation and contribute little to understanding of the real drivers.

Is there any rule-of-thumbs for selection of appropriate explanatory variable? Some variables are of universal importance to the whole focal group of organisms, like the light- and water- availability for the autotrophic plants, but some factors are relevant only to specialized species (e.g. specific soil type for substrate specialists). Further, some factors may be relevant only at particular scale, according to inherent spatial or temporal variability of the desired factor and the actual resolution of its map product and resolution of the species data (Wiens, 1989; Bell *et al.*, 1993; Chase & Knight, 2013; Bernhardt-Römermann *et al.*, 2015). At the largest spatial scales is the evolutionary history and macroclimate recognized (Peterson *et al.*, 1999; Colwell & Rangel, 2010; Peters *et al.*, 2016), while at landscape scale are factors like terrain topography, soil properties or land-use history increasingly important (Whittaker *et al.*, 2001; Fraterrigo *et al.*, 2006; Dambrine *et al.*, 2007; Daly *et al.*, 2009; Zellweger *et al.*, 2015). At the finest scales, where position of single individual is recognized, are the biotic interactions, i.e. facilitation and competition, increasingly important (for examples see Herben et al. 1993, Callaway 1995, Le Roux et al. 2013, Wild et al. 2014, Dolezal et al. 2019a)[2]. Stochasticity, including random disturbances or random dispersal, is relatively large at this scale, but it is believed to have deeper consequences, than only puzzling the ecologists: the effect of fine-scale stochasticity propagate to higher spatial scales, and provide possible explanation to the question: "How can so many plant species, competing for the same resources (the light and water), coexist?" (Shmida & Ellner, 1984; Chesson, 2000).

The climate is generally recognized as the universal driver of species distribution and species richness at broad scales. Even though, little consistency in ecological studies can be found in which climatic parameters they use (Körner & Hiltbrunner, 2018; Gardner *et al.*, 2019). Specifically, indices related to water balance, or water-energy (actual evapotranspiration and water deficit) were recognized to be highly relevant for plants (Mather & Yoshioka, 1968; Stephenson, 1998; Hawkins *et al.*, 2003; Carpenter, 2005), but we can find studies using many other climatic indices, e.g. mean annual temperature, mean growing season temperature, growing season length, maximum

[2] There are many other studies, which are worth mentioning in this thesis, hereafter I preferentially select studies from related study systems and the studies which I personally participated.

temperature in growing season, temperature seasonality, total annual precipitation, soil water content (Jiménez-Alfaro *et al.*, 2018; Gardner *et al.*, 2019). Such inconsistency may be caused by different context of the studies, i.e. spatial extent, geographic area, studied species groups; but it may stem also from arbitrary decisions of the investigators.

Currently, bioclimatic variables from WorldClim grids (Hijmans *et al.*, 2005; Fick & Hijmans, 2017), available globally with spatial resolution of 30 arc sec (ca 1x1 km pixel), are widely used for ecological modelling. Despite the scale of these grids seems to be relatively fine, it may not reflect whole variability present at this scale. These maps are based on weather station data, most of which measure climatic conditions under standardized conditions – thermometers are placed in Stevenson screen on flat place not shaded by trees or other physical objects. Therefore, topographic effects like different exposure to solar radiation caused by slope aspect or effects of forest canopy on microclimates are not covered in the WorldClim or any other climate map based on interpolations of standard weather station data (De Frenne & Verheyen, 2016). Including topographic, and vegetation cover effects into fine-scaled climatic maps would make the species distribution modelling and predictions of climate change impacts on biodiversity more realistic (Bramer *et al.*, 2018; Maclean, 2019). To investigate, if these so-called fine-scaled climatic grids are sufficient for modelling of forest plant communities on the landscape scale, I designed the study using in-situ measured temperatures and spatially modelled topoclimate maps derived from digital elevation model with very fine (5x5m) resolution. This study revealed that substantial part of temperature variability within the landscape is driven by factors not accounted for by WorldClim climate grids and that maximum temperature is better predictor of forest plant communities than mean and minimum temperatures. These results counterpoint the importance of climatic extremes and provide a clue for assessment of the climate change impacts on forest understory.

Insufficient knowledge of the ecological mechanisms and the spatial and temporal scales at which they act, cause serious mismatch between our expectations how the ecosystems should react to environmental change, and the reality. As an example, I show the story of climate change impacts on forest plants distribution: Once it became evident, that global temperature had risen, ecologists started to search for evidence if the elevated temperature is reflected in species distribution. Upward and poleward shifts of range limits were expected, with a magnitude corresponding to the observed change in average temperature (Rosenzweig *et al.*, 2008). Such upward shifts, congruent with expectations (i.e. expected vertical shift calculated as temperature warming rate between surveys divided by an adiabatic temperature lapse rate), were documented by multiple studies in mountain/alpine vegetation (Lenoir *et al.*, 2008; Parolo & Rossi, 2008; Morueta-Holme *et al.*, 2015). Strikingly, forest communities showed a weak response or even response in an opposite direction than expected (Bertrand *et al.*, 2011; Rabasa *et al.*, 2013). Since then, ecologists seek for plausible explanation, why response

of forest plants to warming lags behind warming rates. Forest microclimate seems to be on the top of the list of suspects (De Frenne *et al.*, 2013, 2019; Zellweger *et al.*, 2019). Average temperatures are weakly influenced by forest canopy, which rather buffer the extremes (Geiger *et al.*, 2009; De Frenne *et al.*, 2019; Macek *et al.*, 2019; Zellweger *et al.*, 2019). If this is true, than weakening of climate-warming signal in the forests cannot be attributed to the mean temperatures, but more likely is caused by the buffered high temperature extremes. Moreover, the narrative of range shifts driven unequivocally by temperature was questioned, as interactions with light availability (De Frenne *et al.*, 2015), water-availability (Crimmins *et al.*, 2011) or land-use legacies (Rumpf *et al.*, 2018) affected resulting impact on plant communities (see also Parmesan and Hanley 2015). In case of long-living trees, the unexpected elevational shifts were estimated from differences in distribution of adult trees and tree saplings/seedlings (Rabasa *et al.*, 2013). This approach was later criticized, because differences between density of adult trees and saplings may reflect other factors than the temperature at the year of germination (Máliš *et al.*, 2016). This short example demonstrates, how seemingly straightforward expectation can be in reality biased, if predictors used for modelling are not on the appropriate spatial scale (fine-scaled microclimate vs. coarse-grain macroclimate), temporal scale (considering the life-span of the studied organism), and if proper variables are not selected (average temperature vs. maximum temperature). The complexity of forest microclimate across the landscape and its relevance for understory plants is in detail presented in the third chapter of the thesis.

Species diversity

Measures of species diversity integrate numbers (or abundances) of species belonging to pre-defined species group occurring together at certain area and time (alpha & gamma diversity), or compare differences in species numbers between these samples (beta diversity). What makes the difference between alpha and gamma diversity is the scale: the plot size used by vegetation scientists for alpha diversity evaluation is conventionally ≤ 1000m² (Chytrý & Otýpková, 2003) while the gamma diversity is calculated for larger area, with upper bound at to the total terrestrial area worldwide of nearly 150 million km² hosting ca 300,000 vascular plant species (estimates still differ, see Chapman (2009)). The most intuitive measure of diversity, the species richness, is the summation of individual species present in the sample. Because plants share same fundamental resources for their growth, one would expect similar drivers to be shaping species richness as are the drivers of species spatial distribution. In analogy, species richness is regulated by a hierarchy of drivers acting on different spatial and temporal scales (Clark *et al.*, 2011; Bernhardt-Römermann *et al.*, 2015): broad climatic gradients and evolutionary history acting at the coarsest scales (Mutke & Barthlott, 2005), environmental heterogeneity related to topography and substrate quality at landscape scales (Chytrý *et al.*, 2003; Bruun *et al.*, 2006; Zelený *et al.*, 2010; Lippok *et al.*, 2014) and

biotic interactions and environmental filtering at fine scales (Burton *et al.*, 2011; Chytrý *et al.*, 2015).

After a century of ecological research, we are still missing consensus, which drivers of diversity are the most relevant at each scale (Stevens & Carson, 2002; Michalet *et al.*, 2006; Šímová *et al.*, 2011; Chase & Knight, 2013). Among top explanatory drivers for diversity gradients remains diversity-productivity relationship. Nevertheless, even this relation is scale-dependent, switching from unimodal or even negative at small scales to positive at broad scales (Waide *et al.*, 1999; Whittaker *et al.*, 2001; Rahbek, 2005). This irregularity is caused by interplay of the total species pool and limited number of individuals in a plot at finer scales, controlled by competitive exclusion or productivity per se (Zobel, 1997; Zobel & Pärtel, 2008; Grace *et al.*, 2011). Positive relation dominates at global scales (Waide *et al.*, 1999), but in contradiction to this, many studies on elevational richness gradients found richness peak in middle elevations. Proposed explanation include random arrangement of species ranges within the elevational domain (aka "mid-domain effect", Colwell & Hurtt, 1994; Colwell & Lees, 2000), land-area effects, habitat heterogeneity, or biotic effects like source-sink dynamics (Grytnes, 2003; Grytnes & McCain, 2007). Discussion on the role of neutral processes on formation of spatial patterns of species richness, opened by S. Hubbell (2001) and R. Colwell (Colwell & Hurtt, 1994; Colwell & Lees, 2000) still continues, without a clear solution. Neutral processes can theoretically produce similar patterns to empirical ones, but environmental and biotic drivers cannot be ignored (Colwell *et al.*, 2004, 2016; Zapata *et al.*, 2005; McGill *et al.*, 2006; Adler *et al.*, 2007; Rosindell *et al.*, 2011). Actually, the search for universal explanation of diversity gradients assumes existence of such driver. There are, undoubtedly, some shared limits, like thermal tolerances (Körner & Paulsen, 2004; Clarke, 2014) or shared resources (i.e. light, water, or CO_2 for plants), but individual species differ in the strategy, how to utilize the resources and how to deal with environmental stress. Therefore, the vision of the universal model of diversity may be illusory. Further, the observed diversity patterns are subject to different sources of bias, from observer errors (Lepš & Hadincová, 1992; Kopecký & Macek, 2015; Verheyen *et al.*, 2018) to artefacts caused by differences in sampling intensity (Chao *et al.*, 2014) to methodological artefacts caused by the statistics used to aggregate species occurrence data into diversity measures (Grytnes & Vetaas, 2002; Šizling *et al.*, 2009). Random bias can be averaged-out with sufficient number of replicates, but systematic bias can seriously affect interpretation of the results. A hot debate about apparent mid-domain diversity is the exemplary case: elevational diversity estimates are subject to both sampling bias and statistical artefacts (Colwell & Hurtt, 1994; Colwell & Lees, 2000; Grytnes, 2003; Colwell *et al.*, 2004; Šizling *et al.*, 2009). Study presented in the chapter six of this thesis shed a light on this topic, accounting for possible biases using null-modelling, sampling intensity corrections (Chao *et al.*, 2014), land area corrections and a brand-new mid-point attractor models (Colwell *et al.*, 2016). Here, we found that

unimodal richness gradient is pervasive when corrected for sampling bias, but on the other hand, it can be produced by random sampling from truncated Gaussian distribution of midpoints, suggesting monotonous decline of environmental favourability within the domain of our study. This bridge the gap between our expectations on the productivity-diversity gradient and empirical evidence realized in the field.

Main results

To conclude, relative importance of ecological drivers of plant distribution vary across the scales as these factors display different levels of spatial heterogeneity according to the scale and extent of the study. I assume, that this is not only the artefact of methodology, e.g. the effect of insufficient resolution of environmental grid used in the study (Hengl, 2006), but that this is real phenomenon, conditioned by the nature of environmental heterogeneity. Biotic interactions are most relevant at small spatial scales, where the physical interference between organisms take place, although the effects may propagate at higher spatial scales at long term perspective. In my study on Norway spruce regeneration following bark-beetle outbreak, I identified that facilitative effects of former canopy trees are responsible for spatial aggregation of seedlings during early stand development.

At a landscape scale I focused on climatic heterogeneity modulated by topography and its relevance for plant distribution. Using in-situ measured climatic variables, I found that spatial variability of forest understory plant communities is coupled namely with spatial variability in maximum temperatures. I linked spatial variability in temperatures to topography and used fine-scaled prediction of temperatures for validation on independent set of plant distribution data. This validation proved applicability of my results.

At a country scale, where I touched the fundaments of macroecological theory, I challenged plausibility of several deep-rooted hypotheses, showed that some models are really useful, and I conclude that climate and species identity matters, but neutral drivers are integral part of the story, too. What we can learn from the plant distribution patterns in Himalaya, is that symmetrical Gaussian shape is definitely not very common, so-called 'Rapoport rule' is a pure artefact here, caused by geographic range truncation and that mid-point attractor model can be useful, when interpreted carefully.

1.1 SUMMARY OF THE THESIS AND AUTHOR CONTRIBUTIONS

In this thesis, I aimed to identify factors shaping plant distribution at different spatial scales, link them to causal processes and test general hypothesis on the nature of response curve shapes and species richness patterns. General review of the topic is introduced in the first chapter, followed by five chapters presenting three published studies and two manuscripts.

Studies which I have selected for the thesis deal with plant distribution driven by environmental heterogeneity acting over across several order of magnitude of spatial resolution – from the very local scale (meters; *Paper I*), through the landscape scale (hundreds sq. km; *Paper II*) to the country scale (tens of thousands sq. km; *Papers III; IV; & V*). Research questions and methodology differs accordingly to the scale of the study: from tracking individual seedling's growth and mortality in order to reveal processes responsible for creation of clumped spatial structures in mountain spruce forest, through attributing forest understory community composition to in-situ measured climate, up to 'shuffling' of the whole local flora of Ladakh, complemented with range limits from outside of the study region.

PAPER I *(chapter two)*

Macek, M., Wild, J., Kopecký, M., Červenka, J., Svoboda, M., Zenáhlíková, J., Brůna, J., Mosandl, R., and Fischer, A. 2017. Life and death of *Picea abies* after bark-beetle outbreak: ecological processes driving seedling recruitment. *Ecological Applications* 27:156–167.

MM, JW, MK, MS and AF conceived ideas; AF, RM and Maria Bauer designed and established permanent plots in 1998; MM, JW, MK, JČ, JZ and JB collected field data in 2010 survey; MM analyzed the data; all authors contributed to writing and editing led by MM.

Interesting spatial structures in plant distribution can be found even at the finest scales. In the detailed study, tracing the fate of individual Norway spruce seedlings, we identified processes responsible for creation of clumped spatial pattern of spruce regeneration following the bark beetle outbreak, which was described in previous work of Wild et al. (2014), but the explanation for observed pattern was only speculative. At this scale, competition was the starring actor, but even microclimate variability remained between main suspects. Mortality rates differed between microhabitats, which resulted to highly uneven densities of surviving saplings after a decade since canopy disturbance. It is worth saying that this study was designed hierarchically to capture the variability at the scale of meters, as well as the variability at the landscape scale, where altitudinal gradient turned to be fairly important, but its effect was mediated through seed productivity or germination rate rather than through consecutive seedling mortality.

PAPER II *(chapter three)*

Macek, M., Kopecký, M., and Wild, J. 2019. Maximum air temperature controlled by terrain topography shapes forest plant distribution. *Landscape Ecology* 34:2541-2556.

All authors conceived ideas and experimental design and contributed to text writing and editing. MM coordinated field data collection, analyzed data and led writing.

The landscape-scale study from České Středohoří presented in Paper II dealt with relatively short climatic gradients, because underlying altitudinal gradient spanned only over several hundred vertical meters. Therefore, such data were not suitable for testing the shapes of the response curves, but on the other hand we were able to better delineate effects of climate components and the role of topographic heterogeneity at this scale. We used in-situ measured temperatures and spatial modelling techniques to find biologically most relevant component of forest microclimate at the landscape scale. Maximum temperature turned out to be most influential driver of vegetation dynamics. Maximum temperature exhibited also highest spatial variability conditioned by terrain topography. We demonstrated limitations of input data quality used for ecological modelling by comparing predictive power of fine-scaled topoclimatic grids to coarser climatic grids from Worldclim 2 (Fick & Hijmans, 2017).

PAPER III *(chapter four)*

Dvorský, M., Macek, M., Kopecký, M., Wild, J., and Doležal, J. 2017. Niche asymmetry of vascular plants increases with elevation. *Journal of Biogeography* 44:1418–1425.

All authors conceived the ideas and contributed to text writing and editing led by MD; MM analysed the data. Species occurence data are based on late L. Klimeš botanical surveys. Climate data were collected by MM, JW, MK and JD.

On the country scale, represented by the study from Himalaya (Ladakh region, India), the whole species distribution range along 3,500 m long altitudinal gradient was covered for substantial part of the flora. Luckily, species occurrence data collected by late Leoš Klimeš were sampled systematically using complete floristic inventory for ca 4000 sites (1ha each), providing also true absences needed for logistic regression. This allowed us to quantify response curve shapes, and test the predictions of "asymmetric abiotic stress limitation" hypothesis (Normand *et al.*, 2009). We found asymmetric response shapes to be were quite common, particularly the left-skewed response on elevation gradient, which were found for more than one third of evaluated species. Moreover, the proportion of plants with left skewed response increased with elevation. We interpret this finding as evidence of higher importance of cold temperatures, or short vegetation season, as range limit determinant compared to drought limitation in lower elevations.

PAPER IV *(chapter five)*

Dvorský, M., Macek, M., Kopecký, M., Wild, J., and Doležal, J. (manuscript) Geometric constraints explain elevational range size patterns of vascular plants in Himalaya.

All authors concieved ideas and contributed to writing and editing led by MD. MD compiled plant traits and ranges from literature, MM and JW prepared data for analyses. MM analysed the data, MK and JW consulted design of statistical analyses. Species occurence data were compiled from L. Klimeš botanical surveys (1998-2006) and surveys led by JD and participated by all authors (2008-2015).

Alongside with shape of the response curve, we tested distribution of absolute range sizes along elevational gradient in Himalaya, in order to test predictions of Rapoport's' elevational rule (Stevens, 1992). We employed null modelling approach, to separate non-biological gradients in range size distributions, which resulted in surprising results: the pattern we observed was a pure artefact caused by range truncation by geographic extent of our study. To conclude, we found no support for Rapoport's elevational rule. We also established extensive network of microclimate data loggers and expressed climatic variability to test assumptions of Climate Variability Hypothesis (Janzen, 1967). We conclude that climate variability doesn't increase with elevation in our study area, and therefore basic assumptions of the Climate Variability Hypothesis were not fulfilled.

PAPER V (*chapter six*)

Macek, M., Dvorský, M., Klimeš, A., Wild, J., Doležal, J., and Kopecký, M. (manuscript) Mid-point attractor models of plant species richness along elevational gradient reveal monotonically decreasing climatic favourability shaped by geometric constraints

MM, MD, MK, JW and JD concieved ideas, MD compiled plant traits and ranges from literature, MM prepared data for analyses. Species occurence data were compiled from L. Klimeš botanical surveys (1998-2006) and surveys led by JD and participated by all authors (2008-2015). MM and AK analysed the data, all authors contributed to text writing led by MM.

Species diversity peaking in middle altitudes was reported for various species groups and geographical areas; hot debate about causes of this phenomenon was initiated by the paper by Robert Colwell, attributing the creation of such pattern to biologically neutral processes (aka "mid-domain effect"; Colwell and Hurtt 1994). In his later work, Colwell presented mid-point attractor model, which introduce Gaussian mid-point attractor, compromising between neutral processes and true ecological drivers of diversity (Colwell *et al.*, 2016). Here, we tested consent between proposed null models for elevational species richness and observations from W Himalaya, Ladakh region. We also examined in detail differences between species groups defined by their biogeographical affinity, taxonomic ranking and life form. Our results confirmed usefulness of mid-point attractor model and indicated that species richness pattern is clearly driven by climate and can be decomposed to according to differences between species groups. Nevertheless, observed hump-shaped pattern is accentuated by the

sampling bias, which may be the dominant cause of apparent mid-domain peak in diversity in case of studies based on less intensive sampling.

1.2 REFERENCES

Adler, P.B., Hillerislambers, J. & Levine, J.M. (2007) A niche for neutrality. *Ecology letters*, **10**, 95–104.

Araújo, M.B. & Guisan, A. (2006) Five (or so) challenges for species distribution modelling. *Journal of Biogeography*, **33**, 1677–1688.

Ashcroft, M.B., Cavanagh, M., Eldridge, M.D.B. & Gollan, J.R. (2014) Testing the ability of topoclimatic grids of extreme temperatures to explain the distribution of the endangered brush-tailed rock-wallaby (Petrogale penicillata). *Journal of Biogeography*, **41**, 1402–1413.

Ashcroft, M.B., Chisholm, L.A. & French, K.O. (2008) The effect of exposure on landscape scale soil surface temperatures and species distribution models. *Landscape Ecology*, **23**, 211–225.

Austin, M. (2002) Spatial prediction of species distribution: an interface between ecological theory and statistical modelling. *Ecological Modelling*, **157**, 101–118.

Beck, J., Böller, M., Erhardt, A. & Schwanghart, W. (2014) Spatial bias in the GBIF database and its effect on modeling species' geographic distributions. *Ecological Informatics*, **19**, 10–15.

Bell, G., Lechowicz, M., Appenzeller, A., Chandler, M., DeBlois, E., Jackson, L., Mackenzie, B., Preziosi, R., Schallenberg, M. & Tinker, N. (1993) The spatial structure of the physical environment. *Oecologia*, **96**, 114–121.

Bernhardt-Römermann, M., Baeten, L., Craven, D., De Frenne, P., Hédl, R., Lenoir, J., Bert, D., Brunet, J., Chudomelová, M., Decocq, G., Dierschke, H., Dirnböck, T., Dörfler, I., Heinken, T., Hermy, M., Hommel, P., Jaroszewicz, B., Keczyński, A., Kelly, D.L., Kirby, K.J., Kopecký, M., Macek, M., Máliš, F., Mirtl, M., Mitchell, F.J.G., Naaf, T., Newman, M., Peterken, G., Petřík, P., Schmidt, W., Standovár, T., Tóth, Z., Calster, H. Van, Verstraeten, G., Vladovič, J., Vild, O., Wulf, M. & Verheyen, K. (2015) Drivers of temporal changes in temperate forest plant diversity vary across spatial scales. *Global Change Biology*, **21**, 3726–3737.

Bertrand, R., Lenoir, J., Piedallu, C., Riofrío-Dillon, G., de Ruffray, P., Vidal, C., Pierrat, J.-C. & Gégout, J.-C. (2011) Changes in plant community composition lag behind climate warming in lowland forests. *Nature*, **479**, 517–520.

Böhner, J. & Antonić, O. (2009) *Land-surface parameters specific to topo-climatology*. *Geomorphometry: concepts, software, applications* (ed. by T. Hengl) and H.U. Reuter), pp. 195–226. Elsevier, Amsterdam.

Böhner, J. & Selige, T. (2006) Spatial prediction of soil attributes using terrain analysis and climate regionalisation. *SAGA - Analyses and Modelling Applications: Göttinger Geographische Abhandlungen*, **115**, 13–28.

Boucher-Lalonde, V., Morin, A. & Currie, D.J. (2012) How are tree species distributed in climatic space? A simple and general pattern. *Global Ecology and Biogeography*, **21**, 1157–1166.

Box, G.E.P. (1979) *Robustness in the strategy of scientific model building*. *Robustness i n Statistics* (ed. by R.L. Launer) and G.N. Wilkinson), pp. 201–236. Academic Press, INC.

Bramer, I., Anderson, B.J., Bennie, J., Bladon, A.J., De Frenne, P., Hemming, D., Hill, R.A., Kearney, M.R., Körner, C., Korstjens, A.H., Lenoir, J., Maclean, I.M.D., Marsh, C.D., Morecroft, M.D., Ohlemüller, R., Slater, H.D., Suggitt, A.J., Zellweger, F. & Gillingham, P.K. (2018) Advances in Monitoring and Modelling Climate at Ecologically Relevant Scales. *Advances in Ecological Research*, **58**, 101–161.

Bruun, H.H., Moen, J., Virtanen, R., Grytnes, J.-A., Oksanen, L. & Angerbjörn, A. (2006) Effects of altitude and topography on species richness of vascular plants, bryophytes and lichens in alpine communities. *Journal of Vegetation Science*, **17**, 37–46.

Burton, J.I., Mladenoff, D.J., Clayton, M.K. & Forrester, J. a. (2011) The roles of environmental filtering and colonization in the fine-scale spatial patterning of ground-layer plant communities in north temperate deciduous forests. *Journal of Ecology*, **99**, 764–776.

Callaway, R.M. (1995) Positive Interactions among Plants. *Botanical Review*, **61**, 306–349.

Carpenter, C. (2005) The environmental control of plant species density on a Himalayan elevation gradient. *Journal of Biogeography*, **32**, 999–1018.

Chao, A., Gotelli, N.J., Hsieh, T.C., Sander, E.L., Ma, K.H., Colwell, R.K. & Ellison, A.M. (2014) Rarefaction and extrapolation with Hill numbers: A framework for sampling and estimation in species diversity studies. *Ecological Monographs*, **84**, 45–67.

Chapman, A.D. (2009) Numbers of Living Species in Australia and the World. **2nd**, 84.

Chase, J.M. & Knight, T.M. (2013) Scale-dependent effect sizes of ecological drivers on biodiversity: Why standardised sampling is not enough. *Ecology Letters*, **16**, 17–26.

Chesson, P. (2000) Mechanisms of Maintenance of Species Diversity. *Annual Rewiew of Ecology and Systematics*, **31**, 343–358.

Chytrý, M., Dražil, T., Hájek, M., Kalníková, V., Preislerová, Z., Šibík, J., Ujházy, K., Axmanová, I., Bernátová, D., Blanár, D., Dančák, M., Dřevojan, P., Fajmon, K., Galvánek, D., Hájková, P., Herben, T., Hrivnák, R., Janeček, Š., Janišová, M., Jiráská, Š., Kliment, J., Kochjarová, J., Lepš, J., Leskovjanská, A., Merunková, K., Mládek, J., Slezák, M., Šeffer, J., Šefferová, V., Škodová, I., Uhlířová, J., Ujházyová, M. & Vymazalová, M. (2015) The most species-rich plant communities in the Czech Republic and Slovakia (with new world records). *Preslia*, **87**, 217–278.

Chytrý, M. & Otýpková, Z. (2003) Plot sizes used for phytosociological sampling of European vegetation. *Journal of Vegetation Science*, **14**, 563–570.

Chytrý, M., Tichý, L. & Roleček, J. (2003) Local and regional patterns of species richness in Central European vegetation types along the pH/calcium gradient. *Folia Geobotanica*, **38**, 429–442.

Clark, J.S., Bell, D.M., Hersh, M.H., Kwit, M.C., Moran, E., Salk, C., Stine, A., Valle, D. & Zhu, K. (2011) Individual-scale variation, species-scale differences: inference needed to understand diversity. *Ecology letters*, 1273–1287.

Clarke, A. (2014) The thermal limits to life on Earth. *International Journal of Astrobiology*, **13**, 141–154.

Colwell, R.K., Gotelli, N.J., Ashton, L.A., Beck, J., Brehm, G., Fayle, T.M., Fiedler, K., Forister, M.L., Kessler, M., Kitching, R.L., Klimes, P., Kluge, J., Longino, J.T., Maunsell, S.C., McCain, C.M., Moses, J., Noben, S., Sam, K., Sam, L., Shapiro, A.M., Wang, X. & Novotny, V. (2016) Midpoint attractors and species richness: Modelling the interaction between environmental drivers and geometric constraints. *Ecology Letters*, **19**, 1009–1022.

Colwell, R.K. & Hurtt, G.C. (1994) Nonbiological gradients in species richness and a spurious Rapoport effect. *The American Naturalist*, **144**, 570–595.

Colwell, R.K. & Lees, D.C. (2000) The mid-domain effect: geometric species richness. *Trends Ecol. Evol.*, **15**, 70–76.

Colwell, R.K., Rahbek, C. & Gotelli, N.J. (2004) The mid-domain effect and species richness patterns:what have we learned so far? *The American naturalist*, **163**.

Colwell, R.K. & Rangel, T.F. (2010) A stochastic, evolutionary model for range shifts and richness on tropical elevational gradients under Quaternary glacial cycles. *Philosophical Transactions of the Royal Society B: Biological Sciences*, **365**, 3695–3707.

Comita, L.S., Queenborough, S.A., Murphy, S.J., Eck, J.L., Xu, K., Krishnadas, M., Beckman, N. & Zhu, Y. (2014) Testing predictions of the Janzen-Connell hypothesis: A meta-analysis of experimental evidence for distance- and density-dependent seed and seedling survival. *Journal of Ecology*, **102**, 845–856.

Condit, R., Ashton, P.S., Baker, P., Bunyavejchewin, S., Gunatilleke, S., Gunatilleke, N., Hubbell, S.P., Foster, R.B., Itoh, A., LaFrankie, J. V., Lee, H.S., Losos, E., Manokaram, N., Sukumar, R. & Yamakura, T. (2000) Spatial Patterns in the Distribution of Tropical Tree Species. *Science*, **288**, 1414–1418.

Conrad, O., Bechtel, B., Bock, M., Dietrich, H., Fischer, E., Gerlitz, L., Wehberg, J., Wichmann, V. & Böhner, J. (2015) System for Automated Geoscientific Analyses (SAGA) v. 2.1.4. *Geoscientific Model Development*, **8**, 1991–2007.

Crimmins, S.M., Dobrowski, S.Z., Greenberg, J.A., Abatzoglou, J.T. & Mynsberge, A.R. (2011) Changes in climatic water balance drive downhill shifts in plant species' optimum elevations. *Science*, **331**, 324–327.

Daly, C., Conklin, D.R. & Unsworth, M.H. (2009) Local atmospheric decoupling in complex topography alters climate change impacts. *International Journal of Climatology*, **9999**, n/a.

Dambrine, E., Dupouey, J.L., Laüt, L., Humbert, L., Thinon, M., Beaufils, T. & Richard, H. (2007) Present forest biodiversity patterns in France related to former Roman agriculture. *Ecology*, **88**, 1430–1439.

Dolezal, J., Dvorsky, M., Kopecky, M., Altman, J., Mudrak, O., Capkova, K., Rehakova, K., Macek, M. & Liancourt, P. (2019) Functionally distinct assembly of vascular plants colonizing alpine cushions suggests their vulnerability to climate change. *Annals of Botany*, **123**, 569–578.

Elith, J., Leathwick, J.R. & Hastie, T. (2008) A working guide to boosted regression trees. *Journal of Animal Ecology*, **77**, 802–813.

Ellenberg, H. (1988) *Vegetation ecology of Central Europe*, Cambridge University Press.

Fick, S.E. & Hijmans, R.J. (2017) WorldClim 2: new 1-km spatial resolution climate surfaces for global land areas. *International Journal of Climatology*, **37**, 4302–4315.

Fourcade, Y., Besnard, A.G. & Secondi, J. (2018) Paintings predict the distribution of species, or the challenge of selecting environmental predictors and evaluation statistics. *Global Ecology and Biogeography*, **27**, 245–256.

Fraterrigo, J.M., Turner, M.G. & Pearson, S.M. (2006) Interactions between past land use, life-history traits and understory spatial heterogeneity. *Landscape Ecology*, **21**, 777–790.

De Frenne, P., Rodriguez-Sanchez, F., Coomes, D.A., Baeten, L., Verstraeten, G., Vellend, M., Bernhardt-Romermann, M., Brown, C.D., Brunet, J., Cornelis, J., Decocq, G.M., Dierschke, H., Eriksson, O., Gilliam, F.S., Hedl, R., Heinken, T., Hermy, M., Hommel, P., Jenkins, M. a, Kelly, D.L., Kirby, K.J., Mitchell, F.J.G., Naaf, T., Newman, M., Peterken, G., Petrik, P., Schultz, J., Sonnier, G., Van Calster, H., Waller, D.M., Walther, G.-R., White, P.S., Woods, K.D., Wulf, M., Graae, B.J. & Verheyen, K. (2013) Microclimate moderates plant responses to macroclimate warming. *Proceedings of the National Academy of Sciences*, **110**, 18561–18565.

De Frenne, P., Rodríguez-Sánchez, F., De Schrijver, A., Coomes, D. a., Hermy, M., Vangansbeke, P. & Verheyen, K. (2015) Light accelerates plant responses to warming. *Nature Plants*, **1**, 15110.

De Frenne, P. & Verheyen, K. (2016) Weather stations lack forest data. *Science*, **351**, 234–234.

De Frenne, P., Zellweger, F., Rodríguez-Sánchez, F., Scheffers, B.R., Hylander, K., Luoto, M., Vellend, M., Verheyen, K. & Lenoir, J. (2019) Global buffering of temperatures under forest canopies. *Nature Ecology & Evolution*.

Gardner, A.S., Maclean, I.M.D. & Gaston, K.J. (2019) Climatic predictors of species distributions neglect biophysiologically meaningful variables. *Diversity and Distributions*, 1–16.

Geiger, R., Aron, R. & Todhunter, P. (2009) *The climate near the ground, 7th ed.*, Rowman & Littlefield.

Grace, J.B., Harrison, S. & Damschen, E.I. (2011) Local richness along gradients in the Siskiyou herb flora: R. H. Whittaker revisited. *Ecology*, **92**, 108–120.

Grinnell, J. (1917) The niche-relationships of the California thrasher. *The Auk*, **34**, 427–433.

Grytnes, J.-A. & McCain, C.M. (2007) Elevational trends in biodiversity. *Encyclopedia of Biodiversity*, **5**, 1–8.

Grytnes, J.A. (2003) Ecological interpretations of the mid-domain effect. *Ecology Letters*, **6**, 883–888.

Grytnes, J.A. & Vetaas, O.R. (2002) Species richness and altitude: A comparison between null models and interpolated plant species richness along the Himalayan altitudinal gradient, Nepal. *The American Naturalist*, **159**, 294–304.

Guillera-Arroita, G., Lahoz-Monfort, J.J. & Elith, J. (2014) Maxent is not a presence-absence method: A comment on Thibaud et al. *Methods in Ecology and Evolution*, **5**, 1192–1197.

Guisan, a, Edwards, T. & Hastie, T. (2002) Generalized linear and generalized additive models in studies of species distributions: setting the scene. *Ecological Modelling*, **157**, 89–100.

Guisan, A., Weiss, S.B. & Weiss, A.D. (1999) GLM versus CCA spatial modeling of plant species distribution. *Plant Ecology*, **143**, 107–122.

Guisan, A. & Zimmermann, N.E. (2000) Predictive habitat distribution models in ecology. *Ecological Modelling*, **135**, 147–186.

Hawkins, B.A., Field, R., Cornell, H. V., Currie, D.J., Guégan, J.-F., Kaufman, D.M., Kerr, J.T., Mittelbach, G.G., Oberdorff, T., O'Brien, E.M., Porter, E.E. & Turner, J.R.G. (2003) Energy, water, and broad-scale geographic patterns of species richness. *Ecology*, **84**, 3105–3117.

Hengl, T. (2006) Finding the right pixel size. *Computers & Geosciences*, **32**, 1283–1298.

Herben, T., Krahulec, F., Hadincová, V. & Kováf ova, M. (1993) Small-scale spatial dynamics of plant species in a grassland community over six years. *Journal of Vegetation Science*, **4**, 171–178.

Hijmans, R.J., Cameron, S.E., Parra, J.L., Jones, P.G. & Jarvis, A. (2005) Very high resolution interpolated climate surfaces for global land areas. *International Journal of Climatology*, **25**, 1965–1978.

Hubbell, S.P. (2001) *The Unified Neutral Theory of Biodiversity and Biogeography*, Princeton University Press, Princeton, NJ, US.

Huisman, J., Olff, H. & Fresco, L.F.M. (1993) A hierarchical set of models for species response analysis. *Journal of Vegetation Science*, **4**, 37–46.

Hutchinson, G.E. (1957) Concluding Remarks. *Cold Spring Harbor Symposia on Quantitative Biology*, **22**, 415–427.

Jansen, F. & Oksanen, J. (2015) Extended hierarchical logistic regression (Huisman-Olff-Fresco) model. *Journal of Vegetation Science*, **24**.

Jansen, F. & Oksanen, J. (2013) How to model species responses along ecological gradients - Huisman-Olff-Fresco models revisited. *Journal of Vegetation Science*, **24**, 1108–1117.

Janzen, D.H. (1970) Herbivores and the Number of Tree Species in Tropical Forests. *The American Naturalist*, **104**, 501–528.

Janzen, D.H. (1967) Why mountain passes are higher in the tropics. *The American Naturalist*, **101**, 233–249.

Jiménez-Alfaro, B., Suárez-Seoane, S., Chytrý, M., Hennekens, S.M., Willner, W., Hájek, M., Agrillo, E., Álvarez-Martínez, J.M., Bergamini, A., Brisse, H., Brunet, J., Casella, L., Dítě, D., Font, X., Gillet, F., Hájková, P., Jansen, F., Jandt, U., Kącki, Z., Lenoir, J., Rodwell, J.S., Schaminée, J.H.J., Sekulová, L., Šibík, J., Škvorc, Ž. & Tsiripidis, I. (2018) Modelling the distribution and compositional variation of plant communities at the continental scale. *Diversity and Distributions*, 1–13.

Jucker, T., Hardwick, S.R., Both, S., Elias, D.M.O., Ewers, R.M., Milodowski, D.T., Swinfield, T. & Coomes, D.A. (2018) Canopy structure and topography jointly constrain the microclimate of human-modified tropical landscapes. *Global Change Biology*, **24**, 5243–5258.

Kier, G., Mutke, J., Dinerstein, E., Ricketts, T.H., Küper, W., Kreft, H. & Barthlott, W. (2005) Global patterns of plant diversity and floristic knowledge. *Journal of Biogeography*, **32**, 1107–1116.

Kilibarda, M., Hengl, T., Heuvelink, G.B.M., Gräler, B., Pebesma, E., Perčec Tadić, M. & Bajat, B. (2014) Spatio-temporal interpolation of daily temperatures for global land areas at 1 km resolution. *Journal of Geophysical Research: Atmospheres*, **119**, 2294–2313.

Kopecký, M. & Čížková, Š. (2010) Using topographic wetness index in vegetation ecology: does the algorithm matter? *Applied Vegetation Science*, **13**, 450–459.

Kopecký, M. & Macek, M. (2015) Vegetation resurvey is robust to plot location uncertainty. *Diversity and Distributions*, **21**, 322–330.

Körner, C. & Hiltbrunner, E. (2018) The 90 ways to describe plant temperature. *Perspectives in Plant Ecology, Evolution and Systematics*, **30**, 16–21.

Körner, C. & Paulsen, J. (2004) A world-wide study of high altitude treeline temperatures. *Journal of Biogeography*, **31**, 713–732.

Lawesson, J.E. & Oksanen, J. (2002) Niche characteristics of Danish woody species as derived from coenoclines. *Journal of Vegetation Science*, **13**, 279.

Leempoel, K., Parisod, C., Geiser, C., Daprà, L., Vittoz, P. & Joost, S. (2015) Very high-resolution digital elevation models: Are multi-scale derived variables ecologically relevant? *Methods in Ecology and Evolution*, **6**, 1373–1383.

Lenoir, J., Gégout, J.C., Marquet, P.A., De Ruffray, P. & Brisse, H. (2008) A significant upward shift in plant species optimum elevation during the 20th century. *Science*, **320**, 1768–1771.

Lenoir, J., Graae, B.J., Aarrestad, P.A., Alsos, I.G., Armbruster, W.S., Austrheim, G., Bergendorff, C., Birks, H.J.B., Bråthen, K.A., Brunet, J., Bruun, H.H., Dahlberg, C.J., Decocq, G., Diekmann, M., Dynesius, M., Ejrnæs, R., Grytnes, J.A., Hylander, K., Klanderud, K., Luoto, M., Milbau, A., Moora, M., Nygaard, B., Odland, A., Ravolainen, V.T., Reinhardt, S., Sandvik, S.M., Schei, F.H., Speed, J.D.M., Tveraabak, L.U., Vandvik, V., Velle, L.G., Virtanen, R., Zobel, M. & Svenning, J.C. (2013) Local temperatures inferred from plant communities suggest strong spatial buffering of climate warming across Northern Europe. *Global Change Biology*, **19**, 1470–1481.

Lepš, J. (1990) *Can underlying mechanisms be deduced from observed patterns? Spatial processes in plant communities* (ed. by F. Krahulec), A.D.Q. Agnew), S. Agnew), and J.H. Willems), pp. 1–11. Academia, Praha.

Lepš, J. & Hadincová, V. (1992) How reliable are our vegetation analyses? *Journal of Vegetation Science*, **3**, 119–124.

Lippok, D., Beck, S.G., Renison, D., Hensen, I., Apaza, A.E. & Schleuning, M. (2014) Topography and edge effects are more important than elevation as drivers of vegetation patterns in a neotropical montane forest. *Journal of Vegetation Science*, **25**, 724–733.

Macek, M., Kopecký, M. & Wild, J. (2019) Maximum air temperature controlled by landscape topography affects plant species composition in temperate forests. *Landscape Ecology*, **34**, 2541–2556.

Maclean, I.M.D. (2019) Predicting future climate at high spatial and temporal resolution. *Global Change Biology*, gcb.14876.

Máliš, F., Kopecký, M., Petřík, P., Vladovič, J., Merganič, J. & Vida, T. (2016) Life stage, not climate change, explains observed tree range shifts. *Global change biology*, **22**, 1904–14.

Mather, J.R. & Yoshioka, G.A. (1968) The role of climate in the distribution of vegetation. *Annals of the Association of American Geographers*, **58**, 29–41.

McGill, B.J., Maurer, B. a & Weiser, M.D. (2006) Empirical evaluation of neutral theory. *Ecology*, **87**, 1411–23.

McIntire, E.J.B. & Fajardo, A. (2009) Beyond description: the active and effective way to infer processes from spatial patterns. *Ecology*, **90**, 46–56.

Merow, C., Smith, M.J. & Silander, J. a. (2013) A practical guide to MaxEnt for modeling species' distributions: what it does, and why inputs and settings matter. *Ecography*, **36**, 1058–1069.

Michaelis, J. & Diekmann, M.R. (2017) Biased niches – Species response curves and niche attributes from Huisman-Olff-Fresco models change with differing species prevalence and frequency. *PLOS ONE*, **12**, e0183152.

Michalet, R., Brooker, R.W., Cavieres, L.A., Kikvidze, Z., Lortie, C.J., Pugnaire, F.I., Valiente-Banuet, A. & Callaway, R.M. (2006) Do biotic interactions shape both sides of the humped-back model of species richness in plant communities? *Ecology Letters*, **9**, 767–773.

Mod, H.K., Scherrer, D., Luoto, M., Guisan, A. & Scheiner, S. (2016) What we use is not what we know: environmental predictors in plant distribution models. *Journal of Vegetation Science*, **27**, 1308–1322.

Morueta-Holme, N., Engemann, K., Sandoval-Acuña, P., Jonas, J.D., Segnitz, R.M. & Svenning, J.-C. (2015) Strong upslope shifts in Chimborazo's vegetation over two centuries since Humboldt. *Proceedings of the National Academy of Sciences*, **112**, 201509938.

Mutke, J. & Barthlott, W. (2005) Patterns of vascular plant diversity at continental to global scales. *Biologiske skrifter*, **55**, 521–531.

Normand, S., Treier, U. a., Randin, C., Vittoz, P., Guisan, A. & Svenning, J.-C. (2009) Importance of abiotic stress as a range-limit determinant for European plants: insights from species responses to climatic gradients. *Global Ecology and Biogeography*, **18**, 437–449.

Oksanen, J. & Minchin, P.R. (2002) Continuum theory revisited: what shape are species responses along ecological gradients? *Ecological Modelling*, **157**, 119–129.

Parmesan, C. & Hanley, M.E. (2015) Plants and climate change: Complexities and surprises. *Annals of Botany*, **116**, 849–864.

Parolo, G. & Rossi, G. (2008) Upward migration of vascular plants following a climate warming trend in the Alps. *Basic and Applied Ecology*, **9**, 100–107.

Peters, M.K., Hemp, A., Appelhans, T., Behler, C., Classen, A., Detsch, F., Ensslin, A., Ferger, S.W., Frederiksen, S.B., Gebert, F., Haas, M., Helbig-Bonitz, M., Hemp, C., Kindeketa, W.J., Mwangomo, E., Ngereza, C., Otte, I., Röder, J., Rutten, G., Schellenberger Costa, D., Tardanico, J., Zancolli, G., Deckert, J., Eardley, C.D., Peters, R.S., Rödel, M.O., Schleuning, M., Ssymank, A., Kakengi, V., Zhang, J., Böhning-Gaese, K., Brandl, R., Kalko, E.K.V., Kleyer, M., Nauss, T., Tschapka, M., Fischer, M. & Steffan-Dewenter, I. (2016) Predictors of elevational biodiversity gradients change from single taxa to the multi-taxa community level. *Nature Communications*, **7**.

Peterson, A.T., Soberón, J. & Sánchez-Cordero, V. (1999) Conservatism of ecological niches in evolutionary time. *Science*, **285**, 1265–1267.

Phillips, S.J., Anderson, R.P. & Schapire, R.E. (2006) Maximum entropy modeling of species geographic distributions. *Ecolgical Modelling*, **190**, 231–259.

Rabasa, S.G., Granda, E., Benavides, R., Kunstler, G., Espelta, J.M., Ogaya, R., Peñuelas, J., Scherer-Lorenzen, M., Gil, W., Grodzki, W., Ambrozy, S., Bergh, J., Hódar, J.A., Zamora, R. & Valladares, F. (2013) Disparity in elevational shifts of European trees in response to recent climate warming. *Global Change Biology*, **19**, 2490–2499.

Rahbek, C. (2005) The role of spatial scale and the perception of large-scale species-richness patterns. *Ecology Letters*, **8**, 224–239.

Rapoport, E.H. (1982) *Aerography: geographical strategies of species*, First Engl. Pergamon Press Ltd., Oxford.

Rosenzweig, C., Karoly, D., Vicarelli, M., Neofotis, P., Wu, Q., Casassa, G., Menzel, A., Root, T.L., Estrella, N., Seguin, B., Tryjanowski, P., Liu, C., Rawlins, S. & Imeson, A. (2008) Attributing physical and biological impacts to anthropogenic climate change. *Nature*, **453**, 353–357.

Rosindell, J., Hubbell, S.P. & Etienne, R.S. (2011) The unified neutral theory of biodiversity and biogeography at age ten. *Trends in Ecology & Evolution*, **26**, 340–348.

Le Roux, P.C., Lenoir, J., Pellissier, L., Wisz, M.S. & Luoto, M. (2013) Horizontal, but not vertical, biotic interactions affect fine-scale plant distribution patterns in a low-energy system. *Ecology*, **94**, 671–682.

Rumpf, S.B., Hülber, K., Klonner, G., Moser, D., Schütz, M., Wessely, J., Willner, W., Zimmermann, N.E. & Dullinger, S. (2018) Range dynamics of mountain plants decrease with elevation. *Proceedings of the National Academy of Sciences*, 201713936.

Shmida, A. & Ellner, S. (1984) Coexistence of plant species with similar niches. *Plant Ecology*, **58**, 29–55.

Šímová, I., Storch, D., Keil, P., Boyle, B., Phillips, O.L. & Enquist, B.J. (2011) Global species-energy relationship in forest plots: role of abundance, temperature and species climatic tolerances. *Global Ecology and Biogeography*, **20**, 842–856.

Šizling, A.L., Storch, D. & Keil, P. (2009) Rapoport's rule, species tolerances, and the latitudinal diversity gradient: Geometric considerations. *Ecology*, **90**, 3575–3586.

Stephenson, N.L. (1998) Actual evapotranspiration and deficit: biologically meaningful correlates of vegetation distribution across spatial scales. *Journal of Biogeography*, **25**, 855–870.

Stevens, G. (1992) The elevational gradient in altitudinal range: an extension of Rapoport's latitudinal rule to altitude. *American naturalist*, **140**, 893–911.

Stevens, G.C. (1989) The Latitudinal Gradient in Geographical Range: How so Many Species Coexist in the Tropics. *The American Naturalist*, **133**, 240–256.

Stevens, H.H. & Carson, W.P. (2002) Resource quantity, not resource heterogeneity, maintains plant diversity. *Ecology Letters*, **5**, 420–426.

Strachan, S. & Daly, C. (2017) Testing the daily PRISM air temperature model on semiarid mountain slopes. *Journal of Geophysical Research Atmospheres*, **122**, 5697–5715.

Sutherland, W.J., Freckleton, R.P., Godfray, H.C.J., Beissinger, S.R., Benton, T., Cameron, D.D., Carmel, Y., Coomes, D.A., Coulson, T., Emmerson, M.C., Hails, R.S., Hays, G.C., Hodgson, D.J., Hutchings, M.J., Johnson, D., Jones, J.P.G., Keeling, M.J., Kokko, H., Kunin, W.E., Lambin, X., Lewis, O.T., Malhi, Y., Mieszkowska, N., Milner-Gulland, E.J., Norris, K., Phillimore, A.B., Purves, D.W., Reid, J.M., Reuman, D.C., Thompson, K., Travis, J.M.J., Turnbull, L.A., Wardle, D.A. & Wiegand, T. (2013) Identification of 100 fundamental ecological questions. *Journal of Ecology*, **101**, 58–67.

Thibaud, E., Petitpierre, B., Broennimann, O., Davison, A.C. & Guisan, A. (2014) Measuring the relative effect of factors affecting species distribution model predictions. *Methods in Ecology and Evolution*, **5**, 947–955.

Tolasz, R., Míková, T., Valeriánová, A. & Voženílek, V. eds. (2007) *Climate atlas of Czechia*, 1st edn. Czech Hydrometeorological Institute, Praha - Olomouc.

Vandermeer, J.H. (1972) Niche Theory. *Annual Rewiew of Ecology and Systematics*, **3**, 107–132.

Verheyen, K., Bažány, M., Chećko, E., Chudomelová, M., Closset-Kopp, D., Czortek, P., Decocq, G., De Frenne, P., De Keersmaeker, L., Enríquez García, C., Fabšičová, M., Grytnes, J., Hederová, L., Hédl, R., Heinken, T., Schei, F.H., Horváth, S., Jaroszewicz, B., Jermakowicz, E., Klinerová, T., Kolk, J., Kopecký, M., Kuras, I., Lenoir, J., Macek, M., Máliš, F., Martinessen, T.C., Naaf, T., Papp, L., Papp-Szakály, Á., Pech, P., Petřík, P., Prach, J., Reczyńska, K., Sætersdal, M., Spicher, F., Standovár, T., Świerkosz, K., Szczęśniak, E., Tóth, Z., Ujházy, K., Ujházyová, M., Vangansbeke, P., Vild, O., Wołkowycki, D., Wulf, M. & Baeten, L. (2018) Observer and relocation errors matter in resurveys of historical vegetation plots. *Journal of Vegetation Science*, **29**, 812–823.

Waide, R.B., Willig, M.R., Steiner, C.F., Mittelbach, G., Gough, L., Dodson, S.I., Juday, G.P. & Parmenter, R. (1999) The Relationship Between Productivity and Species Richness. *Annual Review of Ecology and Systematics*, **30**, 257–300.

Watt, A.S. (1947) Pattern and Process in the Plant Community. *The Journal of Ecology*, **35**, 1.

Whittaker, R.J., Willis, K.J. & Field, R. (2001) Scale and species richness: towards a general , hierarchical theory of species diversity. *Journal of Biogeography*, **28**, 453–470.

Wiegand, T. & A. Moloney, K. (2004) Rings, circles, and null-models for point pattern analysis in ecology. *Oikos*, **104**, 209–229.

Wiens, J.A. (1989) Spatial scaling in ecology. *Functional ecology*, **3**, 385–397.

Wild, J., Kopecký, M., Svoboda, M., Zenáhlíková, J., Edwards-Jonášová, M. & Herben, T. (2014) Spatial patterns with memory: Tree regeneration after stand-replacing disturbance in Picea abies mountain forests. *Journal of Vegetation Science*, **25**, 1327–1340.

Wisz, M.S., Pottier, J., Kissling, W.D., Pellissier, L., Lenoir, J., Damgaard, C.F., Dormann, C.F., Forchhammer, M.C., Grytnes, J.A., Guisan, A., Heikkinen, R.K., Høye, T.T., Kühn, I., Luoto, M., Maiorano, L., Nilsson, M.C., Normand, S., Öckinger, E., Schmidt, N.M., Termansen, M., Timmermann, A., Wardle, D.A., Aastrup, P. & Svenning, J.C. (2013) The role of biotic interactions in shaping distributions and realised assemblages of species: Implications for species distribution modelling. *Biological Reviews*, **88**, 15–30.

van den Wollenberg, A.L. (1977) Redundancy analysis an alternative for canonical correlation analysis. *Psychometrika*, **42**, 207–219.

Zapata, F.A., Gaston, K.J. & Chown, S.L. (2005) The Mid-Domain Effect Revisited. *American Naturalist*, **166**, E144–E148.

Zelený, D., Li, C.-F. & Chytrý, M. (2010) Pattern of local plant species richness along a gradient of landscape topographical heterogeneity: result of spatial mass effect or environmental shift? *Ecography*.

Zellweger, F., Braunisch, V., Morsdorf, F., Baltensweiler, A., Abegg, M., Roth, T., Bugmann, H. & Bollmann, K. (2015) Disentangling the effects of climate, topography, soil and vegetation on stand-scale species richness in temperate forests. *Forest Ecology and Management*, **349**, 36–44.

Zellweger, F., Coomes, D., Lenoir, J., Depauw, L., Maes, S.L., Wulf, M., Kirby, K.J., Brunet, J., Kopecký, M., Máliš, F., Schmidt, W., Heinrichs, S., den Ouden, J., Jaroszewicz, B., Buyse, G., Spicher, F., Verheyen, K. & De Frenne, P. (2019) Seasonal drivers of understorey temperature buffering in temperate deciduous forests across Europe. *Global Ecology and Biogeography*, 1–13.

Zobel, M. (1997) The relative role of species pools in determining plant species richness: An alternative explanation of species coexistence? *Trends in Ecology and Evolution*, **12**, 266–269.

Zobel, M. & Pärtel, M. (2008) What determines the relationship between plant diversity and habitat productivity? *Global Ecology and Biogeography*, **17**, 679–684.

CHAPTER TWO:

LIFE AND DEATH OF *PICEA ABIES* AFTER BARK-BEETLE OUTBREAK: ECOLOGICAL PROCESSES DRIVING SEEDLING RECRUITMENT

MARTIN MACEK[1,2], JAN WILD[1,3], MARTIN KOPECKÝ[1,4], JAROSLAV ČERVENKA[4,5], MIROSLAV SVOBODA[4], JITKA ZENÁHLÍKOVÁ[4,5], JOSEF BRŮNA[1], REINHARD MOSANDL[6] AND ANTON FISCHER[7]

[1] *Institute of Botany, The Czech Academy of Sciences, Zámek 1, CZ-252 43, Průhonice, Czech Republic*

[2] *Department of Botany, Faculty of Science, Charles University in Prague, Benátská 2, CZ-128 01, Prague 2, Czech Republic*

[3] *Faculty of Environmental Sciences, Czech University of Life Sciences Prague, Kamýcká 129,CZ- 16521 Prague 6 - Suchdol, Czech Republic*

[4] *Faculty of Forestry and Wood Sciences, Czech University of Life Sciences Prague, Kamýcká 129, CZ-165 21, Prague 6 - Suchdol, Czech Republic*

[5] *Šumava National Park, 1. máje 260,CZ – 385 01 Vimperk, Czech Republic*

[6] *Institute of Silviculture, Technische Universität München TUM, 85354 Freising, Germany*

[7] *Geobotany, Department of Ecology and Ecosystem Management, Center of Life and Food Sciences, Technische Universität München TUM, Hans-Carl-von-Carlowitz-Platz 2, D-85354 Freising, Germany*

Published in: Ecological Applications (2017) 27:156–167.
DOI: 10.1002/eap.1429

2.1 ABSTRACT

The severity and spatial extent of bark-beetle outbreaks substantially increased in recent decades worldwide. The ongoing controversy about natural forest recovery after these outbreaks highlights the need for individual-based long-term studies, which disentangle processes driving forest regeneration. However, such studies have been lacking. To fill this gap, we followed the fates of 2,552 individual seedlings for 12 years after a large-scale bark-beetle outbreak that caused complete canopy dieback in mountain Norway spruce (*Picea abies*) forests in SE Germany. Here we explore the contribution of advance, disturbance-related and post-disturbance regeneration to forest recovery.

Most seedlings originated directly within the three-year dieback of canopy trees induced by bark-beetle outbreak. After complete canopy dieback, the establishment of new seedlings was minimal. Surprisingly, advance regeneration formed only a minor part of all regeneration. However, because it had the highest survival rate, its importance increased over time. The most important factor influencing the survival of seedlings after disturbance was their height. Survival was further modified by microsite: seedlings established on dead wood survived best, whereas almost all seedlings surrounded by graminoids died. For 5 cm tall seedlings, annual mortality ranged from 20% to 50% according to the rooting microsite. However, for seedlings taller than 50 cm, annual mortality was below 5% at all microsites. While microsite modified seedling mortality, it did not affect seedling height growth. A model of regeneration dynamics based on short-term observations accurately predicts regeneration height growth, but substantially underestimates mortality rate - thus predicting more surviving seedlings than were observed.

We found that *Picea abies* forests were able to regenerate naturally even after severe bark-beetle outbreaks owing to advance and particularly disturbance-related regeneration. This, together with microsite-specific mortality, yields structurally and spatially diverse forests. Our study thus highlights the so far unrecognized importance of disturbance-related regeneration for stand recovery after bark-beetle outbreaks.

2.2 KEYWORDS

Advance regeneration, Growth function, Ips typographus, Mortality, Norway spruce, Permanent plots, Salvage logging, Stand-replacing disturbance, Survival

2.3 INTRODUCTION

The key to forest recovery after disturbance is tree regeneration. Its species composition, spatial pattern and structural heterogeneity are crucial for the biodiversity and future resilience of the developing forest (Swanson et al. 2011, Donato et al. 2012). Following the death of mature trees in consequence of a disturbance event, diaspore supply sharply decreases. Successful stand-replacement often depends on the survival and growth of advance regeneration established before the disturbance (Kuuluvainen 1994, Franklin et al. 2002, Svoboda et al. 2012). Increased understory light and released nutrients promote the growth of recruits after disturbance (Metslaid et al. 2007, Kaňa et al. 2012), but regeneration rate depends also on competition with the expanding herb-layer and on biological legacies, such as the amount of coarse woody debris and pit-and-mound topography (Kuuluvainen and Juntunen 1998, Jonášová and Prach 2004).

In contrast to episodic disturbances such as fire or windthrow, bark-beetle outbreak impact is gradual: ongoing canopy tree dieback takes several years (Köster et al. 2009, Edburg et al. 2012). The main differences from episodic high-severity disturbances are: (i) gradual changes in stand microclimate during the dieback of canopy trees; (ii) undisturbed soil surface; and (iii) minimal damage to already established advance regeneration and herb layer vegetation (Kuuluvainen 1994, Storaunet and Rolstad 2004, Fischer et al. 2013, 2015). The regeneration processes after bark-beetle outbreaks are therefore different from those following other disturbances. Knowledge about tree regeneration after stand-replacing fire or windthrow is non-transferable to stand recovery after bark-beetle outbreaks.

The severity and spatial extent of bark-beetle outbreaks substantially increased in recent decades worldwide in different types of coniferous forests (Dale et al. 2001, Schelhaas et al. 2003, Meddens et al. 2012). In Europe, Norway spruce (*Picea abies* (L.) Karst.) forests cover large areas within the boreal forest zone and in the mountains within the temperate zone, where spruce naturally forms almost monodominant stands. These stands are prone to European spruce bark-beetle (*Ips typographus* L.) outbreaks, usually induced by preceding windthrow damage (Brůna et al. 2013, Čada et al. 2016). Recently, these outbreaks have been amplified by series of windstorm events, vast artificial spruce plantations and also by warmer climate causing tree physiological stress and hastened bark-beetle development (Raffa and Aukema 2008, Temperli et al. 2013, Seidl et al. 2014). As a result, recent outbreaks caused almost complete mortality of canopy trees over large areas within short time intervals (Lausch et al. 2011).

Large-scale, stand-replacing disturbances in spruce forests caused severe economic loss in managed forests and at the same time affected many protected areas (Müller et al. 2008). This presented a challenge for both forest managers and nature conservationists and raised important questions about the best management schemes to balance the

requirements of sustainable timber production, biodiversity conservation and other ecosystem services (Wermelinger 2004, Seidl et al. 2008, Beudert et al. 2015). Detailed knowledge of post-disturbance succession is important for nature conservationists because these early-seral stages are crucial for biodiversity (Kouki et al. 2001, Müller et al. 2008, Donato et al. 2012, Lehnert et al. 2013). Recommendations for management of affected stands are urgently needed also by forest managers, who must decide whether the forest will self-replace itself in an acceptable time frame or instead needs salvage logging and replanting. Salvage logging, often applied after bark-beetle outbreaks, has been hotly debated (Lindenmayer and Noss 2006). Its proponents argued that salvage logging followed by tree replanting is needed to control bark-beetle spread and secure stand recovery (Fettig *et al.* 2007; Stadelmann *et al.* 2013), while its opponents questioned the efficiency of salvage logging in controlling bark-beetle epidemics (Grodzki et al. 2006) and argued that this treatment disrupts natural regeneration, adversely affects the self-replacing ability of disturbed stands (Donato et al. 2006, Wild et al. 2014) and negatively influences biodiversity (Kouki et al. 2001, Jonášová and Prach 2008, Thorn et al. 2014).

This controversy has triggered intensive research on natural regeneration and factors affecting stand self-replacement (Kupferschmid et al. 2006, Harvey et al. 2014). However, the regeneration process after bark-beetle outbreaks has been investigated only through studies that did not follow individual seedlings over time (Jonášová and Prach 2004, DeRose and Long 2010, Diskin et al. 2011, Zeppenfeld et al. 2015). Moreover, these studies usually focus only on regeneration over a certain height threshold. The resulting snapshot data covering only a subset of regeneration can easily provide biased results, as it is extremely difficult to infer actual processes behind the observed static patterns (Wiegand et al. 2003). For instance, clumped spatial pattern of spruce seedlings was repeatedly observed, but the processes responsible for the formation of such a pattern remain unclear (Grenfell et al. 2011, Wild et al. 2014). High densities of seedlings on coarse woody debris suggest low mortality on these microsites (Jonášová and Prach 2004, Kupferschmid and Bugmann 2005), but Kathke and Bruelheide (2010) inferred opposite conclusions from regeneration age structure. Advance regeneration, i.e. recruits well-established before the disturbance, is generally thought to be the most important tree cohort for shade-tolerant tree recovery (DeRose and Long 2010, Bače et al. 2015, Burton et al. 2015), but reliable evidence based on temporally replicated surveys is missing. To disentangle conflicting evidence and to provide robust recommendations for the management of *P. abies* forests, long-term studies following the fates of individual seedlings are needed (Fischer and Fischer 2011).

In the present study, we therefore tested the following hypotheses about tree regeneration after stand-replacing bark-beetle outbreaks:

H1: Tree regeneration after the disturbance will be dominated by advance regeneration already established before the disturbance.

H2: Tree regeneration will be structured by microsite-specific seedling performance (i.e. growth and survival rates).

To test these hypotheses, we collected and analyzed individual performance data on *Picea abies* seedlings and saplings during the first 12 years after a stand-replacing bark-beetle outbreak in a naturally regenerated forest in the Bavarian Forest National Park, Germany. To provide recommendations for applied ecology, we also evaluated the potential of short-term post-disturbance monitoring of individual seedlings to yield meaningful predictions of further stand development.

2.4 METHODS

2.4.1 STUDY SITE

We worked in the Bavarian Forest National Park in SE Germany (Fig. 1). The park was established in 1970 and enlarged to its current 240 km² in 1997. Bedrock mostly comprises gneiss and granitic rocks, leading to acidic, podzolised soils. Climate in the park is cold, with long winters and short, but relatively warm summers. Mountain spruce forests form the natural vegetation from about 1150 m a.s.l. up to the highest elevation in the park (1453 m a.s.l.) where mean annual temperature ranges from 5.1 to 3.6°C (Elling et al. 1987). The tree layer is dominated by Norway spruce, accompanied by a small fraction of mountain ash (*Sorbus aucuparia* L.). The European spruce bark-beetle responsible for periodic outbreaks is indigenous to these forests, but its populations show extensive fluctuations depending on forest stand and weather conditions (Wermelinger 2004, Berec et al. 2013). Outbreaks usually cause complete dieback of Norway spruce canopy trees over large areas (Müller et al. 2008).

We studied stands affected by a major outbreak that started in 1993 and culminated between 1996 and 2000. The severity and extent of the canopy dieback were exceptionally high, with complete canopy dieback on about 54 km² (Lausch et al. 2011). The affected stands in the core zone were left to spontaneous development, and this gave us a unique opportunity to study natural tree regeneration after a bark-beetle outbreak.

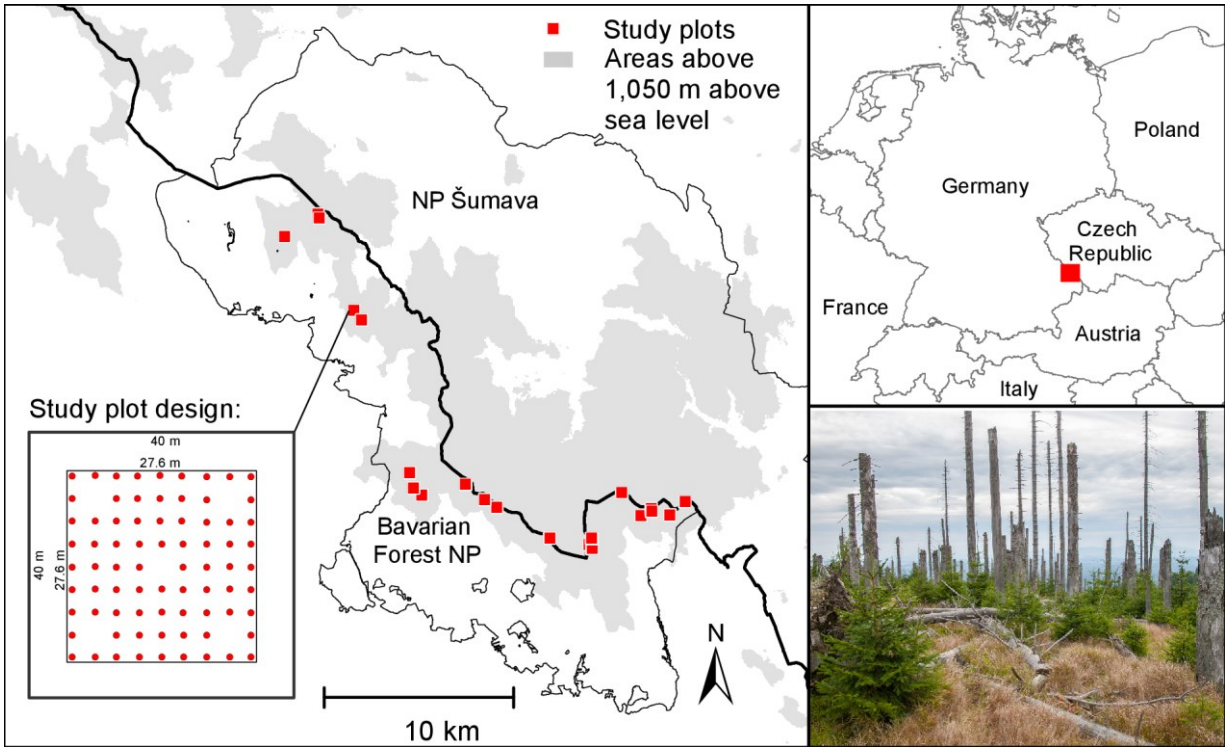

Figure 1. Study site location and plot arrangement: plots are subdivided into a grid of 76 circular sub-plots, 0.5 m² each, spaced 3.35 m apart. All seedlings and saplings present on these sub-plots were permanently labelled and repeatedly measured during the first 12 years after stand-replacing disturbance by a massive bark-beetle outbreak. Inset photograph shows the stand 12 years after the outbreak (during fieldwork in 2010).

2.4.2 DATA COLLECTION

In 1998, Bauer established 24 permanent plots in mountain spruce forests across the park (Bauer 2002, Bauer et al. 2008). The plots covered the whole elevation gradient within the natural spruce forest belt in the region (1155 – 1345 m a.s.l.). Plots were established in stands infested by bark-beetles, complete canopy dieback was reported on all plots by the year 2000. Pre-disturbance stem densities ranged from 269 to 669 stems ha^{-1}, with median 459.5 stems ha^{-1}.

A regular grid of 76 circular sub-plots (0.5 m² each) was established within each 762 m² plot (Fig. 1). All seedlings and saplings rooting in the sub-plots were permanently labelled and numbered. Four parameters were determined for each labelled individual: 1) age in years, 2) absolute height in millimeters, 3) annual height increment in millimeters and 4) rooting microsite. Age was determined according to terminal bud scar and verticil positions, which is reliable for young spruce saplings (Zielonka 2006, Bače et al. 2011). This allowed us to date very precisely the individual seedlings and divide them into three age cohorts: (1) *advance regeneration* - trees established prior to the outbreak (i.e. germinating before 1996); (2) *disturbance-related regeneration* - trees established during the bark-beetle outbreak (i.e. germinating between 1996 and 1999);

and (3) *post-disturbance regeneration* - trees established after complete canopy dieback (i.e. 2000 and later). Rooting microsite type was categorized according to substrate and surrounding vegetation (see Tab. 1). Annual increments and mortality of individual seedlings were measured in the following two years (1999 and 2000).

In 2010, we repeated the same measurements on 21 plots, excluding three plots in the area damaged by windstorm Kyrill. To retain continuity in data, we measured all annual increments of the labelled trees from the last year of measurement in 2000. To get a more representative estimate of regeneration density in each sampled stand, we also counted all juvenile trees growing on each plot.

Table 1. Microsite type definitions and overview of tree proportions on microsites from 1998 (during dieback), 2000 (shortly after dieback) and 2010.

		Proportion of juveniles observed on microsite (weighted plot mean ± *SE*)			Cumulative mortality	Fitted mortality effects	
Microsite	**Description**	1998	2000	2010	1998 – 2010	Odds ratio	Tukey HSD
Dead wood	laying tree logs or coarse woody debris	4.8 ± 1.3	7.3 ± 2.0	12.0 ± 4.4	68.6	0.547	a
Tree base	area surrounding standing trunks up to the distance equal to trunk diameter	15.4 ± 5.1	20.8 ± 5.9	18.0 ± 8.7	85.5	0.632	a
Stump	directly on stumps/snags	14.0 ± 2.9	19.4 ± 3.8	25.0 ± 5.6	77.9	0.665	a
Pits and mounds	windfall pits and mounds	1.7 ± 0.6	1.9 ± 0.4	4.1 ± 0.7	69.8	0.910	abc
Moss	cover predominantly of mosses	15.5 ± 3.2	13.2 ± 3.2	8.5 ± 2.3	93.2	1.215	b
Litter	ground covered by needles, bark or twigs	37.9 ± 4.9	31.2 ± 5.5	29.1 ± 9.0	90.5	1.228	b
Lycopodium	cover predominantly of *Lycopodium annotinum*	5.0 ± 0.9	3.2 ± 0.6	2.5 ± 0.5	93.8	1.428	bc
Graminoid	cover predominantly of *Calamagrostis villosa, Luzula sylvatica* or *Avenella flexuosa*	3.8 ± 0.8	1.9 ± 0.6	0.3 ± 0.3	99.0	2.243	c
Other*	cover predominantly of other species i.e. *Vaccinium, Athyrium, Dryopteris, Oxalis*	1.8 ± 1.3	1.1 ± 0.9	0.3 ± 0.3	97.8	-	-
Total no. of individuals		2550	1045	316	87.6%		

Notes: Numbers are based only on a subset of trees already present in 1998. Tukey HSD letter codes indicate microsite groups with significantly different mortality odds at the 0.05 level. Note that cumulative mortality is a raw value, but fitted odds ratios also reflect tree height as a component of mortality.

2.4.3 Data analysis

We analyzed the survival and growth only of *P. abies*, which formed 99% of all recorded individuals. Other species were too rare for such analyses, and we included them only in a plot-level overview of regeneration density.

Regeneration structure

To assess changes in regeneration structure over time, we calculated proportions of cohorts in the survey years. To test the hypothesis H1, we tested the year 2010 paired differences in plot-level sums of advance regeneration vs. disturbance related plus post-disturbance regeneration by a one-sided Wilcoxon test for paired data.

Growth

To analyze tree growth, we fitted the tree-height series with parametric growth functions through nonlinear mixed-effect models, accounting for the spatially and temporally dependent error structure. Only juveniles surviving the whole period (1998 to 2010) were selected for fitting tree growth. We compared six different growth functions previously used for temperate forest trees (Tab. 2) (Pretzsch 2010).

To fit the models, we used the R software version 3.2 (R Core Team 2015) and the *nlme* function from the *nlme* package (Pinheiro et al. 2013). In the models, we used tree age as a fixed effect and individual trees nested within individual plots as random effects to account for autocorrelation. As an asymptotic tree height parameter, we used the 90th percentile (i.e. 26.85 m) of canopy tree heights measured on our plots before stand dieback (Bauer 2002). To account for heteroscedasticity in tree heights, we used a power variance function. For further analyses, we selected the growth function which fitted best according to the root mean square error (RMSE) and visual inspection of the residuals.

To test the effect of rooting microsite on sapling growth, we added microsite as an additional fixed effect to the best-fitting growth-function model. We used the AIC (Akaike Information Criterion) and a log-likelihood ratio test to explore if the inclusion of rooting microsite improved model fit.

Mortality

To investigate the drivers of juvenile tree mortality, we fitted binomial generalized linear mixed-effect models using the *glmer* function of the *lme4* R package (Bates et al. 2015). We tested log-transformed tree height, rooting microsite and site elevation as fixed effects. Plot ID and survey year were included as crossed random effects. We constructed the minimal adequate model through forward selection of predictors based on the AIC (Crawley 2007). Then, we used a type II Wald χ^2 test to check the statistical significance of the fixed model terms. In the models, we used Laplace approximations

for maximum likelihood estimation. For post-hoc comparison of mortality levels we used Tukey's HSD test.

REGENERATION DYNAMICS MODEL

To investigate whether short-term observation can be used for the prediction of future stand structure, we built a predictive model and compared its output with the observations made after ten years. We used data from only the first three years of sampling (1998 to 2000) to fit the previously selected growth function to all juvenile trees present in 2000. We then made predictions of their heights in the period 2001-2020. For each sapling, we also estimated survival probability according to the marginal prediction of an annual mortality risk model based on rooting microsite, and estimated sapling height for each given year. Individuals surviving to the next year were selected randomly, with weighting based on survival probability.

To evaluate the model, we compared our observations with the predicted numbers of surviving saplings, their densities on different microsites and their height and age structures in the year 2010. We ran this model 1000 times. In each run we tested conformity of mean and distribution function for height by a two-sample t-test and Kolmogorov-Smirnov test and by a discretized Kolmogorov-Smirnov test from the *dgof* R package (Arnold and Emerson 2011) for age structure. Finally, we calculated the number of simulations having predictions significantly deviant ($p < 0.05$) from the observed data.

2.5 RESULTS

REGENERATION STRUCTURE

Initially, in 1998, a total of 2,552 spruce seedlings and saplings were found on the plots, with 86% of them belonging to the disturbance-related cohort. Advance regeneration represented only 14% of all juvenile trees (Tab. 3).

Of the 2,552 juveniles found in 1998, only 316 individuals (12.4%) survived to 2010. Only 38 juveniles got established after complete canopy dieback and survived to 2010. Advance regeneration benefited from lower mortality, and therefore its relative proportion increased over time to 31% in 2010. Despite local variability in proportion of regeneration cohorts (Fig. 2) the advance regeneration does not dominate globally (Wilcoxon test: $V = 13.5$, $p < 0.01$). Contrary, disturbance-related cohort represented the majority of regeneration (58%) even 12 years after the disturbance (Fig. 3). We thus have to reject the H1 hypothesis, that the regeneration will be dominated by the individuals established before the disturbance.

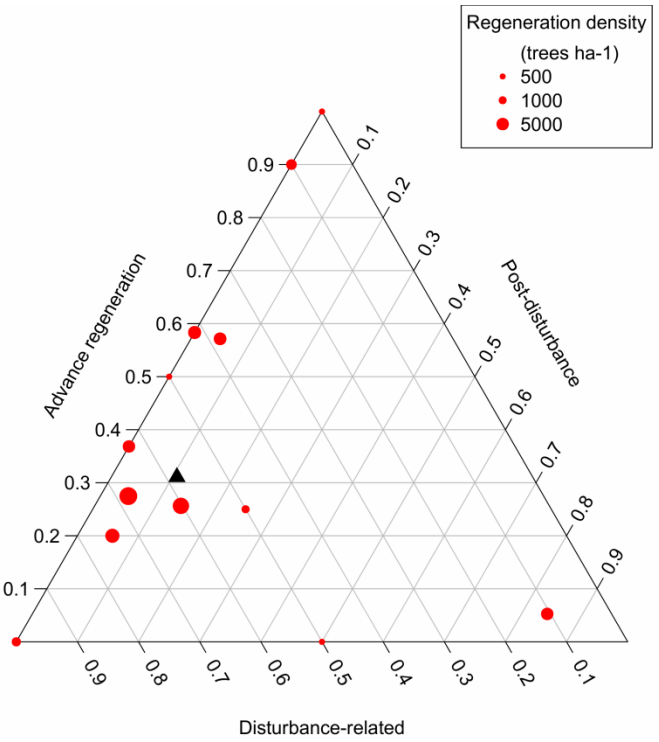

Figure 2. *Cohort contribution to regeneration in 2010 (twelve years after bark-beetle outbreak): total mean (black triangle) and site values (red dots). Size of the dots is proportional to total number of recruits; sites without surviving tracked individuals are not plotted.*

Table 3. Cohort contribution (total no. of individuals and actual percentages ± SEM in parentheses) to spruce population and cumulative mortality starting from 1998 (outbreak culmination) to 2010 (decade after outbreak).

	No. of individuals				Cumulative mortality (%)		
Cohort	1998	1999	2000	2010	1999	2000	2010
Pre-disturbance	363 (14.2 ± 7.2)	308 (16.7 ± 6.9)	238 (22.8 ± 7.2)	110 (31.1 ± 8.6)	15.2	34.4	69.7
Disturbance-related	2189 (85.8 ± 7.2)	1534 (83.2 ± 6.9)	807 (77.2 ± 7.2)	206 (58.2 ± 8.1)	29.9	63.1	90.6
Post-disturbance	0 (0.0 ± 0.0)	1 (0.05 ± 0.1)	1 (0.1 ± 0.2)	38(10.7 ± 6.6)	NA	NA	NA
Total	2552 (100)	1843 (100)	1046 (100)	354 (100)	27.8	59.1	87.6

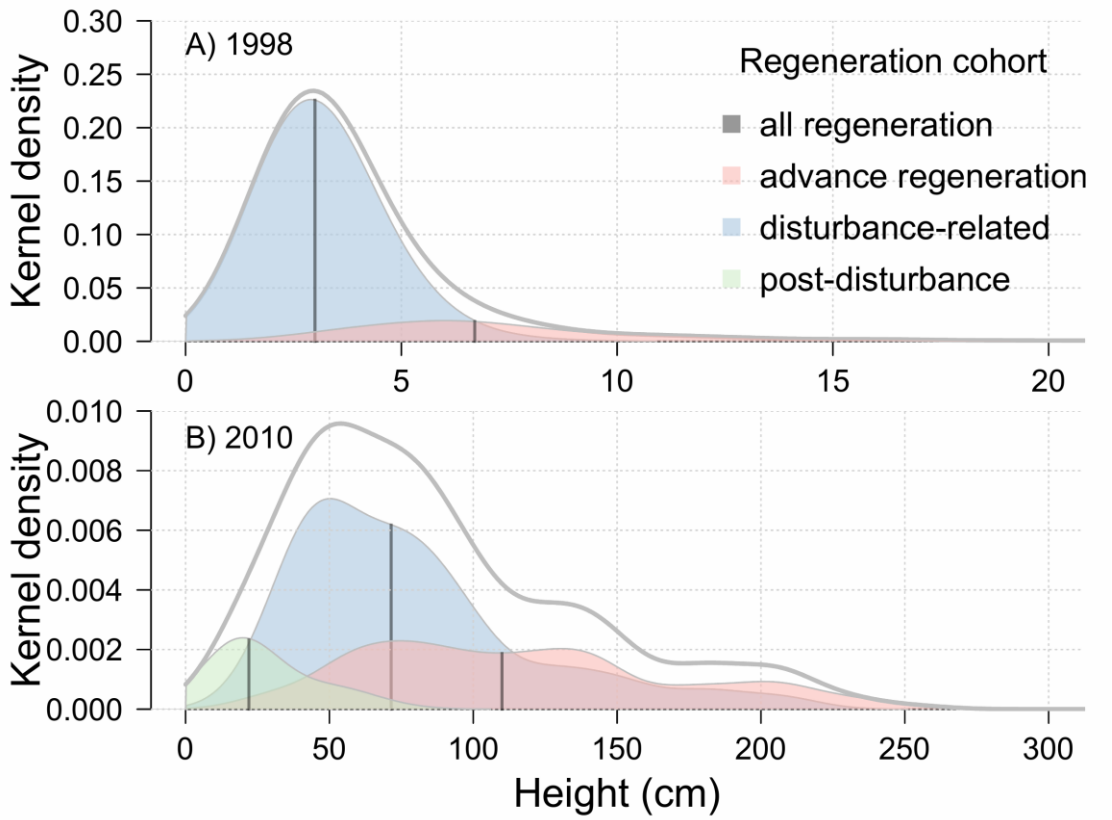

Figure 3. *Height distribution of seedlings and saplings A) in 1998; and B) in 2010. Grey solid line shows height distribution of all regeneration, colored areas show height distributions of separate regeneration cohorts. Vertical lines denote median heights for each cohort separately. Note different scales used. Regeneration during bark-beetle outbreak comprised mostly 1-2 year old seedlings of height < 5 cm established during the outbreak itself (A). Twelve years later (B), the dominance of this disturbance-related cohort was still apparent, but the relative proportion of advance regeneration increased. Only a small fraction of seedlings got established after the canopy dieback.*

In 2010, spruce dominated regeneration with densities varying among plots from 39 to 17,275 individuals ha^{-1}, with a median of 1,601 individuals ha^{-1}. Other tree species were far less abundant: only *Sorbus aucuparia* was present regularly, with median density of 66 individuals ha^{-1} (3.6% of total counts). Light-demanding pioneer species (*Betula* spp., *Salix* spp.) appeared sparsely, together comprising only 0.6% of regeneration. For individual plot values see Appendix S1: Table S1.

Density of regeneration on plots 12 years after the outbreak was 3.9 times the pre-disturbance density of canopy trees (calculated as median of pair-wise ratios). However, regeneration density decreased with increasing elevation by an order of magnitude every 122 m (linear regression, densities log-transformed, $R^2_{adj.} = 0.43$, $F_{1,19} = 16.31$, $p < 0.001$). All plots below 1300 m a.s.l. had regeneration densities higher than their pre-

disturbance stem densities, but above this elevation 5 out of 8 plots had less regeneration than their pre-disturbance numbers of canopy trees.

Growth

Median height rose from 7.3 cm (1998) to 110 cm (2010) for pre-disturbance regeneration and from 3.3 cm to 71.5 cm for disturbance-related regeneration. The median height of post-disturbance regeneration was 26 cm in 2010. During the 12 years after the outbreak, height variability of all regeneration present increased substantially (Fig. 3).

Fitted growth functions differed substantially in residual error structure (Appendix S1: Fig. S1). Logistic and Gompertz growth functions had the lowest RMSE (5 cm and 5.1 cm; Tab. 2). No trends in residual error structure were apparent for the Gompertz growth function. Chapman-Richards, Bertalanffy, Korf and Hossfeld IV growth functions substantially underestimated the height of the youngest recruits, while logistic growth function overestimated it (Appendix S1: Fig. S1). Therefore, we chose the Gompertz growth function for further analyses. Rooting microsite was not related to individual growth rate (approx. log-Likelihood ratio 20.75, p = 0.108; δAIC = +7.24).

In general, young seedlings grew slowly, but their growth gradually accelerated (Fig. 4). The median annual height increment was 1.1 cm for year-2 seedlings (i.e., in their second growing season), but 4 cm and 11 cm for year-10 and year-15 saplings, respectively. Accordingly, the median age needed to reach the height of 10 cm was almost 6 years (6 growing seasons), and to reach breast height (1.3 m) it was almost 16 years.

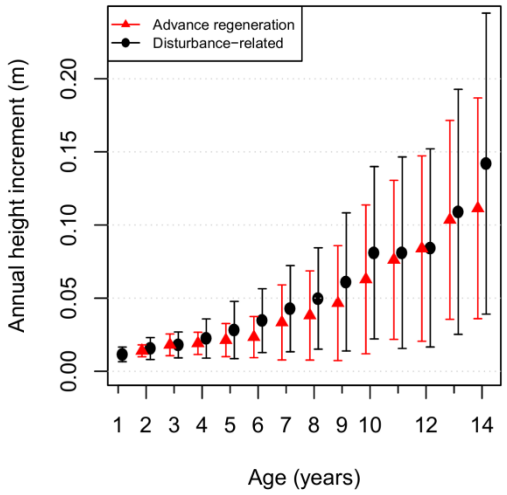

Figure 4. *Annual height increments (mean ±1 SD) observed for juveniles regarding their age and cohort rank.*

***Table 2**. Growth function equations. Asymptotic height (parameter a) was set as 26.85 m for all functions; standard errors (SE) of fixed effect terms are given.*

Growth curve	Equation	RMSE	Parameter estimates ± *SE*
Logistic	height ~ a/(1+c*exp(-b*age))	0.050	b = 0.2191 ± 0.0038 c = 1083.8 ± 26.727
Gompertz	height ~ a*exp(-b*exp(-c*t))	0.051	b = 7.606 ± 0.0406 c = 0.0482 ±0.0014
Chapman-Richards	height ~ a*(1-exp(-b*age)^c)	0.067	b = 0.0131 ± 0.0016 c = 2.103 ± 0.1155
Bertalanffy	height ~ a*(1-exp(-b*age)^3	0.071	b = 0.0236 ± 0.0006
Korf	height ~ a*exp(-b*age^-c)	0.092	b = 11.9955 ±0.6293 c = 0.4099 ± 0.0243
Hossfeld IV	height ~ t^c/(b+t^c/a)	0.100	b = 373.9 ± 8.832 c = 2.02 ± 0.0138

MORTALITY

Smallest seedlings faced the highest mortality (Fig. 5), which sharply decreased with increasing seedling height: tenfold increase in height reduced mortality odds 47.47 times (χ^2 = 356.75; df = 1; p < 0.001). Additionally, mortality was affected by rooting microsite (χ^2 = 93.98; df = 7; p < 0.001). Mortality risk was lowest at wood-related microsites – logs, stumps and tree bases – with odds ratio ranging from 0.55 to 0.66 (Tab. 1). In contrast, graminoid-dominated microsites showed the highest mortality risk (odds ratio 2.24). Seedlings rooting in litter, moss, *Lycopodium* and pits & mounds microsites had a moderate mortality risk (Fig. 5). Mortality risk was independent of plot elevation (χ^2= 0.26; p = 0.62; ΔAIC= +1.8).

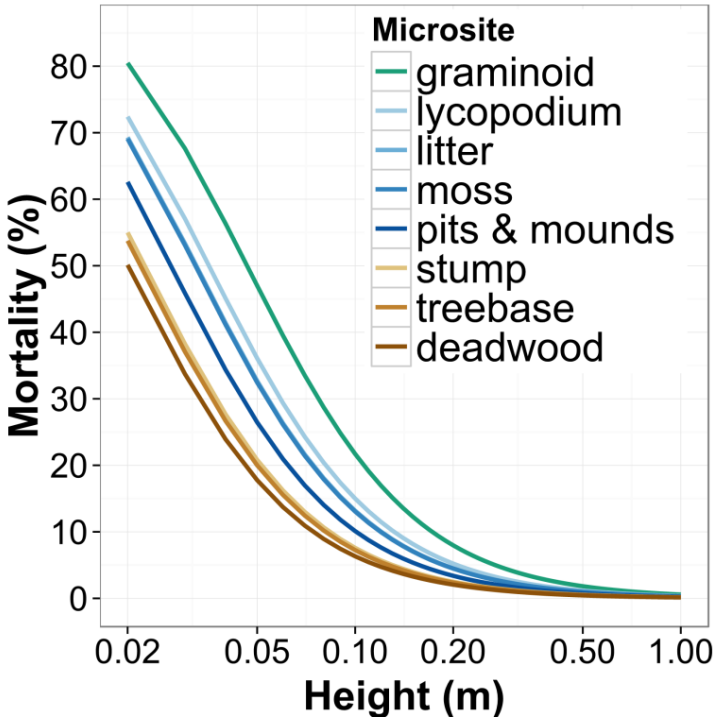

Figure 5. *Annual mortality steeply decreases with height and differs for particular microsites. Overall, the highest mortality was for seedlings growing in graminoid vegetation, whereas seedlings rooting in deadwood had the lowest mortality. Lines show marginal predictions of mortality model.*

Regeneration dynamics model

The predictive model built on data from the first three survey years started with 1028 juvenile trees in 2000. After ten years, all model runs predicted higher numbers of surviving saplings than were actually observed in 2010 (Appendix S1: Table S2). According to the model, the annual mortality dropped below 1% in 2010. While the model overestimates the number of surviving saplings, it predicts regeneration height structure reasonably well. The mean predicted tree height (88 cm) was only slightly lower than the observed mean height (92 cm). Moreover, the difference in the means was significant only for 1% of simulations and K-S test revealed 57.8% simulated empiric distribution functions to be equal with the observed ones (Fig. 6).

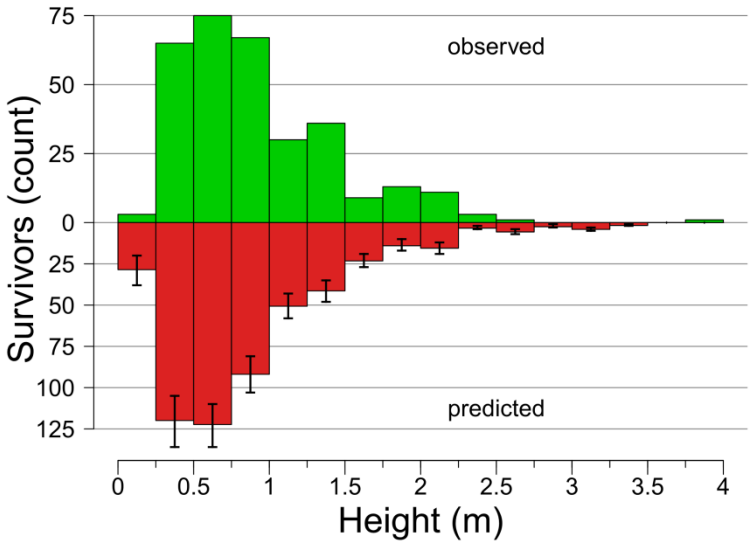

Figure 6. *Observed height distribution (upper green bars) corresponds to the year 2010 predictions (lower red bars), while total number of survivors is systematically overestimated. Error bars delimit 95% simulation interval.*

The model predicted an increase in the amount of pre-disturbance regeneration relative to disturbance-related regeneration, which was similar to that actually observed (K-S test of age distributions insignificant in all simulations). The observed and predicted trends in proportions of trees rooting in specific microsites were similar. The only exception was tree-base microsite, for which the model predicted a higher proportion of juvenile trees than observed (for details see Appendix S1: Table S2).

2.6 Discussion

Regeneration structure

Our hypothesis H1 that advance regeneration would dominate after the bark-beetle outbreak was rejected. Despite high mortality, disturbance-related regeneration outnumbered all other cohorts during the 12-year observation period. After the canopy dieback, seed rain apparently decreased and the proportion of unsuitable patches occupied by graminoids or dense clumps of tree regeneration increased. This explains the minimal establishment of new seedlings after the canopy dieback. The relative importance of advance regeneration increased over the evaluated period because it had the lowest mortality. To the future, we expect the relative proportions of regeneration groups to remain stable because all groups reached low mortality (about 1% annually).

The dominance of disturbance-related regeneration can be ascribed to the timing of several events. The bark-beetle outbreak created a temporal window allowing establishment of numerous seedlings originating mostly from the last mast year in 1995, immediately before the outbreak. These seedlings germinated in 1996, after the outbreak began. The timing of mast seeding preceding an outbreak could be of major significance for regeneration assembly, but mast years are relatively frequent in our study area, occurring on average every three years over the last 20 years (Zeppenfeld et al. 2015). Therefore, a relatively abundant seedling bank could be maintained continuously despite limited long-term survival.

The abundant seedling establishment during canopy dieback suggests that most regeneration usually considered as "advance" – i.e. established before a bark-beetle outbreak – could in fact originate during the disturbance itself. This has far-reaching consequences, because the processes driving regeneration establishment are markedly different before and during a bark-beetle outbreak. Even the shade-tolerant "true" advance regeneration is light-limited and survives mostly in patches under small canopy openings (Metslaid et al. 2007, Nigh et al. 2008, Kathke and Bruelheide 2010). As the stand infested by bark-beetles gradually opens, the seedlings can readily establish on a wider range of microsites until they are outcompeted by expanding vegetation. Canopy trees thus self-replace mostly during disturbance itself. This self-replacing mechanism

leads to the long-term stability of tree species composition and genetic structure of populations. Such positive relationship between conspecific overstory and understory (called 'neighborhood effect') was proposed by Frelich and Reich (1999) as major factor forming forest dynamics. Zeppenfeld et al. (2015) recently showed positive neighborhood effect also in European mountain spruce forest. Our results corroborated this finding but showed that not only advance regeneration, but also disturbance-related regeneration contributed to continuous dominance of spruce.

More precise specification of cohorts in terms of their temporal relationships to disturbance is needed. We propose that the term "advance regeneration" should be used only for those juveniles that have already passed the earlier high-mortality stage and have a higher chance to survive in the understory for a longer time, typically decades. The seedlings established during or just before a disturbance, which experienced different ecological conditions, but share similar seed-source would be called "disturbance-related regeneration". We are convinced that using this more precise differentiation could change the interpretation of many observed tree recovery patterns as well as forest practitioners' perception of disturbance.

Regeneration height growth

We found the absolute increments in early life stages of spruce to be quite small but gradually increasing (Fig. 4). Since it usually takes 6 years for a juvenile to reach 10 cm height (but varying greatly among individuals), this height class includes an important fraction of regeneration even several years after disturbance. Unfortunately, a common practice in forest inventory is to record only seedlings taller than 10 cm or more (Schweiger and Sterba 1997, Heurich 2009, Tomppo et al. 2010, Zeppenfeld et al. 2015). Our data showed that the information about tree regeneration captured by these inventories is incomplete, if not biased. For example, a stand with massive regeneration during a bark-beetle outbreak can be classified by standard forest inventories as having insufficient regeneration even several years after the outbreak.

The quality of fit differed considerably between growth functions used. We chose the Gompertz function as most suitable for fitting height growth of juvenile spruce trees because it showed the best fit and stability of residuals. Rammig et al. (2007) recommended the Bertalanffy growth function for fitting growth of young saplings, but they did not provide comparison with other growth functions. However, their data also showed that Bertalanffy function systematically underpredicts heights in the smallest height category. Since juvenile mortality is tightly coupled with tree height, the selection of an accurate growth function is crucial for the proper prediction of the regeneration process.

Processes structuring regeneration

Seedling microsite preferences are thought to be the main driver of regeneration spatial pattern and density (Kuuluvainen and Kalmari 2003, Wild et al. 2014). Because height-dependent mortality excludes slowly growing individuals from regeneration, we expected that microsites will affect mortality indirectly through differentiated height growth. However, we found no significant effects of microsites on height growth. Published evidence is ambivalent: height growth at wood-related microsites was reported to be lower (Kathke & Bruelheide 2010), unaffected (Kupferschmid and Bugmann 2005), or even higher (Baier *et al.* 2006). Height growth variation thus seems to be influenced by other factors, such as intraspecific competition (Metslaid et al. 2007).

In contrast, we found considerable differences in tree mortality among microsites. Low mortality found on decaying wood and at the bases of standing stems is in accord with the often-reported increase in regeneration densities on these microsites (Kuuluvainen 1994; Kuuluvainen & Kalmari 2003; Bače *et al.* 2012). However, low mortality values contradict Kathke & Bruelheide (2010), who deduced from regeneration age structure that mortality is highest on log and stump microsites. Low mortality without improved growth at these wood-related microsites suggests that spruce regeneration occurs preferentially there due to lower stress-induced mortality, rather than better growth conditions enabling the juveniles to grow out of high mortality stages. Indeed, differences in microsite-specific mortality levels can be attributed to various mechanisms that could include the much greater stress caused by competition in patches occupied by graminoids, lower snow-mold infection rates on microsites with shortened snow cover duration (Cunningham et al. 2006), or better moisture conditions on decayed logs and stumps preventing seedling desiccation (Takahashi and Sakai 2000, Bače et al. 2012). Our hypothesis H2, that regeneration is structured through microsite-specific individual performance, was thus supported, but the main underlying driver was tree mortality rather than height growth.

Our findings of microsite effects on tree mortality allow us to clarify how the clustered spatial pattern of Norway spruce regeneration arises. The previous hypothesis of secondary seed dispersal into snow "tree wells" around trunks and snags was based only on snapshot data (Wild et al. 2014). Here we provide an alternative explanation that improved juvenile survival around tree trunks and snags governs the formation of such a pattern, but these processes could act simultaneously. Further research is needed to disentangle them precisely.

Interestingly, we found no relationship between mortality and elevation. However, sapling densities decreased considerably with elevation: in five stands above 1300 m, we even found regeneration densities lower than the pre-disturbance stem density. The gradient in density is probably driven by decreasing seed production or germination, as

was shown in the Alps (Mencuccini, Piussi & Zanzi Sulli 1995). Recruitment on these sites thus strongly depends on microsite availability and sparse canopies can persist there for decades. Further research is needed to ascertain whether the canopy gaps will be infilled, or if the sparse canopies will persist. With this exception, regeneration densities were several times higher than pre-disturbance canopy density. Self-thinning is thus likely to be the most important driver of future sapling mortality, but this can take decades to manifest in shade-tolerant spruce (Pretzsch 2006).

Evaluation of predictions based on short-term data

We expected that short-term monitoring of individual seedlings after the disturbance would not be sufficient to predict further stand development. Surprisingly, our model based on only three years of monitoring provided satisfactory predictions for some aspects of regeneration structure development. Individually modelled tree growth following the Gompertz function and non-random mortality provided realistic height and age distribution estimates even ten years later, despite height growth being strictly nonlinear and mean height increasing nine-fold in the evaluated period.

However, the same model systematically overestimated the total number of surviving individuals. This is probably a result of underestimated mortality due to increasing competition with other juveniles and expanding graminoids. Kupferschmid *et al.* (2006) achieved better prediction accuracy with a model that included changes in competition. However, we were not able to include competition in our model because competition is not practically possible to parametrize from only three years of data.

Management recommendations

We provide strong evidence that self-replacement of mountain spruce forests after bark-beetle outbreak is possible without any management intervention. Moreover, because most of the regeneration comprises trees that germinated during the gradual stand-dieback, even stands lacking advance regeneration could recover naturally. Although young seedlings with height <10 cm at the time of outbreak suffer high mortality, their role in stand recovery is crucial. Individuals that emerged from such seedlings form the dominant cohort even a decade after the disturbance. Therefore, the practice of counting only seedlings above a pre-defined threshold height, which is frequently employed in current forest inventories, must change, as it excludes potentially important seedlings and can lead to seriously biased management recommendations. We propose that forest inventories should include all regeneration, with height classes weighted by expected future mortality. Similarly, the prediction of regeneration growth should be based on longer (> 3 year) observation; otherwise the tree counts could be strongly overestimated. Although our study was based on observations only in one region, given the ecological similarity of conifer dominated forests in the northern

hemisphere, our results have far reaching consequences, which could be applicable elsewhere.

Spatially structured stands with complex age and height distributions of young trees formed rapidly despite relatively uniform initial conditions. Resulting stand heterogeneity, together with the biological legacies of the former stands, contributes to the high biodiversity of unsalvaged stands (Kouki et al. 2001, Müller et al. 2008, Thorn et al. 2014). Salvage logging can thus damage natural regeneration in the time most critical for seedling establishment and disrupt or postpone the regeneration process. Moreover, excluding soil disturbance caused by salvage logging protects the site from invasion by pioneer and weedy species (Fischer et al. 2015, Nováková and Edwards-Jonášová 2015). Therefore, we consider natural regeneration as an appropriate management practice after bark-beetle outbreaks in natural Norway spruce forests.

2.7 Acknowledgements

We thank Maria L. Bauer for providing the initial data set, the Bavarian Forest National Park administration for support and logistics during field work, Jonathan Rosenthal and Peter Szabo for proofreading and numerous students for field work. We also thank three anonymous reviewers for very useful comments that improved our paper. The work was supported by GACR P504/10/0843 and P504/12/1218, and was part of long-term research development project No. RVO 67985939. M. Svoboda and J. Wild were also supported by the CIGA CULS project No. 20164310.

2.8 References

Arnold, T., and J. Emerson. 2011. Nonparametric goodness-of-fit tests for discrete null distributions. The R Journal:34–39.

Bače, R., M. Svoboda, and P. Janda. 2011. Density and Height Structure of Seedlings in Subalpine Spruce Forests of Central Europe: Logs vs . Stumps as a Favourable Substrate. Silva Fennica 45:1065–1078.

Bače, R., M. Svoboda, P. Janda, R. C. Morrissey, J. Wild, J. L. Clear, V. Čada, and D. C. Donato. 2015. Legacy of Pre-Disturbance Spatial Pattern Determines Early Structural Diversity following Severe Disturbance in Montane Spruce Forests. Plos One 10:e0139214.

Bače, R., M. Svoboda, V. Pouska, P. Janda, and J. Červenka. 2012. Natural regeneration in Central-European subalpine spruce forests: Which logs are suitable for seedling recruitment? Forest Ecology and Management 266:254–262.

Baier, R., R. Ettl, C. Hahn, and A. Göttlein. 2006. Early development and nutrition of Norway spruce (Picea abies (L.) Karst.) seedlings on different seedbeds in the Bavarian limestone Alps – a bioassay. Annals of Forest Science 63:339–348.

Bates, D., M. Mächler, B. Bolker, and S. Walker. 2015. Fitting Linear Mixed-Effects Models Using lme4. Journal of Statistical Software 67:1–48.

Bauer, M. L. 2002. Walddynamik nach Borkenkäferbefall in den Hochlagen des Bayerischen Waldes.

Bauer, M. L., A. Fischer, H. EL Kate, and R. Mosandl. 2008. Verjüngungsdynamik nach großflächigem Borkenkäferbefall in den Fichtenwäldern der Hochlagen des Bayerischen Waldes. Allgemeine Forst und Jagdzeitung 179:43–52.

Berec, L., P. Doležal, and M. Hais. 2013. Population dynamics of Ips typographus in the Bohemian Forest (Czech Republic): Validation of the phenology model PHENIPS and impacts of climate change. Forest Ecology and Management 292:1–9.

Beudert, B., C. Bässler, S. Thorn, R. Noss, B. Schröder, H. Dieffenbach-Fries, N. Foullois, and J. Müller. 2015. Bark Beetles Increase Biodiversity While Maintaining Drinking Water Quality. Conservation Letters 8:272–281.

Brůna, J., J. Wild, M. Svoboda, M. Heurich, and J. Müllerová. 2013. Impacts and underlying factors of landscape-scale, historical disturbance of mountain forest identified using archival documents. Forest Ecology and Management 305:294–306.

Burton, P. J., M. Svoboda, D. Kneeshaw, and K. W. Gottschalk. 2015. Options for Promoting the Recovery and Rehabilitation of Forests Affected by Severe Insect Outbreaks. Pages 495–517 in J. A. Stanturf, editor. Restoration of Boreal and Temperate Forests. CRC Press, Boca Raton, Florida.

Crawley, M. J. 2007. The R Book. John Wiley & Sons, Ltd, Chichester, UK.

Cunningham, C., N. E. Zimmermann, V. Stoeckli, and H. Bugmann. 2006. Growth of Norway spruce (Picea abies L.) saplings in subalpine forests in Switzerland: Does spring climate matter? Forest Ecology and Management 228:19–32.

Čada, V., R. C. Morrissey, Z. Michalová, R. Bače, P. Janda, and M. Svoboda. 2016. Frequent severe natural disturbances and non-equilibrium landscape dynamics shaped the mountain spruce forest in central Europe. Forest Ecology and Management 363:169–178.

Dale, V. H., L. A. Joyce, S. McNulty, R. P. Neilson, M. P. Ayres, M. D. Flannigan, P. J. Hanson, L. C. Irland, A. E. Lugo, C. J. Peterson, D. Simberloff, F. J. Swanson, B. Stocks, and M. B. Wotton. 2001. Climate Change and Forest Disturbances. BioScience 51:723.

DeRose, R. J., and J. N. Long. 2010. Regeneration response and seedling bank dynamics on a Dendroctonus rufipennis -killed Picea engelmannii landscape. Journal of Vegetation Science 21:377–387.

Diskin, M., M. E. Rocca, K. N. Nelson, C. F. Aoki, and W. H. Romme. 2011. Forest developmental trajectories in mountain pine beetle disturbed forests of Rocky Mountain National Park, Colorado. Canadian Journal of Forest Research 41:782–792.

Donato, D. C., J. L. Campbell, and J. F. Franklin. 2012. Multiple successional pathways and precocity in forest development: can some forests be born complex? Journal of Vegetation Science 23:576–584.

Donato, D. C., J. B. Fontaine, J. L. Campbell, W. D. Robinson, J. B. Kauffman, and B. E. Law. 2006. Post-wildfire logging hinders regeneration and increases fire risk. Science 311:352.

Edburg, S. L., J. A. Hicke, P. D. Brooks, E. G. Pendall, B. E. Ewers, U. Norton, D. Gochis, E. D. Gutmann, and A. J. H. Meddens. 2012. Cascading impacts of bark beetle-caused tree mortality on coupled biogeophysical and biogeochemical processes. Frontiers in Ecology and the Environment 10:416–424.

Elling, W., E. Bauer, G. Klemm, and H. Koch. 1987. Klima und Böden: Waldstandorte. Bayerischen Staats- ministerium für Ernährung, Landwirtschaft und Forsten, Grafenau.

Fettig, C. J., K. D. Klepzig, R. F. Billings, A. S. Munson, T. E. Nebeker, J. F. Negron, and J. T. Nowak. 2007. The effectiveness of vegetation management practices for prevention and control of bark beetle infestations in coniferous forests of the western and southern United States. Forest Ecology and Management 238:24–53.

Fischer, A., and H. S. Fischer. 2011. Individual-based analysis of tree establishment and forest stand development within 25 years after wind throw. European Journal of Forest Research 131:493–501.

Fischer, A., H. S. Fischer, M. Kopecký, M. Macek, and J. Wild. 2015. Small changes in species composition despite stand-replacing bark beetle outbreak in Picea abies mountain forests. Canadian Journal of Forest Research 45:1164–1171.

Fischer, A., P. Marshall, and A. Camp. 2013. Disturbances in deciduous temperate forest ecosystems of the northern hemisphere: their effects on both recent and future forest development. Biodiversity and Conservation 22:1863–1893.

Franklin, J. F., T. A. Spies, R. Van Pelt, A. B. Carey, D. A. Thornburgh, D. R. Berg, D. B. Lindenmayer, M. E. Harmon, W. S. Keeton, D. C. Shaw, K. Bible, and J. Q. Chen. 2002. Disturbances and structural development of natural forest ecosystems with silvicultural implications, using Douglas-fir forests as an example. Forest Ecology and Management 155:399–423.

Frelich, L. E., and P. B. Reich. 1999. Neighborhood Effects, Disturbance Severity, and Community Stability in Forests. Ecosystems 2:151–166.

Grenfell, R., T. Aakala, and T. Kuuluvainen. 2011. Microsite Occupancy and the Spatial Structure of Understorey Regeneration in Three Late-Successional Norway Spruce Forests in Northern Europe. Silva Fennica 45:1093–1110.

Grodzki, W., R. Jakuš, E. Lajzová, Z. Sitková, T. Maczka, and J. Škvarenina. 2006. Effects of intensive versus no management strategies during an outbreak of the bark beetle Ips typographus (L.) (Col.: Curculionidae, Scolytinae) in the Tatra Mts. in Poland and Slovakia. Annals of Forest Science 63:55–61.

Harvey, B. J., D. C. Donato, and M. G. Turner. 2014. Recent mountain pine beetle outbreaks, wildfire severity, and postfire tree regeneration in the US Northern Rockies. Proceedings of the National Academy of Sciences 111:15120–15125.

Heurich, M. 2009. Progress of forest regeneration after a large-scale Ips typographus outbreak in the subalpine Picea abies forests of the Bavarian Forest National Park. Silva Gabreta 15:49–66.

Jonášová, M., and K. Prach. 2004. Central-European mountain spruce (Picea abies (L.) Karst.) forests: regeneration of tree species after a bark beetle outbreak. Ecological Engineering 23:15–27.

Jonášová, M., and K. Prach. 2008. The influence of bark beetles outbreak vs. salvage logging on ground layer vegetation in Central European mountain spruce forests. Biological Conservation 141:1525–1535.

Kaňa, J., K. Tahovská, and J. Kopáček. 2012. Response of soil chemistry to forest dieback after bark beetle infestation. Biogeochemistry 113:369–383.

Kathke, S., and H. Bruelheide. 2010. Interaction of gap age and microsite type for the regeneration of Picea abies. Forest Ecology and Management 259:1597–1605.

Köster, K., K. Voolma, K. Jõgiste, M. Metslaid, and D. Laarmann. 2009. Assessment of tree mortality after windthrow using photo-derived data. Annales Botanici Fennici 46:291–298.

Kouki, J., S. Lofman, P. Martikainen, S. Rouvinen, and A. Uotila. 2001. Forest Fragmentation in Fennoscandia: Linking Habitat Requirements of Woodassociated Threatened Species to Landscape and Habitat Changes. Scandinavian Journal of Forest Research:27–37.

Kupferschmid, A. D., P. Brang, W. Schönenberger, and H. Bugmann. 2006. Predicting tree regeneration in Picea abies snag stands. European Journal of Forest Research 125:163–179.

Kupferschmid, A. D., and H. Bugmann. 2005. Effect of microsites, logs and ungulate browsing on Picea abies regeneration in a mountain forest. Forest Ecology and Management 205:251–265.

Kuuluvainen, T. 1994. Gap disturbance, ground microtopography, and the regeneration dynamics of boreal coniferous forests in Finland: a review. Annales Zoologici Fennici 31:35–51.

Kuuluvainen, T., and P. Juntunen. 1998. Seedling establishment in relation to microhabitat variation in a windthrow gap in a boreal Pinus sylvestris forest. Journal of Vegetation Science 9:551–562.

Kuuluvainen, T., and R. Kalmari. 2003. Regeneration microsites of Picea abies seedlings in a windthrow area of a boreal old-growth forest in southern Finland. Annales Botanici Fennici 40:401–413.

Lausch, A., L. Fahse, and M. Heurich. 2011. Factors affecting the spatio-temporal dispersion of Ips typographus (L.) in Bavarian Forest National Park: A long-term quantitative landscape-level analysis. Forest Ecology and Management 261:233–245.

Lehnert, L. W., C. Bässler, R. Brandl, P. J. Burton, and J. Müller. 2013. Conservation value of forests attacked by bark beetles: Highest number of indicator species is found in early successional stages. Journal for Nature Conservation 21:97–104.

Lindenmayer, D. B., and R. F. Noss. 2006. Salvage logging, ecosystem processes, and biodiversity conservation. Conservation Biology 20:949–958.

Meddens, A. J. H., J. A. Hicke, and C. A. Ferguson. 2012. Spatiotemporal patterns of observed bark beetle-caused tree mortality in British Columbia and the western United States. Ecological Applications 22:1876–1891.

Mencuccini, M., P. Piussi, and A. Z. Sulli. 1995. Thirty years of seed production in a subalpine Norway spruce forest: patterns of temporal and spatial variation. Forest Ecology and Management 76:109–125.

Metslaid, M., K. Jõgiste, E. Nikinmaa, W. K. Moser, and A. Porcar-Castell. 2007a. Tree variables related to growth response and acclimation of advance regeneration of Norway spruce and other coniferous species after release. Forest Ecology and Management 250:56–63.

Metslaid, M., K. Jogiste, E. Nikinmaa, W. Moser, and a Porcarcastell. 2007b. Tree variables related to growth response and acclimation of advance regeneration of Norway spruce and other coniferous species after release. Forest Ecology and Management 250:56–63.

Müller, J., H. Bußler, M. Goßner, T. Rettelbach, and P. Duelli. 2008. The European spruce bark beetle Ips typographus in a national park: from pest to keystone species. Biodiversity and Conservation 17:2979–3001.

Nigh, G. D., J. a. Antos, and R. Parish. 2008. Density and distribution of advance regeneration in mountain pine beetle killed lodgepole pine stands of the Montane Spruce zone of southern British Columbia. Canadian Journal of Forest Research 38:2826–2836.

Nováková, M. H., and M. Edwards-Jonášová. 2015. Restoration of Central-European mountain Norway spruce forest 15 years after natural and anthropogenic disturbance. Forest Ecology and Management 344:120–130.

Pinheiro, J., D. Bates, S. DebRoy, D. Sarkar, and the R Core team. 2013. nlme: Linear and Nonlinear Mixed Effects Models. R package version 3.1-108.

Pretzsch, H. 2006. Species-specific allometric scaling under self-thinning: evidence from long-term plots in forest stands. Oecologia 146:572–83.

Pretzsch, H. 2010. Forest Dynamics, Growth and Yield. Springer Berlin Heidelberg.

R Core Team. 2015. R: A language and environment for statistical computing , Vienna, Austria. URL http://www.R-project.org/. R Foundation for Statistical Computing, Vienna, Austria.

Raffa, K., and B. Aukema. 2008. Cross-scale drivers of natural disturbances prone to anthropogenic amplification: the dynamics of bark beetle eruptions. BioScience 58:501–518.

Rammig, A., P. Bebi, H. Bugmann, and L. Fahse. 2007. Adapting a growth equation to model tree regeneration in mountain forests. European Journal of Forest Research 126:49–57.

Seidl, R., W. Rammer, D. Jäger, and M. J. Lexer. 2008. Impact of bark beetle (Ips typographus L.) disturbance on timber production and carbon sequestration in different management strategies under climate change. Forest Ecology and Management 256:209–220.

Seidl, R., M.-J. Schelhaas, W. Rammer, and P. J. Verkerk. 2014. Increasing forest disturbances in Europe and their impact on carbon storage. Nature Climate Change 4:806–810.

Schelhaas, M., G. Nabuurs, and A. Schuck. 2003. Natural disturbances in the European forests in the 19th and 20th centuries. Global Change Biology 9:1620–1633.

Schweiger, J., and H. Sterba. 1997. A model describing natural regeneration recruitment of Norway spruce (Picea abies (L.) Karst.) in Austria. Forest Ecology and Management 97:107–118.

Stadelmann, G., H. Bugmann, F. Meier, B. Wermelinger, and C. Bigler. 2013. Effects of salvage logging and sanitation felling on bark beetle (Ips typographus L.) infestations. Forest Ecology and Management 305:273–281.

Storaunet, K. O., and J. Rolstad. 2004. How long do Norway spruce snags stand? Evaluating four estimation methods.

Svoboda, M., P. Janda, T. A. Nagel, S. Fraver, J. Rejzek, and R. Bače. 2012. Disturbance history of an old-growth sub-alpine Picea abies stand in the Bohemian Forest, Czech Republic. Journal of Vegetation Science 23:86–97.

Swanson, M. E., J. F. Franklin, R. L. Beschta, C. M. Crisafulli, D. A. DellaSala, R. L. Hutto, D. B. Lindenmayer, and F. J. Swanson. 2011. The forgotten stage of forest succession: early-successional ecosystems on forest sites. Frontiers in Ecology and the Environment 9:117–125.

Takahashi, M., and Y. Sakai. 2000. Establishment of tree seedlings and water-soluble nutrients in coarse woody debris in an old-growth Picea – Abies forest in Hokkaido , northern Japan. Canadian Journal of Forest Research 1155:1148–1155.

Temperli, C., H. Bugmann, and C. Elkin. 2013. Cross-scale interactions among bark beetles, climate change, and wind disturbances: a landscape modeling approach. Ecological Monographs 83:383–402.

Thorn, S., C. Bässler, T. Gottschalk, T. Hothorn, H. Bussler, K. Raffa, and J. Müller. 2014. New insights into the consequences of post-windthrow salvage logging revealed by functional structure of saproxylic beetles assemblages. PloS one 9:e101757.

Tomppo, E., T. Gschwantner, R. McRoberts, and M. Lawrence. 2010. National Forest Inventories. (E. Tomppo, T. Gschwantner, M. Lawrence, and R. E. McRoberts, Eds.). Springer Netherlands.

Wermelinger, B. 2004. Ecology and management of the spruce bark beetle Ips typographus - a review of recent research. Forest Ecology and Management 202:67–82.

Wiegand, T., F. Jeltsch, I. Hanski, and V. Grimm. 2003. Using pattern-oriented modeling for revealing hidden information: a key for reconciling ecological theory and application. Oikos 65:209–222.

Wild, J., M. Kopecký, M. Svoboda, J. Zenáhlíková, M. Edwards-Jonášová, and T. Herben. 2014. Spatial patterns with memory: tree regeneration after stand-replacing disturbance in Picea abies mountain forests. Journal of Vegetation Science 25:1327–1340.

Zeppenfeld, T., M. Svoboda, R. J. DeRose, M. Heurich, J. Müller, P. Čížková, M. Starý, R. Bače, and D. C. Donato. 2015. Response of mountain Picea abies forests to stand-replacing bark beetle outbreaks: neighbourhood effects lead to self-replacement. Journal of Applied Ecology 52:1402–1411.

Zielonka, T. 2006. When does dead wood turn into a substrate for spruce replacement? Journal of Vegetation Science 17:739–746.

2.9 SUPPLEMENTARY MATERIALS

Table S1 *Attributes of study localities. Other species include Salix spp. and Betula spp.*

Site	Locality	Latitude (WGS84)	Longitude (WGS84)	Elevation (m a.s.l.)	Aspect	Inclination	1998 tree stems (ha^{-1})	2010 *P. abies* regeneration (ha^{-1})	2010 *S. aucuparia* regeneration (ha^{-1})	2010 other species (ha^{-1})
101	Plattenhausenriegel	48.965384	13.442958	1 302	SW	3.8	413	184	13	0
102	Lusen - Blaue Saule	48.951184	13.481550	1 233	SOS	2.6	550	3321	184	39
103	Lusen – Moorberg	48.948454	13.510177	1 329	O	3.1	531	1497	53	0
104	Reschbachklause	48.962621	13.547129	1 176	S	3.6	556	1825	289	13
201	Gr. Rachel	48.970273	13.388860	1 317	SW	1.4	363	39	0	0
202	Schwarzbach	48.973447	13.533087	1 229	SSO	1.8	656	12340	66	0
203	Reschbachklause	48.966068	13.554480	1 173	NW	1.4	588	2258	39	26
204	Reschbachklause	48.964811	13.554741	1 170	S	1.6	506	4831	131	39
211	Lackenberg	49.102625	13.309456	1 330	NW	2.6	494	801	158	26
214	Gr. Falkenstein	49.091633	13.285603	1 257	S	1.3	394	1693	79	0
301	Plattenhausenriegel	48.975853	13.420128	1 222	WSW	10.4	425	1602	66	0
302	Plattenhausenriegel	48.968806	13.434153	1 222	WSW	7.2	544	5907	158	79
303	Lusen - Moorberg	48.946709	13.512470	1 300	O	31.2	288	53	0	0
304	Lusen - Moorberg	48.951483	13.511743	1 319	O	32.6	275	328	249	0
401	Gr. Rachel	48.981010	13.379838	1 339	SW	9.1	444	276	26	0
402	Gr. Rachel	48.973776	13.382771	1 315	W	8.7	406	66	0	0
403	Reschbachklause	48.963234	13.567973	1 173	WNW	6	669	17276	591	0
404	Reschbachklause	48.969726	13.578729	1 236	SO	10.5	569	3584	53	53
411	Lackenberg	49.100530	13.310432	1 291	S	12.2	269	1050	184	53
412	Kiesruck	49.057351	13.336942	1 155	SW	10.1	319	3361	39	13
413	Kiesruck	49.052849	13.342718	1 227	W	8.6	531	1090	13	53

Table S2. *Regeneration dynamics model: initial conditions in 2000 and observed vs. predicted (median from 1000 simulations) values for 2010. ercentages in parentheses show cohort proportions to total number of survivors in given years.*

	2000	2010	
	Observed	Observed	Model prediction
Total no. of survivors	**1028**	**314**	**555**
Advance regeneration*	229 (22.3%)	108 (34.4%)	164 (29.5%)
Disturbance-related regeneration*	799 (77.7%)	206 (65.6%)	391 (70.5%)
Previous year mortality	43.30%	NA	0.92%
Mean height (m)	0.106	0.920	0.877
Proportion of juveniles on microsites (%)			
Litter	31.52	28.98	27.66
Treebase	21.11	18.15	25.09
Stump	19.75	25.16	23.81
Moss	13.33	8.92	10.07
Timber	7.30	11.78	8.61
Lycopodium	3.21	2.55	2.01
Pits & mounds	1.95	4.14	2.38
Graminoid	1.85	0.32	0.37

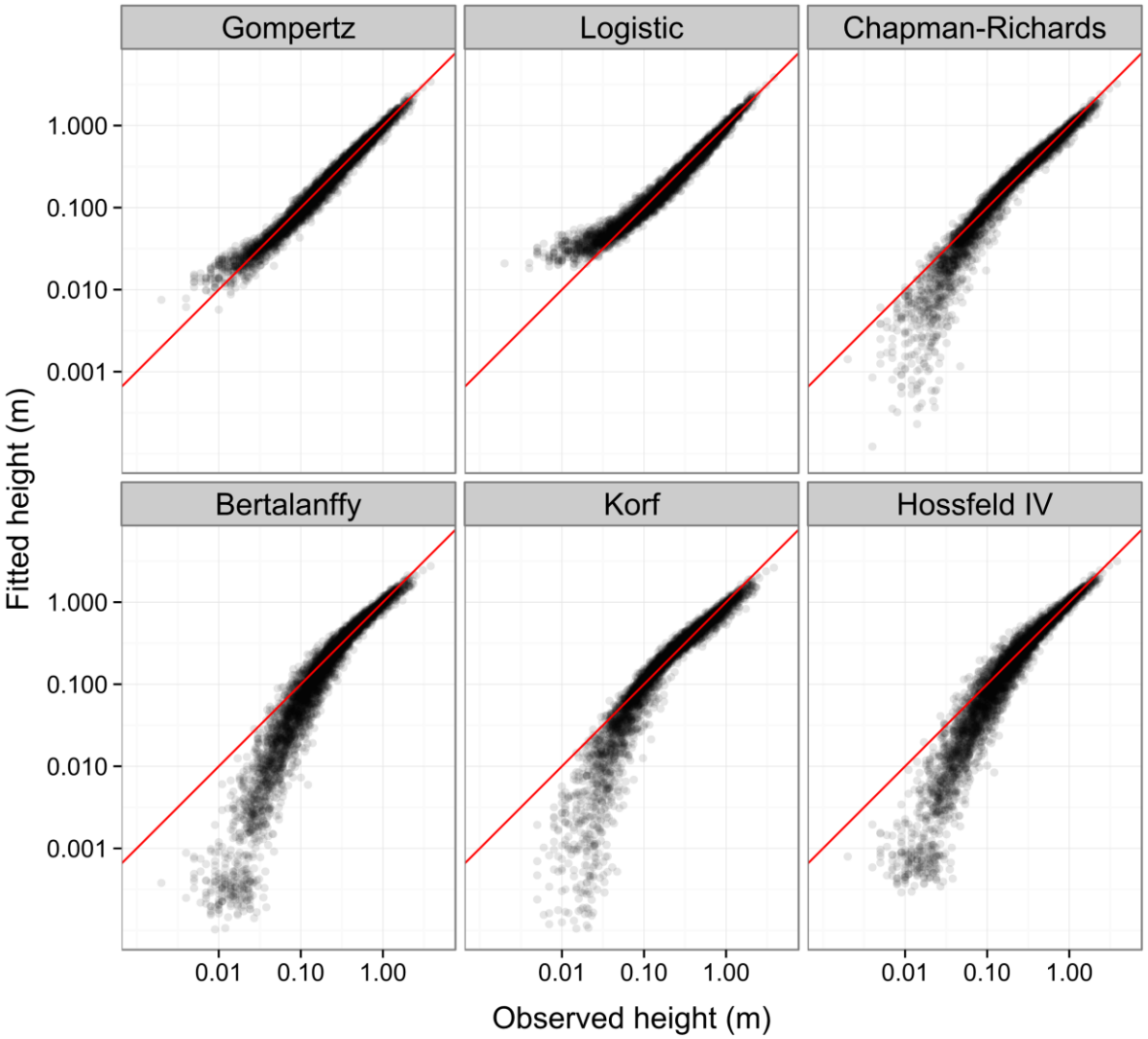

Figure S1. *Comparison of fit for six growth functions. Observed heights are plotted on horizontal axis, fitted values on vertical axis. Line represents 1:1 relation. Fit of Gompertz function is stable for all height classes, logistic function overestimates height of smallest seedlings (up to 0.1 m), while all other growth functions underestimate it.*

CHAPTER THREE:

MAXIMUM AIR TEMPERATURE CONTROLLED BY TERRAIN TOPOGRAPHY SHAPES FOREST PLANT DISTRIBUTION

MARTIN MACEK[1,2], MARTIN KOPECKÝ[1,3] AND JAN WILD[1,4]

1 Institute of Botany of the Czech Academy of Sciences, Zámek 1, CZ-252 43, Průhonice, Czech Republic
2 Charles University, Faculty of Science, Department of Botany, Benátská 2, CZ-128 01, Prague 2, Czech Republic
3 Faculty of Forestry and Wood Sciences, Czech University of Life Sciences Prague, Kamýcká 129, CZ-165 21, Prague 6 - Suchdol, Czech Republic
4 Faculty of Environmental Sciences, Czech University of Life Sciences Prague, Kamýcká 129, CZ-165 21, Prague 6 - Suchdol, Czech Republic

Published in: Landscape Ecology (2019) 34:2541-2556.
DOI: 10.1007/s10980-019-00903-x

3.1 *ABSTRACT*

Context Forest microclimates differ from regional macroclimates because forest canopies affect energy fluxes near the ground. However, little is known about the environmental drivers of understorey temperature heterogeneity and its effects on species assemblages, especially at landscape scales.

Objectives We aimed to identify which temperature variables best explain the landscape-scale distribution of forest plants and to disentangle the effects of elevation, terrain topography and canopy openness on understorey temperatures.

Methods We measured growing season air temperature, canopy cover and plant community composition within 46 plots established across a 400-km2 area in Czech Republic. We linked growing season maximum, mean and minimum temperatures with elevation, canopy cover and topographic proxies for heat load, topographic position, soil moisture and cold air drainage, and created fine-scale topoclimatic maps of the region. We compared the biological relevance of in situ measured temperatures and temperatures derived from fine-scaled topoclimatic maps and global WorldClim 2 maps.

Results Maximum temperature was the best predictor of understorey plant species composition. Landscape-scale variation in maximum temperature was jointly driven by elevation and terrain topography (R2adj. = 0.79) but not by canopy cover. Modelled maximum temperature derived from our topoclimatic maps explained significantly more variation in plant community composition than WorldClim 2 grids.

Conclusions Terrain topography creates landscape-scale variation in maximum temperature, which in turn controls plant species assembly within the forest understorey. Maximum temperature is therefore an important, but neglected microclimatic driver of species distribution across landscapes.

3.2 KEYWORDS

Canopy cover; iButton; Maximum temperature; Microclimate; Species composition; Temperate forest; Terrain attributes; Topoclimate; WorldClim 2

3.3 INTRODUCTION

The relationship between the climate and the distribution of species is at the core of ecology and biogeography. However, this relationship is usually studied using coarse-grained climatic data which do not capture the actual microclimates experienced by organisms (Franklin et al. 2013). Moreover, the selection of climate variables used in species distribution modelling is seldom based on their physiological relevance. Instead, readily available data are preferentially used, with mean annual temperature being the most overused climate variable in ecological modelling (Gardner et al. 2019). The resulting mismatch between coarse-grained climatic data and the real drivers of species distribution acting on fine scales can substantially bias both species distribution models and predictions of species' vulnerability to climate change (Ashcroft et al. 2012, Potter et al. 2013, Slavich et al. 2014). Microclimatic data are therefore essential in assessing climatic effects on the biota (Lembrechts et al. 2018).

Temperature variability across landscapes is driven not only by decreasing temperatures with elevation caused by adiabatic cooling, but also by topographic processes such as anisotropic surface heating, cold air drainage and evaporative cooling (Geiger et al. 2009). Whereas physical processes affecting local temperature variability are well understood, their complexity makes modelling long-term temperature across landscapes challenging. The recent development of miniaturized low-cost data loggers has allowed continuous microclimatic measurements at many sites across entire landscapes (Lookingbill and Urban 2003, Ashcroft et al. 2008, Vanwalleghem and Meentemeyer 2009, Fridley 2009, Wild et al. 2019). Empirical spatial predictions from these measurements suggest that topography-driven temperature variability can be high enough to create local microclimatic refugia able to buffer the effects of climate change on organisms (Ashcroft et al. 2009, Kulonen et al. 2018).

Forest understorey microclimates differ from the macroclimate because tree canopies limit air mixing, absorb incident radiation and force evapotranspiration rates (Geiger et al. 2009, Von Arx et al. 2012). Although the tree canopy has a weak effect on mean temperatures, it can substantially decrease maximum temperatures and increase minimum temperatures near the ground; in other words, forest canopies behave like thermal insulating layers (Vanwalleghem and Meentemeyer 2009, Suggitt et al. 2011, Davis et al. 2019). Therefore, understorey temperatures fluctuate less than those in tree-less habitats (Häntzschel et al. 2005). Because of this decoupling of forest microclimates from conditions above the canopy, topography is possibly a less influential driver of microclimates in forests than in tree-less habitats (Running et al. 1987, Treml and Banaš 2008, Vanwalleghem and Meentemeyer 2009). However, the effect of the forest canopy on understorey temperatures depends on the meteorological situation and on structural attributes and phenological phase of the canopy, making it difficult to generalize the

effects of the canopy, especially at landscape-scales or in the long term (Renaud and Rebetez 2009, Von Arx et al. 2012).

In temperate forests, the diversity of vascular plants is concentrated in the understorey (Gilliam 2007) and understorey plant species are sensitive to fine-scale microclimatic variation (Ashcroft et al. 2008, Tinya et al. 2019). Microclimatic conditions in the understorey are also relevant for tree seedling establishment and growth (Von Arx et al. 2013), causing possible feedbacks in the long-term.

It has been postulated that the effects of climate change in forests can be attenuated by increased canopy cover (De Frenne et al. 2013, Frey et al. 2016). However, the exact mechanism by which this can happen remains unclear because temperatures under forest canopy are not constantly offset from open-area temperatures, but positive offset in minimum and negative offset in maximum temperatures is the usual situation. In addition, the relative importance of different aspects of thermal variability for the forest biota is largely unknown because of a lack of relevant studies and potential interactions with light and moisture microclimatic conditions (Chen et al. 1999, Von Arx et al. 2013). Direct microclimatic measurements are necessary for addressing links between spatial and temporal variation in microclimate and macroclimate, topography, forest structural attributes and plant communities because evidence based on bioindication or standard weather station data may provide misleading results (Harwood et al. 2014).

In the present study, we measured forest understorey temperatures, canopy cover and recorded plant species composition across a broad topographic gradient to: (1) explore how elevation, local topography and canopy cover variation affect understorey temperatures; (2) identify which temperature variable (maximum, mean, or minimum) is the most influential driver of understorey plant communities; and (3) test whether fine-scale empirical topoclimatic model based on forest microclimate measurements can explain gradients in plant species composition better than analogous climatic grids with coarser resolution based on interpolated weather station data, such as WorldClim 2 dataset (Fick and Hijmans 2017).

3.4 METHODS

3.4.1 STUDY AREA

To explore links between local climates, terrain attributes and plant communities at a landscape scale, we set up a network of vegetation plots with *in situ* recorded temperatures in the České Středohoří region, Czech Republic (50°29' – 50°37' N; 13°52'– 14°12'E; Fig. 1). The area is formed by a chain of extinct volcanic hills rising above a sedimentary plateau. Elevations range from 122 m a.s.l. in the Elbe river basin to 837 m a.s.l. at the top of Milešovka hill. The climate is temperate with mean annual temperatures ranging

from 5 to 9°C, mean annual precipitation of 450–600 mm and prevailing westerly winds (Tolasz *et al.*, 2007).

Mostly semi-natural forests cover ca 28 % of the region (Fig. S1 in Electronic Supplementary Material 1). Thermophilous woodlands with sessile oak (*Quercus petraea* agg.) and European hornbeam (*Carpinus betulus*) occur at low elevations and on south-facing slopes, European beech (*Fagus sylvatica*) forests dominate on hilltops and northern slopes, and species-rich forests with limes (*Tilia cordata*, *T. platyphyllos)*, maples (*Acer pseudoplatanus*, *A. platanoides*) and wych elm (*Ulmus glabra*) cover steep slopes and screes.

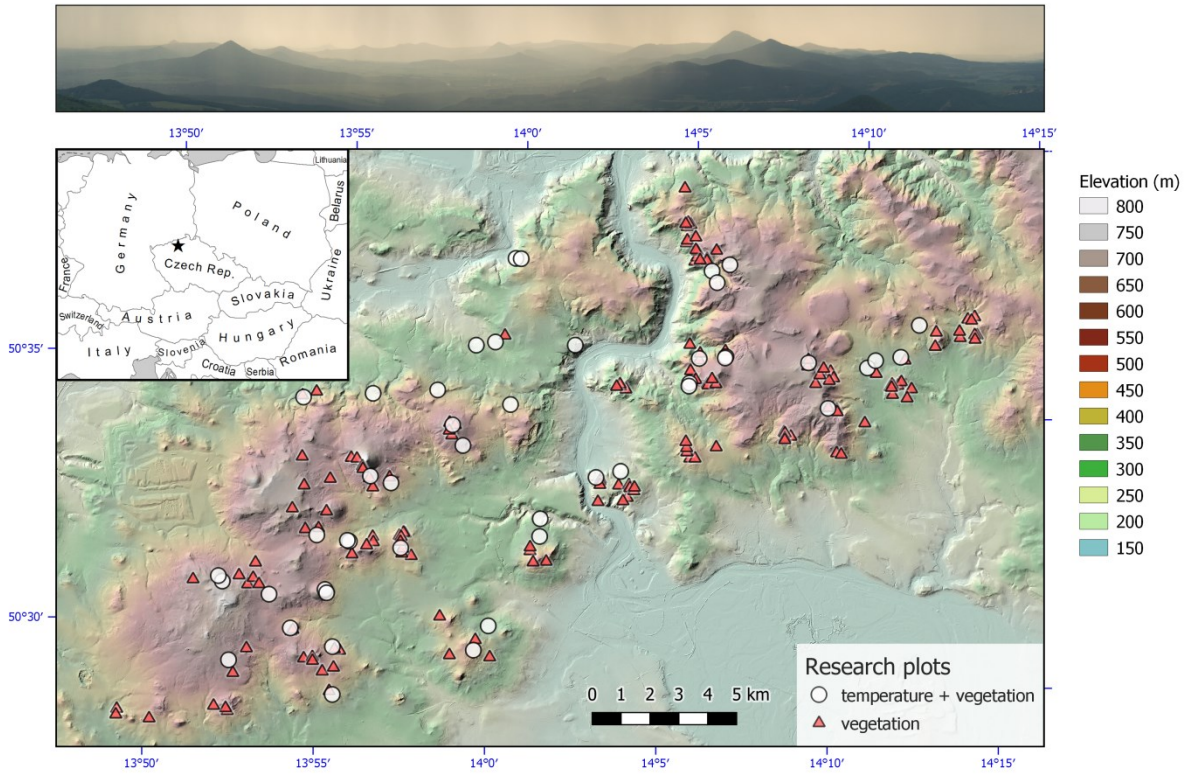

Figure 1 *Study area with sampled forest vegetation plots. White dots indicate the locations 46 plots where we simultaneously ascertained air temperature, canopy cover and plant species composition. Red triangles show the independent dataset of 160 vegetation plots used to evaluate the topoclimatic maps. Elevation is represented by a colour scale; the terrain is visualized using a hillshade effect. The photograph at the top shows a view of the central part of the study area; the inset map shows the position of the study (asterisk) within Central Europe. The geographic projection is S-JTSK Křovák, baseline data by © ČÚZK (DMR 4G digital elevation model with 5×5m resolution).*

3.4.2 DATA COLLECTION

We established 53 plots (10×10 m) in forests distributed across the 400 km2 region according to a stratified random sampling design with strata reflecting main topographic gradients (elevation, slope exposure and topographic wetness; Fig. 1, Fig S7). We excluded recently disturbed stands and coniferous plantations from the selection. We recorded the geographic positions of the plots using differential GPS (GeoExplorer 2008 GeoXH, Trimble Inc., USA) with data post-processing.

TEMPERATURE

At each plot, we measured air temperature with DS1922L iButton Thermochron loggers (Maxim Integrated Inc., San Jose, CA) with a resolution of 0.0625°C placed at a height of 2 m on the north side of a tree trunk and shaded by a passively ventilated plastic shield. The height of 2 m corresponds to the height at which standard meteorological data underlying the reference WorldClim 2 dataset are acquired. The temperature was recorded every three hours over the course of the growing season (1 May to 30 September) in the years 2015 to 2018. We used temperatures collected during the growing season because they are more important drivers of forest plant species distribution than yearly temperatures (Lenoir *et al.*, 2013). As a result of datalogger malfunction or vandalism, we acquired continuous temperature measurements from 46 plots out of 53 in 2015 but obtained a complete record for all four seasons for only 27 plots. Therefore, to maximize the number of plots without missing values, we used for further analyses only data from the 2015 season used the data from the following seasons only to document the consistency of the observed patterns between years (Fig S2).

To identify the temperature variable most relevant for vegetation composition, we compared three variables capturing different aspects of the thermal climate (Ashcroft *et al.*, 2014; Körner & Hiltbrunner, 2018): (i) maximum temperature expressed by the 95th percentile of daily maximum temperatures (Tmax95), (ii*)* mean temperature (Tmean) and (iii*)* minimum temperature expressed by the 5th percentile of daily minimum temperatures (Tmin5).

PLANT COMMUNITY COMPOSITION

At each 100-m2 plot, we identified all vascular plant species growing in the understorey (herbs and woody species < 1.3-m height) and estimated their cover according to the Braun-Blanquet scale (Westhoff and Van Der Maarel 1978) transformed to percentage cover.

Canopy cover

To measure canopy cover at each plot, we took five hemispherical photographs within each plot – one in the plot centre and four on the diagonals 5 m from the plot centre, using a Canon 40D camera with a Sigma 8mm f/3.5 EX fish-eye lens levelled at the height of 1.3 m. We used WinSCanopy v. 2014a (Regent Instruments, Canada) to calculate percent canopy cover over a 50° zenith angle from each photograph and averaged these five canopy cover values into plot mean canopy cover (Canopy).

Topographic variables

To explore links among temperature, topography and vegetation, we extracted the elevation of each plot from a LiDAR-based digital terrain model with a horizontal resolution of 5 m ('DMR 4G', Czech Office for Surveying, Mapping and Cadastre) and calculated three climatically relevant topographic variables: the topographic position index (TPI), potential heat load (HL) and the SAGA wetness index (SWI), all calculated in SAGA GIS ver. 3.0.0 (Conrad et al. 2015).

The topographic position index (TPI) expresses the difference between the elevation of a plot and the mean elevation in its surroundings (Guisan *et al.*, 1999) and captures the topographic exposure of the site, with positive values for ridge or hilltop positions, null on flats or midslopes and negative values on valley bottoms (Fig. S6). The TPI has been successfully used in many studies exploring temperature variation across landscapes (Strachan & Daly, 2017; Jucker *et al.*, 2018). With respect to the scale of topographic variability within our study region, we calculated the TPI using a 250-m radius.

Potential heat load (HL) defined as HL = cos(202.5°–aspect)×tan(slope) was calculated using the function 'anisotropic diurnal heat' in Saga GIS (Böhner & Antonić, 2009). Flat surfaces have zero HL values whereas northerly slopes have negative and southerly slopes positive HL values, with a maximum on SSW-facing slopes (Fig. S7). HL thus reflects maximum temperature patterns across a landscape with respect to diurnal variation in heat fluxes driven by surface exposure to solar radiation (Geiger et al. 2009). Because warm air is not static, local variation in slope and aspect produces unrealistic small-scale variation. We therefore smoothed HL values using a Gaussian filter with a 50-m range.

The topographic wetness index has been successfully used to model cold air pooling (Ashcroft *et al.*, 2008; Kilibarda *et al.*, 2014; Leempoel *et al.*, 2015). We therefore calculated the SAGA wetness index (SWI), a variant of the topographic wetness index (Kopecký & Čížková, 2010) with iteratively adjusted catchment area (Böhner & Selige, 2006) (Fig. S8). Adjusted catchment area produces smoother patterns of the wetness index, especially in flat areas such as valley bottoms, and therefore better reflects the redistribution of cold air than the classical TWI (Böhner and Antonić 2009).

3.4.3 Data analyses

Climatic effects on understorey plant communities

To visualize the main composition gradients, we used global non-metric multidimensional scaling (NMDS) calculated from a Bray-Curtis dissimilarity matrix, and to relate these gradients to environmental variables, we used the *envfit* function from the 'vegan' R package.

To calculate the amount of variation in species composition explained by the climatic variables, we used distance-based redundancy analysis (dbRDA, McArdle and Anderson 2001) calculated with the *dbRDA* function of the 'vegan' package (Oksanen et al. 2017) in R 3.2.5 (R Core Team 2016). We expressed dissimilarity in species composition as the Bray-Curtis index calculated from species percentage cover estimates transformed using a base-2 logarithm to down-weight the influence of the most abundant species (Anderson et al. 2006). We tested the statistical significance of climatic variables using 9,999 permutations.

Absolute values of explained variability in direct multivariate analyses (such as dbRDA) depend on the sample size and compositional heterogeneity of the dataset (Økland 1999). Therefore, it is useful to express explained variability relative to the maximum variability that could be explained by the same number of predictors. To calculate relative importance (RI), we divided the variability in species composition explained by a selected climatic variable by the variability explained by the sample scores on the first ordination axis of the principal coordinates analysis (PCA), which represent the maximum variability that can be explained by a single explanatory variable for the given dataset. We calculated the 95% confidence interval of RI by bootstraping with 9,999 replicates and the adjusted bootstrap percentile (BCa) method from the 'boot' R package (Canty and Ripley 2017).

Elevation, topography and canopy effects on understorey temperature

To explore the effects of terrain topography and canopy cover on the spatial variability of understorey temperature, we constructed empirical models for each temperature variable using multiple linear regression with forward selection based on the BIC criterion. As predictors, we used elevation, topographic indices (TPI, HL and SWI) and canopy cover (Canopy). Prior to the analyses, we standardized elevation and the SWI to zero means, leaving naturally centred variables (HL, TPI) untransformed. Variables entering the model were checked for co-linearity using variance inflation factors (VIF) from the 'car' R package (Fox and Weisberg 2011). All VIF values were below 1.6, indicating low co-linearity of the predictors (see Fig. S7 for correlations between predictors).

To calculate the relative importance of predictors used in the final models, we used LMG metrics from the 'relimpo' R package (Grömping 2006), which calculates the sequential R^2 contribution averaged over all possible orderings among regressors. To express absolute effect size in °C, we subtracted the lowest from the highest predicted values at sampling points where either topographic variables (for elevational effects) or elevation (for topographic effects) were fixed to zero (Ashcroft and Gollan 2013). We evaluated the prediction accuracy of the final topoclimatic models using mean absolute error (MAE) and root-mean-square error (RMSE) statistics based on leave-one-out cross-validation. Because the various temperature variables had different absolute ranges, we also calculated normalized RMSE as absolute RMSE divided by the range of observed values.

Fine-scaled topoclimatic maps vs. WorldClim2

We used these empirically derived models to create high-resolution (5 m) topoclimatic maps for the whole study area (Fig. 3). Our sampling design covered most topographic gradients within the study area (Fig. S8). We checked for spatial autocorrelation in observed temperature variables and in model residuals using Moran's I calculated with the 'ncf' R package (Bjornstad 2018). Because the spatial autocorrelation of model residuals was low, we concluded that the model assumptions were met and that it was not needed to correct for spatial dependence.

To assess the biological relevance of the newly created topoclimatic maps, we used an `independent validation dataset of 160 georeferenced forest vegetation plots without in-situ temperature measurement (see Kopecký and Macek 2015 for a description of the sampling design) sampled across the same region by the authors (Fig. 1). We compared variation in plant species composition explained by temperature variables extracted from our topoclimatic maps to the widely used WorldClim2 gridded climatology with 30 arc-second spatial resolution (Fick and Hijmans 2017). First, for each sample location we extracted Tmax95, Tmean and Tmin from our topoclimate maps and Mean Annual Temperature (bio1; Fig. S9), Max Temperature of Warmest Month (bio5; Fig. S10), Minimum Temperature of Coldest Month (bio6; Fig. S11) from WorldClim 2. Then we used dbRDA (with the same settings as we used to test the effects of in-situ measured temperatures) to assess the variability in understorey species composition explained by temperatures derived from fine-scaled microclimate maps and standard bioclimatic layers.

Understorey temperature variability

To explore the effects of topography and canopy cover on the spatial variability of understorey temperature, we constructed empirical models for each temperature variable using bidirectional elimination of model variables in multiple linear regression based on the Bayesian information criterion (BIC). As predictors we used plot elevation,

topographic variables (TPI, HL and SWI) and canopy cover. Prior to the analyses we standardized elevation and the SWI to zero means, leaving naturally centred variables (HL, TPI) untransformed. Variables entering the model were checked for co-linearity using variance inflation factors (VIF) from the 'car' package (Fox and Weisberg 2011) in R 3.2.5 (R Core Team 2016). All VIF values were below 1.6, indicating low co-linearity of the predictors (Fig. S9). We checked for spatial autocorrelation in observed temperature variables and in model residuals using Moran's I calculated with the 'ncf' R package (Bjornstad 2018). Because the spatial autocorrelation of model residuals was low, we concluded that the model assumptions of independence of residuals were met and that it was not necessary to further correct for spatial dependence.

To calculate the relative importance of predictors used in the final models, we used the sequential R2 contribution averaged over all possible orderings of the regressors, implemented in the 'relimpo' R package as 'LMG' metrics (after Lindeman, Merenda and Gold (1980) in Grömping 2006). To express absolute effect size in degrees Celsius, we subtracted the lowest from the highest predicted values at sampling points where either topographic variables (for elevational effects) or elevation (for topographic effects) were fixed to zero (Ashcroft and Gollan 2013). We evaluated the prediction accuracy of the final topoclimatic models using mean absolute error (MAE) and root-mean-square error (RMSE) statistics based on leave-one-out cross-validation. Because the various temperature variables had different absolute ranges, we also calculated normalized RMSE as absolute RMSE divided by the range of observed values.

Finally, we used these empirically derived models to create high-resolution (5 x 5 m pixel size) topoclimatic maps of Tmax95, Tmean and Tmin5 for the whole study area (Fig. 3). As a supplement to these topoclimatic maps, we provide spatially explicit information about topographic gradients covered by our sampling design (interpolated climate) and those not covered (extrapolated climate) in the supplementary material (Fig. S11).

Effects of in-situ measured temperature on understorey plant communities

To explore the effects of different temperature variables on understorey plant species composition, we performed two complementary multivariate analyses (Økland 1996). First, we explored main gradients in plant species composition and their relationship to environmental variables through indirect ordination and then we used direct ordination to calculate the variation in species composition explained by each in-situ measured temperature variable (Legendre and Lengendre 2012). We expressed dissimilarity in plant species composition as the percentage (aka Bray-Curtis) index (Legendre and Lengendre 2012) calculated from species percentage cover estimates transformed using a base-2 logarithm to decrease the influence of the most abundant species (Anderson et al. 2006).

To explore the main gradients in plant species composition, we used global non-metric multidimensional scaling with primary ('weak') treatment of ties (NMDS) calculated in two dimensions with the 'metaMDS' function from the 'vegan' R package version 2.4-6 (Oksanen et al. 2018). To visualize relationships among the main compositional gradients and environmental variables, we projected all environmental variables onto the NMDS compositional space using the 'envfit' function from the 'vegan' R package.

To calculate the variation in species composition explained by the temperature variables, we used distance-based redundancy analysis (dbRDA, McArdle and Anderson 2001) performed using the 'dbRDA' function from the 'vegan' R package. We tested the statistical significance of temperature variables using 9,999 permutations.

The proportion of variability explained by environmental gradients in direct multivariate analyses (such as dbRDA) tends to be low because explained variability depends on the compositional heterogeneity of the dataset (Økland 1999). It is therefore useful to express the relative importance (RI) of predictors calculated here as the variability explained by the predictor relative to the maximum variability that can be potentially explained by a single predictor. To calculate RI, we divided the variability in species composition explained by each temperature variable by the variability explained by the sample scores from the first ordination axis of the Principal Coordinates Analysis (PCoA) supplied as a single explanatory variable to dbRDA. To provide uncertainty estimates for these RI values, we further calculated the 95% confidence interval of RI for each temperature variable by bootstrapping with 9,999 replicates calculated using the adjusted bootstrap percentile (BCa) method from the 'boot' R package (Canty and Ripley 2017).

TOPOCLIMATIC AND MACROCLIMATIC MAPS IN ECOLOGICAL APPLICATIONS

To assess the biological relevance of the newly created fine-scale topoclimatic maps, we used an independent dataset of 160 georeferenced forest vegetation plots without in situ temperature measurement, sampled across the same region by the authors (see Fig. 1 for the spatial distribution of the plots, Suppl. Fig. S10 for coverage of topographic gradients and Kopecký and Macek (2015) for a description of the sampling design).

We compared variation in plant species composition explained by temperature variables extracted from our high-resolution topoclimatic maps (5 × 5 m pixel size) to the widely used WorldClim 2 climate grids with 30 arc-second (ca 930 × 590 m pixel size at this latitude) spatial resolution (Fick and Hijmans 2017). First, for each sample location we extracted Tmean, Tmax95 and Tmin5 from our topoclimate maps and analogous indices calculated using growing season (May to September) monthly data from WorldClim 2: maximum temperature of the warmest month (WC2 Tmax; Fig. S12),

mean of average monthly temperature (WC2 Tmean; Fig. S13) and minimum temperature of the coldest month (WC2 Tmin; Fig. S14).

We used dbRDA with the same settings as we used to test the effects of in situ measured temperatures to assess the variation in understorey species composition explained by temperatures derived from fine-scale topoclimate maps and from WorldClim 2 climate grids. To test if the fine-scale topoclimate predicts vegetation composition better than analogous WorldClim 2 variables, we compared bootstrapped explained variances (R2) between pairs of models using topoclimatic and analogous WorldClim 2 predictor variables (e.g. Tmax95 vs WC2 Tmax) using one-sided empirical p-values corrected for finite sampling:

Eq. 1: $p = (1+\sum (R2_{topo} \leq R2_{WorldClim\ 2}))/(n+1)$

3.5 RESULTS

UNDERSTOREY TEMPERATURE VARIABILITY

Mean temperatures measured in the growing season 2015 (Tmean) varied by 2.55°C, ranging from 15.02 to 17.57°C across the landscape. Minimum and maximum temperatures were substantially more variable: Tmax95 differed between sites by as much as 6.86°C (Table 1). Similar patterns in Tmax95 and Tmean were found for the next three years on a subset of 27 locations with continuous record (Pearson's correlation coefficient between different years was between 0.9 and 0.97 for Tmax95 and between 0.97 and 0.98 for Tmean). Higher interannual variability was found only for Tmin (Pearson's correlation coefficient between 0.32 and 0.93), Fig. S2-S4.

Table 1 *Environmental variables and their descriptive statistics across the 46 sample sites. Topographic variables were derived from a high-resolution digital elevation model and canopy cover was calculated from hemispherical photographs. Temperature variables were measured using iButton Thermochron data loggers in the vegetation season of 2015 (1st May – 30th September). Mean temperature is calculated as the average from all readings (every 3h).*

Variable	Abbrev.	Units	min	mean	max	sd	range
Elevation	Elev	m	220	427.7	644	109.3	424
Canopy cover	Canopy	%	79	91.8	97	3.37	18
SAGA Wetness Index	SWI	-	5.19	8.77	16.84	2.75	11.65
Heat load	HL	-	-0.55	-0.04	0.43	0.21	0.98
Topographic position index	TPI	m	-39	-0.54	36	16.83	75
95th percentile of daily maximum temperatures	Tmax95	°C	27.29	29.97	34.15	1.57	6.86
Mean temperature	Tmean	°C	15.02	16.13	17.57	0.69	2.55
5th percentile of daily minimum temperatures	Tmin5	°C	4.34	6.88	8.02	0.84	3.68

The final model for Tmax95 with four explanatory variables explained most of the variability in measured temperatures (R2adj. = 0.79); it had RMSE = 0.76°C and no spatial autocorrelation in residuals (Table 2; Fig. 3c). Elevation had a strong negative effect (lapse rate –11.4°C·km–1) with a relative importance of 62.9%. The topographic variables selected in the regression model were the TPI (positive effect, 15.4% RI), HL (positive effect, 15.3% RI) and SWI (negative effect, 6.2% RI). For detailed information on the stepwise model selection see Supplementary Table S15.

The best topoclimatic model for Tmean explained most of the variability (R2adj. = 0.80) and had good prediction accuracy (RMSE = 0.31°C) and no autocorrelation in

model residuals up to the distance of 10 km (Fig. 3f). The model included three variables – elevation, TPI and SWI (Table 3). Tmean decreased with elevation (lapse rate –5.16°C·km–1), which was the most important variable in the model (73% RI). Tmean increased with increasing TPI (14.5% RI) and decreased with increasing SWI (12.4% RI).

Variation in Tmin5 showed low spatial autocorrelation (Fig. 3h) and was difficult to predict (R2adj. = 0.30); the only predictor of Tmin5 selected in the stepwise-selection was SWI (Table 2). The negative relation between Tmin5 and SWI suggests cold air pooling at valley bottoms as the dominant process driving spatial patterns in Tmin5.

Table 2 *Microclimate regression model parameters for minimum, mean and maximum temperatures. The effect size for elevation (Elev. e.s.) was calculated as the range of predicted values for observed plot elevations with all other variables held constant. Topographic effect size (Topo. e.s.) is the range of predicted values for constant elevation and original values of topographic variables. Significance codes: 'n.s.' – not significant; '*' – p < 0.05; '**' – p < 0.01; '***' – p < 0.001. MAE – mean absolute error; RMSE – root-mean-square-error, RMSE norm – normalized root-mean-square-error (RMSE divided by the observed range of values).*

Variable	Intercept	Elev	SWI	TPI	HLI	Canopy	R^2adj.	Elev. e.s.	Topo. e.s.	model p	MAE	RMSE	norm RMSE
Tmax95	29.52 ***	-0.0114 ***	-0.709 **	0.0362 ***	0.00014 ***	n.s.	0.79	4.74	4.27	***	0.62	0.76	0.112
Tmean	15.79 ***	-0.0057 ***	-0.446 ***	0.0141 ***	n.s.	n.s.	0.80	2.36	1.72	***	0.24	0.31	0.123
Tmin5	6.34 ***	n.s.	-0.781 ***	n.s.	n.s.	n.s.	0.30	-	1.87	**	0.57	0.72	0.195

EFFECTS OF IN-SITU MEASURED TEMPERATURE ON UNDERSTOREY PLANT COMMUNITIES

In total, we recorded 196 plant species (median 25.5, min. 4, max. 48 per plot). The main gradient in vegetation composition, as seen on NMDS ordination diagram, can be interpreted as the transition from thermophilous oak woodlands to mesic beech-dominated communities (Fig. 2). The second ordination axis in NMDS followed mainly nutrient status, from communities of acidic soils with Vaccinium myrtillus and Avenella flexuosa to the calcicole and nutrient demanding species like Astrantia major or Viola mirabilis. Whereas Tmax95 and Tmean were both closely related to the first axis of the NMDS ordination, Tmin5 had only weak correlation with the second ordination axis (Fig. 2).

Direct gradient analysis (dbRDA) revealed that species composition was most strongly controlled by Tmax95, less by Tmean and only weakly by Tmin5 (Table 3).

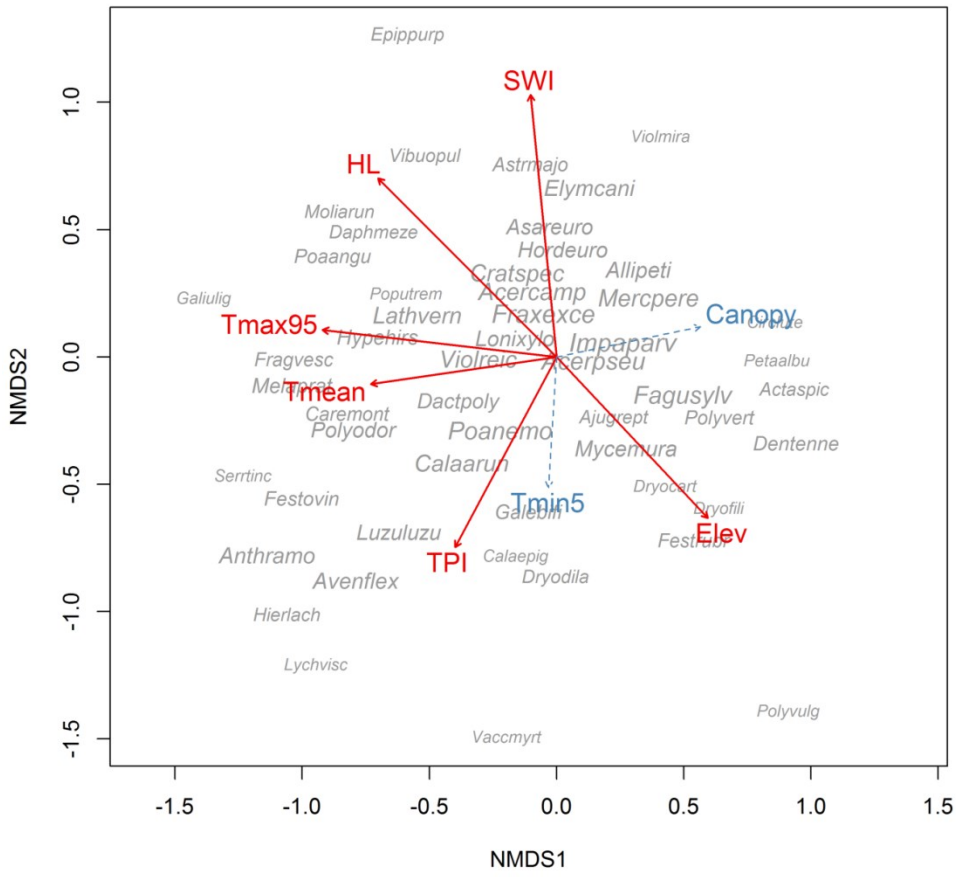

Figure 2 *Ordination diagram from non-metric multidimensional scaling showing main vegetation gradients with passively projected climatic and topographic variables. Environmental variables with statistically significant ($p < 0.05$) correlations with sample scores in the ordination space are depicted by solid red lines; insignificant variables are indicated by a dashed blue lines (see Table 1 for variable abbreviations and descriptions). The contractions of species names are composed of the first four letters of the generic name and the first four letters of the specific epithet; font size is proportional to the species' frequencies in the dataset. In cases of overlapping labels, only the more frequent species was plotted.*

Table 3 *Variation in species composition explained by in situ measured temperatures (Tmax95, Tmean, Tmin5) and the bioclimatic variables bio1 (mean temperature), bio5 (maximum temperature of the warmest month) and bio6 (minimum temperature of the coldest month) extracted from WorldClim 2 climate grids. Explained variation in species composition (R^2 and adjusted R^2) and p-values are based on 9,999 permutations of dbRDA. The shared effect is the fraction of variation jointly explained by in situ measured and corresponding WorldClim 2 variables. Pearson's r is the bivariate correlation between in situ measured and corresponding WorldClim 2 variables.*

variable	n	F model	R^2	R^2 adj.	p	RI_{mean}	$RI_{2.5\%}$	$RI_{97.5\%}$
In situ *measured temperatures*								
Tmax95	46	3.929	0.082	0.061	< 0.001	0.634	0.365	0.822
Tmean	46	3.323	0.070	0.049	< 0.001	0.568	0.269	0.722
Tmin5	46	1.908	0.042	0.020	0.012	0.382	0.139	0.447
Topoclimatic map spatial prediction								
Tmax95	160	9.516	0.057	0.051	< 0.001	0.489	0.306	0.613
Tmean	160	6.897	0.042	0.036	< 0.001	0.374	0.204	0.452
Tmin5	160	4.900	0.030	0.024	< 0.001	0.286	0.141	0.314
WorldClim2 bioclimatic grids								
bio1	160	7.117	0.043	0.037	< 0.001	0.384	0.226	0.454
bio5	160	6.166	0.038	0.031	< 0.001	0.339	0.187	0.401
bio6	160	5.324	0.033	0.026	< 0.001	0.302	0.160	0.350

TOPOCLIMATIC AND MACROCLIMATIC MAPS IN ECOLOGICAL APPLICATIONS

In the independent dataset, microclimatic variables extracted from fine-scale topoclimatic maps (Fig. 3) explained less variability in plant community composition than was explained by in situ measured temperatures in the original dataset, but the ranking of individual variables was the same as for in situ measured temperatures (Table 3). The best predictor of plant community composition was again Tmax95, which was a significantly better predictor of vegetation composition than maximum temperature extracted from WorldClim 2 ($p = 0.005$). However, the explanatory power of Tmean and Tmin5 from topoclimatic maps was not better than that of Tmean ($p = 0.52$) and Tmin ($p = 0.872$) from WorldClim 2.

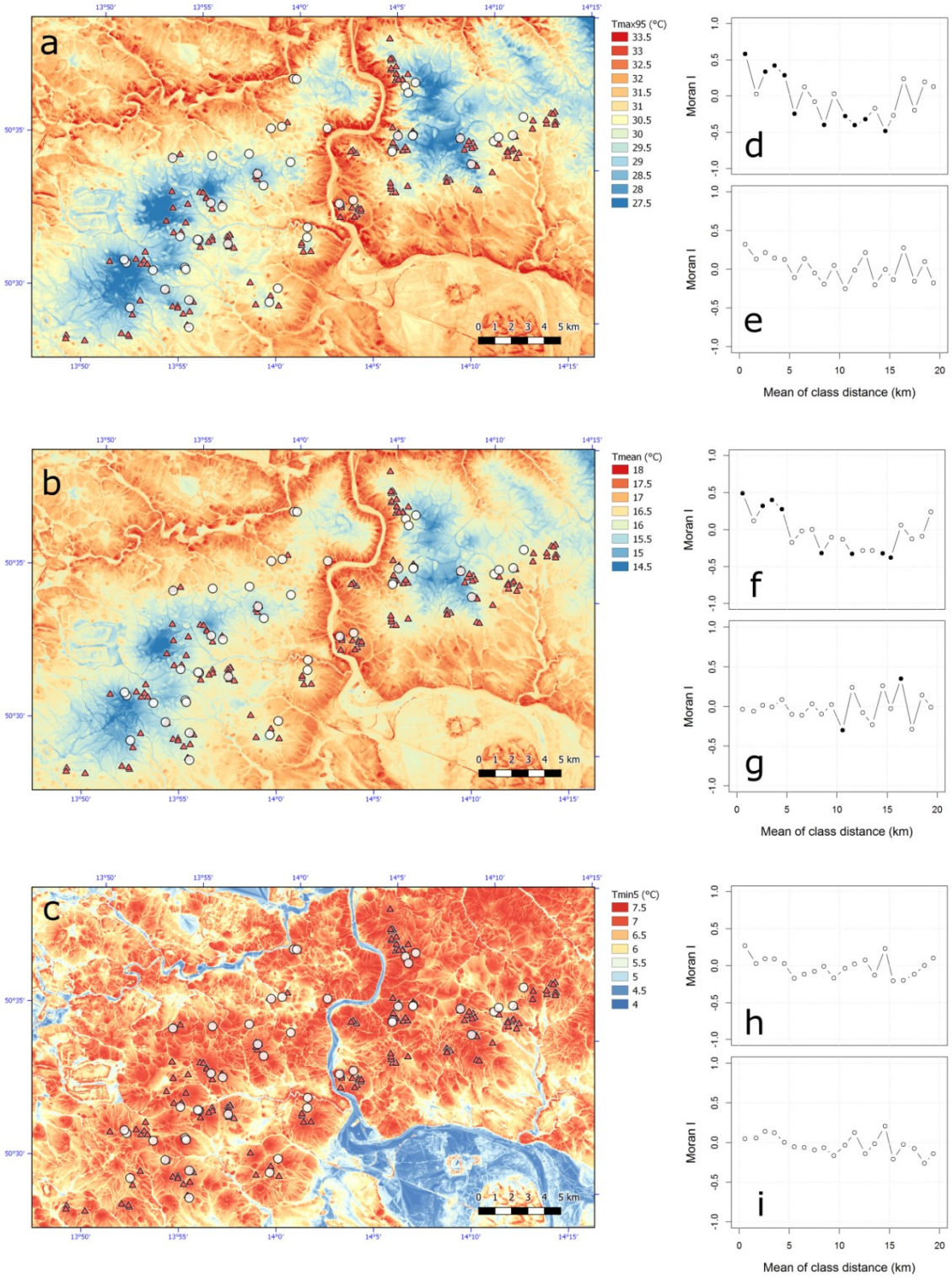

Fig. 3 *Predicted topoclimatic maps for Tmax95 (a), Tmean (b) and Tmin5 (c). Spatial autocorrelation is expressed as Moran's I of measured temperature values (d,f,h) and model residuals (e,g,i) for Tmax95 (d,e), Tmean (f,g) and Tmin5 (h,i). Instances of significant ($p < 0.05$) spatial autocorrelation are plotted as full circles. The model for Tmax95, which was best predictor of plant community composition, explained most of the observed spatial variability and accounted for spatial autocorrelation of residuals at all spatial scales.*

3.6 Discussion

Different sets of topographic variables explained spatial variability in minimum, mean and maximum temperatures, while spatial variability of understorey temperatures driven by differences in canopy openness was insignificant. Maximum temperatures were the most variable in space, with variability controlled jointly by elevation, heat load, topographic position and topographic wetness. Understorey plant community composition was best explained by a gradient of in-situ measured maximum temperatures. Using an independent dataset of vegetation samples, we shoved that the fhad the strongest relation to understory plant community composition. Fine-scaled topoclimatic maps of maximum temperatures can explain forest understorey composition substantially better than the WorldClim 2 gridded climate data, which lack sufficient resolution and do not account for topographic effects other than elevation.

Drivers of understorey temperature variability

It has been suggested that topographic effects on near-surface temperatures are reduced under dense forest canopies (Wilson and Gallant 2000, Körner and Paulsen 2004). However, our results clearly show that topography has a strong effect even in closed-canopy forests. Although we found a significant effect of heat load on maximum temperatures, heat load did not affect mean temperatures significantly, probably because the contrast in temperatures on south-facing slopes is pronounced only around noon on sunny days, which contribute little to seasonal means. By contrast, the SWI, which is a topographic proxy for soil moisture and cold air pooling (Olaya and Conrad 2009, Kilibarda et al. 2014), correlated significantly with all temperature variables. The effect of cold air drainage affecting maximum temperatures during daytime in the growing season seems rather odd. However, beneath the forest canopy, topographically driven downslope flow of the cold air can persist all day, in contrast to conditions above the canopy, where the air flow is reversed during the daytime (Pypker et al. 2007).

Within our study region, the temperature variability driven by topography was comparable to the temperature variability driven by elevation. Terrain topography thus creates contrasting fine-scale microclimatic patterns across the landscape (Fig. 3). Interestingly, the magnitude of topographically driven variability in maximum temperatures observed in our study is in line with values reported from Australia (Ashcroft and Gollan 2012) and France (Joly and Gillet 2017). Similar topographic effects on effective temperatures in the forest understorey have been also demonstrated in Germany, where bioindicated temperature was better predicted by models including the topographic heat load index along with conventional interpolated temperature grids (Reger et al. 2011) Together, these results suggest that topographically driven temperature variability should be considered in ecological studies (Vanwalleghem and Meentemeyer 2009, Ashcroft et al. 2012).

Surprisingly, we did not find any significant correlation between variation in canopy cover and understorey temperature. The average buffering effect of the forest canopy compared to open habitats on maximum air temperatures has been quantified to be ca 2°C in broadleaved forests (Von Arx et al. 2012, Zellweger et al. 2019) and ca 1.4°C in coniferous ones (Davis et al. 2019). The estimated effect of canopy cover, albeit insignificant, in our full model was roughly comparable to these values, tending towards 2.6°C, but with a high standard error of 2.4°C. In contrast to studies reporting significant effects of canopy cover (e.g. Ashcroft and Gollan 2012, Von Arx et al. 2013, Greiser et al. 2018), we did not measure temperature in non-forest habitats. It can therefore be argued that we did not find any effects of canopy cover because we sampled only a limited gradient of canopy cover. However, we selected our plot locations according to a stratified random design with strata defined only by topographic variables; canopy cover in our plots thus reflects typical variation within the region. While most plots were established within close-canopy forests dominating the region, we measured temperatures also in tree-fall gaps and open forests on steep slopes with shallow soils and the range of canopy cover values observed in our study is fully comparable to values reported from other temperate forests, even in studies that also considered canopy gaps (Canham et al. 1990, Valverde and Silvertown 1997, Tinya et al. 2009, Hofmeister et al. 2009). Nevertheless, we acknowledge that part of the unexplained temperature variability can be potentially attributed to variation in other forest structural attributes like canopy height or stem density (Frey et al. 2016, Kovács et al. 2017).

Recently, it has been shown that forest canopy ability to buffer understorey temperatures in temperate deciduous forests does not increase linearly with increasing canopy cover, but is constant beyond a threshold of ca 75% canopy cover (Zellweger et al. 2019). As all sites in our study have canopy cover above 75% (Table 1), lack of effect of canopy cover on measured temperatures is fully in line with Zellweger et al. results. Likewise, Gray et al. (2002) have compared temperatures under closed canopy and canopy gaps of different size, reporting that minimum and mean temperatures were not affected by gaps, but only the maximum air temperatures measured in the largest gaps were significantly affected. Together, these results suggest that there is some threshold value of canopy cover above which the effect of canopy on air temperature is saturated. The temperature variability potentially driven by variation in canopy cover within forest stands is therefore relatively small compared to topography-driven variability (over 4°C in our region).

Effects of in-situ measured temperature on understorey plant communities

We found that maximum temperatures have a stronger effect on understorey plant communities than mean or minimum temperatures. Tmax95 explained 51% of the variability explainable by a single predictor variable in the multivariate analysis, which

indicates a high importance of maximum temperatures. Our results thus support previous studies arguing that not average climatic conditions but rather climatic extremes are the determinants of species distribution and community assembly (Suggitt et al. 2011, Ashcroft and Gollan 2012). The range and spatial heterogeneity observed for maximum temperatures was also broader than that of mean or minimum temperatures (Fig. 3) and which may also contribute to the greater explanatory power of maximum temperatures.

In our opinion, maximum temperature acts on forest plant species as a permanent stress factor rather than an episodic disturbance agent because spatial pattern of maximum temperature was consistent between years (Fig. S2). Plants growing at sites regularly exposed to high maximum temperatures are not only affected by physiological stress caused directly by high temperatures, but they are also exposed to high vapour pressure deficit, which is physically linked to temperature, resulting in high evapotranspiration rates (Kovács et al. 2017, Davis et al. 2019). The effects of high temperature stress on plant communities thus may be accentuated as a result of trade-offs with shade adaptations of forest plants, which make them more sensitive to water deficit under high-temperature conditions (Valladares and Niinemets 2008). Indeed, sites with lower maximum temperatures host typical forest species such as Actaea spicata or ferns Dryopteris carthusiana and D. filix-mas whereas sites on the 'hot' end of the gradient host many plant species that can be found also in forest edges, shrublands or in non-forest habitats, for example Serratula tinctoria, Fragaria vesca or graminoids such as Festuca ovina, Carex montana and Poa anguistifolia (Fig. 2).

The species composition of temperate forest understories changed substantially less than had been expected from the observed changes in mean temperature in the past decades (Bertrand et al. 2011, De Frenne et al. 2013). One explanation for this discrepancy, proposed by De Frenne et al. (2013), is the microclimatic buffering of understorey temperatures caused by increasing canopy cover. However, our results suggest that the potential buffering effect of canopy cover on temperature variability within forests in this region is relatively weak: Even if the relation between canopy cover and maximum temperatures was linear and canopy cover in all our plots was to increase to 100%, the potential difference in buffering effect on maximum temperatures in the forest understorey compared to current situation would not exceed 0.25°C according to the effect reported by Von Arx et al. (2012), but no additional buffering effect with increasing canopy cover can be expected if there is a threshold value in canopy cover above which the temperatures do not further respond to increasing canopy cover, as was reported by Zellweger et al. (2019). Even when the buffering effect is expressed directly as thermophilization of plant communities, using the most extreme estimate of effect sizes from De Frenne et al. (2013) and simulated increase in canopy cover to 100% on all plots, the expected mean buffering effect mitigating plant community thermophilization would be as low as 0.003°C. Such values are far below the expected rise in temperatures

during the 21st century, but also below the observed rise of temperatures in the past decades (IPCC 2014). Our data thus challenge the potential of forests to buffer climate warming by increasing canopy closure at the landscape-scale (De Frenne et al. 2013, Frey et al. 2016). However, significant effects of alternated temperature regime on understorey vegetation can be expected locally in response to moderate to severe canopy disturbance or stand development following such disturbance (Stevens et al. 2015, Brice et al. 2019), but such dynamics is accompanied also by dramatic changes in light, water and nutrient availability, affecting understorey vegetation in a complex way (Canham et al. 1990, Gray et al. 2002, Gálhidy et al. 2005). This makes disentangling the effects of the temperature from other driving forces challenging.

Interestingly, maximum daily temperatures, which proved to be the most determining factor for understorey species composition, have risen globally at a lower rate compared to mean or minimum temperatures (Easterling et al. 1997). The slower increase in maximum temperature and its greater spatial heterogeneity can theoretically be at least partly responsible for the lower rate of change in forest understorey vegetation observed across temperate forests. However, only long-term microclimatic data measured along gradients of canopy cover can disentangle links between the changing climate, forest canopies, topographic complexity and directional change in forest understorey vegetation, so far deduced mostly from indirect evidence based on space-for-time substitutions (Frey et al. 2016, De Frenne et al. 2019) or bioindication (De Frenne et al. 2013).

TOPOCLIMATIC AND MACROCLIMATIC MAPS IN ECOLOGICAL APPLICATIONS

Our findings stress that fine-scale information about maximum temperatures in the growing season is essential for a proper assessment of the effect of climate change and is also vital for species distribution modelling (see also Parmesan et al. 2000, Ashcroft and Gollan 2012, Gardner et al. 2019). The common limitations of currently available global climatic datasets, including WorldClim 2, are their insufficient spatial resolution, possible bias in temperature interpolations and, finally, the fact that weather-station data behind these datasets do not reflect specific forest microclimates and topographic complexity (Bedia et al. 2013, Nadeau et al. 2017, Bramer et al. 2018). Elevation is still the only topographic attribute used in interpolations of WorldClim 2 climate grids (Fick and Hijmans 2017), but we found that other aspects of topographic complexity, including anisotropic heating and cold air pooling can be similarly important at landscape scales. This is the likely reason why maximum temperature from WorldClim 2 explained substantially less variation in species composition than both in situ measured maximum temperatures and maximum temperatures from our interpolated topoclimatic grids. However, the explanatory power of mean temperature was comparable between topoclimatic grids and WorldClim 2. This is probably caused by the lower spatial

variability in mean temperatures and greater relative importance of elevation compared to other topographic attributes, which makes mean temperature predictions in WorldClim 2 more realistic compared to maximum temperature predictions based on the same dataset.

Together, our results show that it is possible to improve bioclimatic maps using topographic variables and thus substantially enhance the ecological relevance of these maps. Therefore, despite substantial improvements in the precision and spatial resolution of global climate grids (Fick and Hijmans 2017), there is still a need to incorporate local topography into these grids (Slavich et al. 2014, Aalto et al. 2017). We show that such topoclimatic maps capture more biologically relevant information and can therefore increase the predictive accuracy of ecological models.

3.7 Conclusion

Elevational gradients together with terrain topography create complex microclimatic mosaics across forested landscapes. Plant species growing in forest understoreys are sensitive to these microclimatic mosaics and most strongly respond to maximum temperature. At landscape scales, maximum temperatures can be successfully modelled using topographic variables derived from high-resolution DEMs, suggesting promising avenues for the refinement of species distribution models and the modelling of species' vulnerability to climate change.

3.8 Acknowledgements

We thank all our colleagues that helped us collect field data. We further thank all three reviewers and the editor for their helpful and constructive comments. This study was supported by the Czech Science Foundation (project 17-13998S), the Grant Agency of Charles University (project 359515) and the Czech Academy of Sciences (project RVO 67985939).

3.9 References

Aalto, J., H. Riihimäki, E. Meineri, K. Hylander, and M. Luoto. 2017. Revealing topoclimatic heterogeneity using meteorological station data. *International Journal of Climatology* 37:544–556.

Anderson, M. J., K. E. Ellingsen, and B. H. McArdle. 2006. Multivariate dispersion as a measure of beta diversity. *Ecology Letters* 9:683–693.

Von Arx, G., M. Dobbertin, and M. Rebetez. 2012. Spatio-temporal effects of forest canopy on understory microclimate in a long-term experiment in Switzerland. *Agricultural and Forest Meteorology* 166–167:144–155.

Von Arx, G., E. Graf Pannatier, A. Thimonier, and M. Rebetez. 2013. Microclimate in forests with varying leaf area index and soil moisture: Potential implications for seedling establishment in a changing climate. *Journal of Ecology* 101:1201–1213.

Ashcroft, M. B., M. Cavanagh, M. D. B. Eldridge, and J. R. Gollan. 2014. Testing the ability of topoclimatic grids of extreme temperatures to explain the distribution of the endangered brush-tailed rock-wallaby (Petrogale penicillata). *Journal of Biogeography* 41:1402–1413.

Ashcroft, M. B., L. A. Chisholm, and K. O. French. 2008. The effect of exposure on landscape scale soil surface temperatures and species distribution models. *Landscape Ecology* 23:211–225.

Ashcroft, M. B., L. A. Chisholm, and K. O. French. 2009. Climate change at the landscape scale: predicting fine-grained spatial heterogeneity in warming and potential refugia for vegetation. *Global Change Biology* 15:656–667.

Ashcroft, M. B., and J. R. Gollan. 2012. Fine-resolution (25 m) topoclimatic grids of near-surface (5 cm) extreme temperatures and humidities across various habitats in a large (200 × 300 km) and diverse region. *International Journal of Climatology* 32:2134–2148.

Ashcroft, M. B., and J. R. Gollan. 2013. Moisture, thermal intertia, and the spatial distributions of near-surface soil and air temperatures: Understanding factors that promote microrefugia. *Agricultural and Forest Meterology* 176:77–89.

Ashcroft, M. B., J. R. Gollan, D. I. Warton, and D. Ramp. 2012. A novel approach to quantify and locate potential microrefugia using topoclimate, climate stability, and isolation from the matrix. Global Change Biology 18:1866–1879.

Bedia, J., S. Herrera, and J. M. Gutiérrez. 2013. Dangers of using global bioclimatic datasets for ecological niche modeling. Limitations for future climate projections. *Global and Planetary Change* 107:1–12.

Bertrand, R., J. Lenoir, C. Piedallu, G. Riofrío-Dillon, P. de Ruffray, C. Vidal, J.-C. Pierrat, and J.-C. Gégout. 2011. Changes in plant community composition lag behind climate warming in lowland forests. Nature 479:517–520.

Bjornstad, O. N. 2018. ncf: Spatial Covariance Functions. R package version 1.2-6. https://CRAN.R-project.org/package=ncf.

Böhner, J., and O. Antonić. 2009. Land-surface parameters specific to topo-climatology. Pages 195–226 in T. Hengl and H. U. Reuter, editors. Geomorphometry: concepts, software, applications. Elsevier, Amsterdam.

Böhner, J., and T. Selige. 2006. Spatial prediction of soil attributes using terrain analysis and climate regionalisation. *SAGA - Analyses and Modelling Applications: Göttinger Geographische Abhandlungen* 115:13–28.

Bramer, I., B. J. Anderson, J. Bennie, A. J. Bladon, P. De Frenne, D. Hemming, R. A. Hill, M. R. Kearney, C. Körner, A. H. Korstjens, J. Lenoir, I. M. D. Maclean, C. D. Marsh, M. D. Morecroft, R. Ohlemüller, H. D. Slater, A. J. Suggitt, F. Zellweger, and P. K. Gillingham. 2018. Advances in Monitoring and Modelling Climate at Ecologically Relevant Scales. *Advances in Ecological Research* 58:101–161.

Brice, M., K. Cazelles, P. Legendre, and M. Fortin. 2019. Disturbances amplify tree community responses to climate change in the temperate–boreal ecotone. *Global Ecology and Biogeography*: DOI: 10.1111/geb.12971.

Canham, C. D., J. S. Denslow, W. J. Platt, J. R. Runkle, T. A. Spies, and P. S. White. 1990. Light regimes beneath closed canopies and tree-fall gaps in temperate and tropical forests. *Canadian Journal of Forest Research* 20:620–631.

Canty, A., and B. D. Ripley. 2017. boot: Bootstrap R (S-Plus) functions.

Chen, J., S. C. Saunders, T. R. Crow, R. J. Naiman, K. D. Brosofske, G. D. Mroz, B. L. Brookshire, and J. F. Franklin. 1999. Microclimate in Forest Ecosystem and Landscape Ecology. *BioScience* 49:288.

Conrad, O., B. Bechtel, M. Bock, H. Dietrich, E. Fischer, L. Gerlitz, J. Wehberg, V. Wichmann, and J. Böhner. 2015. System for Automated Geoscientific Analyses (SAGA) v. 2.1.4. *Geoscientific Model Development* 8:1991–2007.

Davis, K. T., S. Z. Dobrowski, Z. A. Holden, P. E. Higuera, and J. T. Abatzoglou. 2019. Microclimatic buffering in forests of the future: the role of local water balance. *Ecography* 42:1–11.

Easterling, D. R., B. Horton, P. D. Jones, T. C. Peterson, T. R. Karl, D. E. Parker, M. J. Salinger, V. Razuvayev, N. Plummer, P. Jamason, and C. K. Folland. 1997. Maximum and minimum temperature trends for the globe. *Science* 277:364–367.

Fick, S. E., and R. J. Hijmans. 2017. WorldClim 2: new 1-km spatial resolution climate surfaces for global land areas. *International Journal of Climatology* 37:4302–4315.

Fox, J., and S. Weisberg. 2011. An R Companion to Applied Regression. 2nd Edition. *Sage Publications.*

Franklin, J., F. W. Davis, M. Ikegami, A. D. Syphard, L. E. Flint, A. L. Flint, and L. Hannah. 2013. Modeling plant species distributions under future climates: how fine scale do climate projections need to be? *Global Change Biology* 19:473–483.

De Frenne, P., F. Rodriguez-Sanchez, D. A. Coomes, L. Baeten, G. Verstraeten, M. Vellend, M. Bernhardt-Romermann, C. D. Brown, J. Brunet, J. Cornelis, G. M. Decocq, H. Dierschke, O. Eriksson, F. S. Gilliam, R. Hedl, T. Heinken, M. Hermy, P. Hommel, M. a Jenkins, D. L. Kelly, K. J. Kirby, F. J. G. Mitchell, T. Naaf, M. Newman, G. Peterken, P. Petrik, J. Schultz, G. Sonnier, H. Van Calster, D. M. Waller, G.-R. Walther, P. S. White, K. D. Woods, M. Wulf, B. J. Graae, and K. Verheyen. 2013. Microclimate moderates plant responses to macroclimate warming. *Proceedings of the National Academy of Sciences* 110:18561–18565.

De Frenne, P., F. Zellweger, F. Rodríguez-Sánchez, B. R. Scheffers, K. Hylander, M. Luoto, M. Vellend, K. Verheyen, and J. Lenoir. 2019. Global buffering of temperatures under forest canopies. *Nature Ecology & Evolution*.

Frey, S. J. K., A. S. Hadley, S. L. Johnson, M. Schulze, J. A. Jones, and M. G. Betts. 2016. Spatial models reveal the microclimatic buffering capacity of old-growth forests. *Science Advances* 2:e1501392–e1501392.

Fridley, J. D. 2009. Downscaling climate over complex terrain: High finescale (<1000 m) spatial variation of near-ground temperatures in a montane forested landscape (Great Smoky Mountains). *Journal of Applied Meteorology and Climatology* 48:1033–1049.

Gálhidy, L., B. Mihók, A. Hagyó, K. Rajkai, and T. Standovár. 2005. Effects of gap size and associated changes in light and soil moisture on the understorey vegetation of a Hungarian beech forest. *Plant Ecology* 183:133–145.

Gardner, A. S., I. M. D. Maclean, and K. J. Gaston. 2019. Climatic predictors of species distributions neglect biophysiologically meaningful variables. *Diversity and Distributions*:1–16.

Geiger, R., R. Aron, and P. Todhunter. 2009. The climate near the ground, 7th ed. Rowman & Littlefield.

Gilliam, F. 2007. The ecological significance of the herbaceous layer in temperate forest ecosystems. *Bioscience* 57:845–858.

Gray, A. N., T. A. Spies, and M. J. Easter. 2002. Microclimatic and soil moisture responses to gap formation in coastal Douglas-fir forests. *Canadian Journal of Forest Research* 32:332–343.

Greiser, C., E. Meineri, M. Luoto, J. Ehrlén, and K. Hylander. 2018. Monthly microclimate models in a managed boreal forest landscape. *Agricultural and Forest Meteorology* 250–251:147–158.

Grömping, U. 2006. Relative importance for linear regression in R: the package relaimpo. *Journal of Statistical Software* 17:1–27.

Guisan, A., S. B. Weiss, and A. D. Weiss. 1999. GLM versus CCA spatial modeling of plant species distribution. *Plant Ecology* 143:107–122.

Häntzschel, J., V. Goldberg, and C. Bernhofer. 2005. GIS-based regionalisation of radiation, temperature and coupling measures in complex terrain for low mountain ranges. *Meteorological Applications* 12:33–42.

Harwood, T. D., K. Mokany, and D. R. Paini. 2014. Microclimate is integral to the modeling of plant responses to macroclimate. *Proceedings of the National Academy of Sciences* 111:1164–1165.

Hofmeister, J., J. Hošek, M. Modrý, and J. Roleček. 2009. The influence of light and nutrient availability on herb layer species richness in oak-dominated forests in central Bohemia. *Plant Ecology* 205:57–75.

IPCC. 2014. Climate Change 2014: Synthesis Report. Page Core Writing Team, R.K. Pachauri and L.A. Meyer.

Joly, D., and F. Gillet. 2017. Interpolation of temperatures under forest cover on a regional scale in the French Jura Mountains. *International Journal of Climatology* 37:659–670.

Jucker, T., S. R. Hardwick, S. Both, D. M. O. Elias, R. M. Ewers, D. T. Milodowski, T. Swinfield, and D. A. Coomes. 2018. Canopy structure and topography jointly constrain the microclimate of human-modified tropical landscapes. *Global Change Biology* 24:5243–5258.

Kilibarda, M., T. Hengl, G. B. M. Heuvelink, B. Gräler, E. Pebesma, M. Perčec Tadić, and B. Bajat. 2014. Spatio-temporal interpolation of daily temperatures for global land areas at 1 km resolution. Journal of Geophysical Research: *Atmospheres* 119:2294–2313.

Kopecký, M., and Š. Čížková. 2010. Using topographic wetness index in vegetation ecology: does the algorithm matter? *Applied Vegetation Science* 13:450–459.

Körner, C., and E. Hiltbrunner. 2018. The 90 ways to describe plant temperature. *Perspectives in Plant Ecology, Evolution and Systematics* 30:16–21.

Körner, C., and J. Paulsen. 2004. A world-wide study of high altitude treeline temperatures. *Journal of Biogeography* 31:713–732.

Kovács, B., F. Tinya, and P. Ódor. 2017. Stand structural drivers of microclimate in mature temperate mixed forests. *Agricultural and Forest Meteorology* 234–235:11–21.

Kulonen, A., R. A. Imboden, C. Rixen, S. B. Maier, and S. Wipf. 2018. Enough space in a warmer world? Microhabitat diversity and small-scale distribution of alpine plants on mountain summits. *Diversity and Distributions* 24:252–261.

Leempoel, K., C. Parisod, C. Geiser, L. Daprà, P. Vittoz, and S. Joost. 2015. Very high-resolution digital elevation models: Are multi-scale derived variables ecologically relevant? *Methods in Ecology and Evolution* 6:1373–1383.

Legendre, P., and L. Lengendre. 2012. Numerical ecology. *Elsevier*.

Lembrechts, J. J., I. Nijs, and J. Lenoir. 2018, November. Incorporating microclimate into species distribution models. *Ecography*:1–13.

Lenoir, J., B. J. Graae, P. A. Aarrestad, I. G. Alsos, W. S. Armbruster, G. Austrheim, C. Bergendorff, H. J. B. Birks, K. A. Bråthen, J. Brunet, H. H. Bruun, C. J. Dahlberg, G. Decocq, M. Diekmann, M. Dynesius, R. Ejrnæs, J. A. Grytnes, K. Hylander, K. Klanderud, M. Luoto, A. Milbau, M. Moora, B. Nygaard, A. Odland, V. T. Ravolainen, S. Reinhardt, S. M. Sandvik, F. H. Schei, J. D. M. Speed, L. U. Tveraabak, V. Vandvik, L. G. Velle, R. Virtanen, M. Zobel, and J. C. Svenning. 2013. Local temperatures inferred from plant communities suggest strong spatial buffering of climate warming across Northern Europe. *Global Change Biology* 19:1470–1481.

Lookingbill, T. R., and D. L. Urban. 2003. Spatial estimation of air temperature differences for landscape-scale studies in montane environments. *Agricultural and Forest Meteorology* 114:141–151.

McArdle, B. H., and M. J. Anderson. 2001. Fitting multivariate models to community data: A comment on distance-based redundancy analysis. *Ecology* 82:290–297.

Nadeau, C. P., M. C. Urban, and J. R. Bridle. 2017. Coarse climate change projections for species living in a fine-scaled world. *Global Change Biology* 23:12–24.

Økland, R. H. 1996. Are ordination and constrained ordination alternative or complementary strategies in general ecological studies? *Journal of Vegetation Science* 7:289–292.

Økland, R. H. 1999. On the variation explained by ordination and constrained ordination axes. *Journal of Vegetation Science* 10:131–136.

Oksanen, J., F. G. Blanchet, M. Friendly, R. Kindt, P. Legendre, D. McGlinn, P. R. Minchin, R. B. O'Hara, G. L. Simpson, P. Solymos, M. H. H. Stevens, E. Szoecs, and H. Wagner. 2018. vegan: Community Ecology Package. R package version 2.4-6.

Olaya, V., and O. Conrad. 2009. Geomorphometry in SAGA. Pages 293–308 in T. Hengl and H. Reuter, editors. Geomorphometry: concepts, software, applications. Elsevier, Amsterdam.

Parmesan, C., T. L. Root, and M. R. Willig. 2000. Impacts of Extreme Weather and Climate on Terrestrial Biota. *Bulletin of the American Meteorological Society* 81:443–450.

Potter, K. a, H. Arthur Woods, and S. Pincebourde. 2013. Microclimatic challenges in global change biology. *Global Change Biology* 19:2932–2939.

Pypker, T. G., M. H. Unsworth, B. Lamb, E. Allwine, S. Edburg, E. Sulzman, A. C. Mix, and B. J. Bond. 2007. Cold air drainage in a forested valley: Investigating the feasibility of monitoring ecosystem metabolism. *Agricultural and Forest Meteorology* 145:149–166.

R Core Team. 2016. R: A language and environment for statistical computing , Vienna, Austria. URL http://www.R-project.org/. R Foundation for Statistical Computing, Vienna, Austria.

Reger, B., C. Kölling, and J. Ewald. 2011. Modelling effective thermal climate for mountain forests in the Bavarian Alps: Which is the best model? *Journal of Vegetation Science* 22:677–687.

Renaud, V., and M. Rebetez. 2009. Comparison between open-site and below-canopy climatic conditions in Switzerland during the exceptionally hot summer of 2003. *Agricultural and Forest Meteorology* 149:873–880.

Running, S. W., R. R. Nemani, and R. D. Hungerford. 1987. Extrapolation of synoptic meteorological data in mountainous terrain and its use for simulating forest evapotranspiration and photosynthesis. *Canadian Journal of Forest Research* 17:472–483.

Slavich, E., D. I. Warton, M. B. Ashcroft, J. R. Gollan, and D. Ramp. 2014. Topoclimate versus macroclimate: how does climate mapping methodology affect species distribution models and climate change projections? *Diversity and Distributions* 20:952–963.

Stevens, J. T., H. D. Safford, S. Harrison, and A. M. Latimer. 2015. Forest disturbance accelerates thermophilization of understory plant communities. *Journal of Ecology* 103:1253–1263.

Strachan, S., and C. Daly. 2017. Testing the daily PRISM air temperature model on semiarid mountain slopes. *Journal of Geophysical Research Atmospheres* 122:5697–5715.

Suggitt, A. J., P. K. Gillingham, J. K. Hill, B. Huntley, W. E. Kunin, D. B. Roy, and C. D. Thomas. 2011. Habitat microclimates drive fine-scale variation in extreme temperatures. *Oikos* 120:1–8.

Tinya, F., B. Kovács, A. Prättälä, P. Farkas, R. Aszalós, and P. Ódor. 2019. Initial understory response to experimental silvicultural treatments in a temperate oak-dominated forest. *European Journal of Forest Research* 138:65–77.

Tinya, F., S. Márialigeti, I. Király, B. Németh, and P. Ódor. 2009. The effect of light conditions on herbs, bryophytes and seedlings of temperate mixed forests in Őrség, Western Hungary. *Plant Ecology* 204:69–81.

Tolasz, R., T. Míková, A. Valeriánová, and V. Voženílek, editors. 2007. Climate atlas of Czechia. First edition. Czech Hydrometeorological Institute, Praha - Olomouc.

Treml, V., and M. Banaš. 2008. The effect of exposure on alpine treeline position: a case study from the High Sudetes, Czech Republic. *Arctic, Antarctic, and Alpine Research* 40:751–760.

Valladares, F., and Ü. Niinemets. 2008. Shade tolerance, a key plant feature of complex nature and consequences. *Annual Review of Ecology, Evolution, and Systematics* 39:237–257.

Valverde, T., and J. Silvertown. 1997. Canopy closure rate and forest structure. *Ecology* 78:1555–1562.

Vanwalleghem, T., and R. K. Meentemeyer. 2009. Predicting forest microclimate in heterogeneous landscapes. *Ecosystems* 12:1158–1172.

Westhoff, V., and E. Van Der Maarel. 1978. The Braun-Blanquet Approach. Pages 287–399 Classification of Plant Communities. *Springer Netherlands, Dordrecht*.

Wild, J., M. Kopecký, M. Macek, M. Šanda, J. Jankovec, and T. Haase. 2019. Climate at ecologically relevant scales: A new temperature and soil moisture logger for long-term microclimate measurement. *Agricultural and Forest Meteorology* 268:40–47.

Wilson, J. P., and J. C. Gallant. 2000. Secondary topographic attributes. Pages 87–131 in J. P. Wilson and J. C. Gallant, editors. Terrain Analysis: Principles and Applications. *John Wiley & Sons, New York*.

Zellweger, F., D. Coomes, J. Lenoir, L. Depauw, S. L. Maes, M. Wulf, K. J. Kirby, J. Brunet, M. Kopecký, F. Máliš, W. Schmidt, S. Heinrichs, J. den Ouden, B. Jaroszewicz, G. Buyse, F. Spicher, K. Verheyen, and P. De Frenne. 2019. Seasonal drivers of understorey temperature buffering in temperate deciduous forests across Europe. *Global Ecology and Biogeography* DOI: 10.1111/geb.12991

3.10 SUPPLEMENTARY MATERIALS

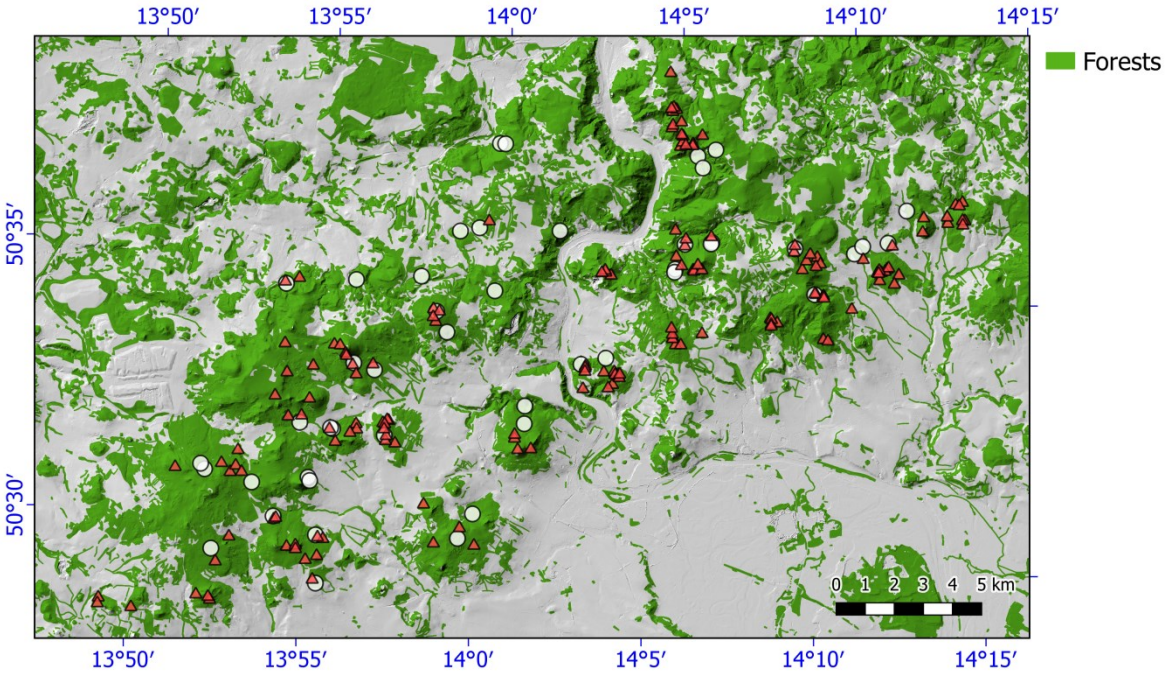

Fig. S1 *Distribution of forested area (green) within study region. Study plots with temperature sensors and plant species composition are displayed with white circles, vegetation-only plots by red triangles in this figure and hereafter.*

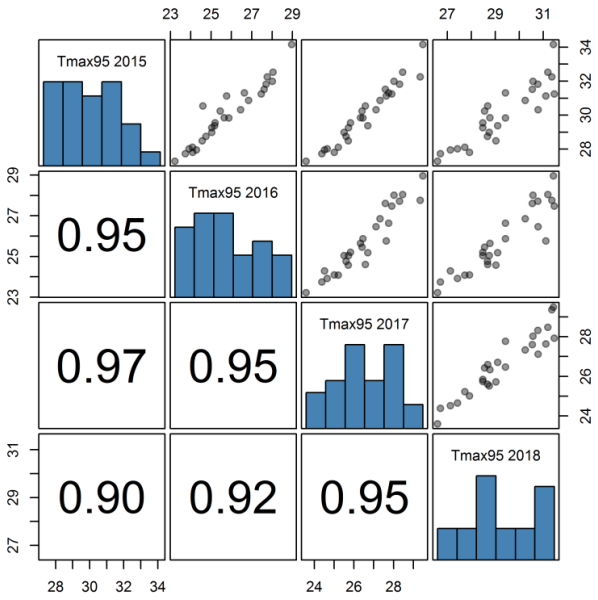

Fig. S2 *Correlation matrix showing in-situ measured maximal temperature (95th percentile of daily maxima; in °C) of the growing seasons 2015 – 2018 (May 1 – September 30). Lower panels show Pearson's correlation coefficients. Despite overall means differ between years, relative differences among locations remained stable.*

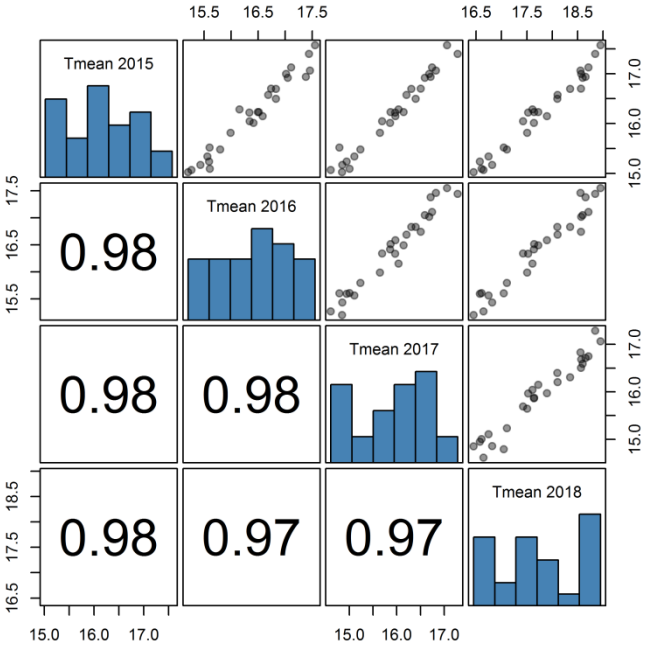

Fig. S3 *Correlation matrix showing in-situ measured growing season (May 1 – September 30) mean temperatures (in °C) for years 2015 – 2018. Lower panels show Pearson's correlation coefficients. Relative positions of sites are stable between years.*

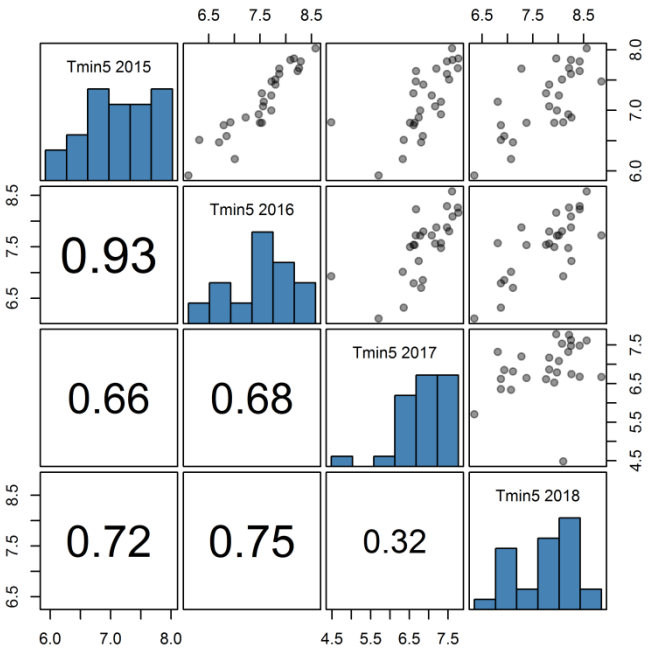

Fig. S4 *Correlation matrix showing in-situ measured minimal temperature (5th percentile of daily minima; in °C) of the growing seasons 2015 – 2018 (May 1 – September 30). Lower panels show Pearson's correlation coefficients. Between-year variability in minimum temperatures was high compared to mean or maximum temperatures.*

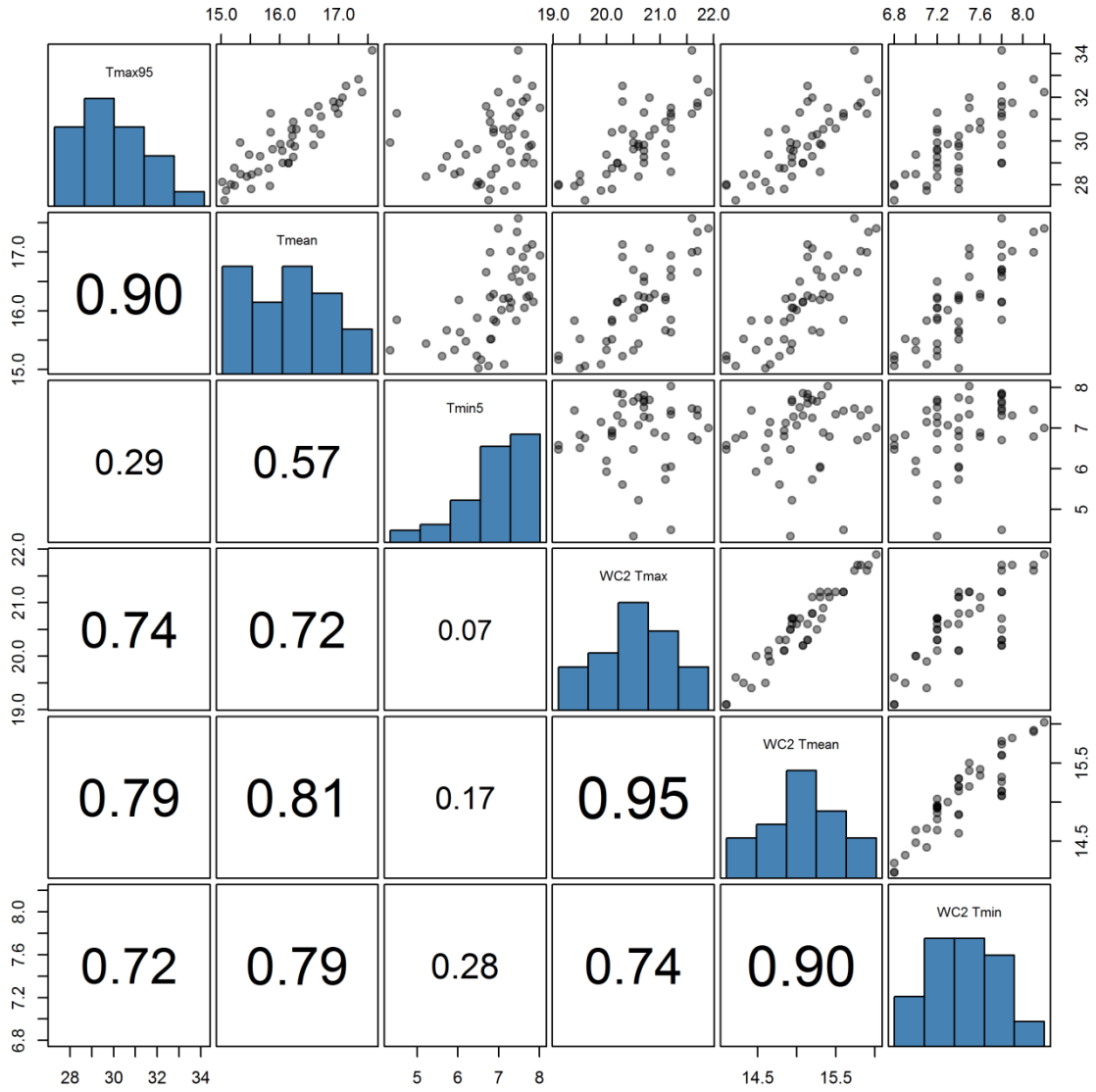

Fig. S5 *Pairwise comparison of climatic characteristics based on in situ measurements and data extracted from Worldclim2 monthly temperature grids for growing season (May to September). Lower panels show Pearson's correlation coefficients. In situ measured variables: 95th percentile of daily maximum temperatures (Tmax95); mean temperature (Tmean); 5th percentile of daily minimum temperatures (Tmin5). Worldclim 2 grids: maximum monthly temperature (WC2 Tmax); average temperature in growing season (WC2 Tmax); minimum from minimum temperatures (WC2 Tmax). All values are in °C.*

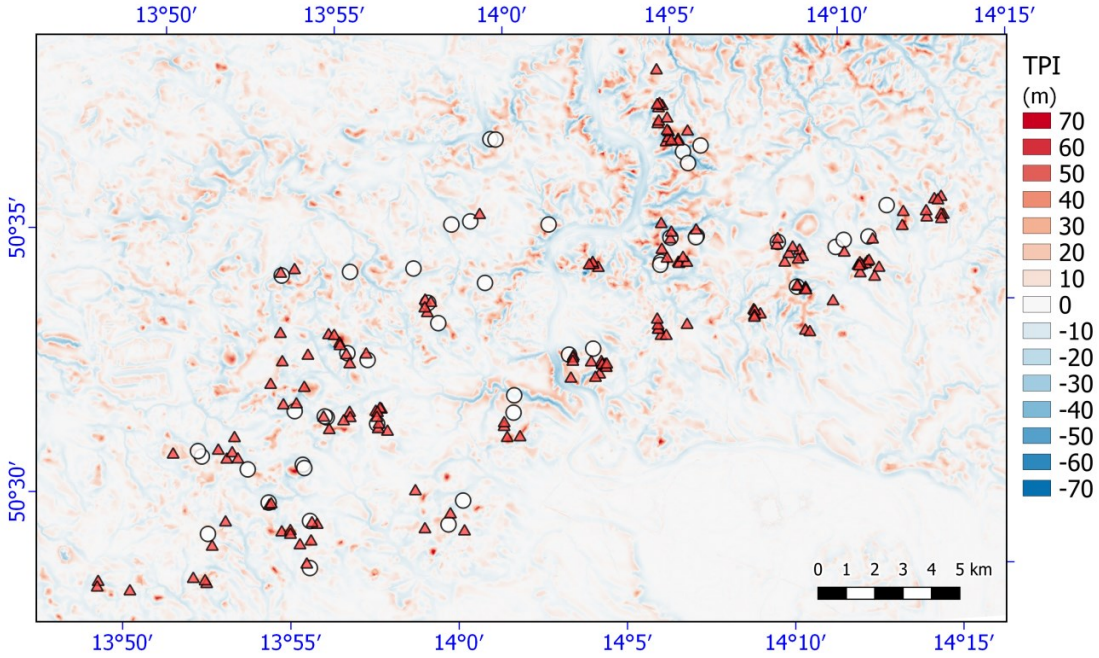

Fig. S6 *Topographic position index (TPI) calculated as difference between actual elevation and averaged elevation in 250m buffer surrounding focal pixel. Positive values (reds) are for areas elevated above surrounding terrain, negative values (blues) represents local depressions. Study plots with temperature sensors and plant species composition are displayed with white circles, vegetation-only plots by red triangles in this figure and hereafter.*

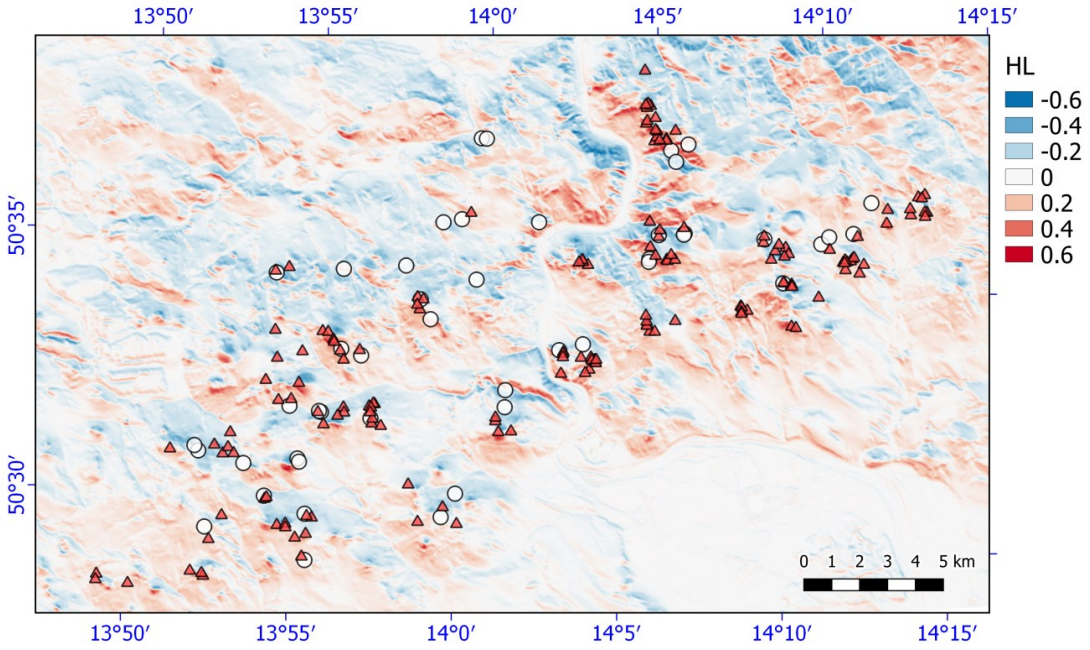

Fig. S7 *Topographic heat load (HL) calculated from slope and aspect. Highest HL values (red) are found on steep SSW (202.5°) facing slopes, zero values (white) on flat areas and negative values (blue) of HL on NNE slopes. HL was calculated using 'diurnal anizotropic heating' function in*

SAGA GIS 3.0.0 with parameter alphamax = 202,5° and resulting surface was smoothed using gaussian filter with 50 m radius.

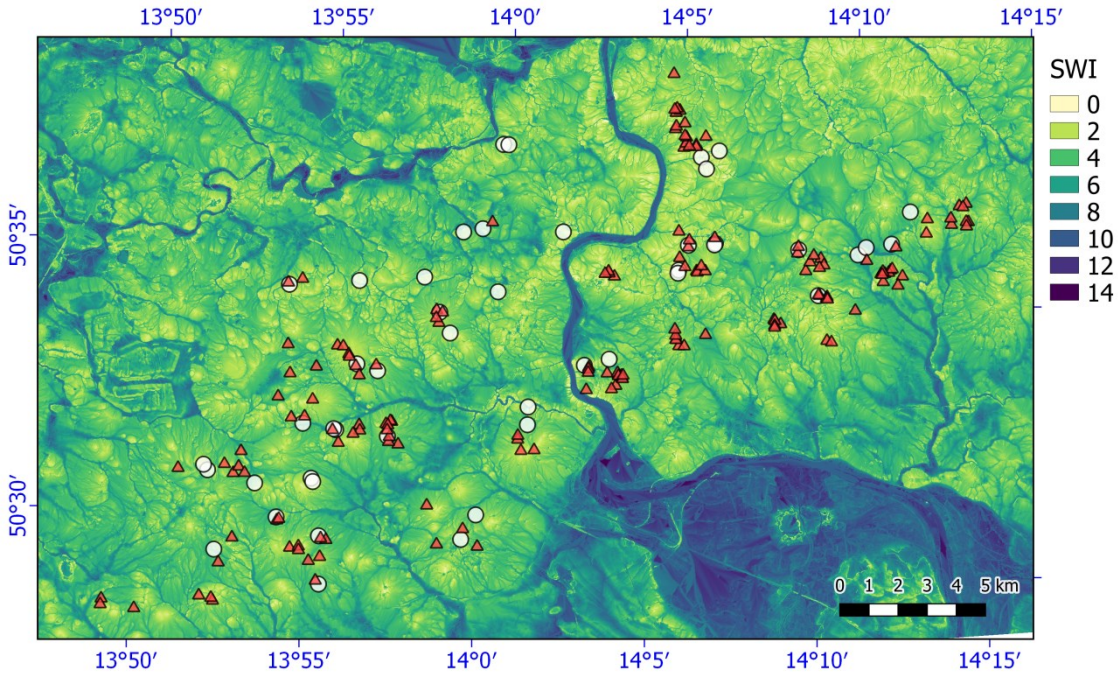

Fig. S8 *SAGA Wetness Index (SWI) was used as a proxy for cold air drainage. High SWI values (blue) denotes area prone to accumulation of cold air, while low SWI (yellow) occurs on well-drained hilltops or ridges.*

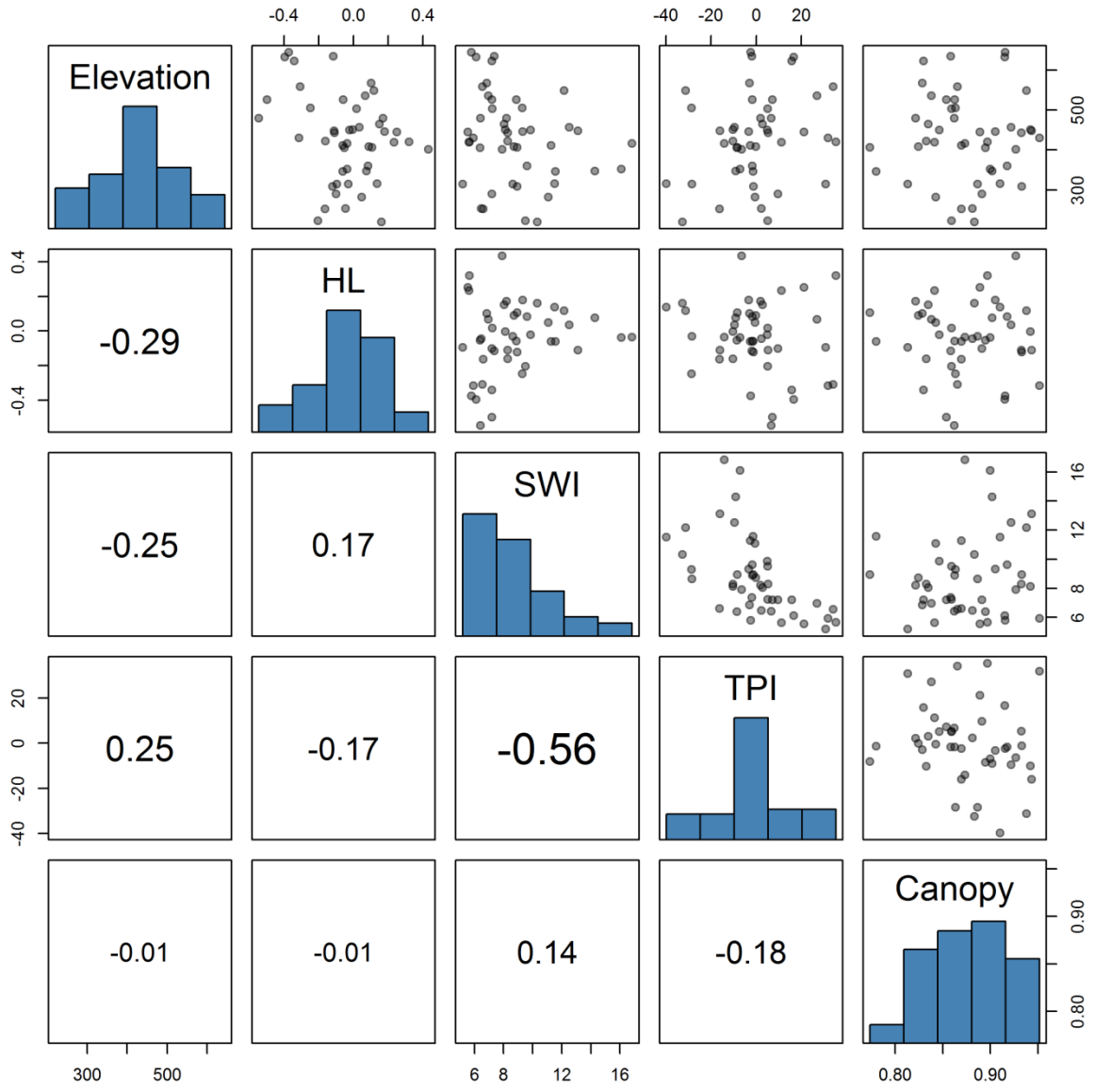

Fig. S9 *Histograms and pairwise comparison of correlation among predictors used to fit measured temperatures on 46 measuring sites: Elevation (m a.s.l.), Canopy - canopy cover (fraction) and topographic attributes HL – heat load (unitless index), SWI – SAGA wetness index (unitless) and TPI – topographic position index (m). Lower panels show Pearson's correlation coefficients.*

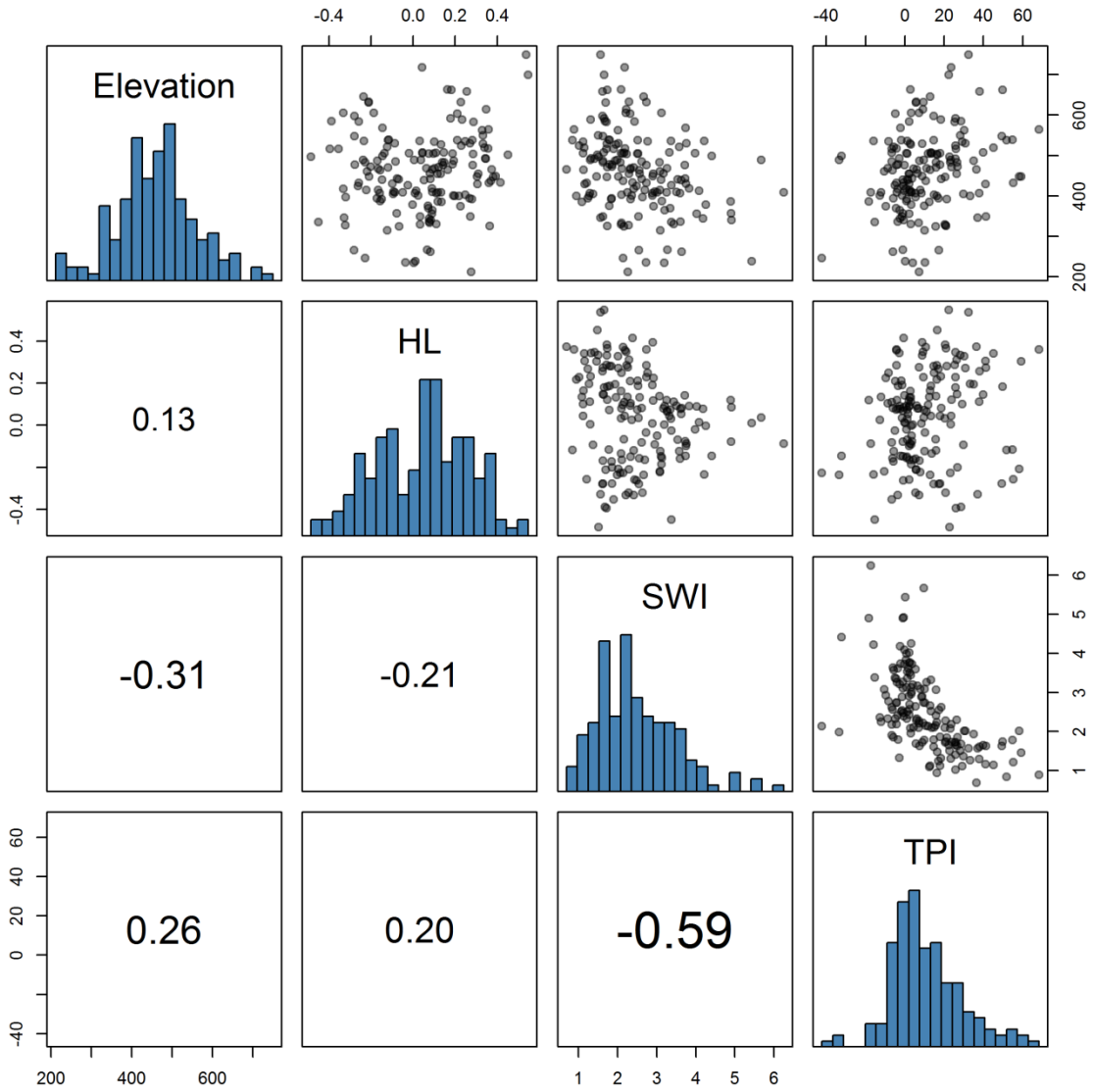

Fig. S10 *Histograms and pairwise comparison of correlation among elevation and topographic attributes for 160 sites with vegetation data only: Elevation (m a.s.l.); and topographic attributes HL – heat load (unitless index), SWI – SAGA wetness index (unitless) and TPI – topographic position index (m). Lower panels show Pearson's correlation coefficients between pairs.*

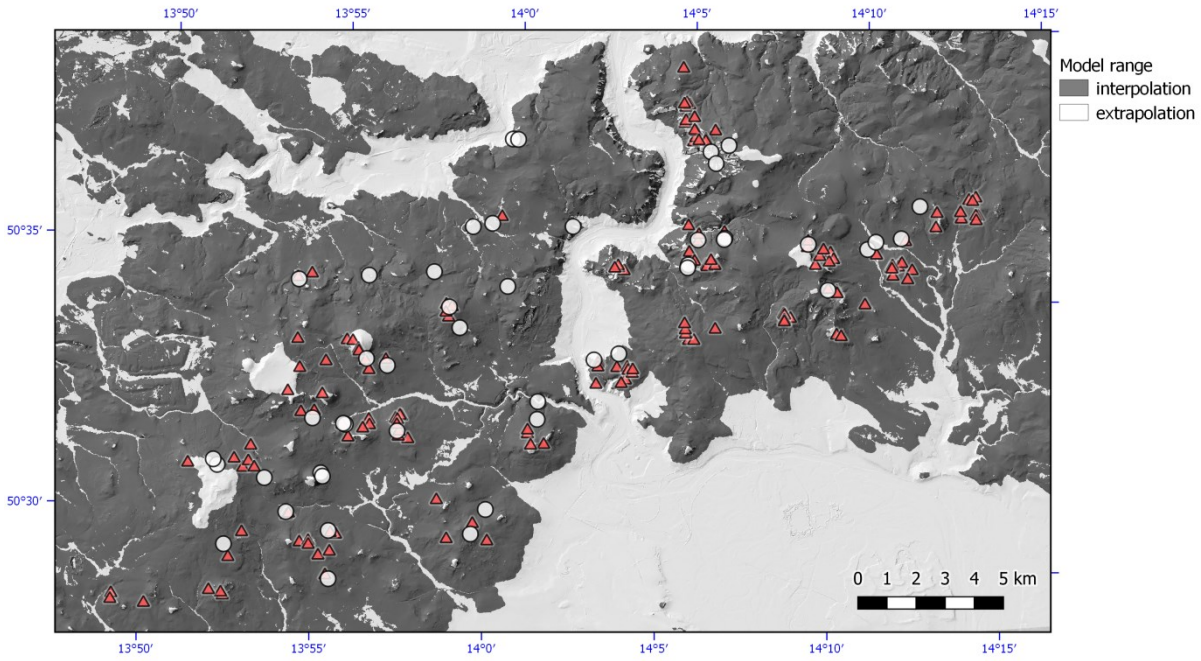

Fig. S11 *Area within the range of terrain parameters used in regression models for temperature (Elevation, Heat Load, Topographic Position Index, SAGA Wetness Index). Dark shaded area represents interpolation between terrain parameters observed on plots with temperature sensors, light shaded area extrapolation outside the range of terrain parameter values.*

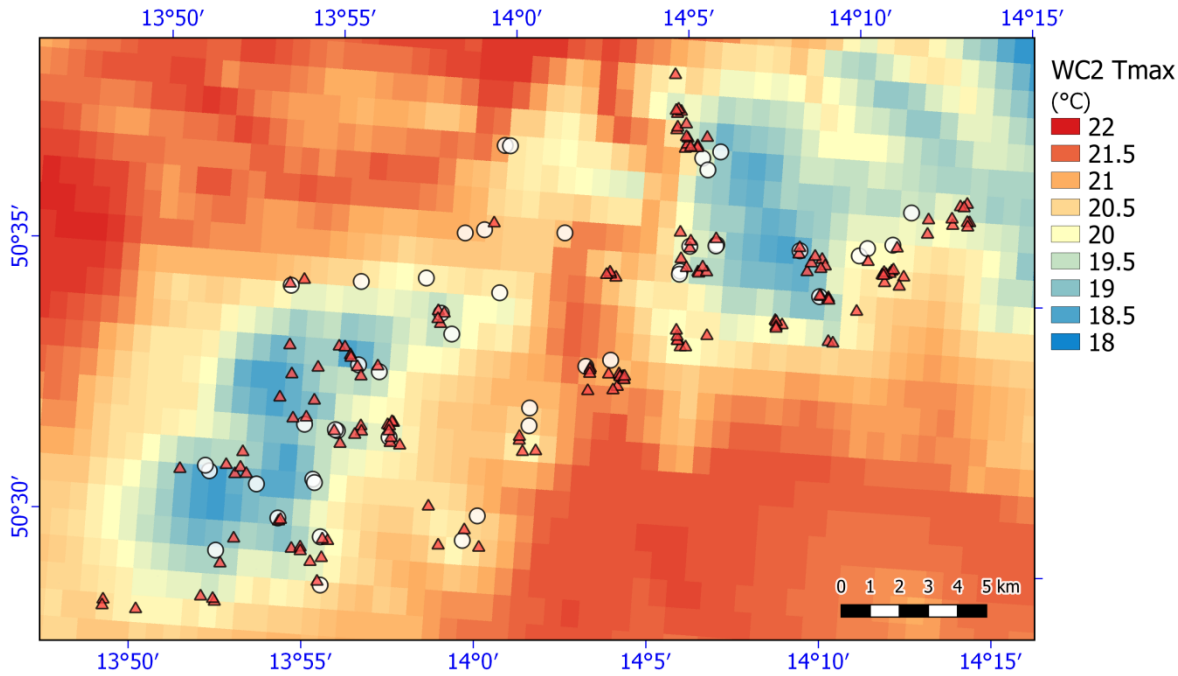

Fig. S12 *Maximum of maximum monthly temperatures in growing season (May-September) from WorldClim2* (Fick & Hijmans, 2017).

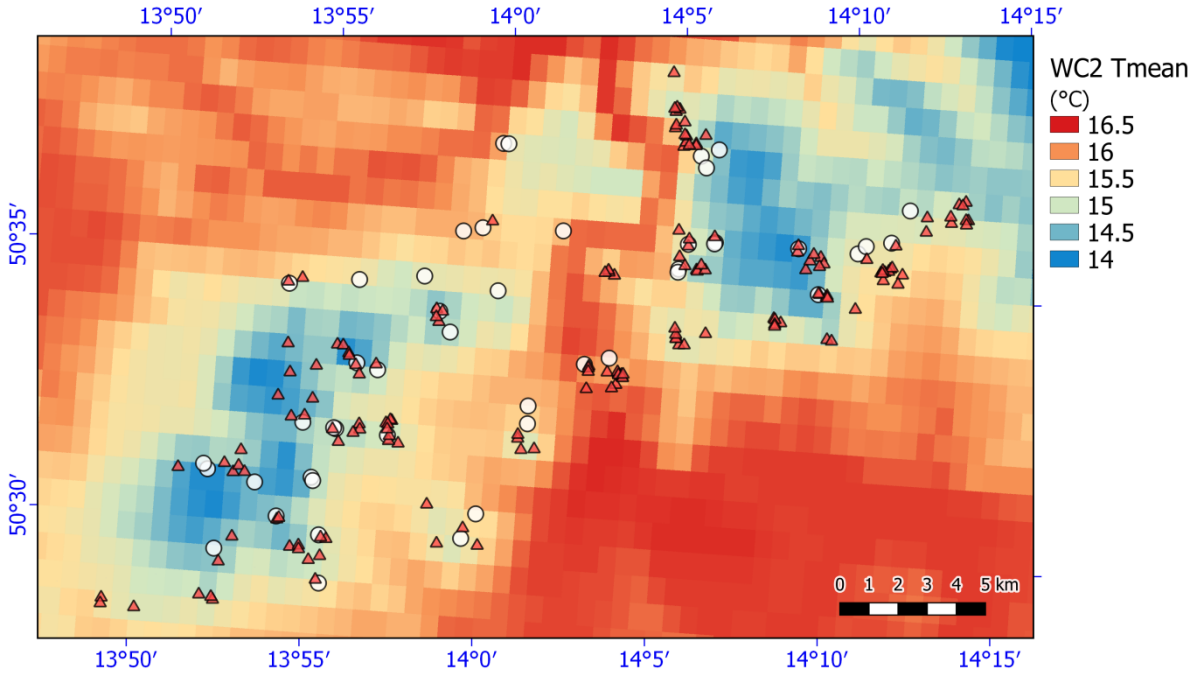

Fig. S13 *Mean of mean monthly temperature in growing season (May-September) from WorldClim2 product (mean annual temperature) for the study area* (Fick & Hijmans, 2017).

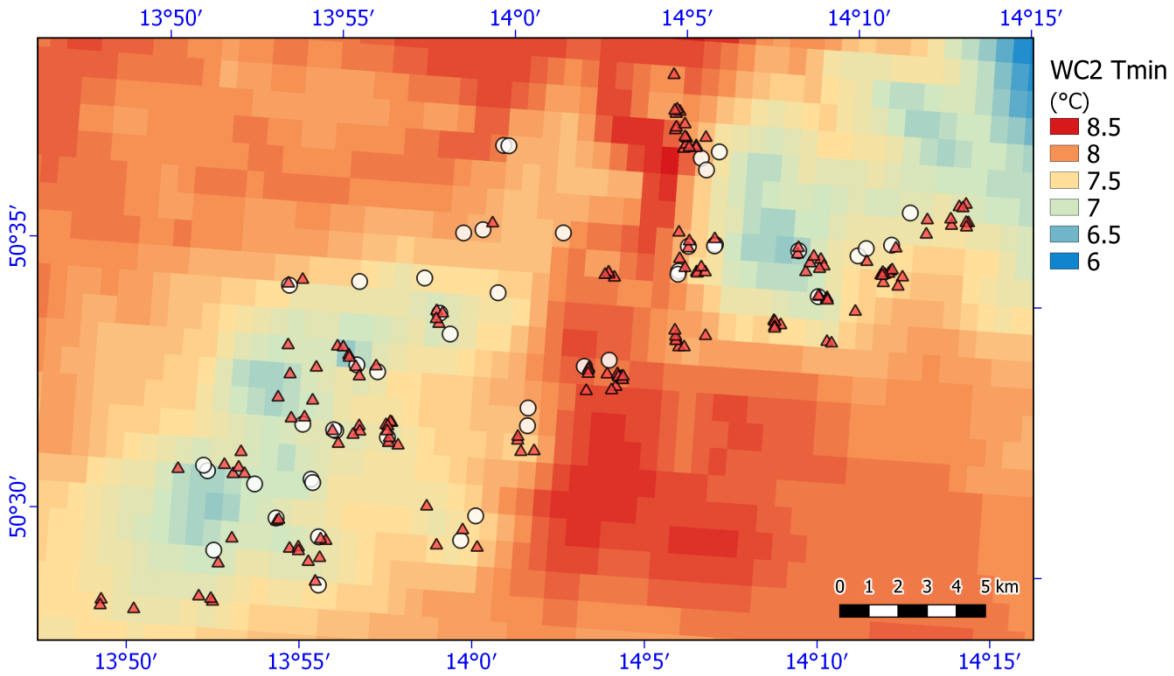

Fig. S14 *Minimum of minimum monthly temperatures in growing season (May-September) from WorldClim2 (WC2 Tmin).*

Table S15 *Model parameters of models compared in stepwise model selection and final model summaries. Set of linear regression models for Tmax95, Tmean and Tmin5 and elevation (Elev), heat load (HL), topographic position index (TPI) and SAGA wetness index (SWI). Models were selected according to BIC, using k = log(n) penalization. Signif. codes: 0 '***' 0.001 '**' 0.01 '*' 0.05 '.' 0.1 ' ' 1*

```
Model selection for Tmax95

Start:  BIC=44.05
Tmax95 ~ 1

         Df Sum of Sq     RSS    BIC F value    Pr(>F)
+ Elev    1    49.981  60.298 20.108 36.4718 2.956e-07 ***
+ HL      1    17.306  92.973 40.026  8.1902  0.006424 **
+ TPI     1     9.916 100.364 43.545  4.3472  0.042906 *
<none>                110.279 44.050
+ Canopy  1     4.952 105.328 45.765  2.0685  0.157448
+ SWI     1     1.220 109.059 47.367  0.4922  0.486632
---

Step:  BIC=20.11
Tmax95 ~ Elev

         Df Sum of Sq     RSS    BIC F value    Pr(>F)
+ TPI     1    25.706  34.593 -1.624 31.9531 1.167e-06 ***
+ SWI     1    16.762  43.536  8.953 16.5560 0.0001982 ***
+ HL      1     6.088  54.210 19.040  4.8294 0.0334133 *
<none>                60.298 20.108
+ Canopy  1     4.762  55.536 20.152  3.6874 0.0614721 .
- Elev    1    49.981 110.279 44.050 36.4718 2.956e-07 ***
---

Step:  BIC=-1.62
Tmax95 ~ Elev + TPI

         Df Sum of Sq     RSS    BIC F value    Pr(>F)
+ HL      1     7.510  27.083 -9.053 11.6458  0.001435 **
+ SWI     1     4.143  30.450 -3.664  5.7144  0.021387 *
<none>                34.593 -1.624
+ Canopy  1     1.635  32.957 -0.023  2.0840  0.156264
- TPI     1    25.706  60.298 20.108 31.9531 1.167e-06 ***
- Elev    1    65.771 100.364 43.545 81.7563 1.674e-11 ***
---

Step:  BIC=-9.05
Tmax95 ~ Elev + TPI + HL

         Df Sum of Sq    RSS     BIC F value    Pr(>F)
+ SWI     1     5.804 21.279 -16.320  11.184  0.001772 **
<none>                27.083  -9.053
+ Canopy  1     1.473 25.610  -7.797   2.358  0.132321
- HL      1     7.510 34.593  -1.624  11.646  0.001435 **
- TPI     1    27.127 54.210  19.040  42.068 7.938e-08 ***
- Elev    1    52.651 79.734  36.789  81.651 2.113e-11 ***
---

Step:  BIC=-16.32
Tmax95 ~ Elev + TPI + HL + SWI

         Df Sum of Sq    RSS     BIC  F value    Pr(>F)
<none>                21.279 -16.320
+ Canopy  1     1.143 20.135 -15.032   2.2711 0.1396660
- SWI     1     5.804 27.083  -9.053  11.1838 0.0017721 **
- HL      1     9.171 30.450  -3.664  17.6708 0.0001386 ***
- TPI     1    12.855 34.134   1.591  24.7700 1.208e-05 ***
- Elev    1    58.340 79.619  40.551 112.4105 2.564e-13 ***
---


Final model summary
Formula = Tmax95 ~ Elev + TPI + HL + SWI
```

```
Residuals:
     Min       1Q   Median       3Q      Max
-1.79375 -0.50041 -0.03022  0.54176  1.30847

Coefficients:
             Estimate Std. Error t value Pr(>|t|)
(Intercept) 29.520733   0.184419 160.074  < 2e-16 ***
Elev        -0.011473   0.001082 -10.602 2.56e-13 ***
TPI          0.036183   0.007270   4.977 1.21e-05 ***
HL           2.280715   0.542555   4.204 0.000139 ***
SWI         -0.708827   0.211956  -3.344 0.001772 **
---
Residual standard error: 0.7204 on 41 degrees of freedom
Multiple R-squared:  0.807,   Adjusted R-squared:  0.7882
F-statistic: 42.87 on 4 and 41 DF,  p-value: 3.943e-14
```

```
Model selection for Tmean

Start:  BIC=-31.87
Tmean ~ 1

         Df Sum of Sq    RSS     BIC F value    Pr(>F)
+ Elev    1    9.4800 11.690 -55.360 35.6828 3.691e-07 ***
+ TPI     1    2.2258 18.944 -33.152  5.1696   0.02792 *
<none>                21.170 -31.871
+ SWI     1    1.1333 20.036 -30.573  2.4887   0.12183
+ HL      1    0.8709 20.299 -29.974  1.8877   0.17642
+ Canopy  1    0.3608 20.809 -28.833  0.7629   0.38718
---

Step:  BIC=-55.36
Tmean ~ Elev

         Df Sum of Sq     RSS     BIC F value    Pr(>F)
+ SWI     1    5.8263  5.8634 -83.270 42.7282 6.054e-08 ***
+ TPI     1    5.4405  6.2492 -80.339 37.4357 2.459e-07 ***
<none>                11.6897 -55.360
+ Canopy  1    0.3387 11.3510 -52.883  1.2830    0.2636
+ HL      1    0.0279 11.6618 -51.641  0.1029    0.7499
- Elev    1    9.4800 21.1697 -31.871 35.6828 3.691e-07 ***
---

Step:  BIC=-83.27
Tmean ~ Elev + SWI

         Df Sum of Sq     RSS     BIC  F value    Pr(>F)
+ TPI     1    1.9543  3.9091 -98.091  20.9974 4.081e-05 ***
<none>                 5.8634 -83.270
+ HL      1    0.2575  5.6058 -81.508   1.9295    0.1721
+ Canopy  1    0.0705  5.7929 -79.998   0.5109    0.4787
- SWI     1    5.8263 11.6897 -55.360  42.7282 6.054e-08 ***
- Elev    1   14.1731 20.0364 -30.573 103.9402 4.786e-13 ***
---

Step:  BIC=-98.09
Tmean ~ Elev + SWI + TPI

         Df Sum of Sq     RSS     BIC  F value    Pr(>F)
<none>                 3.9091 -98.091
+ HL      1    0.2429  3.6662 -97.213   2.7160    0.1070
+ Canopy  1    0.0052  3.9039 -94.323   0.0541    0.8172
- TPI     1    1.9543  5.8634 -83.270  20.9974 4.081e-05 ***
- SWI     1    2.3401  6.2492 -80.339  25.1425 1.016e-05 ***
- Elev    1   14.8959 18.8050 -29.662 160.0443 6.451e-16 ***
---

Final model summary
Formula: Tmean ~ Elev + SWI + TPI

Residuals:
    Min      1Q  Median      3Q     Max
-0.6488 -0.1652 -0.0235  0.1399  0.7876

Coefficients:
```

```
             Estimate Std. Error t value Pr(>|t|)
(Intercept) 15.7964108  0.0780820 202.305  < 2e-16 ***
Elev        -0.0056966  0.0004503 -12.651 6.45e-16 ***
SWI         -0.4463089  0.0890084  -5.014 1.02e-05 ***
TPI          0.0141070  0.0030786   4.582 4.08e-05 ***
---

Residual standard error: 0.3051 on 42 degrees of freedom
Multiple R-squared:  0.8153,  Adjusted R-squared:  0.8022
F-statistic: 61.82 on 3 and 42 DF,  p-value: 1.873e-15
```

```
Model selection for Tmin

Start:  BIC=-13.14
Tmin5 ~ 1

         Df Sum of Sq    RSS      BIC F value    Pr(>F)
+ SWI     1   10.4684 21.341 -27.6715 21.5834 3.076e-05 ***
+ TPI     1    5.3000 26.509 -17.6954  8.7969  0.004861 **
<none>                31.809 -13.1400
+ HL      1    0.5474 31.262 -10.1098  0.7704  0.384854
+ Elev    1    0.1195 31.690  -9.4845  0.1660  0.685698
+ Canopy  1    0.0011 31.808  -9.3129  0.0015  0.969483
---

Step:  BIC=-27.67
Tmin5 ~ SWI

         Df Sum of Sq    RSS     BIC F value    Pr(>F)
<none>                21.341 -27.672
+ Elev    1    0.9094 20.431 -25.846  1.9140    0.1737
+ TPI     1    0.6417 20.699 -25.247  1.3331    0.2546
+ Canopy  1    0.1280 21.213 -24.120  0.2595    0.6131
+ HL      1    0.0009 21.340 -23.845  0.0018    0.9660
- SWI     1   10.4684 31.809 -13.140 21.5834 3.076e-05 ***
---

Final model summary
Formula = Tmin5 ~ SWI

Residuals:
    Min      1Q  Median      3Q     Max
-1.7331 -0.4013  0.1455  0.4669  1.3171

Coefficients:
            Estimate Std. Error t value Pr(>|t|)
(Intercept)   6.3357     0.1564  40.521  < 2e-16 ***
SWI          -0.7805     0.1680  -4.646 3.08e-05 ***
---

Residual standard error: 0.6964 on 44 degrees of freedom
Multiple R-squared:  0.3291,  Adjusted R-squared:  0.3139
F-statistic: 21.58 on 1 and 44 DF,  p-value: 3.076e-05
```

Table S16 *List of species, their abbreviations and frequency in datasets with in-situ temperatures and in independent dataset used for validation of topoclimatic maps. Nomenclature according to: Kubát, K., L. Hrouda, J. Chrtek, Z. Kaplan, J. Kirschner, and J. Štěpánek, editors. 2002. Klíč ke květeně České republiky [Key to the flora of the Czech republic]. Academia, Praha.*

Species	Abbreviation	Frequncy: Temperature + vegetation dataset (n = 46)	Frequency: Vegetation only dataset (n = 160)
Acer campestre	Acercamp	21	47
Acer platanoides	Acerplat	20	53
Acer pseudoplatanus	Acerpseu	28	70
Actaea spicata	Actaspic	3	23
Adoxa moschatellina	Adoxmosc	1	2
Aegopodium podagraria	Aegopoda	11	23
Achillea millefolium agg.	Achimill	0	10
Ajuga reptans	Ajugrept	2	5
Alliaria petiolata	Allipeti	9	47
Anemone nemorosa	Anemnemo	15	40
Anthericum ramosum	Anthramo	3	17
Anthriscus sylvestris	Anthsylv	5	18
Arctium minus agg.	Arctminu	1	3
Asarum europaeum	Asareuro	7	15
Astragalus glycyphyllos	Astrglyc	1	16
Astrantia major	Astrmajo	3	7
Athyrium filix-femina	Athyfili	1	11
Avenella flexuosa	Avenflex	3	19
Betula pendula	Betupend	1	4
Brachypodium pinnatum	Bracpinn	1	21
Brachypodium sylvaticum	Bracsylv	14	40
Bromus benekenii	Brombene	7	45
Bromus erectus	Bromerec	1	0
Calamagrostis arundinacea	Calaarun	15	74
Calamagrostis epigejos	Calaepig	5	17
Campanula persicifolia	Camppers	4	13
Campanula rapunculoides	Camprapu	6	1
Campanula rapunculoides	Camprapu	6	28
Campanula rotundifolia	Camprotu	2	6
Cardaminopsis arenosa ssp. arenosa	Cardaren	1	2
Cardamine impatiens	Cardimpa	3	10
Carex brizoides	Carebriz	1	2
Carex digitata	Caredigi	3	1
Carex montana	Caremont	3	6
Carex muricata agg.	Caremuri	1	17
Carex species	Carespec	1	2

Species	Abbreviation	Frequncy: Temperature + vegetation dataset (n = 46)	Frequency: Vegetation only dataset (n = 160)
Carex sylvatica	Caresylv	4	12
Carpinus betulus	Carpbetu	27	41
Cephalanthera rubra	Cephrubr	1	0
Cerastium lucorum	Ceraluco	0	0
Circaea lutetiana	Circlute	2	2
Cirsium arvense	Cirsarve	0	2
Convallaria majalis	Convmaja	13	40
Cornus species	Cornspec	1	0
Corylus avellana	Coryavel	11	14
Crataegus species	Cratspec	18	27
Dactylis glomerata	Dactglom	3	20
Dactylis polygama	Dactpoly	6	26
Daphne mezereum	Daphmeze	2	6
Dentaria bulbifera	Dentbulb	1	0
Dentaria enneaphyllos	Dentenne	1	1
Deschampsia cespitosa	Desccesp	4	10
Digitalis lutea	Digilute	2	0
Dryopteris carthusiana	Dryocart	7	20
Dryopteris dilatata	Dryodila	4	15
Dryopteris filix-mas	Dryofili	11	38
Elymus caninus	Elymcani	2	21
Epilobium montanum	Epilmont	1	8
Epipactis purpurata	Epippurp	1	3
Euonymus europaeus	Euoneuro	5	4
Euonymus europaeus	Euoneuro	5	3
Euphorbia dulcis	Euphdulc	1	3
Fagus sylvatica	Fagusylv	23	58
Fallopia convolvulus	Fallconv	5	50
Festuca gigantea	Festgiga	8	24
Festuca heterophylla	Festhete	1	15
Festuca ovina	Festovin	4	13
Festuca rubra agg.	Festrubr	1	1
Filipendula ulmaria	Filiulma	1	2
Fragaria moschata	Fragmosc	10	20
Fragaria vesca	Fragvesc	3	21
Frangula alnus	Franalnu	1	1
Fraxinus excelsior	Fraxexce	38	112
Galeopsis bifida	Galebifi	4	1
Galeobdolon luteum	Galelute	13	26
Galeopsis pubescens	Galepube	3	1
Galeopsis speciosa	Galespec	1	7

Species	Abbreviation	Frequncy: Temperature + vegetation dataset (n = 46)	Frequency: Vegetation only dataset (n = 160)
Galeopsis tetrahit agg.	Galetetr	12	60
Galium aparine	Galiapar	8	50
Galium boreale	Galibore	2	2
Galium glaucum	Galiglau	0	1
Galium odoratum	Galiodor	27	90
Galium sylvaticum	Galisylv	9	17
Geranium robertianum	Gerarobe	6	36
Geum urbanum	Geumurba	21	67
Glechoma hederacea	Glechede	1	1
Hedera helix	Hedeheli	4	7
Hepatica nobilis	Hepanobi	16	48
Heracleum sphondylium	Heraspho	1	2
Hierochloe australis	Hieraust	1	0
Hieracium lachenalii	Hierlach	2	7
Hieracium murorum	Hiermuro	4	29
Hieracium sabaudum	Hiersaba	3	2
Hordelymus europaeus	Hordeuro	8	31
Hylotelephium maximum	Hylomaxi	1	9
Hypericum hirsutum	Hypehirs	1	4
Hypericum perforatum	Hypeperf	3	20
Chaerophyllum aromaticum	Chaearom	2	6
Chaerophyllum hirsutum	Chaehirs	1	0
Chaerophyllum temulum	Chaetemu	8	45
Chelidonium majus	Chelmaju	1	2
Impatiens noli-tangere	Impanoli	5	23
Impatiens parviflora	Impaparv	40	138
Juglans regia	Juglregi	2	0
Juncus effusus	Junceffu	1	0
Lamium maculatum	Lamimacu	1	4
Lapsana communis	Lapscomm	2	13
Lathyrus niger	Lathnige	6	21
Lathyrus pratensis	Lathprat	1	0
Lathyrus vernus	Lathvern	14	46
Ligustrum vulgare	Liguvulg	1	2
Lilium martagon	Lilimart	8	15
Lonicera xylosteum	Lonixylo	8	9
Lunaria rediviva	Lunaredi	1	1
Luzula luzuloides	Luzuluzu	7	35
Lychnis viscaria	Lychvisc	1	7
Lysimachia nummularia	Lysinumm	3	6
Maianthemum bifolium	Maiabifo	5	19

Species	Abbreviation	Frequncy: Temperature + vegetation dataset (n = 46)	Frequency: Vegetation only dataset (n = 160)
Melampyrum pratense	Melaprat	5	18
Melittis melissophyllum	Melimeli	2	11
Melica nutans	Melinuta	14	45
Melica uniflora	Meliunif	3	4
Mentha arvensis	Mentarve	1	1
Mercurialis perennis	Mercpere	22	71
Mespilus germanica	Mespgerm	1	0
Milium effusum	Milieffu	11	18
Moehringia trinervia	Moehtrin	14	56
Molinia arundinacea	Moliarun	1	1
Mycelis muralis	Mycemura	9	26
Myosotis species	Myosspec	1	0
Oxalis acetosella	Oxalacet	4	13
Petasites albus	Petaalbu	2	10
Plantago major	Planmajo	1	6
Poa angustifolia	Poaangu	3	5
Poa nemoralis	Poanemo	25	98
Polygonatum multiflorum	Polymult	7	22
Polygonatum odoratum	Polyodor	7	12
Polygonatum verticillatum	Polyvert	2	3
Polypodium vulgare	Polyvulg	1	0
Polypodium vulgare	Polyvulg	1	1
Populus tremula	Poputrem	3	9
Prenanthes purpurea	Prenpurp	3	7
Primula elatior	Primelat	1	0
Primula veris	Primveri	2	7
Prunus avium	Prunaviu	7	21
Prunus spinosa	Prunspin	3	15
Prunella vulgaris	Prunvulg	1	1
Pulmonaria obscura	Pulmobsc	20	47
Pyrus communis	Pyrucomm	2	4
Quercus cerris	Quercerr	1	0
Quercus petraea	Querpetr	34	81
Ranunculus auricomus agg.	Ranuauri	1	8
Ranunculus lanuginosus	Ranulanu	1	5
Ranunculus repens	Ranurepe	1	0
Ribes uva-crispa	Ribeuva	10	7
Rosa canina agg.	Rosacani	14	40
Rosa gallica	Rosagall	1	0
Rubus caesius	Rubucaes	1	0
Rubus fruticosus agg.	Rubufrut	11	53

Species	Abbreviation	Frequncy: Temperature + vegetation dataset (n = 46)	Frequency: Vegetation only dataset (n = 160)
Rubus idaeus	Rubuidae	3	29
Sambucus nigra	Sambnigr	17	37
Sambucus racemosa	Sambrace	1	1
Sanicula europaea	Sanieuro	3	13
Scrophularia nodosa	Scronodo	6	27
Senecio ovatus	Seneovat	11	24
Senecio viscosus	Senevisc	1	3
Serratula tinctoria	Serrtinc	1	0
Sorbus aria agg.	Sorbaria	4	3
Sorbus aucuparia	Sorbaucu	15	52
Stachys sylvatica	Stacsylv	8	32
Stellaria holostea	Stelholo	20	67
Stellaria media	Stelmedi	2	9
Stellaria neglecta	Stelnegl	0	0
Stellaria nemorum agg.	Stelnemo	1	0
Symphytum tuberosum agg.	Symptube	0	4
Tanacetum corymbosum	Tanacory	8	42
Taraxacum sect. Ruderalia	Tarasect	2	4
Tilia cordata	Tilicord	14	18
Tilia platyphyllos	Tiliplat	4	4
Torilis japonica	Torijapo	2	10
Ulmus glabra	Ulmuglab	6	6
Ulmus laevis	Ulmulaev	1	1
Urtica dioica	Urtidioi	21	112
Vaccinium myrtillus	Vaccmyrt	1	13
Veronica chamaedrys	Verocham	7	30
Veronica officinalis	Verooffi	4	14
Viburnum opulus	Vibuopul	2	4
Vicia dumetorum	Vicidume	1	1
Vicia sepium	Vicisepi	1	14
Vicia sylvatica	Vicisylv	0	4
Viola collina	Violcoll	3	7
Viola mirabilis	Violmira	1	2
Viola odorata	Violodor	2	6
Viola reichenbachiana	Violreic	19	46
Viola riviniana	Violrivi	2	12

CHAPTER FOUR:

NICHE ASYMMETRY OF VASCULAR PLANTS INCREASES WITH ELEVATION

MIROSLAV DVORSKÝ[1], MARTIN MACEK[1,2], MARTIN KOPECKÝ[1,3], JAN WILD[1,4] AND JIŘÍ DOLEŽAL[1,5]

1 Institute of Botany, The Czech Academy of Sciences, Zámek 1, CZ-252 43, Průhonice, Czech Republic

2 Department of Botany, Faculty of Science, Charles University, Benátská 2, Praha, CZ-128 01, Czech Republic

3 Department of Forest Ecology, Faculty of Forestry and Wood Sciences, Czech University of Life Sciences Prague, Kamýcká 129, CZ-165 21, Praha 6-Suchdol, Czech Republic

4 Faculty of Environmental Sciences, Czech University of Life Sciences Prague, Kamýcká 129, CZ-165 21, Praha 6-Suchdol, Czech Republic

5 Department of Botany, Faculty of Science, University of South Bohemia, Na Zlaté stoce 1, CZ -370 05, České Budějovice, Czech Republic

Published *in: Journal of Biogeography (2017) 44: 1418–1425.*
DOI: 10.1111/jbi.13001

4.1 ABSTRACT

Aim Species distributions along an environmental gradient are often not symmetric but skewed towards one end of the gradient. Various explanations for this skewness have been proposed but the patterns of niche asymmetry along extensive environmental gradients have been rarely explored. Here we tested three predictions of asymmetric abiotic stress limitation (AASL) hypothesis that predicts a steeper decrease in the probability of occurrence towards the more stressful end of a plant distributional range.

Location Ladakh, arid Himalayas, where drought stress dominates in lower elevation, while the cold stress dominates in upper elevations.

Methods Using data from 4062 plots (2640–6150 m a.s.l.), we explored the shapes of response curves of 395 vascular plant species through Huismann-Ollf-Fresco models. We compared the observed patterns of niche asymmetry along the elevational gradient with null models.

Results Species with symmetric response curves (61.5%) prevailed at lower elevations, while species with left-skewed responses (36.2%) were significantly underrepresented up to 3750 m a.s.l. and occurred significantly more frequently at 5150–5450 m a.s.l. Right-skewed responses were rare (2.3%) along the whole gradient. The steepness of the response increased with elevation. Response types were found in similar proportions across different habitats and functional groups.

Main conclusions Our results support the predictions of AASL hypothesis for cold limits, but not for dry limits. The low proportion of right-skewed responses over the entire gradient suggests an effective adaptation of the local flora to arid conditions, or sufficient opportunity to avoid drought stress through the presence of favourable habitat patches. The accumulation of skewed responses at high elevations likely reflects shared physiological limits of many steppe species, whose distribution abruptly ends at the transition between steppe and alpine zones. Cold therefore represents a stronger barrier to species distribution than drought.

4.2 KEYWORDS

drought stress, Himalaya, HOF model, low temperature stress, skewed response, species range limits, species response curve

4.3 INTRODUCTION

Asymmetric responses of vascular plant species have been reported for various environmental gradients (Oksanen & Minchin, 2002), but its causes are not fully understood (Austin, 2007). Various factors have been proposed to produce asymmetric responses, including physiological constraints and biotic interactions (Austin & Gaywood, 1994; Ettinger & HilleRisLambers, 2013). Recently, Normand *et al.* (2009) introduced the asymmetric abiotic stress limitation (AASL) hypothesis, predicting a steeper decrease in the probability of occurrence towards the physiologically more stressful ends of abiotic gradients. Some aspects of the AASL hypothesis have already been documented, e.g. a considerable proportion of species have been shown to respond asymmetrically to an abiotic gradient (Murphy *et al.*, 2010; Suchrow & Jensen, 2010). However, such findings are not always accepted as a definite proof of the validity of AASL hypothesis (Boucher Lalonde *et al.*, 2012). Moreover, several relevant issues still remain to be explored, for example, the distribution of asymmetric responses in relation to an abiotic stress gradient, the presumably increasing proportion of asymmetric responses with elevated abiotic stress, or the universality of AASL hypothesis predictions.

Increasing evidence suggests that cold limits of vascular plants are determined by distinctly different factors than limits associated with warm areas (Sexton *et al.*, 2009; Pellissier *et al.*, 2013). While cold limits are believed to be primarily driven by abiotic factors (Ettinger *et al.*, 2011; Butterfield, 2015), warm limits are thought to be shaped mostly by biotic factors, particularly competition (Meier *et al.*, 2010; Wisz *et al.*, 2013; but see Cahill *et al.*, 2014). Therefore, the underlying cause of asymmetry in a species response to an environmental gradient could be explained by the varying strength of these factors. Effects of low temperature, including repeated damage by freezing and a short vegetation season, pose physiological constraints on plant growth, development and reproduction, resulting in direct climatic stress (Körner, 2003; Vetaas 2002). Despite an increasing understanding regarding the physiological drivers of cold limits in vascular plants (e.g. Li *et al.*, 2008; Shi *et al.*, 2008; Wiley & Helikker, 2012), there is a lack of studies focusing on the distributional patterns of entire species pools which could demonstrate whether there is a universal temperature threshold. Such an approach however can only be applied to data covering whole species ranges and, importantly, in a region where the vegetation is of the same physiognomy. This is because transitions between physiognomically different vegetation types naturally produce asymmetric distributional patterns (e.g. forest herbaceous species steeply decline at treeline, being bound to the specific forest microclimate; Doležal & Šrůtek, 2002), thus obscuring the response related directly to the temperature decrease.

Similar to cold stress, drought stress is also believed to affect geographic range limits (Osmond *et al.*, 1987). Despite its significance, the role of water availability in shaping species response curves remains speculative. The region of Ladakh provides a

unique opportunity to study species responses along prominent gradients of temperature and soil moisture, which are combined in a single elevational gradient. Lower elevations being dry and warm, while high elevations are cold and relatively moist, with the distribution of plant species reflecting trade-offs between drought and cold tolerance (Klimeš, 2003; Dvorský *et al.*, 2011). Importantly, the elevational gradient in Ladakh accommodates the entire vertical range of most species there, including the highest known occurrences of vascular plants on Earth (Dvorský *et al.*, 2015). Moreover, the upper limit of vegetation in Ladakh is determined climatically, not by physical barriers like permanent snowfields or glaciers. Species′ distributions thus stretch along their full climatic niches (Dvorský *et al.*, 2016). Owing to the overall arid climate, all the vegetation zones are herbaceous such that species ranges are not influenced by transitions of physiognomically different vegetation types. Due to the very low vegetation cover, and consequently the marginal role of biotic interactions, the shapes of responses bear a strong abiotic signal. These characteristics of our study region allow us to filter out major confounding factors, providing unique insights into niche pattern along environmental gradients.

Here, we used a large dataset of plant species occurrences to test three predictions of the AASL hypothesis (Fig. 1). We explored species response curves along a lengthy elevational gradient, starting in dry deserts around 2800 m a.s.l. and ending at the absolute elevational limit of vascular plants at 6150 m a.s.l. Based on the premise that both ends of the elevational gradient are similarly stressful to vascular plants (cold versus dry), we formulated and tested the following hypotheses:

(1) The proportion of species with an asymmetric response increases towards both ends of the elevational gradient.

(2) Species with a right-skewed response prevail at the dry end, and species with a left-skewed response prevail at the cold end of the elevational gradient.

(3) Response curves are increasingly steeper towards both ends of the elevational gradient.

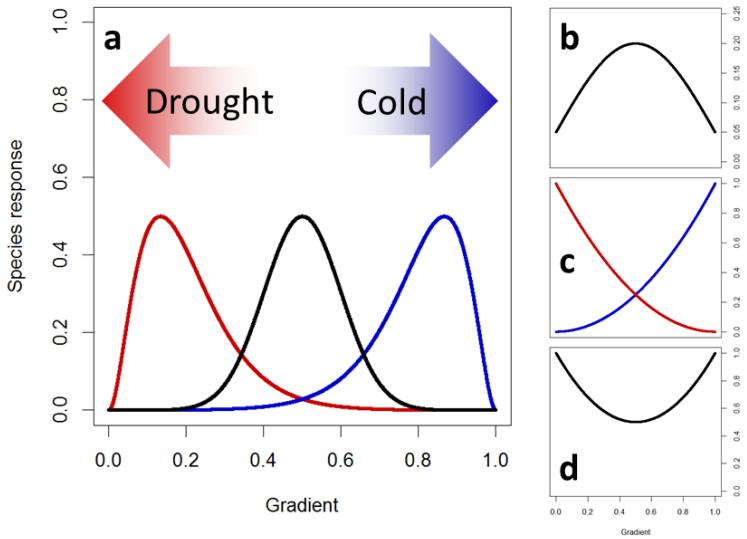

FIGURE 1 *Schematic representation of species responses along an elevational gradient with different stressors at both ends predicted by AASL hypothesis. At lower elevations, the stress caused by drought prevails, while at higher elevations plant distribution is limited by low temperature: a) responses at lower elevations are right-skewed, symmetric in the middle and left-skewed at upper elevations; b) response interval (width of the steep side of the curve) contracts towards both ends of the gradient; c) proportion of species with right-skewed responses increases towards lower elevations and vice versa for species with left-skewed responses; d) proportion of species with a skewed response is lowest in the middle of the gradient.*

4.4 MATERIALS AND METHODS

STUDY REGION

Ladakh is part of the Transhimalayan region in India, Jammu and Kashmir state (Fig. 2). Due to its arid climate (ca. 100 mm yr^{-1}), the vegetation is treeless except for isolated stands along glacial streams composed of low trees (*Salix* spp., *Populus* spp.) and tall shrubs (*Hippophae rhamnoides*, *Myricaria elegans*). The sporadic precipitation accompanied by intense evapotranspiration driven by relatively high summer temperatures results in drought stress being the most limiting abiotic factor at low elevations. At higher elevations, the water regime is more balanced due to the increase in precipitation with elevation and the decrease in evapotranspiration, so that dry conditions are less intensive and low-temperature stress prevails as the dominant limiting factor. Therefore, the most suitable zone is situated approximately in the middle of the elevation gradient (4500–5000), where vegetation attains the highest species richness (Klimeš, 2003). Temperature decreases monotonically with elevation, although on a

local scale the pattern can be influenced by slope, aspect and microtopography (Scherrer & Körner, 2011). The adiabatic lapse rate of atmospheric temperature in this arid region is about 0.8 K per 100 m (Fig. 2). The lowest elevations are semideserts. Cold steppe stretches approximately from 3700 up to 5400 m a.s.l., thus represents the most widespread vegetation type (Dvorský *et al.*, 2011). High elevations host relatively diverse subnival vegetation (Dvorský *et al.*, 2015). Brackish and rarely fresh-water wetlands host azonal vegetation, together with *Kobresia* grasslands and salt marshes.

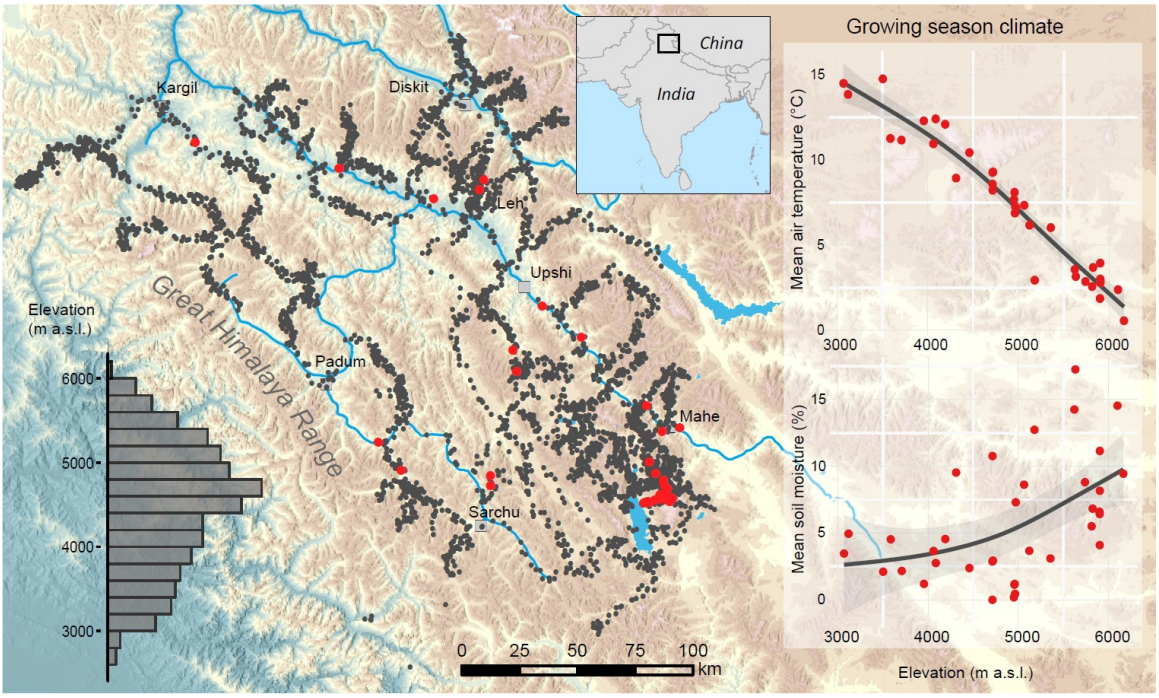

FIGURE 2 *Distribution of vegetation plots and in situ measured climate in the study region in Ladakh, NW Himalayas. Floristic data were collected in 4,150 plots (100×100 m, black dots) and climate measured at 36 sites (red dots) between 2013 and 2014. Histogram on the left side shows the frequency of vegetation plots within respective elevational bands. Mean air temperature of the growing season decreases with elevation (Pearson's r = -0.96), while mean soil moisture increases (Pearson's r = 0.49; graphs on the right side). The trend lines were fitted with GAM and shaded regions represent 95% confidence intervals. Background map is based on SRTM (http://www2.jpl.nasa.gov/srtm/) and OpenStreetMap data.*

CLIMATIC GRADIENTS

We explored the relationship between elevation and climate to test our assumption that elevation is a valid proxy for drought and low-temperature stress. For this purpose, we compared high-resolution interpolated climate data set CHELSA (Karger *et al.*, 2016) and direct field measurements of soil moisture and ground temperature performed with TMS3 data loggers (TOMST, Czech Republic, www.tomst.cz/tms). We extracted mean annual temperature and precipitation values of CHELSA grids for each plot location.

Additionally, average soil moisture and ground temperature (15 cm above ground) during the vegetation season were obtained from field measurements taken by 36 TMS3 units, covering elevational gradient from 3070 to 6150 m a.s.l., recording in 15 minute intervals between August 2013 and September 2014 (Fig. 2). To explore the relationships between climatic variables and elevation, we calculated their linear dependence (Pearson's r) and rank correlation (Spearman's rho).

SPECIES RESPONSES ALONG ELEVATIONAL GRADIENT

Species distributions along the elevation gradient were derived from 95,812 floristic records collected from 1997–2006 at 4,062 localities (each 100 × 100 m) over the entire Ladakh region (Fig. 2). The sampled area is ca. 117,000 km², the vertical range of floristic records begins at 2640 m a.s.l. (Suru Region in the northwest part of Ladakh) and reaches 6150 m a.s.l. (Changthang Region in east Ladakh). As many as 1395 taxa of vascular plants have been recorded (Klimeš & Dickoré, 2006). To reliably quantify shape of species response curves, we analyzed only species with more than 30 occurrences in our dataset, and further excluded: 1) Synanthropic and tree species, because their distribution is determined by human activities, and 2) Aquatic plants, because their distribution reflects the patchy distribution of their habitats.

To quantify species responses along the elevation gradient, we used Huismann-Ollf-Fresco (HOF) hierarchic regression models introduced by Huisman *et al*. (1993) and implemented in the R package `eHOF' (Jansen & Oksanen, 2013). To test the symmetry of the response, we limited the possible model types to unimodal shapes (types IV and V) with model type I (flat response) to control for species with random patterns. To select between the models, we used the model with better fit according to the small-sample-size corrected version of Akaike information criterion (AICc). To increase robustness of the selection, we repeated the model selection 50 times for each species, each time on a different bootstrapped sample of the plots. We used bootstrap sampling with replacement keeping the original frequency of the focal species (Jansen & Oksanen, 2013). Finally, we selected the HOF model type with the most frequent best fit among the bootstrapped samples.

From the resulting species response curves, we calculated three niche parameters for each species: *optimum* as the position of the species response maximum; *central niche* as the part of the gradient where the species response exceeds $e^{-0.5}$ times the species response in the optimum, this corresponds to 1 SD for the Gaussian curve (Heegaard, 2002); *response interval* as the part of the gradient between the optimum and the closer central niche border (cf. Normand *et al*., 2009). To avoid a bias caused by truncated lower elevation limit, we eliminated all species where their central niche was overlapping with elevations below 2800 m a.s.l., and we avoided interpretation of the lower end of the gradient (below 3000 m a.s.l.). A different approach was applied to the upper end of the gradient, since the upper limit of the study corresponds to the current

global limit for vascular plants (Dvorský *et al.*, 2015). To reflect this and to stabilize the response curves, we supplemented the vegetation matrix with 20 artificial plots containing no species, evenly distributed at elevations between 6150 and 6500 m a.s.l. The application of different selection rules described above resulted in a set of 395 species, on which we based all presented results.

Statistical analysis

We tested the independence between the species central niche position on the gradient and its response shape with the use of a null model. The null model simulated a situation where the species response type distribution along the gradient is independent of the central niche position, but keeping the same overall proportion of response types. Therefore, we permuted response types of the species (lef skewed, right skewed, symmetric), while keeping their central niche range, and for each position along the gradient (25 m altitudinal intervals) we calculated proportion of species response types. Species were considered present at a particular elevation if their central niche overlapped with that elevation. We repeated this procedure 10,000 times and calculated 95% and 99% permutation confidence intervals and compared them with observed response type proportions. This procedure generates confidence intervals that reflect an unbalanced species-pool along the gradient and autocorrelation caused by overlapping species ranges.

To test our third hypothesis, we analyzed the pattern of response intervals along the gradient. To control for geometric constraints (Colwell & Lees, 2000), we used a bounded null model, where central niche positions were randomly shifted within the gradient limits applied in our study. Next, using 10,000 permutations we calculated median response intervals of species present at each position along the gradient with interval of 25 m. Finally we calculated 95% and 99% confidence intervals and compared them to observed median response interval values along the gradient.

Species groups

To test if species responses differ among species with different properties, we classified them by their moisture demands and functional group. Three classes of species according to their moisture demand were recognized with regard to their prevailing habitat of occurrence: 1) *dry* (semideserts, steppes); 2) *mesic* (alpine grasslands and meadows, screes, subnival zone); and 3) *moist* (wetlands). Further, we differentiated five functional groups: 1) *graminoids*; 2) *forbs*; 3) *tall shrubs* (>2 m); 4) *low shrubs and subshrubs*; and 5) *ferns and fern allies*. Finally, we tested the differences in the proportions of the particular response types among these species groups using chi-square tests; only groups with more than two species were considered.

4.5 RESULTS

Temperature linearly decreased with increasing elevation (CHELSA mean annual temperature: Pearson's r = -0.95; Spearman's rho = -0.96 and field measurement of mean temperature during vegetation season: r = -0.96; rho = -0.96; Fig. 2). Water availability correlated with elevation moderately (CHELSA mean annual precipitation: r = 0.39; rho = 0.43 and field measurement of mean soil moisture during vegetation season: r = 0.49; rho = 0.54; Fig. 2).

We fitted the HOF models for 395 vascular plant species (Table 1). All modeled species had a distinct elevational optimum (Table 1). Most species (61.5%) displayed a symmetric response (HOF model type IV). Among species with asymmetric responses (HOF model type V), right-skewed responses were rare (2.3%), while left-skewed responses prevailed (36.2%).

TABLE 1 *Response curve types of vascular plant species in Ladakh, India. Responses to elevational gradient of 395 species were determined by HOF models. Proportion of response curve types within respective habitat types and functional groups is shown.*

	Left-skewed		*Symmetric*		*Right-skewed*		*Total*	
	n	*%*	*n*	*%*	*n*	*%*	*n*	*%*
	143	36.2	243	61.5	9	2.3	395	100.0
Habitat type								
Semideserts	4	30.8	8	61.5	1	7.7	13	3.3
Steppes	47	41.2	65	57.0	2	1.8	114	28.9
Grasslands	51	38.1	83	61.9	0	0.0	134	33.9
Screes	21	36.2	35	60.3	2	3.4	58	14.7
Subnival	7	31.8	13	59.1	2	9.1	22	5.6
Wetlands	13	24.1	39	72.2	2	3.7	54	13.7
Functional group								
Graminoids	29	39.2	43	58.1	2	2.7	74	18.7
Forbs	99	34.4	184	63.9	5	1.7	288	72.9
Shrubs	0	0.0	2	100.0	0	0.0	2	0.5
Dwarf shrubs	15	51.7	13	44.8	1	3.4	29	7.3
Ferns, fern allies	0	0.0	1	50.0	1	50.0	2	0.5

The proportion of response curve types was not constant along the elevational gradient (Fig. 3). While asymmetric right-skewed responses were rare along the whole elevational gradient with no clear tendency (Fig. 3a), symmetric response curves prevailed at lower elevations, escaping the upper 95% confidence interval up to 3800 m a.s.l., and the lower 95% confidence interval between 5250 and 5400 m a.s.l. (Fig. 3b). Conversely, asymmetric left-skewed responses accumulated at higher elevations from 4775 to 5400 m a.s.l., while being underrepresented below 3750 m a.s.l. (Fig. 3c).

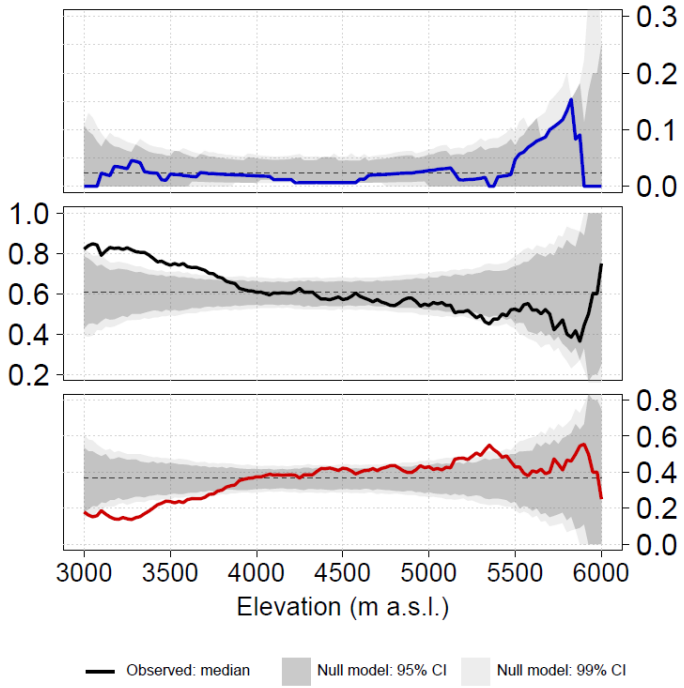

Figure 3 *Proportion of species with (a) right-skewed; (b) symmetric; and (c) left-skewed response types along the elevation gradient. The proportion of left-skewed responses increases almost monotonically between 3000 and 5400 m a.s.l., and is significantly underrepresented at lower elevations up to 3750 m a.s.l. and overrepresented at high elevations (5150 – 5450 m a.s.l.). Right-skewed responses are rare along the whole gradient and show no departure from random expectation. Symmetric responses are significantly overrepresented at lower elevations between 3000 and 3750 m a.s.l., and their proportion decreases with elevation. The unbroken line shows the proportion of species which have their central niche at a given elevation (sampled in 25 m intervals), shaded areas represent 95% and 99% permutation interval of the null model simulating random distribution of response types along an elevation gradient with the same overall proportions. CI, confidence interval.*

Frequency of the response curve types differed neither among species groups defined by moisture demands (Chi-sq. = 4.33, p = 0.36), nor among functional groups (Chi-sq. = 4.63, p = 0.33).

Response interval generally decreased with increasing elevation, and was significantly wider below 3800 m a.s.l., and significantly narrower above 4750 m a.s.l. (Fig. 4).

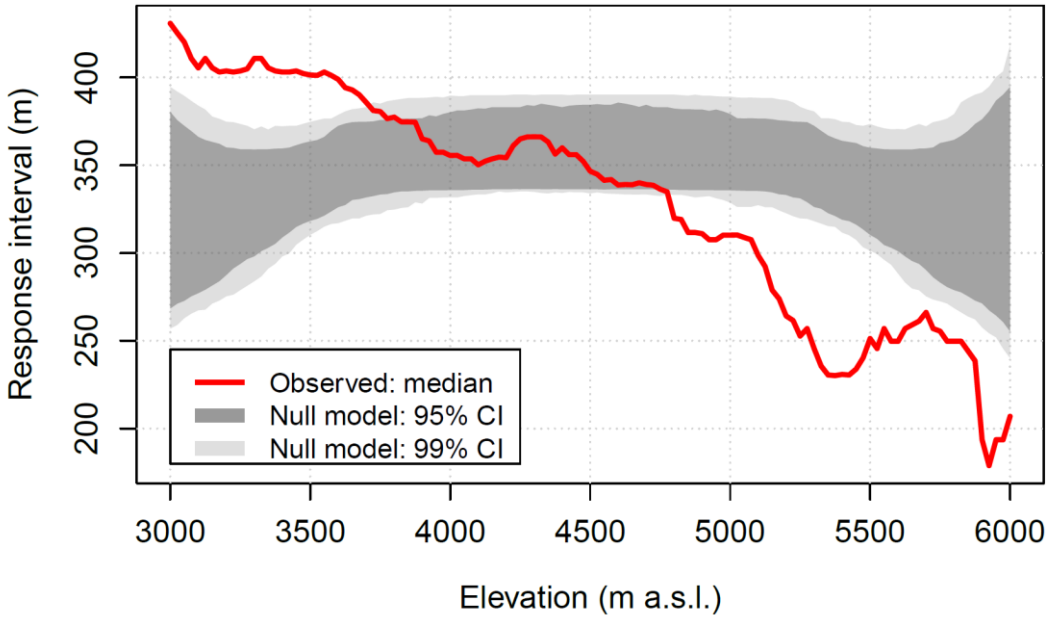

Figure 4 *Response interval decreases with increasing elevation. The line shows the median response interval of species which have their central niche at a particular elevation and shading shows confidence interval of the null model, where the position of each species was shifted randomly along the elevational gradient. The response interval is the distance between optimum and the closer central niche border, the narrower the response interval, the steeper the decrease of the probability of species occurrence along the gradient.*

4.6 Discussion

Over one third of species showed an asymmetric response to the elevational gradient. In fact, this is a conservative estimate with the real proportion probably being higher (due to AICc penalization of HOF model V, which needs one parameter extra compared to model IV). Most of these species had a left-skewed response, meaning that their probability of occurrence decreased faster towards their cold limit. The proportion of the left-skewed responses increased monotonically between 3000 and 5400 m a.s.l. Moreover, the response interval was shortening with increasing elevation, therefore response curves were steeper towards species cold limits. On the other hand, species

with right-skewed responses occurred infrequently along the whole gradient and showed no departure from a random distribution. These findings provide evidence of increasing limitation towards the cold end of species distributions, while no distinct limitation towards lower elevations (drought) occurred. Some studies have already reported a significant proportion of species with steeper responses towards their cold limits (e.g. Normand *et al.*, 2009; Murphy *et al.*, 2010), concluding that the steeper side in asymmetric response curves indicates the direction of the stronger limiting abiotic factor. In our study, however, we also documented an increasing proportion of asymmetric responses as well as an increasing steepness of responses with increasing elevation, thus supporting all crucial aspects of AASL hypothesis.

Our findings suggest that the skewness of a species response curve may depend on the position of its optimum relative to gradient extremes (see also Rydgren *et al.*, 2003). Climatic extremes, more frequently closer to gradient ends, are probably responsible for an abrupt decrease in the probability of occurrence (Zimmermann *et al.*, 2009). Vetaas (2002), for example, demonstrated that extreme cold temperature sets an absolute boundary for survival, while warm temperature does not. Hence, periodic bad years associated with irregular recruitment and a greater likelihood of extinction events may be decisive for the dynamics of marginal populations, causing - in the long run - the asymmetric pattern of distribution. Extreme climatic events during sensitive life stages or vulnerable phenologic phases should therefore be considered decisive factors setting species range limits (Kollas *et al.*, 2014; Doležal *et al.*, 2016). The strong limitation by low temperatures found in our study is in agreement with Butterfield (2015), who reported increasing environmental filtering at the cold end of climatic gradient, with frost having the strongest effect. This could also explain the underrepresentation of left-skewed responses below 3750 m a.s.l. in our study region, where frost practically does not occur during growing season.

Normand *et al.* (2009) reported a quarter of species with a steep decline towards lower water balance, suggesting the importance of drought stress. However, we did not observe such an obvious role of drought. There are two possible explanations why we did not detect strong limitation towards dry conditions. First, temperature and soil moisture differ in their spatial variability. While temperature varies smoothly in space, the distribution of dry and moist habitats is patchy. Plants therefore cannot avoid low ambient temperature at high elevations but can adjust to the spatially variable soil moisture at low elevations (Fig. 2). Although Scherrer & Körner (2011) demonstrated that the ruggedness of the alpine terrain produces substantial variation in mean temperature among micro-habitats,it is the low temperature extremes, that cannot be avoided. On the other hand, plants at lower elevations might avoid excessive drought by preferring relatively moist habitats along glacier streams, in terrain depressions, spring areas or at valley bottoms). As a result, their probability of occurrence declines more gradually towards the dry end of the elevational gradient. For example, *Waldheimia*

tridactylites is almost ubiquitous in the subnival zone, but restricted to gravel bars along streams at lower elevations. In other words, the changes in soil moisture with elevation are not significant enough to cause asymmetry in species response. Second, most species growing in Ladakh have evolved in Central Asia (zonal steppe species) or Tibet (alpine steppe and subnival species; Dickoré, 1995), where palaeoclimatic records show that these regions have always been arid (e.g. Tang *et al.*, 2000). Hence, the plant species in Ladakh seem to be generally well adapted to dry conditions and therefore their individual reaction to increasing drought stress is gradual. Indeed, many species growing in Ladakh have extremely long roots (Klimešová *et al.*, 2011) and are thus decoupled from drought stress by their ability to reach deep soil horizons. A similar effect was observed by Benavides *et al.* (2013), who found that the abundance of juveniles of *Pinus sylvestris*, which are more sensitive to drought stress due to their short roots, was skewed towards higher elevations compared to adults with deep roots. Nevertheless, the lack of right-skewed responses at lower elevations does not exclude drought stress as a possible range-limit determinant, but does suggest that temperature limitation is still the dominant factor even at these elevations. Despite the frost-free period lasting more than six months, the low sum of growing degree days or occasional freezing during winter can limit distribution of many sensitive species.

Some studies stressed the importance of biotic interactions in producing skewed responses (Austin & Smith, 1989). However, in our study region at least, the aboveground competition is negligible due to sparse vegetation cover. To some extent, livestock grazing could affect species distribution (Namgail *et al.*, 2012), but we do not expect a strong elevational gradient in grazing pressure; nomadic shepherds utilize the whole landscape. Hence, we conclude that niche asymmetry could arise merely by two opposing abiotic stress gradients with differing effect strengths.

The fact that we found an accumulation of species with left-skewed responses at 5150–5450 m a.s.l. probably indicates a shared physiological response to low temperature. This elevation is the point where zonal steppe vegetation changes into true alpine vegetation (Dvorský *et al.*, 2015), and where widespread steppe species, often tall graminoids and subshrubs, completely disappear. Although we found no evidence that the proportion of response types differed among habitats or functional groups, we could identify a group of species which responded in a similar way, thus highlighting the existence of a threshold elevation/temperature, which naturally delimits one vegetation zone from another in an otherwise unchanged relief.

In conclusion, we highlight the strong influence of low temperature in determining species range limits. The prevailing gradual decline of the probability of occurrence towards dry conditions suggests that drought is a less restrictive determinant of range limits than cold. Contrary to low temperature, most species can either effectively adapt to drought, or avoid drought stress by preferring places with improved water balance.

Our results support the predictions of the AASL hypothesis that the steeper side of a response curve points to the end of a gradient particularly stressful to a species, and that the species growing closer to the more stressful extremes of the gradient have steeper responses.

4.7 Acknowledgements

Data have been collected by our late colleague Leoš Klimeš. We thank Conor Redmond for language revision and Florian Jansen for advise on HOF models. The study was supported by the Czech Science Foundation (GACR 13-13368S) and was part of long-term research development project No. RVO 67985939.

4.8 Biosketch

The Institute of Botany of The Czech Academy of Sciences has been conducting botanical research in Ladakh, NW India, since 1997. The main focus has been aimed at explaining vegetation patterns in relation to environmental gradients, long-term vegetation monitoring, clonality in plants, the role of cushion plants in plant-plant interactions, and assessing the factors behind the elevational limits of vascular plants.

Author contributions: M.D., M.M., M.K., J.W. and J.D. conceived the ideas; M.M., M.K., J.W. and M.D. analysed the data; and M.D. and M.M. led the writing.

4.9 References

Austin, M.P. (2007) Species distribution models and ecological theory: a critical assessment and some possible new approaches. *Ecological Modelling*, **200**, 1–19.

Austin, M.P. & Gaywood, M.J. (1994) Current problems of environmental gradients and species response curves in relation to continuum theory. *Journal of Vegetation Science*, **5**, 473–482.

Austin, M.P. & Smith, T. M. (1989) A new model for the continuum concept. *Vegetatio*, **83**, 35–47.

Benavides, R., Rabasa, S.G., Granda, E., Escudero, A., Hódar, J. A., Martínez-Vilalta, J. *et al.* (2013) Direct and indirect effects of climate on demography and early growth of *Pinus sylvestris* at the rear edge: changing roles of biotic and abiotic factors. *PLoS One*, **8**, e59824.

Boucher-Lalonde, V., Morin, A. & Currie, D.J. (2012) How are tree species distributed in climatic space? A simple and general pattern. *Global Ecology and Biogeography*, **21**, 1157–1166.

Butterfield, B.J. (2015) Environmental filtering increases in intensity at both ends of climatic gradients, though driven by different factors, across woody vegetation types of the southwest USA. *Oikos*, **124**, 1374–1382.

Cahill, A.E., Aiello-Lammens, M.E., Caitlin Fisher-Reid, M., Hua, X., Karanewsky, C.J., Ryu, H.Y. *et al.* (2014) Causes of warm-edge range limits: systematic review, proximate factors and implications for climate change. *Journal of Biogeography*, **41**, 429–442.

Colwell, R.K. & Lees D.C. (2000) The mid-domain effect: geometric species richness. *Trends in Ecology and Evolution,* **15**, 70–76.

Dickoré, W.B. (1995) Systematische Revision und chorologische Analyse der Monocotyledoneae des Karakorum (Zentralasien, West-Tibet) Flora Karakorumensis I. Angiospermae, Monocotyledoneae. Stapfia, Linz.

Doležal, J., Dvorský, M., Kopecký, M., Liancourt, P., Hiiesalu, I., Macek, M. et al. (2016) Vegetation dynamics at the upper elevational limit of vascular plants in Himalaya. *Scientific Reports*, **6**. doi:10.1038/srep24881

Doležal, J. & Šrůtek, M. (2002) Altitudinal changes in composition and structure of mountain-temperate vegetation: a case study from the Western Carpathians. *Plant Ecology*, **158**, 201–221.

Dvorský, M., Altman, J., Kopecký, M., Chlumská, Z., Řeháková, K., Janatková, K. & Doležal, J. (2015) Vascular plants at extreme elevations in eastern Ladakh, northwest Himalayas. *Plant Ecology & Diversity*, **8**, 571–584.

Dvorský, M., Chlumská, Z., Altman, J., Čapková, K., Řeháková, K., Macek, M. et al. (2016) Gardening in the zone of death: an experimental assessment of the absolute elevation limit of vascular plants. *Scientific Reports*, **6**. doi:10.1038/srep24440

Dvorský, M., Doležal, J., De Bello, F., Klimešová, J. & Klimeš, L. (2011) Vegetation types of East Ladakh: species and growth form composition along main environmental gradients. *Applied Vegetation Science*, **14**, 132–147.

Ettinger, A.K., Ford, K.R. & HilleRisLambers, J. (2011) Climate determines upper, but not lower, altitudinal range limits of Pacific Northwest conifers. *Ecology*, **92**, 1323–1331.

Ettinger, A.K. & HilleRisLambers, J. (2013) Climate isn't everything: competitive interactions and variation by life stage will also affect range shifts in a warming world. *American Journal of Botany*, **100**, 1344–1355.

Heegaard, E. (2002) The outer border and central border for species–environmental relationships estimated by non-parametric generalised additive models. *Ecological Modelling*, **157**, 131–139.

Huisman, J., Olff, H. & Fresco, L.F.M. (1993) A hierarchical set of models for species response analysis. *Journal of Vegetation Science*, **4**, 37–46.

Jansen, F. & Oksanen, J. (2013) How to model species responses along ecological gradients–Huisman–Olff–Fresco models revisited. *Journal of Vegetation Science*, **24**, 1108–1117.

Karger, D.N., Conrad, O., Böhner, J., Kawohl, T., Kreft, H., Soria-Auza, R.W., Zimmermann, N.E., Linder, H.P. & Kessler, M. (2016) CHELSA climatologies at high resolution for the earth's land surface areas (Version 1.1). World Data Center for Climate. doi: 10.1594/WDCC/CHELSA_v1_1.

Klimeš, L. & Dickoré, W.B. (2006) Flora of Ladakh (Jammu & Kashmir, India). A preliminary checklist published at http://www.butbn.cas.cz/klimes. Accessed 23 November 2016.

Klimeš, L. (2003) Life-forms and clonality of vascular plants along an altitudinal gradient in E Ladakh (NW Himalayas). *Basic and Applied Ecology*, **4**, 317–328.

Klimešová, J., Doležal, J., Dvorský, M., De Bello, F. & Klimeš, L. (2011) Clonal growth forms in eastern Ladakh, Western Himalayas: classification and habitat preferences. *Folia Geobotanica*, **46**, 191–217.

Kollas, C., Körner, C. & Randin, C.F. (2014) Spring frost and growing season length co-control the cold range limits of broad-leaved trees. *Journal of Biogeography*, **41**, 773–783.

Körner, C. (2003) Alpine plant life. Springer, Berlin.

Li, M.H., Xiao, W.F., Wang, S.G., Cheng, G.W., Cherubini, P., Cai, X.H. *et al.* (2008) Mobile carbohydrates in Himalayan treeline trees I. Evidence for carbon gain limitation but not for growth limitation. *Tree Physiology*, **28**, 1287–1296.

Meier, E.S., Kienast, F., Pearman, P.B. *et al.* (2010). Biotic and abiotic variables show little redundancy in explaining tree species distributions. *Ecography*, **33**, 1038–1048.

Murphy, H.T., VanDerWal, J. & Lovett-Doust, J. (2010) Signatures of range expansion and erosion in eastern North American trees. *Ecology Letters*, **13**, 1233–1244.

Namgail, T., Rawat, G.S., Mishra, C., van Wieren, S.E. & Prins, H.H. (2012) Biomass and diversity of dry alpine plant communities along altitudinal gradients in the Himalayas. *Journal of Plant Research*, **125**, 93–101.

Normand, S., Treier, U.A., Randin, C., Vittoz, P., Guisan, A. & Svenning J.-C. (2009) Importance of abiotic stress as a range-limit determinant for European plants: insights from species responses to climatic gradients. *Global Ecology and Biogeography*, **18**, 437–449.

Oksanen J. & Minchin, P.R. (2002) Continuum theory revisited: what shape are species responses along ecological gradients? *Ecological Modelling*, **157**, 119–129.

Osmond, C.B., Austin, M.P., Berry, J.A., Billings, W.D., Boyer, J.S., Dacey, J.W.H., Nobel, P.S., Smith, S.D. & Winner, W.E. (1987) Stress physiology and the distribution of plants. *BioScience*, **37**, 38–48.

Pellissier, L., Bråthen, K.A., Vittoz, P., Yoccoz, N.G., Dubuis, A., Meier, E.S., Zimmermann, N.E., Randin, C.F., Thuiller, W., Garraud, L., Van Es, J. & Guisan, A. (2013) Thermal niches are more conserved at cold than warm limits in arctic-alpine plant species. *Global Ecology and Biogeography*, **22**, 933–941.

Rydgren, K., Økland, R.H. & Økland, T. (2003) Species response curves along environmental gradients. A case study from SE Norwegian swamp forests. *Journal of Vegetation Science*, **14**, 869–880.

Sexton, J.P., McIntyre, P.J., Angert, A.L. & Rice, K.J. (2009) Evolution and ecology of species range limits. *Annual Review of Ecology, Evolution and Systematics*, **40**, 415–436.

Shi, P., Körner, C. & Hoch, G. (2008) A test of the growth-limitation theory for alpine tree line formation in evergreen and deciduous taxa of the eastern Himalayas. *Functional Ecology*, **22**, 213–220.

Scherrer, D. & Körner, C. (2011) Topographically controlled thermal-habitat differentiation buffers alpine plant diversity against climate warming. *Journal of Biogeography*, **38**, 406–416.

Suchrow, S. & Jensen, K. (2010) Plant species responses to an elevational gradient in German North Sea salt marshes. *Wetlands*, **30**, 735–746.

Tang, L., Shen, C., Liu, K. & Overpeck, J.T. (2000) Changes in South Asian monsoon: new high-resolution paleoclimatic records from Tibet, China. *Chinese Science Bulletin*, **45**, 87–91.

Vetaas, O.R. (2002) Realized and potential climate niches: a comparison of four Rhododendron tree species. *Journal of Biogeography*, **29**, 545–554.

Wiley, E. & Helliker, B. (2012) A re-evaluation of carbon storage in trees lends greater support for carbon limitation to growth. *New Phytologist*, **195**, 285–289.

Wisz, M.S., Pottier, J., Kissling, W.D. *et al*. (2013) The role of biotic interactions in shaping distributions and realised assemblages of species: implications for species distribution modelling. *Biological Reviews*, **88**, 15–30.

Zimmermann, N.E., Yoccoz, N.G., Edwards, T.C., Meier, E.S., Thuiller, W., Guisan, A. et al. (2009) Climatic extremes improve predictions of spatial patterns of tree species. Proceedings of the National Academy of Sciences, 106, 19723-19728.

CHAPTER FIVE:

GEOMETRIC CONSTRAINTS EXPLAIN ELEVATIONAL RANGE SIZE PATTERNS OF VASCULAR PLANTS IN HIMALAYA

MIROSLAV DVORSKÝ[1], MARTIN MACEK[1,2], MARTIN KOPECKÝ[1,3], JAN WILD[1,4] AND JIŘÍ DOLEŽAL[1,5]

[1]*Institute of Botany, The Czech Academy of Sciences, Zámek 1, CZ-252 43, Průhonice, Czech Republic*
[2]*Department of Botany, Faculty of Science, Charles University, Benátská 2, Praha, CZ-128 01, Czech Republic*
[3]*Department of Forest Ecology, Faculty of Forestry and Wood Sciences, Czech University of Life Sciences Prague, Kamýcká 129, CZ-165 21, Praha 6-Suchdol, Czech Republic*
[4]*Faculty of Environmental Sciences, Czech University of Life Sciences Prague, Kamýcká 129, CZ-165 21, Praha 6-Suchdol, Czech Republic, 5 Department of Botany, Faculty of Science, University of South Bohemia, Na Zlaté stoce 1, CZ -370 05, České Budějovice, Czech Republic*
Corresponding author: Miroslav Dvorský, dvorsky.miroslav@gmail.com

Submitted manuscript

5.1 ABSTRACT

Aim Rapoport´s elevational rule predicts that species' elevational range size increase with increasing elevation. However, this rule has been contradicted and its testing was often associated with null models artefacts. Here we explored the elevational range sizes of 781 vascular plants species in NW Himalayas and separated underlying biological gradients from artefacts caused by the truncation of the elevational gradient and a miss-specified null model. To explore posible climatic drivers of elevational range size, we also assessed the relationship between in-situ measured climatic variables and range size patterns.

Location Northwest Himalaya, Ladakh, India (2650–6150 m a.s.l.).

Time period 1997–2015.

Major taxa studied Vascular plants.

Methods We used a spatially explicit dataset of 102999 species occurrences collected recently in Ladakh and air temperature data collected *in-situ* with TMS microclimatic dataloggers. To summarize range size distribution along the elevational gradient, we used Stevens and bin methods in parallel, because both were used to document Rapoport's rule. To compare observed patterns to the random expectation accounting for geometric constrains of the geographical domain and inherent diversity gradient, we constructed a null model assuming no dependence between range size and its position along elevational gradient.

Results We found no systematic trend in species range size distribution when an appropriate null model was used. Seasonal and diurnal temperature range did not change along the elevational gradient but average daily minimum temperature of the coldest month decreased with elevation.

Main conclusions Our results contradict Rapoport´s elevational rule, and we argue that the often-described patterns supporting this rule may be statistical artefacts caused by an inappropriate null model. Since climate-based hypotheses on range-size drivers gained no direct support in our study, random range sizes imply species-specific drivers of range size variation along elevational gradients.

Keywords: Climatic Variability Hypothesis, cold desert, diurnal temperature range, elevational gradient, Rapoport´s rule, species distribution, species range size, temperature variability, TMS dataloggers

5.2 INTRODUCTION

As broad-scale diversity patterns are co-determined by species´ distributional range sizes, the examination of factors involved in driving distributional ranges plays an important role in ecological theory. Mountains are particularly remarkable for the exceptional biodiversity they support, which is estimated as one-third of all terrestrial species (Körner, 2004). Understanding the processes shaping species´ elevational range sizes can therefore provide insights into the mechanisms influencing the distribution of global biodiversity.

Rapoport´s elevational rule, an extension of Rapoport's latitudinal rule (Stevens, 1989), posits that species´ range sizes increase with elevation (Stevens, 1992). The rationale behind his prediction is that climatic variability increases with elevation, so that species inhabiting more elevated zones are ultimately selected for broader climatic tolerance, which in turn enables them to be spread over larger areas and a broader elevational extent. To date, this is the most commonly-accepted mechanistic explanation of the evolution of range sizes and it is known as the Climatic Variability Hypothesis (CVH): "*the more predictable the environment, the smaller the change in that environment needs to be to serve as an immediate or long-term barrier to dispersal*" (Janzen, 1967). Its logic is appealing and the pattern of increasing range size with elevation has been documented for various taxonomic groups (e.g. Patterson, Pacheco, & Solari, 1996; Fleishman, Austin, & Weiss, 1998; Sanders, 2002; Chatzaki, Lymberakis, Markakis, & Mylonas, 2005; Hausdorf, 2006; Beketov, 2009; Kwon, Kim, & Chun, 2014). On the other hand, a multitude of studies failed to find support for Rapoport´s rule (e.g. Fu, Wu, Wang, Lei, & Chen, 2004; Bhattarai & Vetaas, 2006; Lee, Chun, Song, & Cho, 2013). The debate over such discrepancies eventually led to the conclusion that Rapoport´s rule was a local phenomenon (Rohde, 1996; Gaston et al. 1998; Gaston & Chown, 1999a) with inconsistent predictive value for understanding patterns in species range size (McCain & Knight, 2013). The rule has since been more often referred to as just an effect (Lawton, 1999), which may, or may not be exhibited in specific situations. In addition, the original statistical approach to evaluate Rapoport´s rule (Stevens´ method) was strongly criticized (Colwell & Hurtt, 1994; Gaston et al. 1998; Colwell & Lees, 2000) and other methods were therefore developed (Letcher & Harvey 1994; Lyons & Willig, 1997; Ribas & Schoereder, 2006). The fact that results may depend on the computation method, data quality, scale or taxonomic group is now widely agreed on. In particular, the presence of geographic barriers, truncating the potential range size, was identified as the main confusing factor, and this was even able to reverse the patterns of the underlying biological gradients (Šizling, Storch, & Keil, 2009).

Despite the controversy around Rapoport´s rule, there still is a need to identify the species-specific controls of range size. Experiments with individual species can bring insights into fundamental niches (e.g. Gaston & Chown 1999b; Calosi et al., 2010;

Taschler & Neuner, 2004; Körner et al., 2019), which can be readily related to a species' actual distribution. Such studies are laborious to conduct and are hence too rare to cover a significant number of taxa. Hence, the climate-based hypotheses for variation in range size provide a promising theoretical background because they advocate for a direct testing of the link between species range sizes and the climatic variability or extremes within species range (Pither, 2003; Pintor, Schwarzkopf, & Krockenberger, 2015; Chan et al., 2016). Importantly, they may provide a realistic explanation even in situations when Rapoport´s rule has no explanatory power (Pintor et al., 2015). Therefore, it is not the particular pattern of range size distribution that is of ecological relevance; what are crucial are the underlying mechanisms which enable meaningful generalizations and predictions.

In this paper, we analyzed the distribution of species elevational range sizes in Ladakh, NW Himalaya (ca. 50,000 km², elevational range 2650–6150 m a.s.l.). We used a dataset of 102999 species occurrences recorded between 1997 and 2015, providing spatially explicit information about species distribution combined with temperature data collected *in-situ* with 59 microclimatic dataloggers. Here we 1) describe the pattern of realized distribution of species elevational range sizes; 2) separate underlying biological gradients from artefacts caused by the truncation of elevational gradient and the statistical method used as a null model; 3) explore the temperature patterns along elevational gradient.

5.3 METHODS

STUDY REGION

We studied the elevational ranges of vascular plant species occurring in the Ladakh region, NW India (for a map, see Figure 2 in Dvorský, Macek, Kopecký, Wild, & Doležal, 2017). The area studied covers ca 50,000 km², spanning over almost the complete extent of Ladakh territory under Indian administration. The lowest elevations at the bottoms of the largest river valleys (Upper Indus, Shyok, and their tributaries) go down to 2650 m. Several peaks reach elevation above 7000 m, but the highest known plant occurrence in the region is at 6150 m (Dvorský et al., 2015), which is not far below the globally highest record of vascular plants at 6400 m on the slopes of Mt. Everest, observed, however, almost a century ago (Dentant, 2018). The upper elevational limit of vascular plants in Ladakh is directly set by climatic factors, not by the lack of habitable places (Dvorský et al., 2016).

The climate of Ladakh is determined by the high average elevation of the region and low precipitation caused by a strong rain shadow effect; the main Himalayan Range

blocks most of summer monsoon coming from the south, while Hindu Kush and Karakoram block most of winter snowfall borne by midlatitude westerlies. Therefore, the climate is predominantly arid with 50–300 mm annual precipitation. The aridity is most pronounced at the lowest elevations which experience the highest potential evaporation rates. With increasing elevation, more water becomes available for plants as a result of increasing precipitation and decreasing evaporation (Dvorský et al. 2017). However, above ca. 5000 m, most precipitation falls as snow, though this usually melts the same day (Doležal et al. 2016). The mean annual temperature is about 5°C as reported from Leh (3600 m) and this drops with an adiabatic lapse rate of about -8 °C km^{-1}. The maximum temperature may reach above 30°C, the minimum as low as -40°C, and a great diurnal variation is a typical feature. Freezing air temperatures occur throughout the whole region, with freezing minima occuring regularly year-round above ca 5500m.

Following the climatic gradients, the vegetation zonation starts with deserts and semideserts at lower elevations, succeeded by alpine steppes as the zonal and most widespread vegetation exists between approximately 3700 and 5400 m, and reaches the upper limit in the subnival zone (Hartmann, 2009; Dvorský, Doležal, de Bello, Klimešová, & Klimeš, 2011; Dvorský et al., 2015). Azonal vegetation includes brackish and occasional fresh-water wetlands. The vegetation of river banks and river beds often supports large shrub and tree species, which are otherwise absent from the region. Synanthropic ruderal vegetation includes plant assemblages developed on eutrophicated ground by stables of domestic animals and nearby villages; weedy assemblages grow in irrigated fields up to the limits of cultivation at 4700 m.

DATA SOURCES

We compiled species range data from 4,062 sites (each 100 × 100 m) sampled by the late L. Klimeš during his systematic floristic exploration of Ladakh between 1997 and 2006. This exceptional dataset contains 95,812 species occurences, and we added an additional 7,187 species occurrences recorded between 2008 and 2015 (Fig. 1). The joined dataset contains information about 1395 taxa of vascular plants. However, we excluded all cultivated species, taxonomically unresolved observations and infrequent species with less than 10 observations, from the analyses. This filtering resulted in 781 species analysed in this study.

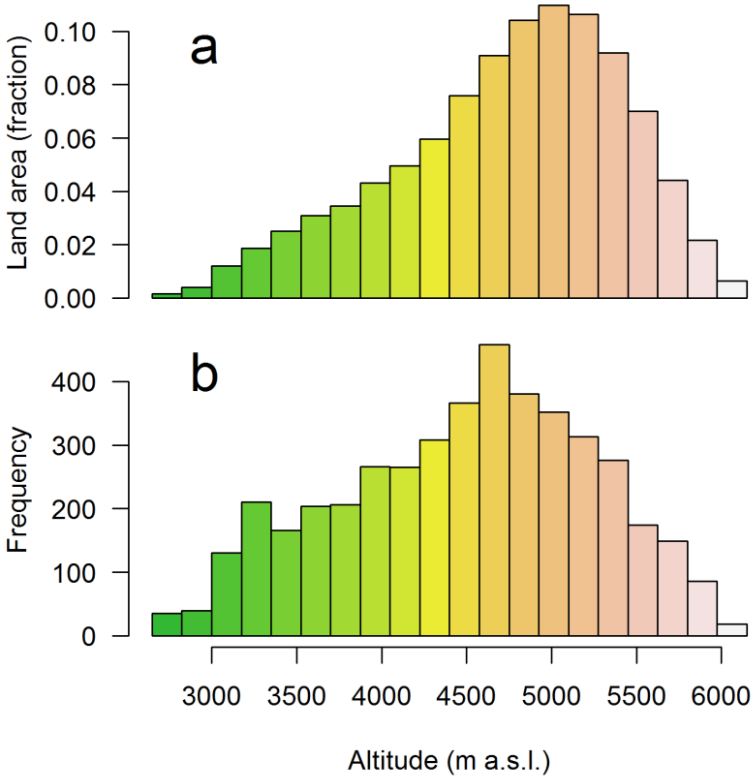

Figure 1 *Histograms showing (a) terrestrial area distribution within the study area as a fraction of total area, excluding glaciated areas and large water bodies and (b) sampling effort expressed as a number of unique sites with plant occurrence records used to calculate elevation ranges of 781 species of vascular plants.*

The elevational gradient in our study region is truncated. While its upper boundary is set by climate, the lower boundary is defined by the geographic extent of the area, and is thus artificial. Therefore, we distinguish between local and regional elevational ranges. The local elevational range is defined by the minimum and maximum elevation of species occurrence contained in the dataset. Regional elevational range size refers to species range in a wider region at comparable latitudes, extracted from the Flora of Pakistan (https://www.tropicos.org/Project/Pakistan), the Flora of China (www.eFloras.org), the Flora of Nanga Parbat (Dickoré & Nüsser, 2000), The Himalayan Uplands Plant database (Dickoré, 2011) and the Global Biodiversity Information Facility (GBIF, https://www.gbif.org). Records from the GBIF were rounded to nearest hundred. Unreliable outliers based on historical records (i.e. proclaimed elevation more than 1000 m apart from other records) were not taken into account and the next reliable occurrence extreme was used instead.

Depending on the phytogeographical affinities, species reached their minima and maxima in different parts within this wider region. Range maxima, if not recorded from Ladakh (which, interestingly, mostly are - about 84 %), come especially from the Central Himalayas and Tibet (for Himalayan and Tibetan elements), or from Karakoram and western Tibet (Central Asian or Pamiran elements). Range minima are, however, disputable. Many Eurasian or Central Asian elements occuring in Ladakh may descend close to sea level in other parts of their distributional range, unrealistically inflating their elevational range under very different climatic conditions. Hence the need for a practical, though artificial delimitation of the Ladakh´s wider region, with macroclimate

as similar as possible. Here, we took into account records from Pakistan, Afghanistan and Tajikistan (most often West Himalayan, Central Asian, Pamiran, or Eurasian elements), southwestern Xinjiang and western Tibet (Tibetan elements), or Himachal Pradesh, Uttarakhand or southern Tibet (Himalayan elements).

Data analyses

To summarize range size distribution along elevational gradient, we used two metrics often used to document Rapoport's rule: 1) the average range size of all species spanning over focal elevational band ("Stevens method"); 2) the average range size of species having their range mid-point in the focal elevational band ("bin method"). Here we divided the whole range of elevations coverd by our field data from Ladakh (2650 - 6150 m) into 20 equal intervals.

To compare observed patterns to the random expectation based on the geometric constrains of the geographical domain, we constructed the null model assuming no dependence between range size and its position along an elevational gradient and accounting for the inherent diversity gradient (Šizling et al. 2009). To construct 1000 realizations of the null model, we randomized species positions along the elevation gradient. For each species in each simulation run, we randomly sampled its upper range limit from the empirical cummulative distribution function of the upper range limits observed in our dataset to account for the decline of species richness with elevation. We used upper limits in randomization because upper limits in our dataset are not affected by range truncation (Fig. 1) and because these species are more strictly limited at their upper elevational limit (Dvorský et al. 2017). Next, we calculated the lower range limit by subtracting the range size from the chosen upper range limit of the sampled species. To calculate the simulated local (truncated) range, we restricting the simulated range by domain limits. Because the observed local ranges are also affected by incomplete sampling and local absence in part of the regional species range, we adjusted simulated local ranges according to the equation:

$$adjLR_i = simLR_i * \sum(simLR)/\sum(obsLR)$$

where adjLRi is the adjusted local range of species *i*; simLRi is the simulated local range of species *i*; ∑(simLR) is the sum of simulated local range over all species; and ∑(obsLR) is the sum of observed local range sizes over all species. Finally, we calculated the mean and 95% confidence intervals of simulated range size distribution metrics at each elevation band.

Climate variability and extremes

Weather stations in Ladakh are scarce and no station operates above 3660 m. Therefore, to assess climate variability and temperature extremes along the whole elevational gradient relevant for our study, we performed our own measurements using 59

TMS3microclimatic dataloggers, recording the air temperature at a height of 0.15 m in 15 min intervals (Wild et al., 2019). This measurement network covered the full range of elevations holding vascular plants in Ladakh (from 3070 m to 6150 m). Here we used annual data from August 2013 to August 2014 to calculate the minimum temperature as the average of the daily minimum temperatures of the coldest month (Pither 2003), the diurnal temperature range (°C) as the average difference between daily maxima and daily minima and the seasonal range (°C) as the difference between the average monthly maximum temperature of the warmest month and the average monthly minimum temperature of the coldest month (Chan et al. 2016). Pearson's coefficient was used to test whether climate variability and minimum temperature are associated with elevation.

5.4 Results

Species elevational ranges

Species' regional elevational range sizes varied between 415 m and 5085 m, with an average range size of 2437 m (Fig. 2). Local range sizes realized within Ladakh varied between 220 m and 2970 m with an average range size of 1563 m (Fig. 2). Regional minima were lower than local minima for most of the species (89.9%) and more than half of the species (56.8%) had their lower regional range limit below the lowest elevations of the whole Ladakh (Fig. 2). In contrast, only 15.9% species were ever spotted at higher elevations than were recorded in Ladakh and only two species (0.26%) were reported from elevations higher than the highest vascular plant occurrence currently known in Ladakh.

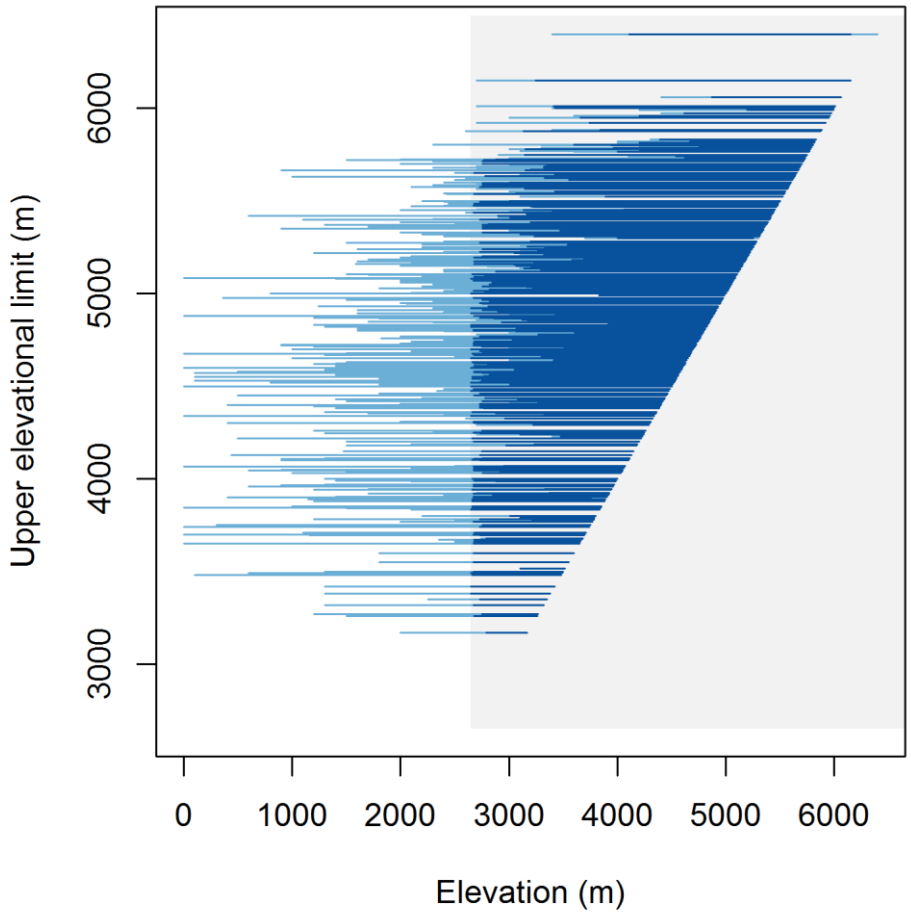

Figure 2 *Range distribution for 781 vascular plant species occuring in Ladakh sorted according their upper elevational limit. Species local ranges in Ladakh are drawn by dark blue lines, regional ranges by light blue lines and shaded area represents elevations existing in Ladakh, setting the domain limit for our null models. While local upper range limits usually represent regional upper range limits, most local ranges are truncated at their lower elevational limit. This geometric constraint results in an apparent increase of range size with elevation as predicted by Rapoport´s rule, however, this artificial pattern disappears when we look at species elevational ranges in the whole region.*

Range size distribution

The average regional range size examined by Stevens' method monotonously decreased with increasing elevation (Fig. 3). This general pattern was expected under the null model, slight deviations from the null model confidence interval were found for elevations < 3500 m, where range sizes were narrower, and for elevations 4000–4750 m, where range sizes were broader than expected. Local range sizes were considerably smaller than regional range sizes due to their truncation at the domain boundary (Fig. 3). The observed relation between average range size and elevation was decreasing between 2650 and 3500 m, then increasing up to 5500 m and then decreasing again

towards 6150 m. This pattern was well reproduced by the null model, with significant deviations only at the lowest elevations (<3000 m) and between 4500 m and 5250 m.

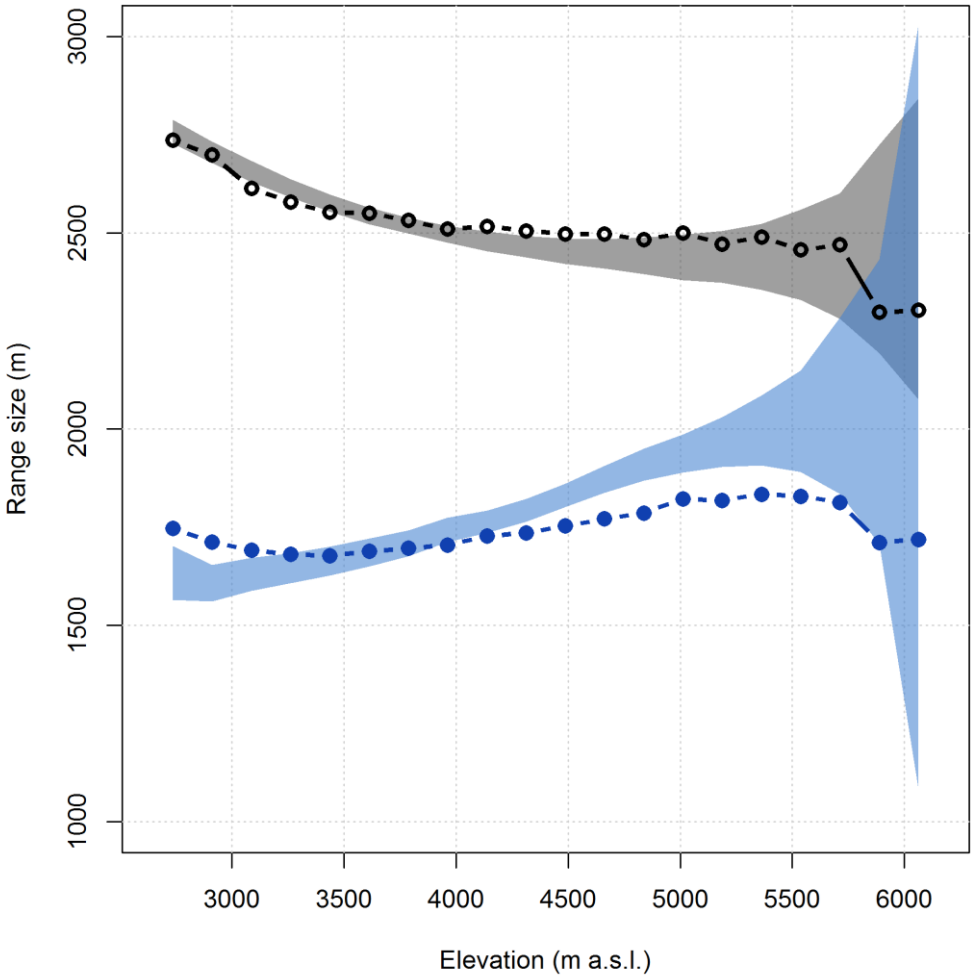

Figure 3 *Range size distribution calculated with Stevens' method generally follows the prediction from the null model. Open circles and the gray-filled area represent observed average range size of species present in particular elevation belt based on regional data from Ladakh and adjacent regions and 95% conf. int. from the respective null model. Full blue circles and blue area represents average range size of species present in particular elevation belt based on local data from Ladakh and 95% conf. int. of the null model. Difference between the local and regional range sizes is caused by range truncation, local absence in part of the gradient and by possible range size underestimation due to incomplete sampling.*

Range size examined by 'bin' methods resulted in decreasing range size with elevation for regional range and unimodal relation for local ranges (Fig. 4). These shapes were expected by random chance; regional range size distributions followed exactly the

prediction of the null model, while local range size deviated from the random expectation at low elevation bins (< 3400 m) and at around 4000 m.

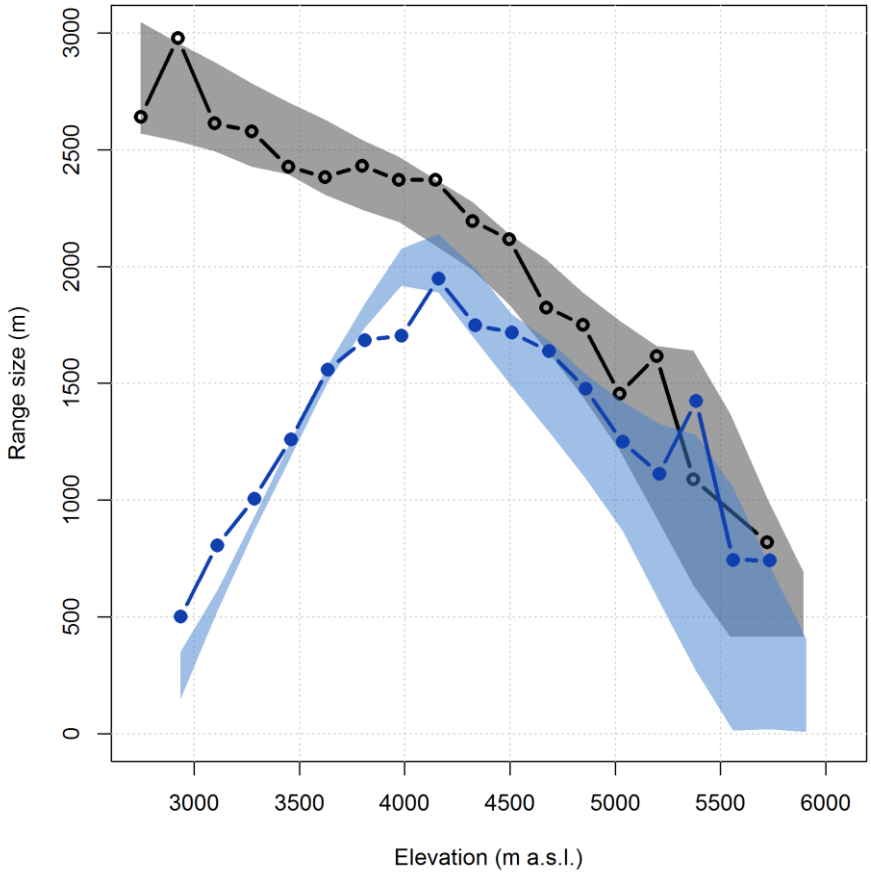

Figure 4 *Range size distribution calculated with 'bin' method is hardly affected by artefacts caused by calculating average range size of species according to their mid-point position. Observed regional range size is plotted by open circles and respective null model is grey-shaded area. Full circles and blue shaded area refer to the local range size. The bin method is sensitive to geometric constrains, because the position of mid-point cannot be closer to the domain limit than half of the range. The observed pattern in regional range size corresponds with null model prediction. Observed local range sizes had the same unimodal shape as prediction from the null model, but significant deviation were found in several bins.*

Temperature variability and extremes

The observed seasonal temperature range was between 35.5°C and 63.8°C (mean = 45.7°C; s.d. = 5.2°C) and the diurnal temperature range was between 5.9°C and 27.6°C (mean = 17.2°C; s.d. = 4.7°C;). Neither of the two climatic variability indices were associated with elevation (Fig. 5). The correlation between climate variability and elevation was insignificant for both seasonal range (cor = -0.145, p = 0.26) and for diurnal range (cor = 0.02, p = 0.87). The average temperature minima of the coldest

month ranged between -32°C and -8.9°C and strongly decreased with increasing elevation by 0.0062°C m^{-1}, (cor = -0.91, $p < 0.001$).

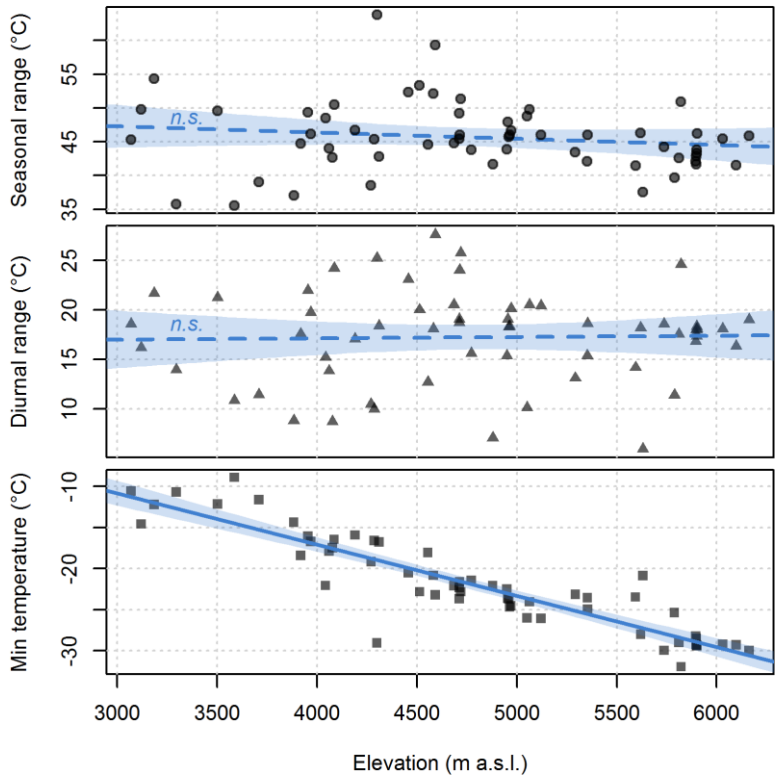

Figure 5 *Temperature variability along the elevation gradient based on in-situ measurements: seasonal range (top), diurnal range (middle) and average minimum temperature of the coldest month (bottom). A significant relation with elevation was found only for minimum temperature (slope = -0.0062, $p < 0.001$). The full line represents significant fit, dashed line unsignificant fit of linear regression models and shaded areas 95% confidence intervals around these lines.*

5.5 Discussion

Patterns of range size distribution observed along elevational gradient followed the expectation of the null models which assume decreasing diversity towards high elevations and random position of range sizes. The discrepancy between patterns observed on local and regional scales was caused by range truncation close to the geographic limit of the studied region. Our results based on real distribution data thus fully support the previous results based on simulated data, showing that the presence of geographic limits can reverse the relation between observed range size distribution and the underlying intrinsic ecological gradient (Šizlink et al., 2009). From this perspective, the effects of range truncation observed in our study provide an example of how strong such artefacts can be, and complement previous studies showing that species´ eleva-

tional range sizes are distributed randomly, irrespective of elevation (e.g. Bhattarai and Vetaas, 2006; Lee et al., 2013; Zhou et al., 2019).

Having refuted the pattern predicted by Rapoport´s rule, we have to ask what drives range size variability in our study system? From the multitude of factors influencing range size evolution, climate-based hypotheses are still top of the list of possible explanations (Pintor et al., 2015; Chan et al., 2016), especially for perennial plants. In theory, climatic tolerance is strongly influenced by the climatic variability (or extremes) an organism experiences, and elevational range size broadens with increasing tolerance (Gilchrist, 1995; Ghalambor, Huey, Martin, Tewksbury, & Wang, 2006; Sheldon & Tewksbury, 2014). Our climatic measurements suggest that the whole elevational gradient experiences a similar high magnitude of temperature variability, both seasonal and diurnal, typical of a continental desert climate, which can be one reason why we found a random arrangement of species ranges when geometric constraints were considered. Even though the freezing minima increased with elevation, the absence of any trend in elevational range size distribution means that higher freezing resistance does not translate into broader ranges either. This is in contrast to tropical mountains, where plants growing in low elevations never experience freezing temperatures and evolutionary adaptations to freezing temperatures may dramatically affect species elevational range.

The role of climate in structuring species´ elevational ranges, while intuitively acting at a certain level, may thus be overemphasized (Nowrouzi, Andersen, Bishop, & Robson, 2018). It can be well illustrated by the often-neglected fact that the elevational ranges of all lowland species are naturally truncated at sea level. From the perspective of climatic tolerance, these species would flourish several hundred metres below their current limit if there was land (cf. vegetation of the Dead Sea region, -400 m a.s.l.). Narrow ranges of lowland species, or the support for Rapoport´s rule often observed on islands (e.g. Chatzaki et al., 2005; Ogwu et al., 2019) may thus have other reasons (e.g. geometric constraints), rendering the attempts to establish a direct link between range size and climate debatable.

Species range sizes are distributed randomly in our study system, hence every elevation harbours a mixture of species with different ranges. The subnival zone provides a clear example. Highly specialized species with some of the narrowest ranges (ranking within 10 species with narrowest ranges of all Ladakh species with more than 30 occurrences) make a considerable proportion of the local species pool, e.g. *Ladakiella klimesii, Eritrichium hemisphaericum, Desideria pumila* or *Draba himachalensis* (Dvorský et al., 2015). These species must endure the particularly challenging conditions at the cold edge of vascular plant life, but adaptations to these extreme conditions become useless towards the lowlands where other qualities are demanded in order to succeed, e.g. competitive strength, tolerance of grazing, and, perhaps the most im-

portant in arid Ladakh, drought resistance. A similar trade-off is common in other taxonomic groups, too, with upper thermal tolerance declining with an improvement in the ability to tolerate low temperatures (Gaston & Chown, 1999b; Stillman, 2003; Calosi, Bilton, Spicer, & Atfield, 2008; Dixon et al., 2009; Calosi et al., 2010). Thus, the reverse of what Rapoport´s rule would predict, narrow-ranged high-elevation species, seems to be a logical consequence of ecological specialization.

The species pool of the subnival zone, however, also contains broad-ranged species. In fact, of the 11 species growing above 6000 m there are five species which simultaneously occur as low as 3500 m and their ranges are thus among the broadest in the whole regional species pool. Of those five, three species (*Aphragmus oxycarpus, Waldheimia tridactylites, Stellaria decumbens*) are ubiquitous above ca. 5600 m, and spread along streams downwards from their high-elevation centre, and subsequently have a skewed elevational distribution with the longer tail towards lower elevations (Dvorský et al. 2017). These species take advantage of improved moisture conditions near glacial streams at their low elevation limit, but disappear when the increasing competition from clonal graminoids leaves no space in the beneficial proximity of watercourses. Indeed, biotic interactions influence the warm ends of a species distribution more than climate (Normand et al., 2009; Meier et al., 2010; Wisz et al., 2013). The elevation itself therefore matters not so much to plant distribution, and species elevational range size without the knowledge of the range of microclimate a species experiences can be misleading (Scherrer and Körner, 2011; Dvorský et al., 2015).

To provide one more example, we compare two species with similar ecology and elevational centre of distribution (4500–5000 m), but one having the broadest range size from all plant species growing in Ladakh, while the other is narrow-ranged. *Kobresia schoenoides*, spanning between 2680 and 5650 m, is a strong competitor and its stout dense tufts are avoided by grazing animals. Its habitat requirements, mesic to wet grasslands and turf along streams, lake margins and wetlands, are the same as for *Gentianella pygmaea*, which does not occur below 4520 m, being small and a weak competitor. Moreover, it is easily eliminated by grazing. Therefore, the main difference behind the opposite elevational extent of these two species is not their ability to withstand a wider range of climatic conditions, but their different ability to cope with competition and disturbance. This example illustrates that species distribution can be shaped by many non-climatic drivers which can override the importance of the climatic ones (see also Sexton et al., 2009; Boulangeat et al., 2012). This, despite „*an almost suicidal tendency for many ecologists to celebrate complexity and detail at the expense of bold, first-order phenomena*“ (Lawton 1999), seems to be the most probable conclusion from our analyses.

In summary, our results support the conclusions of a meta-analysis by McCain & Knight (2013) that the predictive value of Rapoport´s elevational rule is at best weak,

and that elevational gradients in range sizes are the exception rather than the rule. We argue that the often-described patterns supporting this rule may be statistical artefacts caused by an inappropriate null model. Since climate-based hypotheses on range size drivers gained no direct support in our study, random range sizes imply species-specific responses, influenced both by climatic and non-climatic factors.

5.6 ACKNOWLEDGEMENTS

Leoš Klimeš, our late colleague who disappeared in Ladakh in 2007, collected most of the data; all credit to him for making Ladakh one of the best botanically explored parts of the whole High Asia. Our study was supported by the Czech Science Foundation (project GACR 17-19376S) and the Czech Academy of Sciences (project RVO 67985939).

5.7 References

Beketov, M. A. (2009). The Rapoport effect is detected in a river system and is based on nested organization. *Global Ecology and Biogeography, 18:* 498-506.

Bhattarai, K. R., & Vetaas, O. R. (2006). Can Rapoport's rule explain tree species richness along the Himalayan elevation gradient, Nepal?. *Diversity and Distributions, 12:* 373-378.

Boulangeat, I., Gravel, D., & Thuiller, W. (2012). Accounting for dispersal and biotic interactions to disentangle the drivers of species distributions and their abundances. *Ecology Letters, 15:* 584-593.

Calosi, P., Bilton, D. T., Spicer, J. I., & Atfield, A. (2008). Thermal tolerance and geographical range size in the Agabus brunneus group of European diving beetles (Coleoptera: Dytiscidae). *Journal of Biogeography, 35:* 295-305.

Calosi, P., Bilton, D. T., Spicer, J. I., Votier, S. C., & Atfield, A. (2010). What determines a species' geographical range? Thermal biology and latitudinal range size relationships in European diving beetles (Coleoptera: Dytiscidae). *Journal of Animal Ecology, 79*: 194-204.

Chan, W. P., Chen, I. C., Colwell, R. K., Liu, W. C., Huang, C. Y., & Shen, S. F. (2016). Seasonal and daily climate variation have opposite effects on species elevational range size. *Science*, 35: 1437-1439.

Chatzaki, M., Lymberakis, P., Markakis, G., & Mylonas, M. (2005). The distribution of ground spiders (Araneae, Gnaphosidae) along the altitudinal gradient of Crete, Greece: species richness, activity and altitudinal range. *Journal of Biogeography, 32:* 813-831.

Colwell, R. K., & Hurtt, G. C. (1994). Nonbiological gradients in species richness and a spurious Rapoport effect. The American Naturalist, 144: 570-595.

Colwell, R. K., & Lees, D. C. (2000). The mid-domain effect: geometric constraints on the geography of species richness. *Trends in Ecology & Evolution, 15:* 70-76.

Dentant, C. (2018). The highest vascular plants on Earth. *Alpine Botany, 128:* 97-106.

Dickoré, W. B. (2011). Himalayan upland plant database of Bernhard Dickoré, Munich Herbaria, accessed on the GBIF portal.

Dickoré, W. B., & Nüsser, M. (2000). Flora of Nanga Parbat (NW Himalaya, Pakistan): An annotated inventory of vascular plants with remarks on vegetation dynamics (Vol. 19). Botanic Garden and Botanical Museum Berlin-Dahlem.

Dixon, A. F., Honěk, A., Keil, P., Kotela, M. A. A., Šizling, A. L., & Jarošík, V. (2009). Relationship between the minimum and maximum temperature thresholds for development in insects. *Functional Ecology, 23:* 257-264.

Doležal, J., Dvorský, M., Kopecký, M., Liancourt, P., Hiiesalu, I., Macek, M., ... & Borovec, J. (2016). Vegetation dynamics at the upper elevational limit of vascular plants in Himalaya. *Scientific Reports, 6:*24881.

Dvorský, M., Altman, J., Kopecký, M., Chlumská, Z., Řeháková, K., Janatková, K., & Doležal, J. (2015). Vascular plants at extreme elevations in eastern Ladakh, northwest Himalayas. *Plant Ecology & Diversity, 8:*571-584.

Dvorský, M., Doležal, J., de Bello, F., Klimešová, J., & Klimeš, L. (2011). Vegetation types of East Ladakh: species and growth form composition along main environmental gradients. *Applied Vegetation Science, 14:*132-147.

Dvorský, M., Chlumská, Z., Altman, J., Čapková, K., Řeháková, K., Macek, M., ... & Doležal, J. (2016). Gardening in the zone of death: an experimental assessment of the absolute elevation limit of vascular plants. *Scientific Reports, 6:*24440.

Dvorský, M., Macek, M., Kopecký, M., Wild, J., & Doležal, J. (2017). Niche asymmetry of vascular plants increases with elevation. *Journal of Biogeography, 44:*1418-1425.

Fleishman, E., Austin, G. T., & Weiss, A. D. (1998). An empirical test of Rapoport's rule: elevational gradients in montane butterfly communities. *Ecology, 79:*2482-2493.

Fu, C., Wu, J., Wang, X., Lei, G., & Chen, J. (2004). Patterns of diversity, altitudinal range and body size among freshwater fishes in the Yangtze River basin, China. *Global Ecology and Biogeography, 13:*543-552.

Gaston, K. J., & Chown, S. L. (1999a). Why Rapoport's rule does not generalise. *Oikos*, 309-312.

Gaston, K. J., & Chown, S. L. (1999b). Elevation and climatic tolerance: a test using dung beetles. *Oikos*, 584-590.

Gaston, K. J., Blackburn, T. M., & Spicer, J. I. (1998). Rapoport's rule: time for an epitaph?. *Trends in Ecology & Evolution, 13:*70-74.

Ghalambor, C. K., Huey, R. B., Martin, P. R., Tewksbury, J. J., & Wang, G. (2006). Are mountain passes higher in the tropics? Janzen's hypothesis revisited. *Integrative and Comparative Biology, 46,* 5-17.

Gilchrist, G. W. (1995). Specialists and generalists in changing environments. I. Fitness landscapes of thermal sensitivity. *The American Naturalist, 146:*252-270.

Hartmann, H. (2009). *A summarizing report on the phytosociological and floristical explorations (1976-1997) in Ladakh (India)*. Druckerei Landquart VBA, 7302 Landquart, Switzerland.

Hausdorf, B. (2006). Latitudinal and altitudinal diversity patterns and Rapoport effects in north-west European land snails and their causes. *Biological Journal of the Linnean Society, 87:*309-323.

Janzen, D. H. (1967). Why mountain passes are higher in the tropics. *The American Naturalist, 101,* 233-249.

Körner, C. (2004). Mountain biodiversity, its causes and function. *Ambio*, 11-17.

Körner, C., Riedl, S., Keplinger, T., Richter, A., Wiesenbauer, J., Schweingruber, F., & Hiltbrunner, E. (2019). Life at 0° C: the biology of the alpine snowbed plant *Soldanella pusilla*. *Alpine Botany*, 1-18.

Kwon, T. S., Kim, S. S., & Chun, J. H. (2014). Pattern of ant diversity in Korea: An empirical test of Rapoport's altitudinal rule. *Journal of Asia-Pacific Entomology, 17:*161-167.

Lawton, J. H. (1999). Are there general laws in ecology?. *Oikos, 84:*177-192.

Lee, C. B., Chun, J. H., Song, H. K., & Cho, H. J. (2013). Altitudinal patterns of plant species richness on the Baekdudaegan Mountains, South Korea: mid-domain effect, area, climate, and Rapoport's rule. *Ecological Research, 28:*67-79.

Letcher, A. J., & Harvey, P. H. (1994). Variation in geographical range size among mammals of the Palearctic. *The American Naturalist, 144:*30-42.

McCain, C. M., & Knight, B.K. (2013). Elevational Rapoport's rule is not pervasive on mountains. *Global Ecology and Biogeography, 22:*750-759.

Meier, E. S., Kienast, F., Pearman, P. B., Svenning, J. C., Thuiller, W., Araújo, M. B., ... & Zimmermann, N. E. (2010). Biotic and abiotic variables show little redundancy in explaining tree species distributions. *Ecography, 33:*1038-1048.

Normand, S., Treier, U. A., Randin, C., Vittoz, P., Guisan, A., & Svenning, J. C. (2009). Importance of abiotic stress as a range-limit determinant for European plants: insights from species responses to climatic gradients. *Global Ecology and Biogeography, 18:*437-449.

Nowrouzi, S., Andersen, A. N., Bishop, T. R., & Robson, S. K. (2018). Is thermal limitation the primary driver of elevational distributions? Not for montane rainforest ants in the Australian Wet Tropics. *Oecologia, 188:*333-342.

Ogwu, M. C., Takahashi, K., Dong, K., Song, H. K., Moroenyane, I., Waldman, B., & Adams, J. M. (2019). Fungal elevational Rapoport pattern from a high mountain in Japan. *Scientific Reports, 9:*6570.

Patterson, B. D., Pacheco, V., & Solari, S. (1996). Distribution of bats along an elevational gradient in the Andes of south-eastern Peru. *Journal of Zoology, 240:*637-658.

Pintor, A. F., Schwarzkopf, L., & Krockenberger, A. K. (2015). Rapoport's Rule: Do climatic variability gradients shape range extent?. *Ecological Monographs, 85:*643-659.

Pither, J. (2003). Climate tolerance and interspecific variation in geographic range size. *Proceedings of the Royal Society of London. Series B: Biological Sciences, 270:*475-481.

Ribas, C. R., & Schoereder, J. H. (2006). Is the Rapoport effect widespread? Null models revisited. *Global Ecology and Biogeography, 15:*614-624.

Rohde, K. (1996). Rapoport's rule is a local phenomenon and cannot explain latitudinal gradients in species diversity. *Biodiversity Letters, 3:*10-13.

Sanders, N. J. (2002). Elevational gradients in ant species richness: area, geometry, and Rapoport's rule. *Ecography, 25:*25-32.

Sexton, J. P., McIntyre, P. J., Angert, A. L., & Rice, K. J. (2009). Evolution and ecology of species range limits. *Annual Review of Ecology, Evolution, and Systematics, 40*:415-436.

Sheldon, K. S., & Tewksbury, J. J. (2014). The impact of seasonality in temperature on thermal tolerance and elevational range size. *Ecology, 95:*2134-2143.

Scherrer, D., & Körner, C. (2011). Topographically controlled thermal-habitat differentiation buffers alpine plant diversity against climate warming. *Journal of Biogeography, 38:*406-416.

Stevens, G. C. (1989). The latitudinal gradient in geographical range: how so many species coexist in the tropics. *The American Naturalist, 133:*240-256.

Stevens, G. C. (1992). The elevational gradient in altitudinal range: an extension of Rapoport's latitudinal rule to altitude. *The American Naturalist, 140:*893-911.

Stillman, J. H. (2003). Acclimation capacity underlies susceptibility to climate change. *Science, 301:*65-65.

Šizling, A. L., D. Storch, & P. Keil. 2009. Rapoport's rule, species tolerances, and the latitudinal diversity gradient: Geometric considerations. *Ecology, 90:*3575–3586.

Taschler, D., & Neuner, G. (2004). Summer frost resistance and freezing patterns measured *in situ* in leaves of major alpine plant growth forms in relation to their upper distribution boundary. *Plant, Cell & Environment, 27:*737-746.

Wild, J., Kopecký, M., Macek, M., Šanda, M., Jankovec, J., & Haase, T. (2019). Climate at ecologically relevant scales: A new temperature and soil moisture logger for long-term microclimate measurement. *Agricultural and Forest Meteorology*, 268:40-47.

Wisz, M. S., Pottier, J., Kissling, W. D., Pellissier, L., Lenoir, J., Damgaard, C. F., ... & Heikkinen, R. K. (2013). The role of biotic interactions in shaping distributions and realised assemblages of species: implications for species distribution modelling. *Biological Reviews, 88:*15-30.

Zhou, Y., Ochola, A. C., Njogu, A. W., Boru, B. H., Mwachala, G., Hu, G., ... & Wang, Q. (2019). The species richness pattern of vascular plants along a tropical elevational gradient and the test of elevational Rapoport's rule depend on different life-forms and phytogeographic affinities. *Ecology and Evolution, 9:*4495-4503.

CHAPTER SIX:

MID-POINT ATTRACTOR MODELS OF PLANT SPECIES RICHNESS ALONG ELEVATIONAL GRADIENT REVEALS MONOTONICALLY DECREASING CLIMATIC FAVOURABILITY SHAPED BY GEOMETRIC CONSTRAINTS

MARTIN MACEK[1,2], MIROSLAV DVORSKÝ[1], ADAM KLIMEŠ[1,2], JAN WILD[1,3], JIŘÍ DOLEŽAL[1,4] & MARTIN KOPECKÝ[1,5]

1 Institute of Botany, The Czech Academy of Sciences, Zámek 1, CZ-252 43, Průhonice, Czech Republic

2 Department of Botany, Faculty of Science, Charles University, Benátská 2, Praha, CZ-128 01, Czech Republic

3 Faculty of Environmental Sciences, Czech University of Life Sciences Prague, Kamýcká 129, CZ-165 21, Praha 6-Suchdol, Czech Republic

4 Department of Botany, Faculty of Science, University of South Bohemia, Na Zlaté stoce 1, CZ -370 05, České Budějovice, Czech Republic

5 Department of Forest Ecology, Faculty of Forestry and Wood Sciences, Czech University of Life Sciences Prague, Kamýcká 129, CZ-165 21, Praha 6-Suchdol, Czech Republic

Corresponding author: Martin Macek, e-mail: martin.macek@ibot.cas.cz

Manuscript

6.1 Abstract

Midpoint attractor models (MPA) were introduced recently as a promising statistical tool capable of reproducing unimodal empirical elevational species richness gradients and differentiating the underlying gradient of environmental favourability from neutral effects forced by geometric constraints. Here we used a comprehensive dataset of the elevational distribution of 1054 vascular plant species growing in NW Himalaya to evaluate model performance in a system constrained geographically at low elevations and physiologically at high elevations. We tested how the inclusion of functionally, biogeographically and taxonomically distinct species groups affects model performance. We compared two alternative variants of MPA, with respect to fit to the data and interpretation of mid-point attractor parameters. MPA successfully fitted species richness gradients, both of vascular plants as a whole, and of separate species groups. The greatest variability was between biogeographic elements, while taxonomic subsetting by families revealed limited variability of midpoint attractor parameters. The two MPA variants provided similar fit to the data, but with considerable differences in midpoint attractor parameters. MPA proved to be useful model, able to synthesise underlying ecological drivers and neutral constraints on species richness.

6.2 Keywords

Mid-domain effect; midpoint attractor; Himalaya; plant species richness; sampling bias; neutral theory; null models; elevational gradient, climatic favorability, geometric constrains, species ranges

6.3 INTRODUCTION

Species diversity patterns along altitudinal and latitudinal gradients have always fascinated scientists (Lomolino 2001). Monotonic decrease of diversity with increasing elevation used to be a generally accepted and universal pattern attributed to general decrease of temperature with elevation, but conflicting evidence of humped-shaped species diversity patterns resulted in a search for alternative explanations of empirical diversity patterns (Rahbek 1995, 2005). Mid-elevation peaks were found more frequently in dry climates, where productivity at low elevations is limited by increasing aridity caused by high evaporation rates and low precipitation (McCain 2009). Furthermore, anthropogenic ecosystem disturbances have been concentrated mostly in lowlands, with negative effects on the biodiversity documented (Nogués-Bravo et al. 2008). However, the observed mid-elevation diversity peak may be just an artefact of the sampling effort or the method used to estimate elevational diversity pattern from available observations (Colwell and Hurtt 1994, Grytnes and Vetaas 2002). When the species range is estimated from point-samples, it is likely that the absolute range would be underestimated and this consequently causes the underestimation of actual diversity, especially at the domain margins and when the sampling effort is limited.

A simple and ecologically neutral explanation of diversity peak at middle elevations emerged with the concept of 'mid-domain effect' (MDE), using only geometric constraints and random placement of species ranges within these constraints (Colwell and Hurtt 1994, Colwell and Lees 2000). MDE predicts formation of symmetrical, hump-shaped distributions, just by random overlap of species ranges placed within the domain. Mid-domain effect thus represents an ecologically neutral null model, simulating how the richness pattern within a bounded domain would look, when species range placement is not governed by climate suitability. The support for MDE varied widely among studies, according to the geographic extent and organism group studied (see Dunn et al. 2007 for review). The MDE prediction is more likely to fit empirical richness patterns when species ranges and the scale of analysis are both large (Jetz and Rahbek 2001, Dunn et al. 2007). When a domain hosts a higher proportion of large-ranged species, the overlap in the middle of the domain is more likely. Second, MDE fit is expected to be stronger when the environmental gradients are weak (Colwell et al. 2005), or under conditions of high environmental tolerances (Rangel and Diniz-Filho 2005). On the other hand, small-ranged (relative to domain size) species are usually found along prominent gradients with sharply changing environmental conditions; such systems are accordingly less prone to the influence of MDE.

While MDE quickly attained recognition of biogeographers, it had also been strongly criticized (Zapata et al. 2005, Currie and Kerr 2008, but see Colwell et al. 2004, 2005). MDE opponents stressed the conceptual difficulties in defining domain boundaries, as well as purported latent effects of environmental factors on the range size frequency

distribution used to generate mid-domain null models (Hawkins et al. 2005) or evidence that water-energy hypothesis can provide a better fit to empirical richness gradients than MDE (Hawkins et al. 2003). It is true that, with the exception of islands and other domains with sharp ecotones (e.g. lakes and their aquatic life), practically no other parts of global surface have effective hard boundaries. This seems to be the major constraint for the application of MDE in practice – how to define the domain and its boundaries? As a rule of thumb, the lowest elevation of land surface in the study area (usually the sea-level) is considered as the lower domain limit. In contrast, the decision where to set the upper limit is more arbitrary – it can be the elevation of the highest summit in the area, but also the physiological limit for survival of the organisms studied (Grytnes 2003a, Zapata et al. 2005). The growing body of macroecological studies on diversity distributions reveals that most authors regret they cannot define their domain unambiguously, and are accordingly cautious interpreting their results. Currently, there seems to be a consensus that the effects of geometric constraints can jointly influence the observed richness pattern together with other ecological drivers of diversity, and its contribution can eventually be separated and quantified. In fact, MDE is not important for what it does explain, but rather for what it does not. The unexplained residuals from MDE model require further explanation, because they may include deterministic, non-random biologically-relevant drivers (Colwell and Lees 2000).

To overcome the limitations of MDE, the mid-point attractor model (MPA) was recently developed, extending the conceptual framework of MDE by replacing a uniform distribution of midpoint positions within the domain by a midpoint attractor with Gaussian distribution (Colwell et al. 2016). The MPA model is more flexible than MDE because the Gaussian attractor allows MPA to fit also skewed hump shapes, peaking apart from the center of the domain. The Gaussian attractor has two parameters, the first identifies the position of the peak of Gaussian curve (hereafter called parameter A), and second (parameter B) is the standard deviation of the Gaussian curve, an inverse measure of attractor′s strength. The curve is truncated by the limits of the domain. The position and shape of mid-point attractor can be interpreted as an ecologically meaningful shared 'optimum', favouring diversity of the studied taxa, shifting the MPA model from purely neutral towards a model with biological meaning.

However, even the MPA model has several limitations and assumptions to be met. Artefacts in underlying empirical data, i.e. incomplete sampling of species diversity and arbitrary decisions about where to set domain boundaries, may confound the model-fitting and interpretation. Furthermore, species whose fundamental niche goes beyond the environmental gradient present in the domain will have their realized range truncated, i.e. one or both of their range boundaries will likely be aligned with the domain boundary. The presence of such species may cause deviations from normal distribution of midpoints. To deal with this issue, Colwell et al. (2016) proposed modification of the MPA algorithm. While the primary MPA model (hereafter called MPA 1)

uses a doubly truncated normal distribution as a midpoint sampler, a modified algorithm (MPA 2) samples midpoints from complete Gaussian distribution and then adjusts midpoints of the species with ranges exceeding domain boundaries to the closest possible position to respective domain boundary that will keep the complete species range within the domain boundaries. Both variants prevent the simulated species ranges from overlapping domain boundaries, but the second approach increases the probability that species range limit is placed directly on domain limit. The fit to the data presented by Colwell at al. (2016) was comparable between the alternative MPA model modifications, but the consequences of the decision which model to use on estimated model parameter values and their interpretation were not sufficiently discussed.

The basic assumption underlying the MPA is the existence of a universal, unimodal gradient of environmental favourability that underlies the realized richness patterns in a bounded domain. In reality, the ecological niche of taxonomically or functionally related groups of organisms tends to be similar, and this niche conservatism is mirrored in the pattern of species richness along altitudinal and latitudinal gradients (Peterson et al. 1999, Wiens and Graham 2005). Moreover, species richness patterns of distinct taxonomic or functional groups may follow different climatic drivers (Hawkins et al. 2003, Šímová et al. 2011). In plants, water-energy measures (i.e. annual precipitation, actual evapotranspiration, potential evapotranspiration) or climatic extremes (temperature minima and maxima) are usually considered the most relevant climatic variables controlling species ranges and richness. While the average temperature universally decreases with elevation, other climatic measures potentially controlling species richness exhibit more complex relation to altitudinal gradients (McCain and Grytnes 2010). It is therefore legitimate to ask how the inclusion of ecologically distinct groups of species affects the resulting species richness curve and, consequently, model performance. The decision how to define a species group used for richness assessment is usually made ad-hoc; taxonomic or life-form criteria are usually applied (Zhou et al. 2019). In the case of plants, studies dealing with altitudinal richness gradients generally consider either all vascular plants (Grytnes and Vetaas 2002, Grytnes 2003b), or selected functional or taxonomic groups, such as ferns (Watkins et al. 2006, Colwell et al. 2016), epiphytes (Cardelús et al. 2006), trees (Carpenter 2005, Rana et al. 2019) or palms (Bachman et al. 2004). However, studies aiming to directly address differences among groups are surprisingly scarce (Grytnes and Beaman 2006, Peters et al. 2016, Rana et al. 2019).

In this paper we use a comprehensive dataset on vascular plant diversity from the Ladakh region in the Western Himalaya to explore diversity patterns along an altitudinal gradient spanning more than 3500 m. We tested the performance of the MDE and MPA models, addressing elevational diversity patterns in the study area, where the lower domain boundary is defined geographically by a regional boundary, while the

upper domain boundary is set by climatic hospitability to vascular plant life. We aimed to compare the performance of different models for plant diversity along this altitudinal gradient and to decompose effects of geographic constraints, sampling bias, species functional grouping, phylogenetic structure and biogeographic origin on realized diversity patterns and their interpretation.

6.4 Methods

Empirical species diversity data

We studied diversity patterns along an elevation gradient in NW Himalaya, Ladakh region, India (Fig. 1). This region is partly isolated from adjacent areas by biogeographical barriers – glaciated ranges of Great Himalaya to the south, and Karakoram Range to the north-west. To the east, the region is connected to the Tibetan plateau. Orographic barriers are also responsible for a strong rain-shadow effect, causing overall aridity in the region, with total annual precipitation as low as 100 mm·year-1. Elevations with available unglaciated land area span from 2650 to ca 7050 m a.s.l., but the highest occurrences of vascular plants have been reported from 6150 m a.s.l. (Dvorský et al. 2015). Combined effects of low temperature stress and aridity restrict regional species ranges and dominant life forms (Dvorský et al. 2017). The prevailing vegetation is treeless due to high aridity, except for shrubby formations along streams. At higher elevations, where the water regime is more balanced due the decrease in evapotranspiration, low temperature is the dominant limiting factor (Dvorský et al. 2015).

We compiled species ranges using 95,812 georeferenced floristic records from the study region collected on 4062 plots (1 ha each) in surveys conducted between 1997-2006 and from 7187 floristic records made in 2008-2015, maintained by the Institute of Botany of the Czech Academy of Sciences. The total extent of the study area covered by field sampling is ca. 50,000 km2 and the vertical range of floristic records spans from 2650 m a.s.l. in Suru Region in northwest Ladakh to 6150 m a.s.l. in Changthang Region, in eastern Ladakh. We excluded all cultivated plant species and taxonomically unresolved records from the genus Taraxacum. This selection resulted in a dataset comprising 90,489 records of 1054 plant species, used for further analyses. For each species we identified the elevation of its lowest and highest occurrence in the dataset.

To assess the contribution of various species groups to the overall diversity pattern, we classified the species according to the following criteria: taxonomic rank (family level), biogeographical affinity, and life form (annuals, graminoids, forbs, shrubs, and trees). Detailed classification of species and the rules applied can be found in Appendix 1.

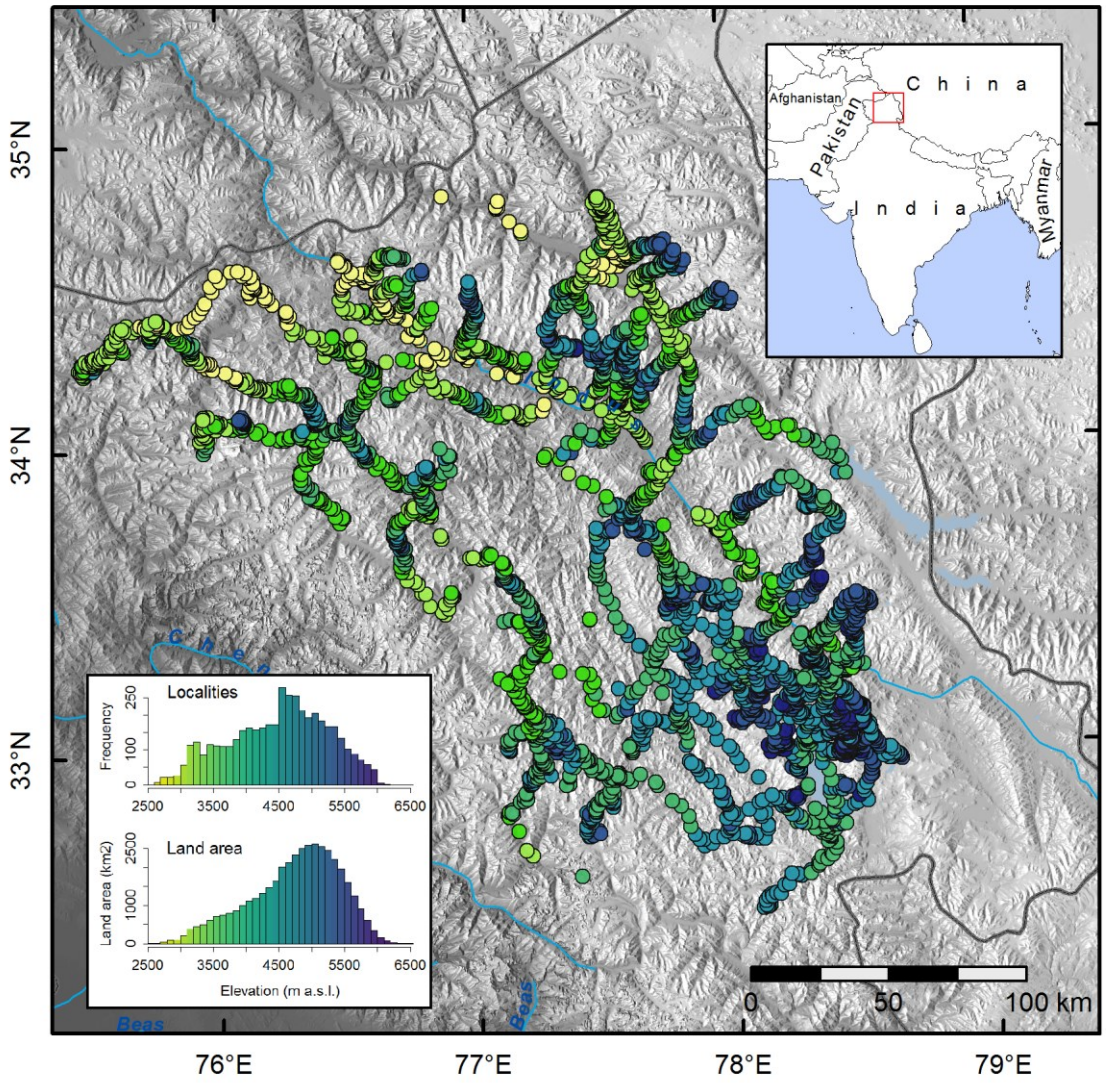

Figure 1 *Study area with sampling localities. Inset histograms show sampling effort and terrestrial land-area by 100m elevation bands. Hillshade and land area histogram is based on digital elevation model (Jarvis A., H.I. Reuter, A. Nelson, E. Guevara, 2008, Hole-filled seamless SRTM data V4, International Centre for Tropical Agriculture (CIAT), available from http://srtm.csi.cgiar.org)*

Data analyses

We defined our domain by the extent of elevations with species occurrence data, i.e. 2650 m a.s.l. as the lower domain limit, and 6150 m a.s.l. as the upper domain limit. We then transformed elevation values to unit domain values for model fitting purposes and back-transformed values for the interpretation of results.

To calculate empirical elevational species richness (ESR), we used the interpolation method, supposing that each species is continuously present to elevations between its extreme occurrences (Grytnes and Vetaas 2002). Interpolation method ESR was then

calculated as number of overlapping species ranges in 100 elevations uniformly placed along the elevation gradient of the modeling domain.

We performed two independent analyses to reveal how is ESR affected by sampling bias and uneven distribution of planimetric area along elevational gradient. First, we calculated ESR from species ranges based on a limited number of observations. We subsampled floristic records used for ESR calculation to mimic limited sampling effort. We used sequence of samples consisting of 5% to 95% records sampled randomly without replication from the full dataset. We repeated this procedure 1,000 times and calculated median ESR for each sampling intensity. Second, we calculated species richness in elevational bands using incidence data from point samples and applied corrections for sampling effort and total land area. This method is less sensitive to elevational richness pattern distortion close to domain boundaries (Grytnes and Vetaas 2002). We calculated uncorrected empical richness as the number of species present in 35 elevational bands (100-m each). To account for sampling effort we calculated total species richness using the abundance-based asymptotic richness estimator from the iNEXT R package (Chao et al. 2014, Hsieh et al. 2019), and to account for total land area in elevation belts we divided elevation gradient into 35 variable elevational bands with equal total land area.

To compare congruence between different null models and ESR, we used a mid-domain effect (MDE) model (Colwell and Lees 2000) and four modifications of mid-point attractor (MPA) models (after Colwell et al. 2016).

To fit the MDE model, we randomly sampled midpoint positions for each species from a uniform probability distribution function restricted by interval [half range; 1 – half range]. This restriction ensures that sampled ranges cannot extend beyond domain limits (Colwell and Hurtt 1994). We repeated the sampling 1000 times and stored median and the 95% confidence interval (2.5 and 97.5 percentiles) from species richness predicted by MDE models.

The MPA model fits empirical diversity using a Gaussian attractor defined by two parameters: the parameter A, which controls location of the attractor‘s peak, and parameter B, which is the standard deviation of the attractor, controlling the strength of the attractor. We tested two variants of MPA as proposed by Colwell et al. (2016), differing in the probability distribution function used for midpoint sampling – algorithm MPA 1 uses a doubly truncated Gaussian probability density function, where truncation prevents sampled ranges from extending beyond domain limits. Algorithm MPA 2 uses a full Gaussian probability density function, and in case that sampled midpoint distance from the domain limit is less than half range distance, it is moved to half range distance to prevent ranges from extending beyond domain boundaries. For each algorithm MPA 1 and MPA 2 we tested two different settings: first, with mid-point attractor parameter A values restricted to the unit [0, 1] interval (i.e. constrained to lie

within the domain) and parameter B restricted to the unit [0, 1] interval, henceforth referred to as algorithm MPA 1a and MPA 2a, respectively. This first setting for A and B corresponds to the original setting used by Colwell et al. (2016). In the second setting, the mid-point attractor parameter A is allowed to fall outside the domain limits, within an interval restricted to [-0.5, 1.5], and parameter B is limited to the interval [0, 2] (algorithm MPA 1b and MPA 2b). This second setting allows mid-point attractor to be located below/above actual domain limits, which is a possible scenario in our high-altitude study area. We compiled MPA models using Bayesian inference through 'RStan' package (Stan Development Team 2018). Flat priors were used to define both parameters. For Bayesian inference, we used a likelihood function for midpoint distribution, directly, instead of using a goodness-of-fit measure for empirical species richness as proposed by Colwell et al. (2016). Our approach gives equal weight to each species, whereas the original approach gives more weight to wide-ranged species. We used four chains and 1000 iterations for warmup and 1000 post-warmup iterations, with a thinning factor of five, resulting in 800 draws used for model inference. We stored posterior mean and 95% credible interval values of estimated mid-point attractor parameters A and B, and median and 95% credible intervals for predicted species richness values (PSR) at 100 evenly spaced positions along the elevation gradient for each model.

For model performance evaluation, we calculated four goodness-of-fit measures based on median PSR and ESR: Pearson correlation (cor); mean absolute error (MAE); root mean squared error (RMSE); and normalized RMSE (RMSE divided by total species richness).

We fitted MDE and MPA models to the full species list and to subsets of species, with species groups selected according to taxonomic rank, biogeographic affinity, or life-form. Only groups with more than 10 species were used for model fitting. We tested effects of decomposition of the total diversity into species groups using taxonomic, biogeographic and life-form criterion on MPA model parameters A and B. We quantified between-group variability in midpoint attractor position as the standard deviation of MPA parameter A and variability in attractor strength as average MPA parameter B, using posterior mean parameter estimates for the selected species groups. We used randomized species classification (randomization without replication) to provide a null expectation, given numbers and sizes of species groups equal to the actual groups. We expected that, if the applied grouping criterion were ecologically relevant, the variability in MPA parameter A (attractor position) would be higher and average MPA parameter B (inverse measure of attractor strength) would be lower as compared to the null expectation. Increased variability on parameter A indicates differenciation of midpoint positions between the groups and lower parameter B indicates higher homogeneity of midpoint positions within the groups. We used a one-tailed F-test to test our hypothesis that variability of MPA parameter A will be higher and a one-tailed paired t-test to test

the hypothesis that average MPA parameter B will be lower for empirical parameter estimates compared to null expectations for ecologically differenciated species groups.

All statistical analyses were performed in R 3.4.4 (R Core Team 2018).

6.5 Results

Many species ranges had their lower range limit at - or close to - the lower limit of the domain (Fig. 2). The ESR curve was unimodal and positively skewed, peaking at 3875 m a.s.l. (0.35 on unit domain); maximum ESR was 660 species (Fig. 3). However, species diversity completely diminished towards upper elevations and reached zero below the physical limit of available unglaciated land-area at high elevations.

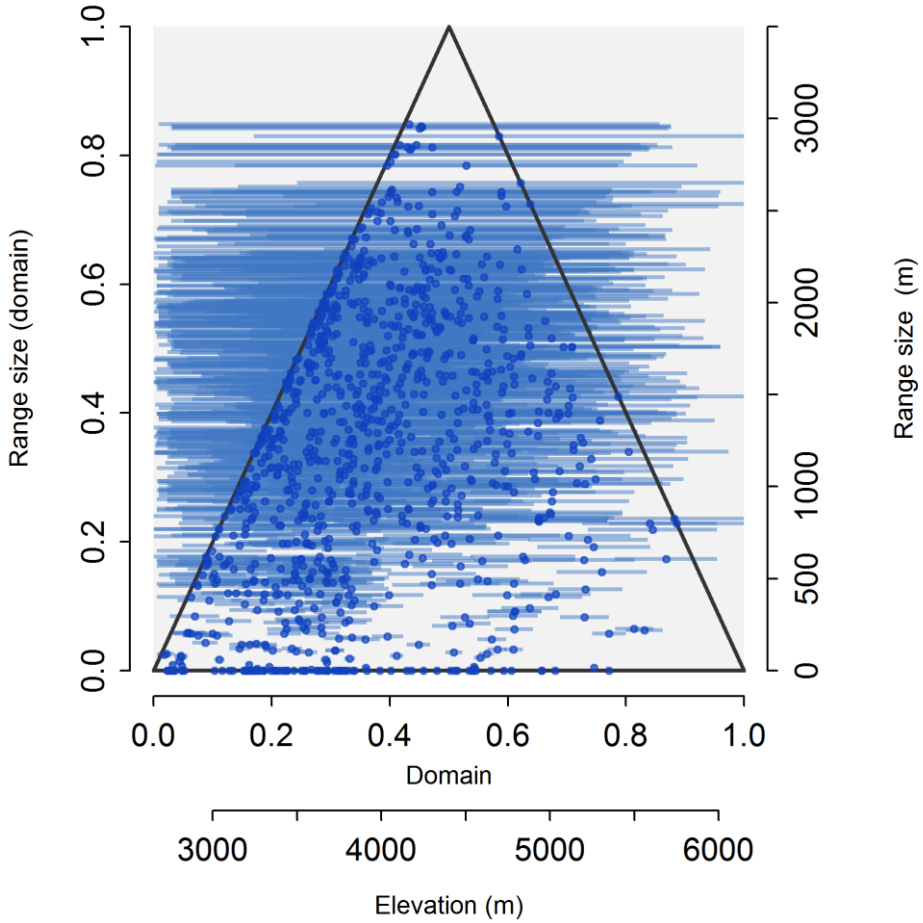

Figure 2 *Empirical species ranges. Position of species range mid-point (x-axis) is plotted by points against its range size (y-axis). Horizontal lines display species range defined by minimum and maximum elevation of occurrence. Triangle bounds possible locations of midpoints within the domain.*

Sampling bias

Random subsampling of the species-occurrence dataset affected the shape of the ESR (Fig. 3). Richness estimates based on interpolation method at the domain margins

proved to be the most sensitive to simulated less-intensive sampling. The lower part of the elevational domain was more sensitive to sampling bias than the upper part. The shape of the ESR converged as sampling effort increased. With very limited sampling effort (<10% of the original dataset) the ESR became more symmetric, with its peak closer to domain midpoint.

Species richness estimate from point-samples in elevational bands produced hump shaped patterns, too (Fig. 4). Applying an asymptotic estimate for total species richness in altitudinal bands conserved a hump-shaped pattern, with maximum of 769 species estimated for altitudinal band 3,650 – 3,750 m a.s.l. (Fig. 4b). When band planimetric area was standardized, a hump was less pronounced, reaching maximum values at 3,280-3,500 m, both uncorrected and corrected for sampling intensity (Fig. 4c,d).

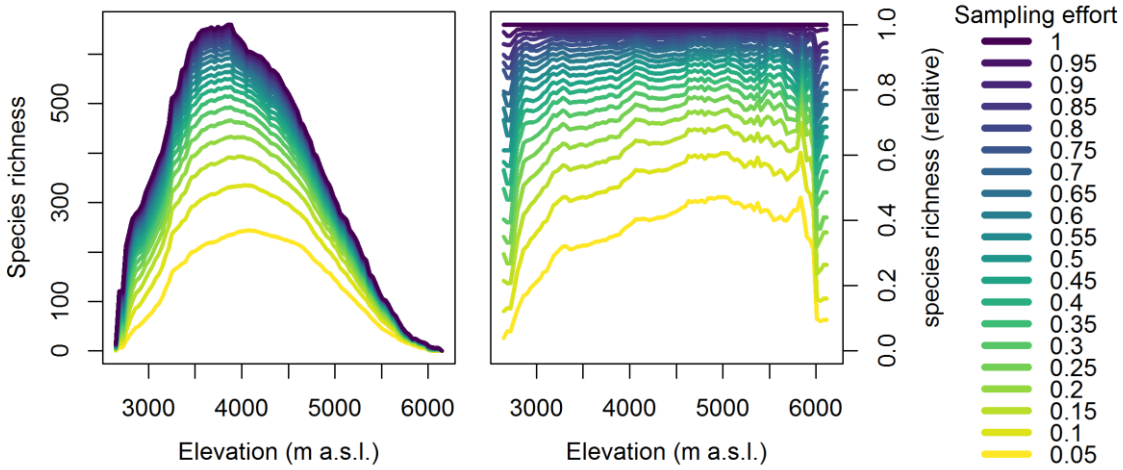

Fig. 3 *Species richness estimates for limited sampling effort using the range interpolation method. Sampling bias is relatively most pronounced at domain margins and in the lower part of the gradient. Absolute (left) and relative (to the full dataset, right) species richness estimated using random fractions (0.05-1) of species occurrence records.*

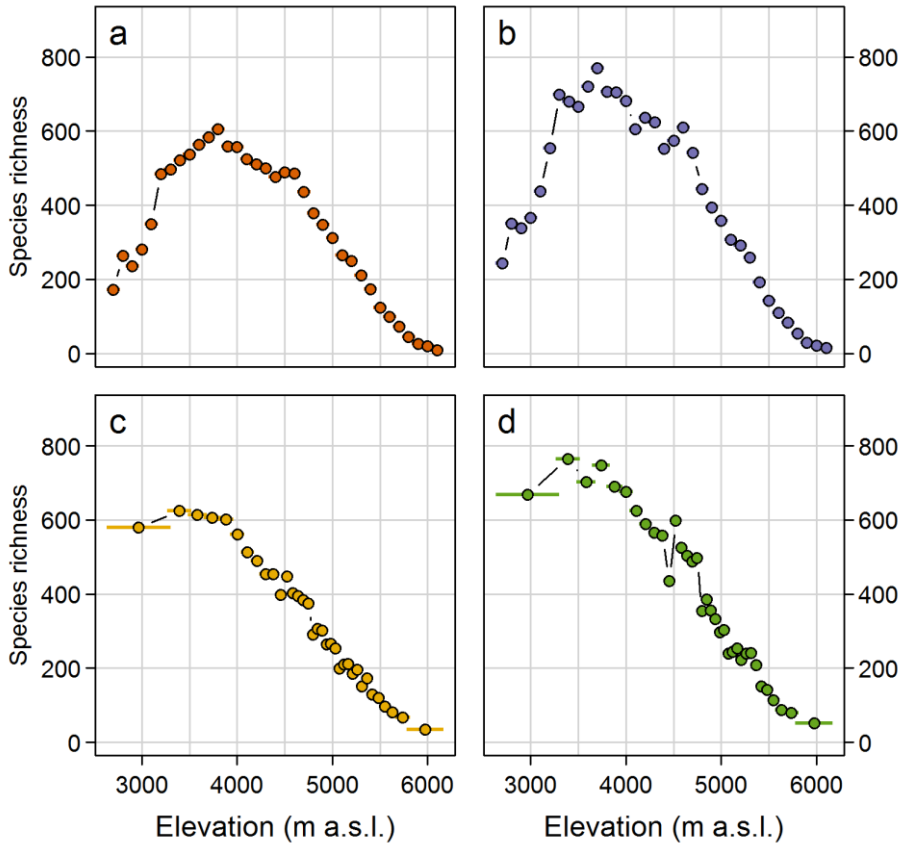

Figure 4 Estimated species richness using point-samples in 35 elevational bands, a) using equally spaced 100-m elevational bands, b) using equally spaced 100-m elevational bands corrected for sampling intensity using asymptotic richness estimate, c) using variable bandwidth with equal planimetric land area, d) using variable bandwidth with equal planimetric land area corrected for sampling intensity using asymptotic richness estimate. Horizontal whiskers indicate width of elevational bands used.

Model performance

Full dataset

MDE prediction produced a symmetrical, bell-shaped curve, which reproduced the empirical species richness pattern poorly, underestimating diversity at lower elevations and overestimating diversity at upper elevations (Fig. 5a, f). All MPA models fitted the empirical species richness well, with algorithm MPA 1b providing best results (Fig. 5; table 1). Algorithms MPA 1 and 2 differed only slightly in the goodness-of-fit metrics, but they provided significantly different estimates of midpoint attractor parameters. Midpoint attractor position estimated by MPA 1b was situated below the lower domain limit. Algorithm MPA 2b produced similar midpoint attractor position estimates as

algorithm MPA 2a, with the attractor centered approximately at the observed peak of diversity.

Table 1 *Estimated parameters and model performance for evaluated richness models using the full set of species. Parameter A controls the Gaussian mid-point attractor location (in m a.s.l.); parameter B controls strength (standard deviation, in m) of the Gaussian mid-point attractor. Fit between observed and predicted elevational richness is presented by goodness-of-fit measures: Pearson correlation (cor); mean absolute error (MAE); root-mean-squared error (RMSE) and normalized root-mean-squared error (nRMSE).*

Richness model	Param. A mean (95% CI)	Param. B mean (95% CI)	cor	MAE	RMSE	nRMSE
MDE	-	-	0.718	140.88	155.74	0.148
MPA1a	2848 (2659; 3114)	1078 (946; 1185)	0.993	17.66	25.86	0.025
MPA1b	2431 (1324; 3044)	1229 (989; 1595)	0.994	16.67	24.49	0.023
MPA2a	3913 (3873; 3949)	600 (570; 630)	0.990	26.03	32.90	0.031
MPA2b	3913 (3876; 3948)	600 (570; 632)	0.990	26.02	32.94	0.031

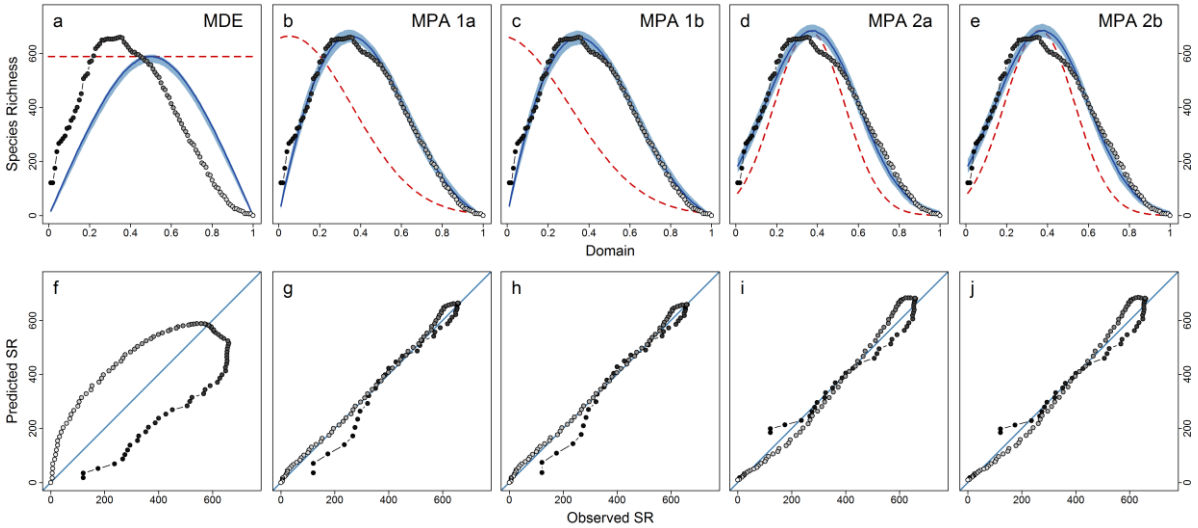

Figure 5 Observed elevational species richness and null model predictions for MDE model (a, f); MPA 1a (b, g); MPA 1b (c, h); MPA 2a (d, i); and MPA 2b (e, j). Upper panels (a-e) shows empirical richness (dots); predicted species richness by null models (blue line and light blue area for median and 95% confidence/credible interval) and the probability function of the mid-point attractor (dashed red line). Lower panels (f-j) display predicted vs. observed species richness and the 1:1 line. While the MDE model provided poor fit to the empirical richness, all variants of the MPA models provided excellent fit.

Species grouping

Splitting the dataset into species groups significantly affected MPA shape parameters (Fig. 6), but goodness-of-fit measures were on average worse than for whole vascular plant richness (Appendix 2, Table S1).

Grouping based on life-form resulted in a the marginally significant ($p < 0.1$) effect on the variance of attractor positions (parameter A) only for model MPA 2b. A marginally significant effect on attractor strength (parameter B) was found for all four MPA models (Table 2). The absolute difference from random expectation was, however, largest among tested grouping criteria, but the low number of life-form groups ($n = 5$) resulted in low test power.

Grouping based on biogeographical affinity significantly affected both attractor position and strength in all MPA models. Attractor location for Eurasian, Mediterranean, Eurasian and Cosmopolitan biogeographic elements was estimated to lie below the lower domain limit by the model MPA 1b. In contrast, the midpoint attractor for Tibetan elements was located at 5290 m a.s.l., far above mid-point attractors of other biogeographic groups (Fig. 6).

Grouping according to taxonomic rank marginally affected the variance of attractor position (parameter A) only in the MPA 1a model, and affected attractor strength (parameter B) in models MPA 2a and MPA 2b (Table 2). Attractor position estimated by MPA 1b for 13 out of 23 families lay below domain limit. The highest attractor position was reported consistently by all MPA models for family *Saxifragaceae*. A very weak attractor (MPA 1b parameter B > 3000 m) was reported for four families (*Brassicaceae, Crassulaceae, Papaveraceae,* and *Saxifragaceae*).

Table 2 Variability in parameter estimates according to the species grouping criterion applied. An F-test was applied to test the effects of grouping on the variance of attractor location (parameter A) and a t-test to test effects on attractor strength (parameter B).

Groups	Model	Parameter A					Parameter B				
		SD (obs)	SD (rnd)	F-value	p-value	Signif	Avg. (obs)	Avg (rnd)	t-value	p-value	Signif
Life form	MPA1a	208.5	19.4	0.81	0.579		714.8	1160.4	-1.97	0.060	(.)
(N = 5)	MPA1b	518.0	40.0	1.46	0.362		857.4	1688.4	-1.71	0.082	(.)
	MPA2a	217.4	62.5	5.38	0.066	(.)	480.6	703.6	-2.05	0.055	(.)
	MPA2b	230.9	109.1	1.82	0.287		498.4	926.4	-1.70	0.082	(.)
Biogeographic	MPA1a	621.9	146.7	17.97	< 0.001	***	826.8	1025.3	-2.97	0.007	**
(N = 11)	MPA1b	950.9	344.7	7.61	0.002	***	1048.8	1355.9	-2.95	0.007	**
	MPA2a	342.1	86.5	15.63	< 0.001	***	541.5	643.1	-3.26	0.004	**
	MPA2b	380.0	134.5	7.98	0.001	**	572.3	672.3	-2.72	0.011	*
Taxonomic	MPA1a	536.5	382.1	1.97	0.060	(.)	1115.2	1212.6	-0.69	0.249	
(N = 23)	MPA1b	931.8	714.2	1.70	0.110		1773.2	1846.5	-0.26	0.400	
	MPA2a	250.1	200.3	1.56	0.153		594.0	794.5	-2.84	0.005	**
	MPA2b	267.2	313.9	0.72	0.772		637.2	1111.3	-2.91	0.004	**

Significance codes: 0 *** < 0.001 ** < 0.05 (.) < 0.1

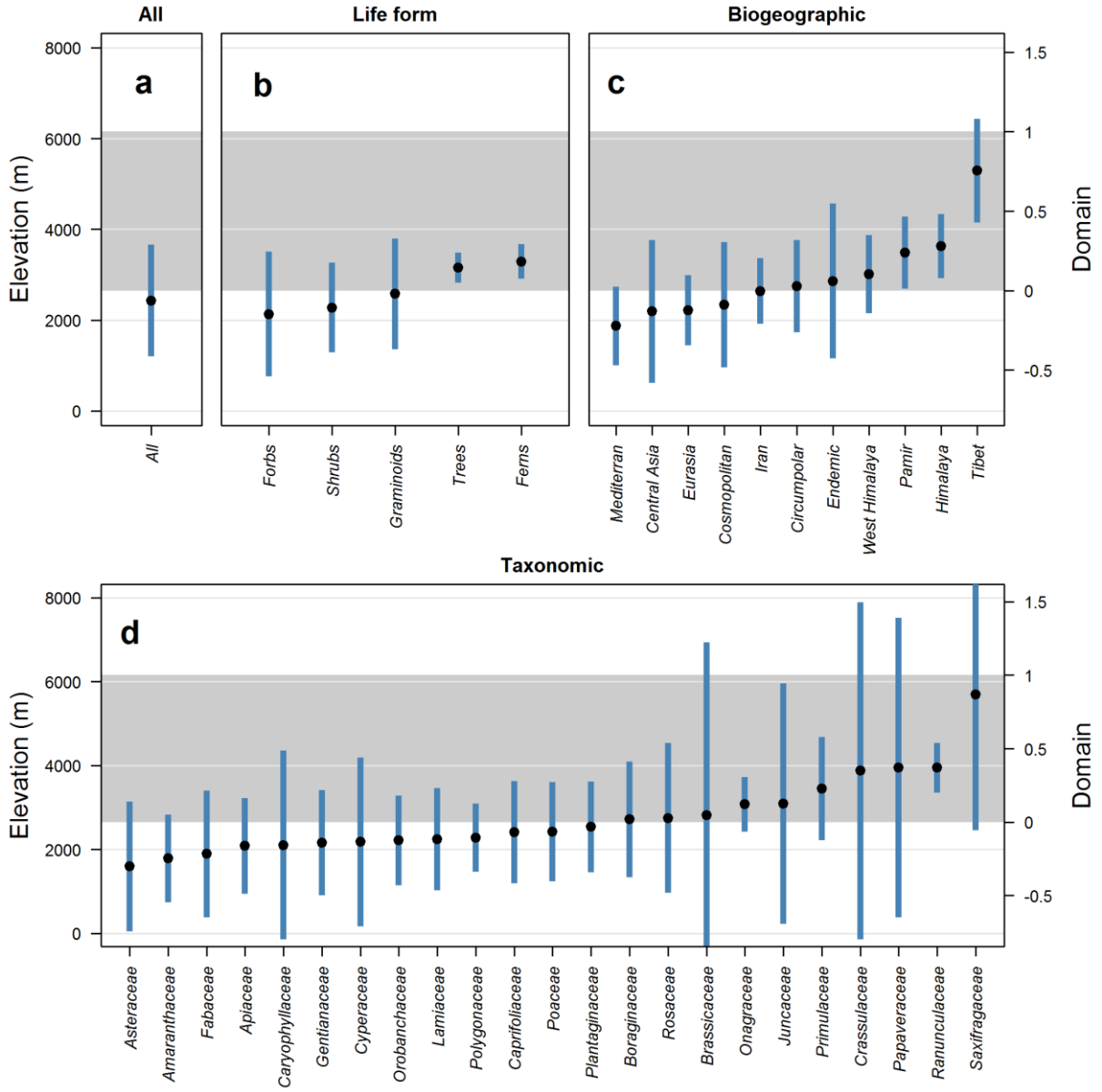

Figure 6 *Estimated mid-point attractor position and strength using the MPA 1b model for species groups: a) full dataset; b) life-form groups; c) biogeographic elements; d) taxonomic rank (family). Gaussian mid-point attractor position (parameter A) is plotted by dots and its strength (standard deviation of Gaussian attractor (parameter B) as a vertical blue bar. The shaded area depicts domain limits. Note that if a mid-point attractor is located below domain limit, then only a monotonically decreasing part of the Gaussian curve was used for mid-point sampling.*

6.6 Discussion

Empirical observations and sampling bias

Despite intensive sampling effort, the actual species ranges may have been slightly underestimated. Underestimation of species ranges leads to underestimated diversity, especially close to domain boundaries, when the interpolation method for richness estimation is used (Grytnes and Vetaas 2002). Simulation of less intensive sampling

effort in this study showed that empirical species richness at lower part of the elevational gradient is more sensitive to range underestimation with limited sampling, while in the upper part of the elevational gradient estimated diversity was less affected (Fig. 3). Nevertheless, a hump-shaped richness pattern remained apparent in alternative point-sample based richness estimation, even when sampling effort was accounted for (Fig. 4). When we corrected for land area using equal-area bands, the hump was less pronounced, peaking at 3,280-3,500 m. Therefore, we conclude that the unimodal elevational richness pattern has a real basis, although accentuated by sampling bias and land area distirubion to a certain degree – either controlled by neutral processes or in underlying climate gradients, as discussed below.

MDE and MPA models performance

MPA models fitted almost perfectly the empirical species richness curves, regardless of the MPA algorithm used. The full set of regional vascular plant species richness was matched with a correlation coefficient > 0.99, reached by all four alternative MPA models. This is in contrast to MDE, which failed to reproduce the observed, positively-skewed diversity pattern because MDE produces only symmetric, humped-shaped curves (Fig. 5). The clear advantage of MPA models is in their flexibility, which allows them to fit different curves, using only two additional parameters (Gaussian attractor position and strength) compared to MDE, which has none.

However, the shape parameters of mid-point attractors were sensitive to the model algorithm used. The MPA model parameters A and B were restricted to a unit range in the original work of Colwell et al. (2016), but we see no strict reason for this limitation, because the center of diversity may in fact lie outside the domain, especially when the studied region covers only a part of altitudinal gradient, as in this case. When we allowed the midpoint attractor to be located outside the domain (model MPA 1b), the model fit to the data slightly increased and the estimated attractor position (parameter A) for all species was situated at 2430 m a.s.l., about 220 m below the domain limit. When the midpoint attractor peak is situated below the domain limit, then the underlying distribution function within the domain is monotonically decreasing part of Gaussian curve. When this is true, then the unimodality of empirical species richness must be caused solely by neutral processes linked to geometric constraints, in conjunction with an approximately Gaussian distribution of environmental favorability for the group in question.

The mid-point attractor probability function of the MPA 2 algorithm places species ranges at domain boundaries with substantially higher probability than the MPA 1 algorithm. In contrast, the MPA 1 algorithm compensated for the truncation of the midpoint attractor distribution by shifting the midpoint attractor to lower elevations; in the case of MPA 1b (attractor not restricted by domain limits), the estimated mid-point attractor was situated even below the lower domain limit for the whole flora, for 13

families; four biogeographic groups and three life-forms (Appendix Table S1). The maximum difference in estimated mid-point attractor position between the MPA 1b and MPA 2b models for same species group was as much as 2250 m. The discrepancy between models was accentuated when we fitted species groups with a center of diversity in lower elevations, probably as a consequence of a high proportion of truncated ranges. The sensitivity of MPA parameters to model assumptions means that midpoint position must be interpreted with caution, particularly if a substantial portion of evaluated species ranges reach domain limits. Despite the fact that many species ranges were truncated in our study domain, the algorithm MPA 1 performed equally well, or even slightly better than MPA 2. Because the interpretation of the underlying midpoint attractor probability function is also more straightforward for algorithm MPA 1, we recommend this algorithm for further use. We also question the restriction of parameter B to unit definition range. There is no strict mathematical reason of such restriction, this limitation in Colwell et al. (2016) was strictly arbitrary. Theoretically, if parameter B was set to infinity, than the MPA 1 would be equal to MDE. We recorded, in several instances, that the estimated value for parameter B exceeded the unit interval in the MPA 1b models for certain species groups, when the a priori range for parameter B was set to the [0,2] interval. This result indicates low climatic control on midpoint placement for these groups, or, in other words, high ecological plasticity of the group.

Ecological interpretations

The absolute decline of species richness towards high elevations is climatically determined, as was confirmed experimentally in our study region (Klimeš and Doležal 2010, Dvorský et al. 2016). Conditions above the elevation of the highest vascular plant occurrence are clearly inhospitable: annual mean temperature falls below –10°C and freezing temperatures occur here every single day of the year (Klimeš and Doležal 2010, Dvorský et al. 2015). The upper limits of plant species in this area belong to the highest records on Earth (Dvorský et al. 2015) and we repeatedly searched for plants growing above the current highest record at 6150 m a.s.l., but so far with negative results. We are therefore confident that the upper range limits used in this study are not truncated due to the geographic extent of our study area, but are set by species´ physiological tolerance.

A different picture can be seen at the lower limit of our modelling domain. Species richness at the lowest elevations may be limited by increasing aridity, but not so strictly as by the low temperatures at upper domain limits (Dvorský et al. 2017). Climate in the lower parts of Ladakh is arid, but even moisture-demanding species can find suitable habitats along streams and on occasional spring fens. However, the decline in species richness towards the lower domain limit have several non-biological explanation: Elevations below 3000 m a.s.l. in the study region are geographically restricted to valleys of the Indus, Dras and Shyok rivers in the NW part of the region (Fig. 1). It is thus

possible that species growing in comparable elevations in adjacent regions are truly missing from the same elevations in Ladakh, simply due to dispersal limitations and/or stochastic extinctions of small populations, following the principles of the species-area relationship.

To assess how common range truncation may be, by geographic constraints, we conducted a literature survey on species range limits in adjacent regions (see Appendix 1 for the description of data sources). We identified 615 species (60% of the total plant diversity), that were reported from lower elevations in other regions than their actual lowest elevation of occurence in Ladakh. This finding provides additional support to our conclusion that climatic favourability (which underlies ESR in Ladakh) is monotonically decreasing with elevation, while the unimodality in observed richness is controlled by neutral processes. With regard to regional climatic gradients, this means that thermal tolerance is the driving factor of plant diversity rather than productivity, which is limited by water deficit in lower part of elevational gradient in Ladakh, similarly to conclusions of Šímová et al. (2011) about drivers of global tree diversity. This inference is not in conflict with a hump-shaped pattern of total diversity, using the asymptotic point-sample estimates, because this approach corrects only for sampling bias, while the inherent species-area relationship, controlled by available land area, still has an impact.

Species groups

The fit of MPA models to the full set of species was almost perfect, therefore dataset separation into distinct species groups could not have improved the overall model fit. On the contrary, we observed slightly worse fit for separately-fitted groups than for the whole plant diversity of the area. Nevertheless, the evaluation of models for species subsets revealed considerable variation in attractor shape parameters among the groups (Fig. 6). We interpret the perfect fit to the full species set, despite the presence of ecologically distinct species groups, as the analogy to the central limit theorem, predicting that regardless of the distribution of separate samples, the summation converges towards normal distribution (see also Šizling et al. 2009). This is likely the reason why the Gaussian attractor is so successful in MPA models. The only model parameter that suggests ecological divergence among species groups contributing to the overall richness pattern, is the inflated (for all species, compared to within groups) attractor parameter B, regulating the strength of the attractor. When we separated species to groups using various grouping criteria, the strength of midpoint attractor generally increased.

Species groupings based on their biogeographical affinity had the greatest significance for attractor positions and strength. This is not so surprising given that climatic niche is mirrored in both altitudinal and latitudinal range. Similarly, Rana et al. (2019) concluded that trees with different biogeographic affinity in E Himalaya greatly differed

in their elevation predominance, but mixing of the groups in the middle elevations couldn't explain the formation of richness peak.

Surprisingly, phylogenetic signal in attractor parameters was relatively weak. With the exception of the family Saxifragaceae, midpoint attractor positions were greatly overlapping and midpoint attractors were relatively weak. Variability in thermal tolerances within the taxonomic groups at the rank of families is obviously still high, probably due to parallel evolution of adaptations to climatic stress. Notably, the twelve species found at elevations ≥6,000 m belonged to six different families. This example illustrates well the limited niche conservatism with respect to thermal tolerances at the level of families (see also Prinzing et al. 2001).

Classification based on life-form provided seemingly striking results: the midpoint attractor in the MPA 1b model for trees was located higher than for forbs, graminoids or shrubs (Fig. 6b). This result may seem contradictory, but only at first glance: midpoint attractor strength was much higher for trees, which means that their midpoints are restricted to elevations around 3,000 – 3,500 m, while the midpoints of the latter life-forms are distributed more evenly along the altitudinal gradient. Drought limitation and human pressure may be responsible for a steeper decline of tree species richness at low elevations as compared to other groups and physiologic constraints control the upper tree-line (Dolezal et al. 2019b).

Here we compared fit to separate models for each group, but integration of species grouping into one model is potentially feasible. The question is, what then should be the optimization criterion, when the fit to the empirical richness of less complex model treating all species together is equal or even better than fit to subdivided dataset. This is critical for understanding the ecology of species, hiding otherwise behind the universal richness gradient.

6.7 Conclusions

Mid-point attractor models are useful in fitting and interpretation of empirical richness data. However, interpretation must be done with caution, because model parameters are sensitive to the setting of model algorithm and the two parameters of midpoint attractor interact in their effects.

Our results showed that unimodal species richness pattern in the Himalaya is jointly driven by a general climatic suitability gradient and also by neutral processes, including domain boundary effects. Sampling bias is a potential source of richness underestimation, especially at the geographically truncated domain boundaries, but with our extensive dataset it played a minor role. The inclusion of ecologically distinct groups did not decrease goodness-of-fit measures, but it weakened the strength of the midpoint attractor. According to differences in midpoint attractor parameters among

species groups, the main distinction criterion was biogeographic affinity, rather than taxonomic rank or life-form.

6.8 Acknowledgements

We gratefully thank Robert K. Colwell who provided critical feedback and helped to improve the manuscript. Majority of species occurrence data were collected by late Leoš Klimeš, who disappeared during his research in Ladakh in 2007. Our study was supported by the Czech Science Foundation (project GACR 17-19376S) and the Czech Academy of Sciences (project RVO 67985939).

6.9 References

Bachman, S., W. J. Baker, N. Brummitt, J. Dransfield, and J. Moat. 2004. Elevational gradients, area and tropical island diversity: an example from the palms of New Guinea. *Ecography* 27:299–310.

Cardelús, C. L., R. K. Colwell, and J. E. Watkins. 2006. Vascular epiphyte distribution patterns: Explaining the mid-elevation richness peak. *Journal of Ecology* 94:144–156.

Carpenter, C. 2005. The environmental control of plant species density on a Himalayan elevation gradient. *Journal of Biogeography* 32:999–1018.

Chao, A., N. J. Gotelli, T. C. Hsieh, E. L. Sander, K. H. Ma, R. K. Colwell, and A. M. Ellison. 2014. Rarefaction and extrapolation with Hill numbers: A framework for sampling and estimation in species diversity studies. *Ecological Monographs* 84:45–67.

Colwell, R. K., N. J. Gotelli, L. A. Ashton, J. Beck, G. Brehm, T. M. Fayle, K. Fiedler, M. L. Forister, M. Kessler, R. L. Kitching, P. Klimes, J. Kluge, J. T. Longino, S. C. Maunsell, C. M. McCain, J. Moses, S. Noben, K. Sam, L. Sam, A. M. Shapiro, X. Wang, and V. Novotny. 2016. Midpoint attractors and species richness: Modelling the interaction between environmental drivers and geometric constraints. *Ecology Letters* 19:1009–1022.

Colwell, R. K., and G. C. Hurtt. 1994. Nonbiological gradients in species richness and a spurious Rapoport effect. *The American Naturalist* 144:570–595.

Colwell, R. K., and D. C. Lees. 2000. The mid-domain effect: geometric species richness. *Trends Ecol. Evol.* 15:70–76.

Colwell, R. K., C. Rahbek, and N. J. Gotelli. 2004. The mid-domain effect and species richness patterns:what have we learned so far? *The American Naturalist* 163.

Colwell, R. K., C. Rahbek, and N. J. Gotelli. 2005. The Mid-Domain Effect: There's a Baby in the Bathwater. *The American Naturalist* 166:E149–E154.

Currie, D. J., and J. T. Kerr. 2008. Tests of the mid-domain hypothesis: A review of the evidence. *Ecological Monographs* 78:3–18.

Dolezal, J., M. Kopecky, M. Dvorsky, M. Macek, K. Rehakova, K. Capkova, J. Borovec, F. Schweingruber, P. Liancourt, and J. Altman. 2019. Sink limitation of plant growth determines tree line in the arid Himalayas. *Functional Ecology* 33:553–565.

Dunn, R. R., C. M. McCain, and N. J. Sanders. 2007. When does diversity fit null model predictions? Scale and range size mediate the mid-domain effect. *Global Ecology and Biogeography* 16:305–312.

Dvorský, M., J. Altman, M. Kopecký, Z. Chlumská, K. Řeháková, K. Janatková, and J. Doležal. 2015. Vascular plants at extreme elevations in eastern Ladakh, northwest Himalayas. *Plant Ecology and Diversity* 8:571–584.

Dvorský, M., Z. Chlumská, J. Altman, K. Čapková, K. Řeháková, M. Macek, M. Kopecký, P. Liancourt, and J. Doležal. 2016. Gardening in the zone of death: an experimental assessment of the absolute elevation limit of vascular plants. *Scientific Reports* 6:24440.

Dvorský, M., M. Macek, M. Kopecký, J. Wild, and J. Doležal. 2017. Niche asymmetry of vascular plants increases with elevation. *Journal of Biogeography* 44:1418–1425.

Grytnes, J. A. 2003a. Ecological interpretations of the mid-domain effect. *Ecology Letters* 6:883–888.

Grytnes, J. A. 2003b. Species-richness patterns of vascular plants along seven altitudinal transects in Norway. *Ecography* 26:291–300.

Grytnes, J. A., and J. H. Beaman. 2006. Elevational species richness patterns for vascular plants on Mount Kinabalu, Borneo. *Journal of Biogeography* 33:1838–1849.

Grytnes, J. A., and O. R. Vetaas. 2002. Species richness and altitude: A comparison between null models and interpolated plant species richness along the Himalayan altitudinal gradient, Nepal. *The American Naturalist* 159:294–304.

Hawkins, B. A., J. A. F. Diniz-Filho, and A. E. Weis. 2005. The mid-domain effect and diversity gradients: is there anything to learn? *The American Naturalist* 166.

Hawkins, B. A., R. Field, H. V. Cornell, D. J. Currie, J.-F. Guégan, D. M. Kaufman, J. T. Kerr, G. G. Mittelbach, T. Oberdorff, E. M. O'Brien, E. E. Porter, and J. R. G. Turner. 2003. Energy, water, and broad-scale geographic patterns of species richness. *Ecology* 84:3105–3117.

Hsieh, T. C., K. H. Ma, and A. Chao. 2019. iNEXT: iNterpolation and EXTrapolation for species diversity. R package version 2.0.19.

Jetz, W., and C. Rahbek. 2001. Geometric constraints explain much of the species richness pattern in African birds. *Proceedings of the National Academy of Sciences* 98:5661–5666.

Klimeš, L., and J. Doležal. 2010. An experimental assessment of the upper elevational limit of flowering plants in the western Himalayas. *Ecography* 33:590–596.

Lomolino, M. V. 2001. Elevation gradients of species-density : historical and prospective views. *Global Ecology and Biogeography* 10:3–13.

McCain, C. M. 2009. Global analysis of bird elevational diversity. *Global Ecology and Biogeography* 18:346–360.

McCain, C. M., and J.-A. Grytnes. 2010. Elevational Gradients in Species Richness. Pages 1–10 *Encyclopedia of Life Sciences*. John Wiley & Sons, Ltd, Chichester.

Nogués-Bravo, D., M. B. Araújo, T. Romdal, and C. Rahbek. 2008. Scale effects and human impact on the elevational species richness gradients. *Nature* 453:216–219.

Peters, M. K., A. Hemp, T. Appelhans, C. Behler, A. Classen, F. Detsch, A. Ensslin, S. W. Ferger, S. B. Frederiksen, F. Gebert, M. Haas, M. Helbig-Bonitz, C. Hemp, W. J. Kindeketa, E. Mwangomo, C. Ngereza, I. Otte, J. Röder, G. Rutten, D. Schellenberger Costa, J. Tardanico, G. Zancolli, J. Deckert, C. D. Eardley, R. S. Peters, M. O. Rödel, M. Schleuning, A. Ssymank, V. Kakengi, J. Zhang, K. Böhning-Gaese, R. Brandl, E. K. V. Kalko, M. Kleyer, T. Nauss, M. Tschapka, M. Fischer, and I. Steffan-Dewenter. 2016. Predictors of elevational biodiversity gradients change from single taxa to the multi-taxa community level. *Nature Communications* 7.

Peterson, A. T., J. Soberón, and V. Sánchez-Cordero. 1999. Conservatism of ecological niches in evolutionary time. *Science* 285:1265–1267.

Prinzing, A., W. Durka, S. Klotz, and R. Brandl. 2001. The niche of higher plants: Evidence for phylogenetic conservatism. *Proceedings of the Royal Society B: Biological Sciences* 268:2383–2389.

R Core Team. 2018. R: A Language and Environment for Statistical Computing.

Rahbek, C. 1995. The elevational gradient of species richness: a uniform pattern? *Ecography* 18:200–205.

Rahbek, C. 2005. The role of spatial scale and the perception of large-scale species-richness patterns. *Ecology Letters* 8:224–239.

Rana, S. K., K. Gross, and T. D. Price. 2019. Drivers of elevational richness peaks, evaluated for trees in the east Himalaya. *Ecology* 100:1–12.

Rangel, T. F. L. V. B., and J. A. F. Diniz-Filho. 2005. Neutral community dynamics, the mid-domain effect and spatial patterns in species richness. *Ecology Letters* 8:783–790.

Šímová, I., D. Storch, P. Keil, B. Boyle, O. L. Phillips, and B. J. Enquist. 2011. Global species-energy relationship in forest plots: role of abundance, temperature and species climatic tolerances. *Global Ecology and Biogeography* 20:842–856.

Šizling, A. L., D. Storch, E. Sizlingova, J. Reif, and K. J. Gaston. 2009. Species abundance distribution results from a spatial analogy of central limit theorem. *Proceedings of the National Academy of Sciences* 106:6691–6695.

Stan Development Team. 2018. RStan: the R interface to Stan. R package version 2.17.3.

Watkins, J. E., C. Cardelús, R. K. Colwell, and R. C. Moran. 2006. Species richness and distribution of ferns along an elevational gradient in Costa Rica. *American Journal of Botany* 93:73–83.

Wiens, J. J., and C. H. Graham. 2005. Niche conservatism: Integrating evolution, ecology, and conservation biology. *Annual Review of Ecology, Evolution, and Systematics* 36:519–539.

Zapata, F. A., K. J. Gaston, and S. L. Chown. 2005. The Mid-Domain Effect Revisited. *The American Naturalist* 166:E144–E148.

Zhou, Y., A. C. Ochola, A. W. Njogu, B. H. Boru, G. Mwachala, G. Hu, H. Xin, and Q. Wang. 2019. The species richness pattern of vascular plants along a tropical elevational gradient and the test of elevational Rapoport's rule depend on different lifeforms and phytogeographic affinities. *Ecology and Evolution*:ece3.5027.

6.10 SUPPLEMENTARY INFORMATION

APPENDIX 1: SUPPLEMENTARY TEXT

6.10.1 SPECIES CLASSIFICATION

Naturalness of occurrence:

Cultivated species (crops, fruits, vegetables, ornamental and medicinal plants) – adventive or cultural species of uncertain origin; their distribution is fully bound to human settlements in irrigated oases and gardens. These species were excluded from analysis.

Ruderal species – indigenous species, or naturalized adventive species, occupying mostly disturbed semi-natural habitats (field margins, along roads, eutrophic places in settlements). Although their occurrence is spontaneous, the distribution and density of their habitats is more or less influenced by human activities. 155 species.

Species from natural habitats; distribution of these indigenous species is considered uninfluenced by human activities. 899 species.

Biogeographical elements.

Only species groups with more than 10 species were used for separate model fitting

1. Central Asiatic steppe and desert elements, widely distributed in semi-arid to arid areas of Inner Asia, or mountains of High Asia - Mongolia, Altai, Tian Shan, Pamir, Karakorum, Tibet. 167 species (C AS).
2. Circumpolar distribution, taxa occurring in temperate to arctic zones of Europe, Asia and N America, occasionally to Antarctic South America. 81 species (CIRCPOL).
3. Cosmopolitan taxa distributed almost world-wide, although predominantly in temperate zones, either anthropogenically (weeds) or naturally (mostly water plants). 14 species (COSMO).
4. Microarealophytes or relatively widely distributed local taxa of the Upper Indus Valley, S Karakorum, Zanskar and SW Tibet. 39 species (ENDEM).
5. Distribution covering temperate to Arctic Europe, occasionally N Africa, and Asia, sub.=,humid to arid areas, often temperate subhumid Euro-Siberian types. 140 species (EURAS).
6. (Sino-)Himalayan elements, subhumid to perhumid areas of the Outer Himalayas (S slopes), usually extending along the S rim of the Tibetan Plateau from E Afghanistan, N Pakistan or Kashmir to SE Tibet and China. 131 species (HIMAL).
7. Irano-Turanian elements, occurring in subarid to subhumid winter-rain areas on the border of temperate and subtropical regions of SW Asia, approximately from Turkey to W Himalaya, or east of Iran only. 45 species (IRAN).
8. Taxa widely distributed mainly in warm-arid areas from the Mediterranean and N Africa to SW Asia, occasionally eastwards 24 species (MEDITER).

9. Adventive flora spreading from the New World, usually temperate elements occupying disturbed habitats. 9 species (NEW WORLD).
10. Subtropical and tropical elements of the Old World – Africa, Arabia, India, China, Japan, Malaysia, occasionally as far east as Oceania and Australia. 9 species (PALEOTROP).
11. Pamiran elements, taxa concentrated mainly in montane-alpine winter rain regions on the western fringe of High Asia,Tian Shan, Pamir, W Himalaya. 59 species (PAMIR).
12. Taxa with pantropic distribution. 3 species (PANTROP).
13. Tibetan elements, alpine or subnival high-altitude flora of the Tibetan Plateau itself, or occasionally (disjunctively) occurring also in N Karakorum, E Pamir and Central Tian Shan. 126 species (TIBET).
14. West Himalayan elements, taxa concentrating in moderately monsoon-influenced, subhumid to subarid regions of the Inner West Himalayas, approximately E Afghanistan, SW Karakorum, Kashmir to W Nepal. 205 species (W HIM).

Phylogenetic classification

Species were grouped according to their taxonomic position at the rank of families. Only families with more than 10 representatives were used for richness modelling (species number in parentheses):

Amaranthaceae (38), Apiaceae (23), Boraginaceae (39), Brassicaceae (61), Caprifoliaceae (11), Caryophyllaceae (37), Asteraceae (133), Crassulaceae (12), Cyperaceae (50), Gentianaceae (34), Lamiaceae (28), Fabaceae (57), Onagraceae (13), Orobanchaceae (19), Papaveraceae (22), Plantaginaceae (21), Poaceae (132), Polygonaceae (32), Primulaceae (19), Ranunculaceae (51), Rosaceae (40), Saxifragaceae (20).

In total, 892 species were used for analysis of species richness according to phylogenetic grouping.

Life-form classification

1. Graminoids. 193 species
2. Forbs. 769 species
3. Trees – trees and large woody shrubs > 2 m. 10 species
4. Shrubs - shrubs, dwarf shrubs, subshrubs, shrublets, lianas. 55 species
5. Ferns - ferns, fern-allies. 26 species

6.10.2 LITERARURE SURVEY ON RANGE LIMITS

Elevational range limits in regions adjacent to our study area (Ladakh, India) were compiled from the following resources: the Flora of Pakistan (https://www.tropicos.org/Project/Pakistan), the Flora of China (www.eFloras.org), the Flora of Nanga Parbat (Dickoré & Nüsser, 2000), The Himalayan Uplands Plant database (Dickoré, 2011) and the Global Biodiversity Information Facility (GBIF, https://www.gbif.org). Records from the GBIF were rounded to nearest hundred. Unreliable outliers based on historical records (i.e. proclaimed elevation more than 1000 m apart from other records) were not taken into account and the next closest, reliable occurrence extreme was used instead.

APPENDIX 2: SUPPLEMENTARY TABLES

Table S1 *Model results ordered by species grouping applied and model used. Number of species (n), Goodness-of-fit measures: Pearson correlation (cor), mean absolute error (MAE), root mean squared error (RMSE, normalized root mean squarred error (nRMSE)*

Grouping	Model	Species group	n	Atractor: mean	Atractor: sd	Goodness of fit			
				estimate (95% CI)	estimate (95% CI)	cor	MAE	RMSE	nRMSE
none	MDE	-	1054	-	-	0.718	140.875	155.743	0.148
	MPA1a	-	1054	2848 (2659; 3114)	1078 (946; 1185)	0.993	17.655	25.862	0.025
	MPA1b	-	1054	2431 (1324; 3044)	1229 (989; 1595)	0.994	16.665	24.493	0.023
	MPA2a	-	1054	3913 (3873; 3949)	600 (570; 630)	0.990	26.025	32.897	0.031
	MPA2b	-	1054	3913 (3876; 3948)	600 (570; 632)	0.990	26.015	32.936	0.031
Biogeo-graphic	MDE	Central Asia	167	-	-	0.813	22.820	25.202	0.151
		Circumpolar	81	-	-	0.791	10.980	12.160	0.150
		Cosmopolitan	14	-	-	0.174	3.215	3.643	0.260
		Endemic	39	-	-	0.822	4.260	4.958	0.127
		Eurasia	140	-	-	0.147	34.875	38.711	0.277
		Himalaya	131	-	-	0.700	16.305	18.459	0.141
		Iran	45	-	-	0.291	9.650	11.126	0.247
		Mediterran	24	-	-	0.024	6.220	7.161	0.298
		Pamir	59	-	-	0.804	7.900	8.836	0.150
		Tibet	126	-	-	0.923	11.785	13.628	0.108
		West Himalaya	205	-	-	0.630	35.050	39.134	0.191
	MPA1a	Central Asia	167	3391 (2772; 3776)	819 (599; 1122)	0.995	3.190	4.379	0.026
		Circumpolar	81	3203 (2692; 3684)	854 (605; 1164)	0.992	1.970	2.481	0.031
		Cosmopolitan	14	3007 (2663; 3495)	663 (407; 1118)	0.888	1.100	1.510	0.108
		Endemic	39	3497 (2704; 4115)	1112 (573; 2330)	0.988	1.255	1.563	0.040
		Eurasia	140	2825 (2657; 3109)	609 (505; 698)	0.982	4.200	6.784	0.048
		Himalaya	131	3645 (3234; 3850)	706 (558; 969)	0.990	2.760	3.699	0.028
		Iran	45	3085 (2691; 3454)	588 (396; 796)	0.984	1.405	1.996	0.044
		Mediterran	24	2868 (2659; 3217)	611 (451; 864)	0.941	1.375	2.194	0.091
		Pamir	59	3625 (2914; 3987)	733 (492; 1194)	0.989	1.620	2.236	0.038
		Tibet	126	5071 (4691; 5910)	990 (636; 1748)	0.992	4.020	5.204	0.041
		West Himalaya	205	3155 (2717; 3495)	805 (631; 1007)	0.994	4.290	5.665	0.028
	MPA1b	Central Asia	167	3279 (1872; 3769)	866 (611; 1435)	0.995	3.280	4.431	0.027
		Circumpolar	81	2744 (1061; 3684)	1018 (576; 1676)	0.992	1.955	2.455	0.030
		Cosmopolitan	14	2181 (972; 3337)	920 (475; 1594)	0.881	1.115	1.547	0.110
		Endemic	39	2860 (1009; 4142)	1701 (602; 5350)	0.986	1.585	1.886	0.048
		Eurasia	140	2212 (1001; 2979)	773 (549; 1059)	0.983	4.360	6.646	0.047
		Himalaya	131	3628 (3240; 3853)	710 (558; 950)	0.990	2.720	3.712	0.028
		Iran	45	2640 (1079; 3447)	727 (429; 1183)	0.984	1.460	2.020	0.045
		Mediterran	24	1869 (937; 3060)	863 (532; 1244)	0.950	1.420	2.088	0.087
		Pamir	59	3489 (1677; 3976)	795 (486; 1680)	0.989	1.675	2.227	0.038
		Tibet	126	5291 (4678; 7361)	1143 (659; 2521)	0.991	4.345	5.678	0.045
		West Himalaya	205	3012 (1776; 3481)	858 (649; 1284)	0.993	4.400	5.824	0.028

***Table S2** continued*

Grouping	Model	Species group	n	Atractor: mean estimate (95% CI)	Atractor: sd estimate (95% CI)	Goodness of fit cor	MAE	RMSE	nRMSE
Biogeo-graphic	MPA2a	Central Asia	167	4036 (3955; 4111)	482 (427; 548)	0.994	3.950	5.007	0.030
		Circumpolar	81	3948 (3828; 4057)	516 (437; 623)	0.990	2.350	2.926	0.036
		Cosmopolitan	14	3385 (2707; 3844)	779 (399; 1732)	0.954	0.700	1.010	0.072
		Endemic	39	4062 (3866; 4242)	564 (443; 755)	0.985	1.015	1.501	0.038
		Eurasia	140	3527 (3436; 3615)	457 (401; 533)	0.985	4.555	6.269	0.045
		Himalaya	131	3924 (3825; 4019)	540 (466; 630)	0.987	3.110	4.122	0.031
		Iran	45	3608 (3459; 3727)	434 (341; 554)	0.977	1.660	2.392	0.053
		Mediterran	24	3307 (2751; 3639)	621 (394; 1063)	0.969	1.110	1.706	0.071
		Pamir	59	4023 (3910; 4148)	474 (395; 577)	0.993	1.300	1.761	0.030
		Tibet	126	4610 (4517; 4704)	530 (467; 612)	0.984	5.320	6.031	0.048
		West Himalaya	205	3850 (3777; 3923)	504 (455; 566)	0.992	4.960	6.251	0.030
	MPA2b	Central Asia	167	4035 (3962; 4107)	482 (435; 540)	0.994	3.905	4.976	0.030
		Circumpolar	81	3941 (3823; 4054)	513 (437; 615)	0.989	2.435	3.090	0.038
		Cosmopolitan	14	2846 (1082; 3809)	1170 (432; 3183)	0.946	0.780	1.114	0.080
		Endemic	39	4057 (3859; 4241)	572 (445; 750)	0.985	1.000	1.478	0.038
		Eurasia	140	3525 (3426; 3611)	458 (392; 538)	0.985	4.510	6.183	0.044
		Himalaya	131	3920 (3814; 4014)	542 (475; 626)	0.987	3.145	4.132	0.032
		Iran	45	3615 (3474; 3732)	433 (344; 578)	0.975	1.695	2.464	0.055
		Mediterran	24	3152 (1718; 3631)	693 (383; 1457)	0.973	1.060	1.631	0.068
		Pamir	59	4021 (3906; 4146)	479 (396; 583)	0.992	1.350	1.826	0.031
		Tibet	126	4615 (4531; 4710)	531 (473; 607)	0.984	5.220	5.985	0.047
		West Himalaya	205	3849 (3769; 3917)	508 (456; 565)	0.993	4.790	6.070	0.030
Life form	MDE	Graminoids	193	-	-	0.791	22.420	24.860	0.129
		Forbs	769	-	-	0.722	101.425	112.598	0.146
		Trees	10	-	-	0.288	2.840	3.219	0.322
		Shrubs	55	-	-	0.602	11.430	12.570	0.229
		Ferns	26	-	-	0.102	3.895	4.275	0.164
	MPA1a	Graminoids	193	3048 (2678; 3495)	1037 (809; 1274)	0.991	3.970	5.428	0.028
		Forbs	769	2833 (2661; 3144)	1120 (979; 1228)	0.993	13.995	20.050	0.026
		Trees	10	3334 (2804; 3598)	286 (144; 557)	0.972	0.440	0.762	0.076
		Shrubs	55	3062 (2668; 3541)	755 (536; 993)	0.992	1.375	2.033	0.037
		Ferns	26	3313 (2884; 3493)	376 (254; 637)	0.942	0.820	1.378	0.053
	MPA1b	Graminoids	193	2575 (1125; 3502)	1218 (813; 1779)	0.991	4.145	5.497	0.028
		Forbs	769	2131 (1054; 2924)	1371 (1074; 1738)	0.993	13.295	18.620	0.024
		Trees	10	3154 (1293; 3573)	328 (145; 929)	0.972	0.440	0.762	0.076
		Shrubs	55	2276 (990; 3448)	986 (582; 1431)	0.992	1.340	1.918	0.035
		Ferns	26	3291 (2746; 3501)	384 (254; 712)	0.941	0.830	1.395	0.054
	MPA2a	Graminoids	193	3943 (3855; 4026)	598 (535; 681)	0.992	4.410	5.139	0.027
		Forbs	769	3929 (3877; 3975)	611 (575; 650)	0.988	20.225	25.950	0.034
		Trees	10	3618 (3322; 3856)	373 (199; 811)	0.969	0.455	0.820	0.082
		Shrubs	55	3851 (3716; 3977)	462 (382; 576)	0.990	1.905	2.439	0.044
		Ferns	26	3446 (3257; 3597)	359 (258; 537)	0.959	0.670	1.170	0.045

***Table S2** continued*

Grouping	Model	Species group	n	Atractor: mean	Atractor: sd	Goodness of fit			
				estimate (95% CI)	estimate (95% CI)	cor	MAE	RMSE	nRMSE
Life form	MPA2b	Graminoids	193	3942 (3846; 4033)	599 (534; 675)	0.991	4.540	5.308	0.028
		Forbs	769	3930 (3882; 3974)	611 (574; 650)	0.988	20.430	26.100	0.034
		Trees	10	3544 (1966; 3869)	455 (199; 1809)	0.969	0.460	0.825	0.082
		Shrubs	55	3853 (3722; 3978)	464 (376; 593)	0.989	1.930	2.499	0.045
		Ferns	26	3448 (3251; 3601)	363 (258; 550)	0.961	0.680	1.158	0.045
Habitat	MDE	Ruderals	155	-	-	0.103	41.470	46.878	0.302
		Natural	899	-	-	0.804	101.855	114.032	0.127
	MPA1a	Ruderals	155	2720 (2652; 2869)	578 (519; 646)	0.965	6.855	11.432	0.074
		Natural	899	3286 (2918; 3543)	977 (836; 1172)	0.996	12.545	16.941	0.019
	MPA1b	Ruderals	155	1388 (915; 2221)	856 (687; 987)	0.972	5.740	10.025	0.065
		Natural	899	3274 (2853; 3518)	983 (842; 1190)	0.996	12.745	17.099	0.019
	MPA2a	Ruderals	155	3483 (3398; 3576)	482 (419; 557)	0.974	6.910	9.690	0.063
		Natural	899	3995 (3954; 4035)	581 (551; 613)	0.989	23.270	28.704	0.032
	MPA2b	Ruderals	155	3485 (3387; 3572)	482 (416; 564)	0.974	6.900	9.691	0.063
		Natural	899	3993 (3952; 4032)	581 (552; 612)	0.989	23.405	28.738	0.032
Taxonomic	MDE	Amaranthaceae	38	-	-	0.574	7.735	8.767	0.231
		Apiaceae	23	-	-	0.602	3.910	4.412	0.192
		Boraginaceae	39	-	-	0.534	5.995	7.072	0.181
		Brassicaceae	61	-	-	0.961	3.100	3.736	0.061
		Caprifoliaceae	11	-	-	0.550	2.310	2.733	0.248
		Caryophyllaceae	37	-	-	0.808	4.885	5.503	0.149
		Compositae	133	-	-	0.562	20.385	22.980	0.173
		Crassulaceae	12	-	-	0.910	1.230	1.546	0.129
		Cyperaceae	50	-	-	0.944	2.575	3.285	0.066
		Gentianaceae	34	-	-	0.745	4.615	5.150	0.151
		Juncaceae	10	-	-	0.720	2.115	2.335	0.234
		Lamiaceae	28	-	-	0.638	5.030	5.645	0.202
		Leguminosae	57	-	-	0.750	6.875	7.778	0.136
		Onagraceae	13	-	-	0.530	3.330	3.814	0.293
		Orobanchaceae	19	-	-	0.586	3.640	4.157	0.219
		Papaveraceae	22	-	-	0.928	1.950	2.317	0.105
		Plantaginaceae	21	-	-	0.559	3.855	4.268	0.203
		Poaceae	132	-	-	0.720	17.875	20.098	0.152
		Polygonaceae	32	-	-	0.555	6.970	7.744	0.242
		Primulaceae	19	-	-	0.862	2.120	2.683	0.141
		Ranunculaceae	51	-	-	0.865	5.135	5.889	0.115
		Rosaceae	40	-	-	0.886	3.290	3.971	0.099
		Saxifragaceae	20	-	-	0.906	1.580	2.025	0.101

***Table S2** continued*

Grouping	Model	Species group	n	Atractor: mean estimate (95% CI)	Atractor: sd estimate (95% CI)	Goodness of fit cor	MAE	RMSE	nRMSE
Taxonomic	MPA1a	Amaranthaceae	38	2916 (2658; 3395)	753 (553; 1006)	0.966	1.920	2.818	0.074
		Apiaceae	23	3048 (2669; 3597)	836 (528; 1256)	0.982	0.770	1.046	0.045
		Boraginaceae	39	3340 (2715; 3973)	1038 (588; 1758)	0.935	2.365	3.052	0.078
		Brassicaceae	61	3546 (2684; 5112)	2408 (1340; 3434)	0.978	2.525	3.098	0.051
		Caprifoliaceae	11	3224 (2679; 3935)	777 (377; 2328)	0.970	0.450	0.806	0.073
		Caryophyllaceae	37	3176 (2677; 4199)	1568 (858; 3110)	0.951	2.470	2.921	0.079
		Compositae	133	2828 (2655; 3184)	1147 (954; 1399)	0.944	7.270	9.291	0.070
		Crassulaceae	12	4065 (2765; 5811)	1811 (485; 3412)	0.928	1.045	1.387	0.116
		Cyperaceae	50	3174 (2668; 3882)	1491 (875; 2997)	0.972	1.900	2.319	0.046
		Gentianaceae	34	3075 (2668; 3648)	932 (615; 1399)	0.982	1.095	1.447	0.043
		Juncaceae	10	3698 (2729; 5360)	1352 (350; 3339)	0.925	1.110	1.360	0.136
		Lamiaceae	28	3108 (2671; 3682)	949 (581; 1591)	0.977	1.135	1.550	0.055
		Leguminosae	57	2981 (2661; 3512)	1131 (834; 1491)	0.966	2.510	3.131	0.055
		Onagraceae	13	3559 (2785; 3905)	436 (215; 908)	0.987	0.435	0.716	0.055
		Orobanchaceae	19	3129 (2676; 3682)	740 (436; 1248)	0.974	0.835	1.163	0.061
		Papaveraceae	22	4176 (2782; 5736)	1648 (511; 3393)	0.952	1.455	1.850	0.084
		Plantaginaceae	21	3175 (2676; 3752)	850 (492; 1463)	0.955	1.185	1.521	0.072
		Poaceae	132	3053 (2682; 3504)	954 (714; 1223)	0.989	3.350	4.372	0.033
		Polygonaceae	32	3035 (2675; 3480)	598 (409; 831)	0.989	0.960	1.364	0.043
		Primulaceae	19	3730 (2834; 4142)	733 (356; 1862)	0.945	1.160	1.575	0.083
		Ranunculaceae	51	3942 (3501; 4175)	591 (427; 1020)	0.989	1.355	1.674	0.033
		Rosaceae	40	3443 (2716; 4046)	1160 (594; 2440)	0.977	1.490	1.825	0.046
		Saxifragaceae	20	5186 (3665; 6096)	1747 (662; 3309)	0.973	0.855	1.197	0.060
	MPA1b	Amaranthaceae	38	1786 (929; 3025)	1044 (678; 1388)	0.966	1.995	2.755	0.073
		Apiaceae	23	2080 (945; 3481)	1143 (602; 1780)	0.979	0.870	1.127	0.049
		Boraginaceae	39	2717 (1046; 3943)	1378 (616; 2780)	0.938	2.355	3.052	0.078
		Brassicaceae	61	2818 (972; 6813)	4110 (1772; 6767)	0.976	2.555	3.103	0.051
		Caprifoliaceae	11	2410 (969; 3718)	1219 (435; 4717)	0.970	0.480	0.837	0.076
		Caryophyllaceae	37	2103 (947; 4239)	2247 (1064; 5877)	0.963	2.135	2.498	0.068
		Compositae	133	1590 (930; 2727)	1547 (1144; 1918)	0.954	6.475	8.307	0.062
		Crassulaceae	12	3870 (1089; 7488)	4020 (702; 6853)	0.928	1.060	1.414	0.118
		Cyperaceae	50	2175 (937; 3750)	2016 (996; 4344)	0.973	1.850	2.296	0.046
		Gentianaceae	34	2158 (976; 3471)	1257 (720; 1905)	0.982	1.060	1.442	0.042
		Juncaceae	10	3089 (1004; 7278)	2869 (460; 6685)	0.888	1.380	1.643	0.164
		Lamiaceae	28	2242 (929; 3618)	1220 (514; 2055)	0.980	1.030	1.453	0.052
		Leguminosae	57	1890 (949; 3170)	1511 (1002; 2140)	0.969	2.325	2.926	0.051
		Onagraceae	13	3075 (1147; 3842)	651 (212; 1664)	0.983	0.570	0.877	0.067
		Orobanchaceae	19	2214 (977; 3476)	1066 (543; 1738)	0.971	0.975	1.262	0.066
		Papaveraceae	22	3944 (1230; 7397)	3570 (679; 6869)	0.938	1.720	2.115	0.096
		Plantaginaceae	21	2536 (1001; 3830)	1078 (472; 2096)	0.951	1.230	1.584	0.075
		Poaceae	132	2423 (1011; 3438)	1182 (763; 1695)	0.988	3.650	4.625	0.035

Grouping	Model	Species group	n	Atractor: mean estimate (95% CI)	Atractor: sd estimate (95% CI)	Goodness of fit cor	MAE	RMSE	nRMSE
Taxonomic	MPA1b	Polygonaceae	32	2274 (948; 3370)	811 (447; 1256)	0.988	1.050	1.466	0.046
		Primulaceae	19	3446 (1338; 4250)	1235 (371; 5658)	0.947	1.150	1.628	0.086
		Ranunculaceae	51	3947 (3538; 4176)	591 (424; 917)	0.989	1.385	1.721	0.034
		Rosaceae	40	2743 (1025; 4139)	1784 (631; 5434)	0.977	1.545	1.877	0.047
		Saxifragaceae	20	5695 (1938; 7761)	3235 (797; 6781)	0.965	1.010	1.373	0.069
	MPA2a	Amaranthaceae	38	3742 (3510; 3926)	547 (413; 758)	0.988	1.265	1.677	0.044
		Apiaceae	23	3618 (2992; 3944)	674 (423; 1275)	0.967	1.090	1.425	0.062
		Boraginaceae	39	3935 (3693; 4126)	625 (471; 857)	0.932	2.455	3.034	0.078
		Brassicaceae	61	4234 (4017; 4441)	755 (598; 1000)	0.979	2.050	2.584	0.042
		Caprifoliaceae	11	3679 (2937; 4027)	590 (280; 1551)	0.936	0.680	1.149	0.104
		Caryophyllaceae	37	4070 (3804; 4272)	660 (500; 945)	0.960	2.300	2.665	0.072
		Compositae	133	3847 (3674; 3987)	722 (616; 872)	0.967	5.420	6.839	0.051
		Crassulaceae	12	4253 (3766; 4666)	607 (336; 1591)	0.942	0.800	1.183	0.099
		Cyperaceae	50	3998 (3657; 4218)	755 (566; 1100)	0.943	2.775	3.253	0.065
		Gentianaceae	34	3824 (3531; 4073)	627 (458; 914)	0.959	1.535	2.196	0.065
		Juncaceae	10	4016 (3369; 4376)	536 (267; 1810)	0.962	0.680	0.917	0.092
		Lamiaceae	28	3897 (3648; 4108)	562 (414; 824)	0.974	1.190	1.694	0.061
		Leguminosae	57	3877 (3618; 4076)	702 (555; 933)	0.945	3.325	3.925	0.069
		Onagraceae	13	3811 (3640; 3962)	284 (182; 448)	0.986	0.460	0.735	0.057
		Orobanchaceae	19	3697 (3297; 3950)	539 (351; 933)	0.968	0.960	1.296	0.068
		Papaveraceae	22	4311 (3996; 4583)	619 (416; 1075)	0.959	0.990	1.478	0.067
		Plantaginaceae	21	3755 (3136; 4039)	617 (376; 1287)	0.977	0.710	1.082	0.052
		Poaceae	132	3896 (3785; 3997)	580 (501; 670)	0.991	3.230	3.903	0.030
		Polygonaceae	32	3711 (3530; 3878)	465 (349; 645)	0.988	1.030	1.432	0.045
		Primulaceae	19	4007 (3765; 4223)	455 (317; 707)	0.936	1.375	1.674	0.088
		Ranunculaceae	51	4109 (3986; 4237)	457 (376; 566)	0.989	1.365	1.727	0.034
		Rosaceae	40	4061 (3856; 4246)	582 (462; 754)	0.966	1.805	2.256	0.056
		Saxifragaceae	20	4705 (4359; 5152)	702 (447; 1310)	0.962	0.985	1.312	0.066
	MPA2b	Amaranthaceae	38	3755 (3523; 3944)	544 (408; 756)	0.988	1.285	1.704	0.045
		Apiaceae	23	3576 (2352; 3944)	716 (425; 1564)	0.970	1.010	1.353	0.059
		Boraginaceae	39	3910 (3621; 4135)	640 (470; 954)	0.934	2.435	2.989	0.077
		Brassicaceae	61	4231 (4012; 4456)	754 (593; 1006)	0.978	2.110	2.636	0.043
		Caprifoliaceae	11	3576 (1431; 4157)	847 (297; 4570)	0.939	0.660	1.122	0.102
		Caryophyllaceae	37	4065 (3830; 4280)	672 (499; 957)	0.960	2.280	2.631	0.071
		Compositae	133	3846 (3679; 3999)	724 (612; 877)	0.967	5.385	6.810	0.051
		Crassulaceae	12	4281 (2764; 5970)	988 (327; 5708)	0.944	0.790	1.196	0.100
		Cyperaceae	50	4010 (3708; 4255)	740 (555; 1102)	0.943	2.780	3.253	0.065
		Gentianaceae	34	3821 (3497; 4054)	627 (459; 943)	0.960	1.550	2.169	0.064
		Juncaceae	10	3980 (3234; 4305)	617 (283; 2915)	0.963	0.650	0.911	0.091
		Lamiaceae	28	3886 (3576; 4139)	572 (412; 873)	0.975	1.170	1.666	0.059
		Leguminosae	57	3876 (3588; 4070)	705 (547; 936)	0.945	3.300	3.899	0.068
		Onagraceae	13	3808 (3648; 3980)	290 (190; 511)	0.988	0.420	0.693	0.053
		Orobanchaceae	19	3667 (3002; 3945)	567 (350; 1279)	0.963	1.020	1.378	0.073

Grouping	Model	Species group	n	Atractor: mean	Atractor: sd	Goodness of fit			
				estimate (95% CI)	estimate (95% CI)	cor	MAE	RMSE	nRMSE
Taxonomic	MPA2b	Papaveraceae	22	4297 (4014; 4602)	647 (425; 1083)	0.961	1.000	1.442	0.066
		Plantaginaceae	21	3738 (3143; 4020)	598 (377; 1258)	0.974	0.770	1.151	0.055
		Poaceae	132	3895 (3782; 3991)	581 (506; 679)	0.991	3.200	3.866	0.029
		Polygonaceae	32	3713 (3518; 3860)	463 (352; 628)	0.988	0.985	1.445	0.045
		Primulaceae	19	4006 (3808; 4207)	456 (319; 714)	0.933	1.380	1.709	0.090
		Ranunculaceae	51	4109 (3989; 4235)	453 (368; 569)	0.989	1.330	1.687	0.033
		Rosaceae	40	4060 (3860; 4247)	583 (450; 783)	0.965	1.825	2.277	0.057
		Saxifragaceae	20	4752 (4295; 5948)	872 (446; 3456)	0.966	0.930	1.251	0.063